



City Research Online

City, University of London Institutional Repository

Citation: Papadrakakis, Manolis (1978). Gradient and relaxation nonlinear techniques for the analysis of cable supported structures. (Unpublished Doctoral thesis, City, University of London)

This is the submitted version of the paper.

This version of the publication may differ from the final published version.

Permanent repository link: <https://openaccess.city.ac.uk/id/eprint/21924/>

Link to published version:

Copyright: City Research Online aims to make research outputs of City, University of London available to a wider audience. Copyright and Moral Rights remain with the author(s) and/or copyright holders. URLs from City Research Online may be freely distributed and linked to.

Reuse: Copies of full items can be used for personal research or study, educational, or not-for-profit purposes without prior permission or charge. Provided that the authors, title and full bibliographic details are credited, a hyperlink and/or URL is given for the original metadata page and the content is not changed in any way.

City Research Online:

<http://openaccess.city.ac.uk/>

publications@city.ac.uk

GRADIENT AND RELAXATION
NONLINEAR TECHNIQUES
FOR THE ANALYSIS OF
CABLE SUPPORTED STRUCTURES

A Thesis submitted by Manolis Papadrakakis
for the degree of Doctor of Philosophy

The City University,
Department of Civil Engineering,
July, 1978.

*"Endlessly one could thank, for one
is nothing without those amongst whom
one lived, from whom one learnt, on
whose knowledge one builds up. If only
I, in my way, can some day be of use !"*

George Dibbern

CONTENTS

PAGE NO

LIST OF COMPUTER PROGRAMS

ABSTRACT

ACKNOWLEDGEMENTS

CHAPTER 1 : INTRODUCTION	20 - 42
1.1. The Characteristics of Tension Structures	20
1.2. State of the Art	25
1.3. Review of the Literature	30
CHAPTER 2 : ENERGY SEARCH APPROACH	43 - 78
2.1. Energy Formulations	43
2.2. Unconstrained Minimization	46
2.3. Assumptions	50
2.4. The Total Potential Energy	51
2.5. The Gradient Vector	53
2.6. The Matrix of Second Partial Derivatives	55
2.7. Scaling Effects of Iterative Methods	59
2.8. Termination Criteria	66
2.9. Test Problems	69
CHAPTER 3 : GRADIENT METHODS	79 - 102
3.1. Introduction	79
3.2. The Conjugate Gradient Algorithm	81

3.3.	The Single Variable Search	84
3.3.1.	Methods for Bracketing the Solution	85
3.3.2.	Methods for Approximating the Minimum	87
3.4.	Buchholdt's Method	93
3.5.	Extensions of the CG Algorithm	95
3.5.1.	Polak and Ribiere Algorithm	95
3.5.2.	Sorenson's Version	96
3.6.	The Memory Gradient Method	97
3.7.	The Inversion of a Matrix by the CG Method	101

CHAPTER 4 : NUMERICAL STUDIES ON CONJUGATE GRADIENT METHODS 103-129

4.1.	Fletcher and Reeves Method (CGFR)	103
4.2.	Stanton's Method (CGST)	106
4.3.	Other CG Algorithms	110
4.4.	Comparative Study	113
4.5.	Conclusions	125

CHAPTER 5 : RELAXATION METHODS 130-179

5.1.	Dynamic Relaxation	130
5.1.1.	Historical Development	130
5.1.2.	Formulation of the Iterative Procedure	133
5.1.3.	Asymptotic Convergence of Dynamic Relaxation	135
5.1.4.	Evaluation of the Optimum Iteration Parameters	139
5.1.5.	Stability of Dynamic Relaxation	143

5.2.	Methods with Three Term Recursion Formulae	145
5.3.	Relation Between Dynamic Relaxation and Tchebycheff methods	149
5.4.	Relation Between Conjugate Gradient and Tchebycheff methods	151
5.5.	The Residual Polynomial	152
5.6.	The Conjugate Gradient - Tchebycheff Method	154
5.7.	Assessment of the Dynamic Relaxation Parameters	158
5.8.	"A Priori" Evaluation of Dynamic Relaxation Parameters	162
5.9.	Automatic Adjustment of the Dynamic Relaxation Parameters	164
5.10.	The Use of Kinetic Damping	168
5.11.	Successive Overrelaxation	171
5.12.	The Successive Overrelaxation Parameter	175
5.13.	Automatic adjustment of the SOR Parameter	176
5.14.	Application of the Successive Overrelaxation Method to Cable Structures	178
CHAPTER 6 : THE SPECIAL EIGENVALUE PROBLEM		180-212
6.1.	Introduction	180
6.2.	The Power Method	182
6.2.1.	Improving the Convergence of the Power Method	184
6.3.	The Method of Steepest Descent	187
6.4.	The Method of Conjugate Gradients	189

6.5.	Optimization of the Conjugate Gradient Algorithm	191
6.5.1.	Fried's Method	181
6.5.2.	Geradin's Method	193
6.6.	Convergence and Initial approximation	194
6.7.	Gershgorin Theorem	197
6.8.	Coordinate Relaxation	198
6.9.	Numerical Studies	199
6.10.	Conclusions	208

CHAPTER 7 : NUMERICAL STUDIES ON RELAXATION METHODS 213-247

7.1.	Dynamic Relaxation Method	213
7.2.	Automatic Adjustment of Dynamic Relaxation Parameters	223
7.3.	Kinetic Damping	228
7.4.	The Conjugate Gradient-Tchebycheff Method	230
7.5.	Successive Overrelaxation Method	234
7.6.	Comparative Study	237
7.7.	Conclusions	241

CHAPTER 8 : STIFFNESS METHODS 248-273

8.1.	Linear Equation Systems	248
8.1.1.	Introduction	248
8.1.2.	Jenning's Compact Storage Scheme for the Solution of Symmetric Linear Simultaneous equations	251

8.2.	Nonlinear Equation Systems	255
8.2.1.	Introduction	255
8.2.2.	Newton Raphson Type Methods	259
8.2.3.	Incremental Stiffness Procedure	266
8.2.4.	The Perturbation Method	267

CHAPTER 9 :	COMPARATIVE STUDY	274-292
-------------	-------------------	---------

9.1.	Example 1 : Suspension Cable	274
9.2.	Example 2 : Counterstressed Dual Cable	275
9.3.	Example 3 : Orthogonal Hyperbolic Paraboloid Prestressed Net	277
9.4.	Example 4 : Three Dimensional Counterstressed Dual Cable Structure	288
9.5.	Example 5 : Large Prestressed Net	288
9.6.	Conclusions	290

CHAPTER 10 :	ULTIMATE LOAD ANALYSIS	293-320
--------------	------------------------	---------

10.1.	Introduction	293
10.2.	Mathematical Formulation	294
10.3.	Nonlinear Solution Techniques for Ultimate Load Analysis	299
10.4.	Numerical Studies	300
10.4.1.	Example 3 : Hyperbolic Paraboloid	300
10.4.2.	Example 4 : Three Dimensional Counterstressed Dual Cable Structure	307
10.5.	Conclusions	318

CHAPTER 11 : GENERAL CONCLUSIONS AND SUGGESTIONS
FOR FURTHER WORK

321-329

11.1. Conclusions

321

11.2. Suggestions for Further Work

327

REFERENCES

330-357

LIST OF COMPUTER PROGRAMS

Computer Programs for Gradient Methods

- CGFRIN : The linear CG algorithm with the residuals and the stiffness matrix being modified after each iteration.
- CGFRIP : The linear CG algorithm with the product Kp_i being obtained as the product Kx_i and the stiffness matrix being modified after each iteration.
- CGFRIL : A Newton Raphson iterative technique, with linear solutions obtained from the CG algorithm.
- CGFR : Davidon's linear search as modified by Fletcher and Reeves.
- CGST : Stanton's technique for bracketing the solution in conjunction with the regular falsi-bisection algorithm.
- CGSR : A combined Stanton-Davidon linear search.
- CGMEM : The memory gradient method.
- CGBUC : Buchholdt's method.
- CGSTPR : Stanton's linear search with Polak and Ribiere's algorithm for β .
- CGSDSR : Stanton's linear search with Sorenson's algorithm for β .

The symbol "-SC" after the abbreviated name of the method means a scaled version of the method, while the symbol "-Rn" means that a reinitialization process has been applied every after n iterations.

Computer Programs for the Evaluation of the Extreme Eigenvalues

- EIGP : The power method.
- EIGSD : The steepest descent method.
- EIGFR1 : The CG algorithm with Fried's modification (equation (6.36)).
- EIGFR2 : The CG algorithm with Fried's modification (equation (6.35)).
- EIGCG : The conjugate gradient algorithm.
- EIGGER : The CG algorithm with Geradin's modifications.
- EIGCR : The coordinate relaxation method.

The letter "B" after the abbreviated name of the method means that the Bradbury and Fletcher orthogonalization process has been applied.

Computer Programs for Relaxation Methods

- DRGR : The DR method with an "a priori" evaluation of the relaxation parameters and Geradin's algorithm for the estimation of the extreme eigenvalues.
- DRGRFS : The DR method with Flanders and Shortley iteration parameters.
- DRGRYN : The DR method with Young's iteration parameters.
- DRAUT : The DR method with automatic adjustment of the iteration parameters.
- DRKR : The DR method with kinetic damping and a velocity criterion to avoid divergence.

All the above methods have been applied in their scaled versions. The symbol "-UNSC" has been used after the abbreviated name when the unscaled version of the method has been applied.

- CGTCH : A combination of the CG algorithm and the DRAUT method.
- SORNL : The SOR method with the stiffness matrix being updated at each iteration.
- SORES : The SOR method with the stiffness matrix being held constant and resetting only the residuals.
- SORES : The SOR method with Carre's algorithm for the automatic evaluation of parameter ω .
- SORESH : The SOR method with Hageman's technique for the automatic evaluation of parameter ω .

Computer Programs for Stiffness Methods

- NTRA : The Newton Raphson iteration method with a semi-bandwidth Gaussian elimination technique.
- NTRAJE : The Newton Raphson iteration method with Jennings's compact storage elimination technique.

ABSTRACT

The purpose of this work is to investigate the efficiency of numerical nonlinear solution procedures when applied to the static analysis of cable supported structures. Gradient and relaxation methods are developed and compared with existing nonlinear solution techniques. In order to obtain a more general picture of the performances of the above methods, stiffness methods with Newton Raphson iterative schemes have also been included in the comparative study.

Chapter 1 examines the behaviour and characteristics of cable supported structures and investigates the analytical requirements for static analysis. A state of the art of numerical solution techniques used to analyse these structures is presented. An extensive review of published work in relation to the analysis of single unstiffened cables, dual cables and cable networks is also presented.

Chapter 2 approaches the solution of the structural problem through total energy formulations. Three basic energy formulations are discussed with particular emphasis given to the total potential energy formulation. The principles of the unconstrained minimization method are considered and different search techniques for approximating the minimum are discussed. Expressions for the gradient vector of the total potential energy are obtained and the tangent stiffness matrix is evaluated as the matrix of the second partial derivatives

of the total potential energy formulation. Different scaling techniques are reviewed and the effects of the termination criterion used, for different methods of analysis, on the final accuracy of the methods is also discussed.

In Chapter 3 there is an extensive theoretical treatment of gradient methods for the nonlinear solution of structural problems. Particular emphasis is given to the conjugate gradient algorithm and the modifications proposed by various investigators since it first appeared in 1952. A number of one dimensional linear searches are studied which approximate the minimum along the p direction and determine the scalar parameter α for the next iteration. And extensions of the conjugate gradient algorithm for the evaluation of the scalar parameter β , as proposed by Sorenson and Polak and Ribiere are discussed. Finally, the memory gradient method which employs a two dimensional linear search for a simultaneous evaluation of α and β is also presented.

Chapter 4 examines the efficiency of the methods discussed in Chapter 3 when applied to the nonlinear solution of a number of test problems. The problems are selected to have varying numbers of degrees of freedom and the respective stiffness matrices to have differing condition numbers in order to study the response of the methods for different structural characteristics. The Fletcher and Reeves method with Davidon's linear search with a cubic equation to approximate the minimum, Stanton's algorithm for bracketing the solution and the regula falsi-bisection algorithm to approximate the minimum, a

combined algorithm of Davidon and Stanton's techniques, Buchholdt's method, Polak and Ribiere's algorithm, Sorenson's version, the memory gradient method and a number of linearized conjugate gradient algorithms are developed and their convergence characteristics are compared. The effects of scaling and reinitialization are also studied.

In Chapter 5 there is a theoretical investigation of relaxation methods and in particular the dynamic relaxation and the successive overrelaxation methods. A rigorous examination of the characteristic properties of dynamic relaxation is carried out. The method is treated as a standard eigenvalue problem for error vectors and expressions for the iteration parameters are developed with respect to the minimum and maximum eigenvalue of the current stiffness matrix. A theoretical comparison of a number of pure iterative methods is performed and relationships between the iteration or scalar parameters of the conjugate gradient method, the dynamic relaxation method, the Jacobi semi-iterative method, and the Tchebycheff methods, are established. This suggests that all these methods in fact belong to the same family of methods called "three term recursion formulae". A combined conjugate gradient and Tchebycheff type method is also studied. A method for the automatic evaluation of the dynamic relaxation parameters is developed by the author which can guarantee convergence for almost any arbitrary initial estimate of the minimum and maximum eigenvalues of the current stiffness matrix. The concept of using kinetic energy damping instead of viscous damping in the dynamic relaxation iterative process is also examined. Finally, the

successive overrelaxation method is modified to be applicable to the nonlinear analysis of structural problems, and two ongoing processes for automatic evaluation of the optimum overrelaxation parameter ω , proposed by Carre and Hageman, are also examined.

Chapter 6 is devoted to a theoretical and numerical investigation of the problem of finding the minimum and maximum eigenvalues of a symmetric matrix. The power method, the steepest descent method, the conjugate gradient method, and the coordinate relaxation method, are among the techniques examined and compared in this Chapter. Several other modifications to the initial conjugate gradient algorithm are also studied, including the modification proposed by Fried for the evaluation of the scalar parameter β and the one proposed by Geradin. An orthogonalization process is also applied to alleviate the dependency of the convergence of the method on the initial approximation for the final eigenvector.

In Chapter 7 numerical studies of the relaxation methods discussed in Chapter 5 are performed. Alternative forms of the dynamic relaxation methods with an "a priori" evaluation of the iteration parameters (using one of the methods discussed in Chapter 6), with automatic adjustment of the relaxation parameters based on the method developed in Chapter 5, and with the incorporation of kinetic damping, are applied for different test problems. Techniques to avoid the occurrence of instability of the method, when the current maximum eigenvalue of the iteration matrix becomes greater than the estimated maximum eigenvalue,

are also developed and compared. Finally, the efficiency of the successive overrelaxation method, with both constant and adjustable relaxation parameters is examined and compared with the efficiency of the dynamic relaxation method.

In Chapter 8 a review of methods operating through the formulation of the overall stiffness matrix is carried out. The efficiency of these methods is dependent on both the method employed to perform the linear solution when this is necessary and the nonlinear technique used to approximate the nonlinear equilibrium position in each iteration. A compact store elimination scheme, proposed by Jennings, is studied in conjunction with the Gaussian elimination procedure. Three different classes of nonlinear techniques are discussed together with the area in which each one has proved to be more suitable.

Chapter 9 performs a general comparative study of the convergence characteristics of the best methods from each classification (gradient, relaxation and stiffness methods), and examines the advantages and disadvantages involved in the application of the methods to the nonlinear elastic analysis of cable supported structures with members being allowed to slacken. The computer time required to obtain a certain degree of accuracy, the storage requirements and the cost involved are all examined and compared in an effort to select the most suitable method for each particular class of problem.

In Chapter 10 the ultimate load carrying capacity of cable structures is studied, with members being allowed to slacken and

with the inclusion of nonlinear stress-strain relationships. Two different solution procedures are employed : the stiffness method with or without the compact store elimination scheme in conjunction with Newton Raphson iteration, and Stanton's conjugate gradient algorithm. The convergence of the methods are tested for different values of the termination parameter ϵ and load increments. A continuous stress-strain curve as proposed by Jonatowski is used and provision for the cable members to reload following a different path is also included. Finally, Chapter 11 reviews the general conclusions resulting from the experience gained from the theoretical and numerical treatment of the methods discussed in this work, together with suggestions for further research.

ACKNOWLEDGEMENTS

I am deeply indebted to Dr. M. R. Barnes for his helpful supervision and guidance throughout the preparation of this work. I also would like to thank him for his patient reading of the manuscript and for giving some useful suggestions. His help is very much appreciated.

I would like to thank my colleagues Barry Topping and David Wakefield for their assistance during my stay at The City University.

I am also grateful to the staff of the Skinners Library and the Computer Unit of the University for their help.

The typing of the thesis was done very effectively by Miss M. Williams, for which I am very grateful.

Finally, I would like to thank my wife Anne-Marie for her care of our daughter Isadora and myself. This work would not have been completed without her constant encouragement and understanding.

CHAPTER 1

INTRODUCTION

The capacity to transmit forces and moments by tension loaded cables is found in animate and inanimate nature. The oldest cable nets were built millions of years ago by spiders. The history of the development of nets, produced by people, is lost in antiquity. Many Etruscan and Roman frescos and mosaics show scenes with hunting nets, fishing nets and ship nets. While in China at about 65 AD was recorded the use of vine ropes and metal chains in suspension structures.

Nevertheless the few records which are available on net structures, in contrast to structures subjected to compression and bending, indicate that major achievements were not attained until recently.

In bridge building, the single cable let to double and multi-cable suspension bridges. The first cable suspension bridge was built by James Finley in Pennsylvania in 1810. Following the example of bridges, roofs were also suspended from cables in the last century (Laurent 1837, "Lorient Arsenal", Engineering News Record, October 27, 1921). The designs of V. G. Shookhov in Nijny-Novgorod (Russia) in 1896 are generally regarded as the first engineering surface structures in which roof membranes are supported directly on the cable systems. Following this there was a period of inactivity in the erection of cable network structures, and it was not until 1954 that the next significant structure of this type was constructed: the Raleigh Arena in North Carolina (USA). Since then a great number of cable supported

structures have been built all over the world with resulting advances in scale, methods of erection and prefabrication, jointing and clamping details, and numerical design and analysis procedures.

Although tensile structures built to date show a steady increase in scale, they perform more or less conventional functions. On the other hand, there are a number of projects, in different stages of development, that would utilize a membrane envelope to enclose a park, a resort, an office building, or even several city blocks. It is in this area of very wide span structures that the advantages of tension systems could become most significant. Since both the technology and the need for such applications exist, their realization is likely to be a matter of time (Varga [294]).

1.1. The Characteristics of Tension Structures

The primary characteristic of tension structures, is that the main structural elements, transmitting the applied loads to bearing structures, consist of high strength flexible cables with the ability to sustain only tensile forces. The absence of bending moments permits the full utilization of the cross section of the cables, with permissible stresses not limited by instability effects.

Architects and Engineers have a strong interest in utilizing suspension systems. This interest results from two factors. The first factor is aesthetic; the inherent flexibility of the cables permits further opportunities for architectural expression. The second factor is economic. The use of high tensile components gives

light weight structures capable of covering large areas without supporting columns, and with the minimum steel consumption. In addition they can be mounted on site very rapidly.

The analysis of cable suspended structures differs from that of ordinary Civil Engineering structures, because they possess the unique characteristic, that for a given loading condition, the internal forces and the resulting geometry necessary to maintain equilibrium are interdependent. The usual assumption of infinitesimal deformations leads to erroneous results when applied to these type of structures. Thus a valid analysis must include finite deformations and their effect on internal forces, i.e., the equations of equilibrium must be written corresponding to the distorted configuration of the structure. This means that the principal of superposition loses its validity and that the governing equations become nonlinear.

Buchholdt [50], has introduced an expression for the degrees of mechanical freedom for discrete pinjointed assemblies as

$$DMF = f - m + p \quad (1.1)$$

where f is the number of degrees of freedom of the joints, m is the number of members and P is the number of linearly independent force vectors which can be superimposed without disturbing the equilibrium configuration. The assembly is classified as a structure when $DMF = 0$, and as a structural mechanism when $DMF > 0$. The advantage of equation (1.1) is that the existence of mechanical freedom can be detected by considering the number of ways in which an assembly can be prestressed, instead of considering its Kinematic properties. Structural mechanisms do

not possess an unstrained geometry and it is necessary to relate the deflections to a known equilibrium position of the structure. The geometry of the known equilibrium position replaces the undeformed geometry of a rigid structure.

Large displacements in cable systems arise mainly as a result of large rotations experienced by the elements of the structure and not as a result of high strains. Furthermore, the stress-strain curve for cables typically used in modern constructions exhibit linear characteristics only up to about 50% of their breaking strength, assuming the cables to be prestressed [290]. Thus a rigorous investigation of the behaviour of cable structures must include both nonlinear stress-strain relationships and geometric nonlinearities; particularly when studying ultimate load carrying capacity. In addition to continuous stress-strain nonlinearities, discontinuous nonlinearities, such as cable slackening may occur. Under these combined nonlinearities numerical search for an equilibrium position should strictly be treated as path dependent.

Another major characteristic of suspension structures, and in particular of cable networks, is that the stiffness matrix is inherently ill-conditioned. For a stiffness matrix of a linear structure, the elements of the i th column $K_{1i}, K_{2i}, \dots, K_{ni}$, are the nodal forces required to maintain an imposed displacement state of $U_i = 1$ with all other displacements zero. For a nonlinear cable system the same physical explanation applies to the tangent stiffness matrix. For a shallow network structure, as in Figure 1.1, the horizontal node forces required to maintain this imposed displacement state may be considerably larger than the force applied at the same joint and at the same direction as the unit vertical

displacement. Thus the absolute value of the terms representing the horizontal node forces, $K_{l-2,i}$, $K_{l-1,i}$, $K_{j-2,i}$, $K_{j-1,i}$, $K_{k-2,i}$, $K_{k-1,i}$, $K_{m-2,i}$, $K_{m-1,i}$, $K_{i-2,i}$, $K_{i-1,i}$, may be considerably larger than the diagonal term $K_{i,i}$. This difference becomes greater the more flat is the network. Thus, for this type of structure, every third equation of the stiffness matrix, will usually have a main diagonal term which is smaller in magnitude than the other terms of the same row. This peculiarity is one of the characteristics of poorly conditioned matrices (see Chapter 2, Section 2.8).

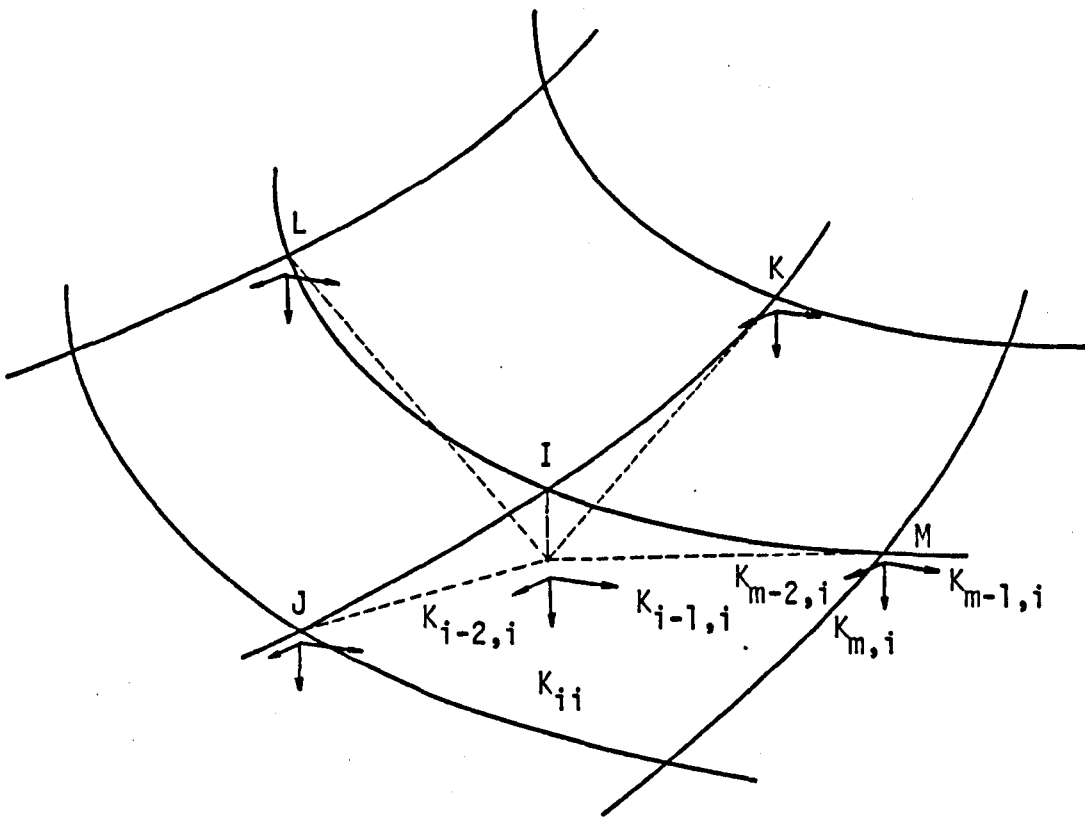


Figure 1.1

Apart from static behaviour, the analysis of tension systems involves a special consideration of two major aspects. The first is the initial shape determination which is directly coupled to the prestress distribution, and the second is the dynamic behaviour; the light-weight and flexibility of tension structures making them particularly sensitive to dynamic loads.

Some examples of tension systems are shown in Figures 1.2 through 1.5.

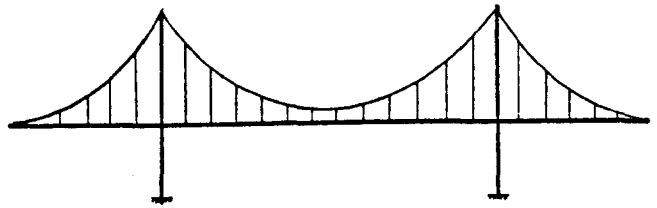
1.2. State of the Art

For the purpose of analysis cable structures may be treated either as continuous or as discrete systems. In the first half of the "sixties" most of the published work treated the system as continuous. For such analyses the cable net is assumed to be replaced by an equivalent flexible membrane which takes up the shape of the middle surface of the net. The majority of the methods in this category are linearized methods which usually include some type of iteration correction for the nonlinear terms, although a direct treatment of the nonlinear equations has also been attempted.

In terms of practical structures, however, the "membrane" approach is somewhat limited. Only those cable nets with an easily defined mathematical shape can be analysed and irregularities in boundary shapes and cable mesh are difficult to allow for. Moreover, the "membrane" analogy is an approximation which gets progressively worse as the coarseness of the cable grid increases.

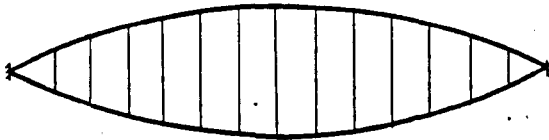


Simple cable

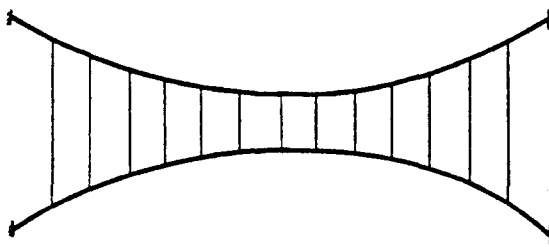


Stiffened cables

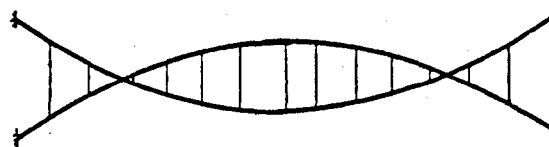
Fig. 1.2 Single cable structures



Girder

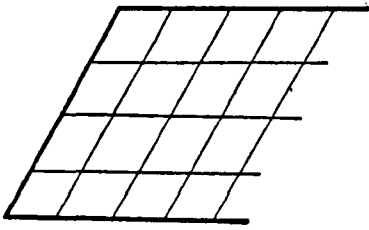


Truss

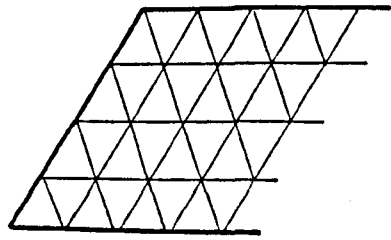


Girder-truss

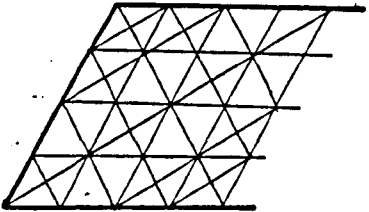
Fig. 1.3 Dual cable structures



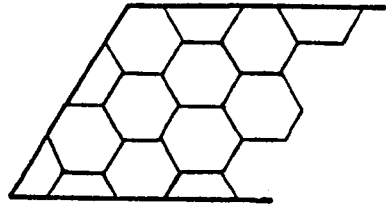
Doubly threaded net



Triply threaded net

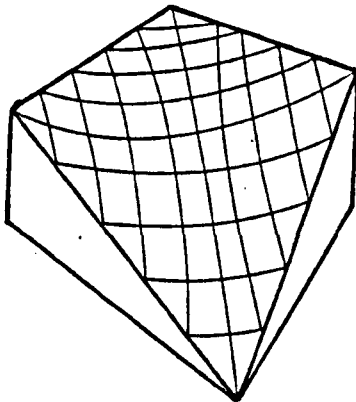


Quadruply threaded net

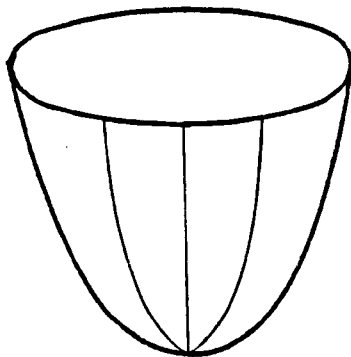


Hexagonal grid

Fig. 1.4 Cable net mesh patterns



Anticlastic
(negative curvature)



Sinclastic
(positive curvature)

Fig. 1.5 Three dimensional cable networks

For those cases where the net has a fine mesh and can be adequately represented by a membrane, considerable computational advantage can be gained, since the number of unknowns remains relatively small. Less time and storage is needed and the computations are reasonably free from round-off errors.

The discrete idealization has the advantage of suiting better the true nature of the cable structure, which is inherently discrete. This idealization must be regarded as a more accurate method than the previous one, because it can be easily applied to structures with complex shape and widely different cable properties, can take into account arbitrary types of support conditions, and permits an accurate treatment of the nonlinear effects.

The laws of mechanics when applied to the discretized structure lead to the formulation of algebraic field equations rather than differential equations. These equations can be categorized as either force or displacement. The force methods are usually difficult to automate for general purpose programs, although when practicable the formulation may lead to a system with fewer equations. The displacement method is generally more suited to computer application, and particularly to nonlinear analyses where geometric nonlinearities are predominant, as indeed is the case with cable supported structures. Some mixed formulations have also been used, particularly when the effects of flexible boundaries are included.

A considerable number of authors have investigated the nonlinear displacement equations that govern the behaviour of discrete cable net structures and have developed different iteration schemes for their solutions. One common approach, despite the demands on computer

storage, is the stiffness formulation of the overall matrix with nonlinear terms taken into account by various iterative schemes. For minimising the computer storage requirements, sparse matrix techniques, bandwidth optimization and frontal methods of solution are widely reported. In addition to these, techniques for reducing the size of the problem by static condensation or substructuring are also available.

Other approaches to the solution of the resultant nonlinear equations are the vector or explicit methods which do not require the formation of an overall stiffness matrix and equilibrium and compatibility conditions are treated separately. Most direct energy minimization methods and the dynamic relaxation method belong to this category. This type of approach offers several advantages. The effort required to formulate the problem is reduced because the energy formulation is simply the scalar sum of the energy contribution of the individual elements. The need for the assembled stiffness matrix of the structure is eliminated and a substantial saving in computer storage is achieved. Also divergence problems of finding solutions to nonlinear simultaneous equations may be more easily avoided.

The inelastic response of the cables has also been considered with different approximations to the nonlinear stress-strain curve; the ultimate carrying capacity of a complete structure being predicted using an incremental load procedure.

Finally, some simplified techniques have also been considered for the preliminary stage of analysis.

1.3. Review of the Literature

This review of the technical literature includes publications on the numerical static solution of single cable, dual cable and cable network structures. Stiffened cable structures as used in suspension bridge type of construction are not included in the review.

Pugsley [237] first considered the changes in cable geometry due to applied load by deriving the differential equations for inextensible cables. He also considered the use of flexibility or influence coefficients [238] for a single cable by dividing the cable into a number of equal segments. Jawerth [150, 151] was the first to carry out work of importance in dual cable structures by presenting a method of analysis that was valid for three different cable systems and the corresponding vertical loads. The resulting equations were solved by iteration. Bandel [10] in 1959, presented an analysis for orthogonal hyperbolic cable nets using a finite element or a finite difference approach and derived a set of linear algebraic equations for vertical displacements of the joints. In reference [11], Bandel presented a procedure for a single cable under three dimensional loading and temperature change by dividing the cable into several straight line segments and using an iteration procedure for the linearised equations.

Michalos and Birnstiel [196] and Jennings [152] have used a force method to analyse the displaced position of a single cable subjected to change in vertical loading. The cable is treated as straight segments between load points. A method of successive approximations is used with the horizontal component of cable tension

and a cable shear assumed as force unknowns, while in each iteration the resulting geometry is calculated and the initial assumptions corrected. An approximate force method was later used by Krishna and Sparks [170], to analyse counterstressed cable structures with vertical ties. Influence coefficients were derived for each tie location, taking into account approximately the nonlinear load deflection characteristics but applying superposition of the upper and lower systems.

Schleyer [267, 268] has published several studies on the analysis of cable structures treating them as continuous systems. The governing partial differential equation was derived with the assumptions that the horizontal displacements are small and that the cables in each direction lie in two orthogonal vertical planes. Schleyer's method was essentially a linearised approach, and his attempt to incorporate the nonlinear effects by means of iterative corrections were not entirely successful.

Zetlin [312, 313] proposed a design procedure for counterstressed cable structures that considered only uniformly distributed loading and vertical displacements. On the assumption that the cables have small sag to span ratios and the loads are normal to the chord of the cable, Morales [208] published a method of solution for cable tensions without the use of cable movements or displacements as parameters. Continuous and the discontinuous theories are developed by Stein [276] for calculating an orthogonal hyperbolic paraboloid net bounded by completely rigid edges; polynomials being used to represent the load system. Eras and Elze [96] presented a finite element method for determining the vertical deflections of an orthogonal net subjected to vertical loads. The linearised equations offered only first order convergence and appeared under certain

conditions to be subject to problems of non-convergence. Krishna [235] used an averaging displacement procedure for the nonlinear terms and improved the convergence of the method.

In 1963 Siev [271] proposed a method for determining the displacements of a general net, including the effect of horizontal displacements and changes in geometry. An iteration procedure was used to solve the linearised nodal equilibrium equations. The same procedure was used for two dimensional networks, neglecting horizontal displacements [272]. Siev also suggested incrementing the loads when the problem is highly nonlinear. Dean and Ugate [92] presented a close form solution for three dimensional nets having two, three, or four sets of cables. The method is based on the two dimensional analogue of the classical string polygon problem, with the assumptions of vertical loading only, and boundaries lying at a constant elevation. Buchanan and Akin [44] extended this closed form solution procedure, to cable nets with arbitrary boundaries using the reflection method. The reflection approach considers any arbitrary shape structural net to be a loaded portion of a larger net with zero boundary elevations. The simultaneous equations are considerably reduced as they are equal to the number of internal boundary or loaded points.

Shore and Bathish [265] replaced the orthogonal cable network by an equivalent thin elastic membrane without shear rigidity. The general governing nonlinear partial integral-differential equation is derived and its solution is obtained by using a Fourier double series. Based on the same approach Gero [124, 125] proposed a closed form solution using a simplified method. Kawagushi and Chin [175], solved the nonlinear differential integral equations of the membrane by finite difference approximation.

Johnson and Brotton [162] applied the Newton Raphson approach for the analysis of three dimensional networks, and expressions for the elemental tangent stiffness matrix were also given. A classification and a comparison of different iterative methods, based on a stiffness formulation, by means of their convergence characteristics was carried out by Poskitt [234]. Correlations between theoretical and experimental results were made and a new method, valid only for certain type of cable structures was also presented.

Mollman [199], treating the system as discrete, derived general nonlinear equations for cable nets in tensor form and developed a theorem concerning the uniqueness of the solution. By introducing certain approximations, he further developed Schleyer's equation for a continuous system. Mollman and Mortensen [200] applied a modified Newton Raphson iteration method for the solution of the governing nonlinear equations. The initial stiffness matrix was kept constant throughout the iterative procedure and inverted only once; tension changes, and hence the geometric stiffness contributions being estimated in order to improve convergence. The nonlinear terms were treated as residual loads. Comparisons have been made with the results obtained from a continuous idealization of a special type of cable net. In another publication, Mollman [202] derived the nonlinear equilibrium equations for a plane prestressed cable structure composed of members of the following three kinds: (a) simple tension members, (b) simple compression members and (c) flexible shallow cable members. The equations are again linearised by using second order terms from each cycle as a load vector in the next cycle of iteration. A Choleski triangular decomposition is

used for the stiffness matrix. A comprehensive treatment of the analysis of cable structures has been given by the same author [205] with many extensions to his previous work. A simple formula for the ultimate carrying capacity of certain cable nets is also presented. Williams [302] considered a cable net in the form of a surface of revolution with radial and circumferential surface, using Mollmohr's nonlinear equation.

Thornton and Birnstiel [282] derived a set of nonlinear simultaneous algebraic equations for a general cable network using a discrete element idealization. Two solution procedures are considered. Firstly the "method of continuity", in which the nonlinear set of simultaneous algebraic equations is transformed into a set of nonlinear differential equations that is numerically integrated. Secondly the "incremental load method", in which the loads are applied incrementally and the equations are solved at each load level by means of an iterative technique. The second method proved more effective in terms of computing time requirements. Jensen [158] used a combination of load increments and iteration for the governing nonlinear equilibrium equations.

An approach to the solution of the deformation of prestressed cable structures which did not require the formation and storage of an overall stiffness matrix was presented by Buchholdt. His theory is based on the minimization of the total potential energy. In his early papers [46, 47, 48, 49, 50], the descent direction towards the minimum is the steepest descent direction. The conjugate gradient direction was presented in [53, 54], and a numerical comparison of five different descent directions was presented in [56]. In all the above cases the step length calculations are made from the minimization of the local total

potential energy's fourth order polynomial with respect to the step length. In 1971 Buchholdt [55] was the first to propose a Taylor expansion scheme for the gradient vector and derived expressions for the 2nd, 3rd and 4th terms. A numerical solution was also presented, but although it was found more stable than the Newton Raphson solution, from the computational point of view the above process is less attractive. A modified Newton Raphson approach with step length control was also developed.

Bogner [29] removed the assumptions that the prestressed forces are sufficient to preclude cable slackening under the application of loads, and presented a general minimization method based on the Fletcher and Powell algorithm. He considered a conventional truss analysis, allowing the cables to go slack and the truss members to buckle. The post-buckled configuration of the structure was traced.

The problem of combined geometric and material nonlinearities in cable structures was first considered by Greenberg [129] who developed an algebraic expression for a representative stress-strain curve to simulate cable behaviour. An averaging stiffness coefficient approach is used to accelerate convergence. Another stress-strain curve was proposed by Jonatowski and Birnstiel [160] who used an iterative procedure to evaluate the unstressed lengths of the cables.

Murray [209] and Murray and Willems [210], have presented a total potential energy minimization procedure using the Fletcher and Reeves conjugate gradient algorithm, and the Fletcher and Powell variable metric method, for the elastic and inelastic analysis of tension structures. The Ramberg and Osgood [241] stress-strain curve and the one proposed by Greenberg were studied and compared.

Saafan [253] also considered the effects of nonlinear stress-strain properties in cable structures. He proposed a scheme similar to that used by Haug and Powell [135], which applied only a fraction of the residual loads in each Newton Raphson iteration.

In the work proposed by Avent [9], a field approach to nonlinear analysis of arbitrary net systems is used by formulating a walk-through technique. Tottenham and Khan [287] have compared a continuous approach, derived from first principles by Williams [302], and a discrete approach. The error involved in treating a physically discrete system as an equivalent continuous system was found to be small, particularly for nets with fine meshes. Buchanan [45] presented a continuous approach for a single cable. The governing differential equations are solved by a perturbation technique as proposed by Van Dyke [293].

Dynamic relaxation has also been used for the solution of the nonlinear equations of tension structures. Day and Bunce [91] used an approximate upper bound for the time increment, while the optimum time coefficient was obtained from a trial run. Barnes [13] derived an approximate expression for evaluating close bounds to the critical time interval. The masses are then adjusted so as to give the same critical time in each node. Membrane cladding elements are also considered. The same method is also used to cope with member slackening and buckling of the membrane cladding [43]. A force transfer procedure is utilized for a special type of cable structures. In reference [17] comparisons were given using viscous and kinetic damping procedures.

Mollman [201] and Greenberg [130] have considered the loads applied along the cables, but assumed the cable to take the shape of a shallow parabola, thus limiting the application only to cases when it is justifiable to assume the loads to be applied uniformly and laterally to the cables. Reference [114] examines the difference in the forces and displacements obtained assuming the loads are applied to the joints rather than to the cables. Buchholdt and McMillan [57] used the conjugate gradient minimization procedure for the analysis of vertically and laterally loaded cables. The total potential energy was expressed in this case as an eighth order polynomial with respect to the step length. An exact analytical general solution to the static response of a single cable under arbitrary loading has been given by Irvine and Sinclair [147]. Explicit expressions for the tension within the cable and the displacements are derived as functions of a single independent variable, the Lagrangian coordinate, associated with the unstrained profile.

Braga and Care [35] presented a method of analysis taking into account the actual loads as applied along the cables. A method is described for the distribution of the loading to the nodes. The nodal loads then are updated at each iteration according to the actual deformation. Burtley and Harvey [64] also examined the effect of a uniformly distributed load along the cables. Foster and Baufait [109] presented the effect of precast panels on the behaviour of cable networks.

Epstein and Tene [95], presented a method of solution based on a general approach for solving nonlinear problems in structural mechanics as presented by Budiansky [43]. The method provides

exact equilibrium equations valid for arbitrary large strains and displacements and makes use of exact kinematic equations and a general nonlinear stress-strain relationship approximated by a polynomial. The method, however, made large demands on computer storage. Argyris [7] developed a modified derivation of the complete element stiffness matrix, particularly adopted for the nonlinear analysis of prestressed networks. Krishna [173] presented various iterative schemes and compared their efficiency with reference to their application to cable net problems.

Kar and Okazaki [166] used a Newton Raphson type of solution for highly nonlinear cable net problems. The new iterative technique presented, represents an effort to scale down the over-estimated displacements by the ratio of the largest applied load, at any cycle of iteration, to its corresponding equilibrium load, calculated on the basis of the linearised solution. The efficiency of the method is demonstrated by comparisons with other iterative methods. They also suggested that for highly nonlinear cases, incrementing the loads may improve the rate of convergence.

Several investigators have considered the effect of flexible boundaries on cable structures. Mollman [206] presented a study on this problem using two methods: (a) the displacement method applied to the complete structure and (b) a mixed method in which the horizontal components of the cable forces and vertical deflections in the net are used as unknowns together with displacements of the boundary structure. Buchholdt et al [58] applied the conjugate gradient method to a similar problem. The inclusion of flexible boundaries increased the condition number of equations and a scaling technique was used to accelerate the convergence. Mixed formulations were also used by Kawamata and Magara [177] and

Saitoh and Kurok [254]. The basic equations are derived from the stationary conditions of the total energy of the function expressed in terms of the nodal displacements and the member forces. Asplaud [8] described a force method to analyse orthogonal nets.

Urelius and Fowler [291] examined the varying influence of design parameters on the overall behaviour of a cable truss. They also compared the accuracy of approximate design equations, previously proposed by Zetlin, with that of a stiffeners Newton Raphson type solution procedure. Sand and Hagiescu [255] examined the influence of the characteristics of boundary structures on the forces and displacements in counterstressed cable structures. Noesgen [215] and Gero [126] studied the behaviour of large cable network structures under various combinations of design parameters by modelling them to similar networks with fewer cables. Buchholdt [60] also examined the same problem. Krishna and Natarajan [172] presented a study of the influence of nonlinearity of vertical and lateral deformations hyperbolic paraboloid nets.

A development of the approximate solution given by Schleyer [268] and Mollman [201] has been described by Krishna and Agrawal [174]. The method can be applied to a single cable, cable trusses and cable networks of restricted shape. Bhupinder and Bhusham [24] proposed a continuum method for anisotropic cable networks.

Jonatowski [161] presented a numerical procedure for determining the deformation response of suspension structures as the the loading is increased from the initial state to the ultimate carrying capacity of the structure. The nonlinear stress-strain relation of Jonatowski and Birnstiel [160] is used. The cables are allowed to go slack and expressions for the stress-strain relation-

ships are derived as the cable unloads and reloads during the application of loading.

Aizaiwa et al [2,280] first applied the static perturbation technique for the solution of the nonlinear equations of cable structures. The derivation of the characteristic equations of the perturbation method with respect to the load increment parameter λ is outlined. The load is applied in one increment and no iteration correction procedure is performed. A comparison was also carried out with the Newton Raphson approach and it was suggested that the perturbation method should be superior to the Newton Raphson approach from the standpoint of computational time, although these conclusions were not substantiated with numerical examples.

Finally Foster and Sandberg [292] discussed the peculiarities of stiffness matrices arising during the nonlinear solution process of cable structures. They investigated cases where in addition to large off-diagonal terms, the geometric stiffness approach can result in the generation of negative diagonal terms. In those cases the Choleski square root method for inverting the stiffness matrix cannot be used since it is restricted to symmetric positive definite matrices. The second Choleski algorithm, the Grout reduction, which is mathematically similar to the Gauss elimination method, was recommended. They also found that for relatively small problems the Gauss elimination method is more practical and accurate, while for larger problems the Grout reduction was more advantageous.

In this thesis nonlinear methods of analysis have been developed and compared for the static solution of cable supported structures with varying degrees of freedom. A number of conjugate gradient methods, with one and two dimensional linear search and linearized algorithms without linear search, have been used. Relaxation methods have also been developed and compared. The dynamic relaxation method has been used in three different forms : with the iteration parameters being evaluated "a priori", with automatic adjustment of the iteration parameters, and with the incorporation of kinetic energy damping instead of viscous damping. A number of methods, for the estimation of the minimum and maximum eigenvalue of the stiffness matrix have been also compared and the best one has been employed for the "a priori" evaluation of the dynamic relaxation iteration parameters.

A combined dynamic relaxation and conjugate gradient algorithm has been developed and the efficiency of the successive overrelaxation method with and without automatic evaluation of the relaxation parameter has been studied for problems with stiffness matrices not possessing property "A". Stiffness methods, in conjunction with the Newton Raphson iterative algorithm, have also been included in a general comparative study for small and large problems. The effects of nonlinear stress-strain relationships and slackening of cable members have been studied and the efficiencies of two different methods of solution, namely the stiffness approach with Newton Raphson

iterations and the conjugate gradient algorithm with one dimensional linear search, have been compared.

CHAPTER 2
ENERGY SEARCH APPROACH

2.1. Energy Formulations

The energy search approach to structural analysis is based upon the application of mathematical programming methods to appropriate energy functions. The structural analysis problem can be envisaged as the search for a stationary point for the energy function of the structure.

There are three commonly used energy formulations of the structural analysis problem ; each one being associated with a corresponding energy principle. The displacement method is related to the principle of the total potential energy, the force method is equivalent to the complementary energy approach, and the mixed force-displacement formulation to the Reissner energy principle.

(i) The principle of stationary potential energy states that of all geometrically admissible sets of displacements satisfying the boundary conditions, that which makes the total potential energy, π , stationary satisfies the equilibrium conditions and is the actual displacement state x^* . It follows that

$$\left. \frac{\partial \pi}{\partial x_i} \right|_{x = x^*} = 0 \quad i = 1, 2, \dots, n \quad (2.1)$$

where
$$\pi = U - \sum_{i=1}^n P_i x_i \quad (2.2)$$

U = the strain energy in terms of displacements.

Furthermore, if

$$\pi(x^*) < \pi(x) \quad (2.3)$$

for any virtual displacement from x^* , then the associated equilibrium position is stable. The potential energy formulation is a minimum principle.

(ii) The principle of complementary energy states that of all force sets P_k that satisfy the equations of equilibrium and the boundary conditions, that which makes the complementary energy, π^* , stationary satisfies the compatibility conditions. It follows that

$$\left. \frac{\partial \pi^*}{\partial P_k} \right|_{P = P^*} = 0 \quad k = 1, 2, \dots, m \quad (2.4)$$

where

$$\pi^* = -V + \sum_{k=1}^m P_k x_k \quad (2.5)$$

V = the strain energy in terms of the member loads P_k .

Furthermore, if

$$\pi^*(P^*) > \pi(P) \quad (2.6)$$

for any virtual displacement from x^* , then the associated equilibrium position is stable. The complementary energy formulation is a maximum principle.

(iii) The Reissner's principle of stationary energy states that among all states of stress and displacement that satisfy the equilibrium equations and the force-displacement relations,

the actual one makes the Reissner energy, J , stationary. It follows that

$$\left. \frac{\partial J}{\partial z_i} \right|_{z = z^*} = 0 \quad i = 1, 2, \dots, \ell \quad (2.7)$$

Reissner's energy function is formulated in terms of forces and displacements and is a stationary principle.

First to implement the energy search approach for the solution of structural problems was the Case Western University group. An exploratory study was carried out in References [28, 189]. In References [187, 188] studies for three dimensional structures that can be represented by straight truss and frame members are reported. Schmit et al [262] applied the energy approach to plate and shell type of structures, where energy search methods based on gradient minimization algorithms were shown to be computationally competitive with conventional stiffness approaches.

For geometrically nonlinear problems the formulation of the total energy is usually simpler if the displacement method is used, for materially nonlinear problems if the force method is used, and for combined nonlinearities if a mixed method is used. In other words, the Reissner's principle should be more appropriate for problems with material and geometric nonlinearities. But, since it is neither a maximum nor a minimum, an additional step is required in order to apply the standard methods of optimization : The calculation of the so-called residual function

$$R(x) = \sum_{i=1}^n \left(\frac{\partial J}{\partial x_i} \right)^2 \quad (2.8)$$

which has a minimum of zero at the solution x^* .

In the case of the analysis of cable structures with combined nonlinearity, it is felt that since only axial member forces need to be considered, the additional complication of applying the Reissner's energy principle can not be justified. Thus the principle of the minimum potential energy will be considered herein.

2.2. Unconstrained Minimization

An unconstrained function minimization technique is an algorithm for choosing test points x , not obeying any constraint requirements, which provides information about the function $F(x)$ and the location of its minimum. Minimization techniques are divisible into two general classes according to the approach taken in the selection of test points. In the first category, the nonsequential search, a complete set of test points is chosen prior to the initiation of testing. Each trial solution is compared with the "best" obtained up to that time and there is a strategy for determining what the next trial solution will be. One approach is to choose the test points at random according to an n -dimensional probability density function [39]. A second approach is the so called factorial technique [31] where the test points are chosen in a specific geometric pattern. Attempts have been made to place the selection of a set of test points on a mathematical rather than an intuitive or random basis [179].

The second category, the sequential search, is appropriate for continuous and differentiable analytic functions. The sequential techniques seek to move from a given point x_i a distance t along a direction ϕ_i using the recursive relations

$$x_{i+1} = x_i + t_i \phi_i \quad (2.9)$$

in such a way that the value of the function F at the new point x_{i+1} is reduced :

$$F(x_{i+1}) < F(x_i)$$

Direct search methods are those which do not require the explicit evaluation of any partial derivatives of the functions and rely only on values of the objective function together with information gained from earlier iterations. Gradient methods on the other hand are those which select the direction ϕ_i using values of the partial derivatives of the objective function with respect to the independent variables, as well as values of the objective function itself and information gained from earlier iterations.

Many of the direct search methods lack convergence proofs and are subjected to premature convergence. However in structural problems, where derivatives of the objective function are easily evaluated, gradient methods have predominantly been used .

"Gradient" suggests the idea of the direction of fastest improvement towards a solution since the gradient vector points in the direction in which the function increases or decreases most rapidly.

A third category of unconstrained minimization techniques are those which utilize the second derivative of the object function. Among these methods, the Newton Raphson procedure and the quasi-Newton techniques are most often used.

Given a function $F(x)$, for which all the first partial derivatives $\frac{\partial F}{\partial x_i}$, $i = 1, \dots, n$, exist at all points, a necessary condition for a minimum to exist is

$$\frac{\partial F}{\partial x_1} = \frac{\partial F}{\partial x_2} = \dots = \frac{\partial F}{\partial x_i} = 0 \quad (2.10)$$

A sufficient condition for a point satisfying equations (2.10) to be a minimum is that all the second partial derivatives

$\frac{\partial^2 F}{\partial x_j \partial x_k}$ ($j, k = 1, \dots, n$) exist at this point and that $D_i > 0$

for $i = 1, 2, \dots, n$, where

$$D_i = \begin{vmatrix} \frac{\partial^2 F}{\partial x_1^2} & \frac{\partial^2 F}{\partial x_1 \partial x_2} & \dots & \frac{\partial^2 F}{\partial x_1 \partial x_n} \\ \dots & \dots & \dots & \dots \\ \frac{\partial^2 F}{\partial x_n \partial x_1} & \dots & \dots & \frac{\partial^2 F}{\partial x_n^2} \end{vmatrix} \quad (2.11)$$

i.e. the principal minors of the matrix of second partial derivatives must all be positive [198].

A convenient model for representing simple functions $F(x)$ with only two independent variables, is to represent the function graphically using Cartesian co-ordinates in a three dimensional space. In this three dimensional model such geometric ideas as tangent, gradient, curvature and perpendicularity are easily

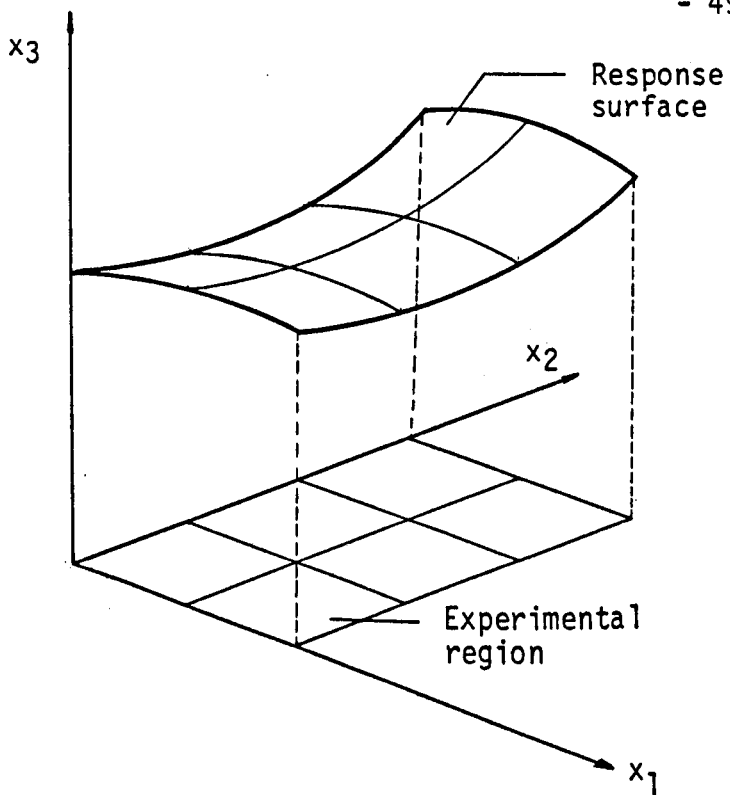


Fig. 2.1. Isometric representation of a response surface

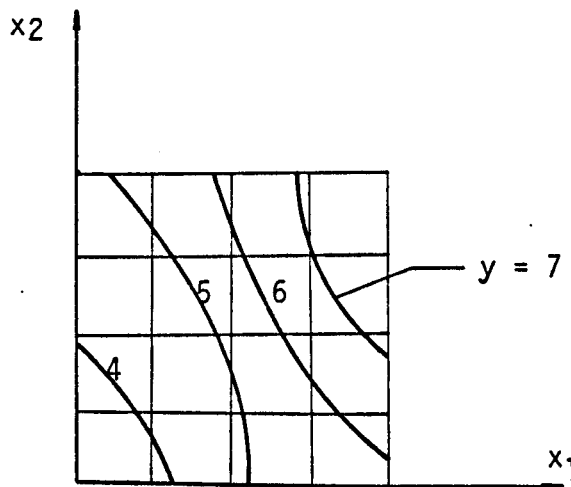


Fig. 2.2. Contour representation of a response surface

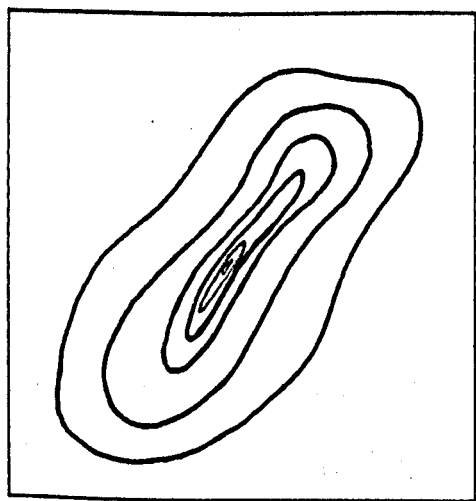


Fig. 2.3. Unimodal Function

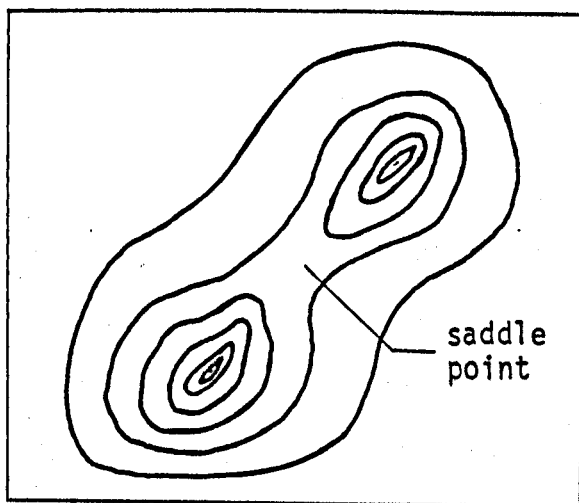


Fig. 2.4. Bimodal Function

visualised. Suppose $y = y(x_1, x_2)$, then points y_i form a surface called the "response surface" (this name originated from the studies of Biologists and Statisticians for whom the criterion y is often the response of a living organism to environmental factors x_1 and x_2). The response surface of Fig. 2.1 is termed two dimensional because only two co-ordinates are needed to specify a point on it. Figure 2.2 shows another way of depicting a response surface, by means of contour lines through points of equal values of the function y . Figure 2.3 shows a unimodal function where there is only one hump in the surface to be explored, while Fig. 2.4 shows a bimodal function with two optima and a saddle point.

2.3. Assumptions

For the nonlinear elastic analysis of cable structures the following assumptions have been made :

- a. The cables are straight lines between nodes.
- b. Structural members are of uniform cross section.
- c. The external forces are applied at the points of intersection of the cables and do not vary during the process of deformation, either in magnitude or in direction.
- d. The system consists of cables or cables and struts with no flexural or torsional rigidity.
- e. The cables cannot resist compression.
- f. The elastic extensions of the cables are small compared with their length.

- g. The supports are fixed.
- h. The stress-strain relationship is linear.

In Chapter 10, where ultimate load studies are carried out, assumption h is excluded.

2.4. The Total Potential Energy

The total potential energy of any body is given by

$$\pi = U + V \quad (2.12)$$

where U is the strain energy or potential energy of the internal forces, and V is the potential energy of the external forces acting on the body.

For an arbitrary unstiffened cable system

$$U = \sum_1^m U_{jn} \quad (2.13)$$

where U_{jn} is the strain energy associated with segment jn and m is the total number of cable segments, while

$$V = \sum_1^N \sum_1^{NDF} F_{in} x_{in} \quad (2.14)$$

with F_{in} is the external force at node n in direction i ,

x_{in} is the displacement of node n in direction i ,

N is the total number of interior nodes in the system,

NDF is the number of degrees of freedom

The strain energy of a cable segment can be expressed in terms of the total stress and total strain as follows :

$$\begin{aligned}
 U_{jn} &= \int \int_{\text{vol } \epsilon} \sigma d\epsilon \\
 &= \frac{1}{2} \int_0^L \sigma \epsilon dx
 \end{aligned}
 \tag{2.15}$$

with $\epsilon = \epsilon^0 + \epsilon^a$, where ϵ^0 is the strain before the application of the incremental force, P, and ϵ^a is the additional strain after the application of the incremental force.

Under the assumption (h), equation (2.15) becomes

$$\begin{aligned}
 U_{jn} &= \frac{1}{2} AE \int_0^L \epsilon^2 dx \\
 &= \frac{1}{2} AE \int_0^L (\epsilon^0 + \epsilon^a)^2 dx \\
 &= \frac{1}{2} AEL (\epsilon^0)^2 + AE\epsilon^0 \int_0^L \epsilon^a dx + \frac{1}{2} AE \int_0^L (\epsilon^a)^2 dx
 \end{aligned}
 \tag{2.16}$$

The first term on the right hand side of equation (2.16) is the strain energy present prior to imposition of an additional disturbance. The second term depends on the initial stress and yields the geometric stiffness. The third term depends on the additional strain due to the incremental force P, and is no different from the conventional small deflection case, yielding the elastic stiffness.

Under the assumption (f), equation (2.16) can be further modified as follows

$$\begin{aligned}
 U_{jn} &= \frac{1}{2} \frac{AE}{L} (e^0)^2 + P^0 e^a + \frac{1}{2} \frac{AE}{L} (e^a)^2 \\
 &= U^0 + P^0 e^a + U^a
 \end{aligned}
 \tag{2.18}$$

where e^0 is the extension and L the initial length of member jn before the application of the incremental force P , and e^a is the additional extension (from the initial state) after the application of the load increment.

2.5. The Gradient Vector

The gradient vector of the total potential energy is of great importance not only to the gradient methods but virtually to any iterative nonlinear solution procedure. It represents the out of balance forces arising from the difference between the applied nodal load and the vector sum of the internal forces in the members intersecting at the same joint.

From equation (2.12) the partial derivative of the total potential energy with respect to the displacement at the n^{th} node in the i direction is

$$\frac{\partial \pi}{\partial x_{in}} = \sum^k \frac{\partial U_{jn}}{\partial x_{in}} - F_{in}
 \tag{2.19}$$

with k being the number of segments connected directly to node n .

Using the strain energy expression of equation (2.18), equation (2.19) can be written

$$\begin{aligned} \frac{\partial \pi}{\partial x_{in}} &= \sum^k \left(p^0 \frac{\partial e_{jn}}{\partial x_{in}} + \frac{AE}{L} e_{jn} \frac{\partial e_{jn}}{\partial x_{in}} \right) - F_{in} \\ &= \sum^k (p^0 + \bar{P}) \frac{\partial e_{jn}}{\partial x_{in}} - F_{in} \quad (2.20) \\ &= \sum^k P_{jn} \frac{\partial e_{jn}}{\partial x_{in}} - F_{in} \end{aligned}$$

in which P_{jn} is the total force in cable segment j-n after the application of the load increment, and e_{jn} is the elongation of the cable segment from the initial or prestress configuration. Note, that for simplicity, the superscript a has been omitted from e in expression (2.20) and hereafter.

The elongation e_{jn} can be expressed as

$$e_{jn} = [L_{jn}^2 + h(x)]^{\frac{1}{2}} - L_{jn} \quad (2.21)$$

in which

$$h(x) = \sum_{i=1}^{NDF} [(2(X_{in} - x_{ij}) + (x_{in} - x_{ij})) (x_{in} - x_{ij})] \quad (2.22)$$

where X_{in} and x_{in} denote respectively the initial co-ordinate and the displacement of joint n.

Differentiating equation (2.21) with respect to x_{in} gives

$$\frac{\partial e_{jn}}{\partial x_{in}} = \frac{1}{2[L_{jn}^2 + h(x)]^{\frac{1}{2}}} \cdot \frac{\partial h(x)}{\partial (x_{in} - x_{ij})} \cdot \frac{\partial (x_{in} - x_{ij})}{\partial x_{in}} \quad (2.23)$$

From equation (2.22)

$$\frac{\partial h(x)}{\partial (x_{in} - x_{ij})} = 2(X_{in} - X_{ij}) + 2(x_{in} - x_{ij}) \quad (2.24)$$

Then substituting equation (2.24) into equation (2.23)

$$\frac{\partial e_{jn}}{\partial x_{in}} = \frac{1}{(L_{jn} + e_{jn})} \left[(X_{in} - X_{ij}) + (x_{in} - x_{ij}) \right] \frac{\partial (x_{in} - x_{ij})}{\partial x_{in}} \quad (2.25)$$

and finally substituting the above equation into equation (2.20),
the gradient vector becomes

$$\frac{\partial \pi}{\partial x_{in}} = \sum^k \frac{P_{jn} [(X_{in} - X_{ij}) + (x_{in} - x_{ij})]}{(L_{jn} + e_{jn})} - F_{in} \quad (2.26)$$

and correspondingly

$$\frac{\partial \pi}{\partial x_{ij}} = - \sum^k \frac{P_{in} [(x_{in} - X_{ij}) + (x_{in} - x_{ij})]}{(L_{jn} + e_{jn})} - F_{ij} \quad (2.27)$$

2.6. The Matrix of the Second Partial Derivatives

Let the gradient vector of the total potential energy at joint j, in the i^{th} direction and at a position Δ in displacement space be

$$\left(\frac{\partial \pi}{\partial x_{ij}} \right)_{\Delta}$$

with the corresponding gradient vector at position $\Delta + d\Delta$ in displacement space :

$$\left(\frac{\partial \pi}{\partial x_{ij}}\right)_{\Delta + d\Delta}$$

Expanding the last vector by Taylors theorem we obtain

$$\begin{aligned} \left(\frac{\partial \pi}{\partial x_{ij}}\right)_{\Delta + d\Delta} &= \left(\frac{\partial \pi}{\partial x_{ij}}\right)_{\Delta} + \left[\frac{\partial^2 \pi}{\partial x_r \partial x_{ij}}\right]_{\Delta} \cdot (dx_r) \\ &+ \frac{1}{2!} \left[\frac{\partial^3 \pi}{\partial x_s \partial x_r \partial x_{ij}}\right]_{\Delta} \cdot (dx_s)^T \cdot (dx_r) \quad (2.28) \\ &+ \frac{1}{3!} \left[\frac{\partial^4 \pi}{\partial x_k \partial x_s \partial x_r \partial x_{ij}}\right]_{\Delta} \cdot (dx_k) \cdot (dx_s)^T \cdot (dx_r) \\ &+ \dots \end{aligned}$$

Since the potential energy of the applied load system is linear in x , the change in the gradient vector due to an incremental change in the displacement space is given by

$$\begin{aligned} \left(\frac{\partial \pi}{\partial x_{ij}}\right)_{\Delta + d\Delta} &= \left(\frac{\partial \pi}{\partial x_{ij}}\right)_{\Delta} + \left[\frac{\partial^2 U}{\partial x_r + \partial x_{ij}}\right] \cdot (dx_r) \quad (2.29) \\ &+ \dots \end{aligned}$$

Assuming the changes in displacements to be so small that their higher powers are negligible, equation (2.29) may be written as

$$\left(\frac{\partial \pi}{\partial x_{ij}}\right)_{\Delta + d\Delta} - \left(\frac{\partial \pi}{\partial x_{ij}}\right)_{\Delta} = \left[\frac{\partial^2 U}{\partial x_r \partial x_{ij}}\right] (dx_r) \quad (2.30)$$

Since the vector of the left hand side of equation (2.30) represents the change in residual force components due to a change dx_r in displacement space, the matrix of the second

partial derivatives of the strain energy can be identified as the stiffness matrix of the assembly.

Differentiating equation (2.20) with respect to the displacement vector x_r , we have

$$\frac{\partial^2 U_{jn}}{\partial x_{in} \partial x_r} = \sum^k \left(\frac{\partial P_{jn}}{\partial e_{jn}} \cdot \frac{\partial e_{jn}}{\partial x_{in}} \cdot \frac{\partial e_{jn}}{\partial x_r} + P_{jn} \frac{\partial^2 e_{jn}}{\partial x_{in} \partial x_r} \right) \quad (2.31)$$

We now want to find expressions for the following terms in equation (2.31)

$$\frac{\partial e_{jn}}{\partial x_{in}}, \quad \frac{\partial^2 e_{jn}}{\partial x_{in} \partial x_r} \quad \text{and} \quad \frac{\partial P_{jn}}{\partial e_{jn}}$$

The first derivative of the elongation e_{jn} is given by equation (2.25), which can be written in matrix form as follows

$$\begin{bmatrix} \frac{\partial e_{jn}}{\partial x_{1j}} \\ \frac{\partial e_{jn}}{\partial x_{2j}} \\ \frac{\partial e_{jn}}{\partial x_{3j}} \\ \frac{\partial e_{jn}}{\partial x_{1n}} \\ \frac{\partial e_{jn}}{\partial x_{2n}} \\ \frac{\partial e_{jn}}{\partial x_{3n}} \end{bmatrix} = \frac{1}{L_{jn} + e_{jn}} \begin{bmatrix} - (X_1 + x_1) \\ - (X_2 + x_2) \\ - (X_3 + x_3) \\ + (X_1 + x_1) \\ + (X_2 + x_2) \\ + (X_3 + x_3) \end{bmatrix} = \begin{bmatrix} -c \\ +c \end{bmatrix} \quad (2.32)$$

where $X_i = X_{in} - X_{ij}$

$$x_i = x_{in} - x_{ij}$$

Differentiating now equation (2.25) with respect to x_r we obtain the expression

$$\frac{\partial e_{jn}}{\partial x_r} \cdot \frac{\partial e_{jn}}{\partial x_{in}} + (L_{jn} + e_{jn}) \frac{\partial^2 e_{jn}}{\partial x_r \partial x_{in}} = \frac{\partial (x_{in} - x_{ij})}{\partial x_r} \cdot \frac{\partial (x_{in} - x_{ij})}{\partial x_{in}} \quad (2.33)$$

which gives

$$\frac{\partial^2 e_{jn}}{\partial x_r \partial x_{in}} = \frac{1}{(L_{jn} + e_{jn})} \left(\frac{\partial (x_{jn} - x_{ij})}{\partial x_r} \cdot \frac{\partial (x_{in} - x_{ij})}{\partial x_{in}} - \frac{\partial e_{jn}}{\partial x_r} \cdot \frac{\partial e_{jn}}{\partial x_{in}} \right) \quad (2.34)$$

Equation (2.34) may be written in matrix form as follows :

$$\frac{\partial^2 e_{jn}}{\partial x_r \partial x_{in}} = \frac{1}{(L_{jn} + e_{jn})} \begin{bmatrix} 1 & 0 & 0 & -1 & 0 & 0 \\ 0 & 1 & 0 & 0 & -1 & 0 \\ 0 & 0 & 1 & 0 & 0 & -1 \\ -1 & 0 & 0 & 1 & 0 & 0 \\ 0 & -1 & 0 & 0 & 1 & 0 \\ 0 & 0 & -1 & 0 & 0 & 1 \end{bmatrix} - \frac{1}{(L_{jn} + e_{jn})^3} \begin{bmatrix} -(X_1 + x_1) \\ -(X_2 + x_2) \\ -(X_3 + x_3) \\ (X_1 + x_1) \\ (X_2 + x_2) \\ (X_3 + x_3) \end{bmatrix} \begin{bmatrix} -(X_1 + x_1) \\ -(X_2 + x_2) \\ -(X_3 + x_3) \\ (X_1 + x_1) \\ (X_2 + x_2) \\ (X_3 + x_3) \end{bmatrix} \quad (2.35)$$

$$= \frac{1}{(L_{jn} + e_{jn})} \begin{bmatrix} I & -I \\ -I & I \end{bmatrix} - \frac{1}{(L_{jn} + e_{jn})^3} \begin{bmatrix} CC^T & -CC^T \\ -CC^T & CC^T \end{bmatrix}$$

And from linear stress-strain relationships :

$$\frac{\partial P_{jn}}{\partial e_{jn}} = \frac{EA}{(L_{jn} + e_{jn})} \quad (2.36)$$

Substituting now equations (2.32), (2.35) and (2.36) into equation (2.31) a final expression for the stiffness matrix may be obtained :

$$\frac{\partial^2 U_{jx}}{\partial x_{in} \partial x_r} = \frac{EA}{(L_{jn} + e_{jn})} \begin{bmatrix} CC^T & -CC^T \\ -CC^T & CC^T \end{bmatrix} + \frac{P_{jn}}{(L_{jn} + e_{jn})} \begin{bmatrix} (I - CC^T) - (I - CC^T) \\ -(I - CC^T) & (I - CC^T) \end{bmatrix} \quad (2.37)$$

The first term of the right hand side of the above expression is the elastic stiffness matrix according to linear theory and the second term is the geometric stiffness matrix of the pin-jointed member jn .

2.7. Scaling Effects on Iterative Methods

Consider the system of linear equations

$$Ax = b \quad (2.38)$$

the solution of which is given by $x = A^{-1}b$. The components of x are functions of the given components of A and b . Consider now the effect on x of small changes of A and b . If certain types of small relative changes of the components of A and b give rise to relatively large changes of the components of x , then the system is said to be ill-conditioned. Ill-conditioning

This number may be used as a measure for the ill-conditioning of a matrix. In a general way it may be said that the larger the condition number, the more ill-conditioned the system of equations.

The characteristic invariants of a space for a linear problem are the eigenvalues of the stiffness matrix. These are proportional to the square of the principal axes of a constant energy ellipsoid in the space. The more the condition number approaches the optimum value the more the energy contours become spherical. It is clear geometrically that a n -dimensional sphere is the optimal function space, since one gradient move from any point would be adequate to reach the minimum (Figure 2.5a). In general the number p is also a measure of the deviation of the function space from optimal. A large condition number means a narrow energy ellipsoid (Figure 2.5b).

It has been shown by Hestenes and Stiefel [137] that the accumulation of round-off errors and the eventual instability of the conjugate gradient method, depends on the ellipticity of the total potential energy function. The round-off errors cause the sequences of vectors p_i and g_i (ref : Chapter 3) to deviate from the orthogonality and A -orthogonality conditions, which in turn slow down the convergence.

An improvement in the efficiency of gradient methods can be achieved not by finding better search directions but rather by transforming the function space itself, in an effort to decrease the condition number. There are two commonly used ways of improving the condition number :

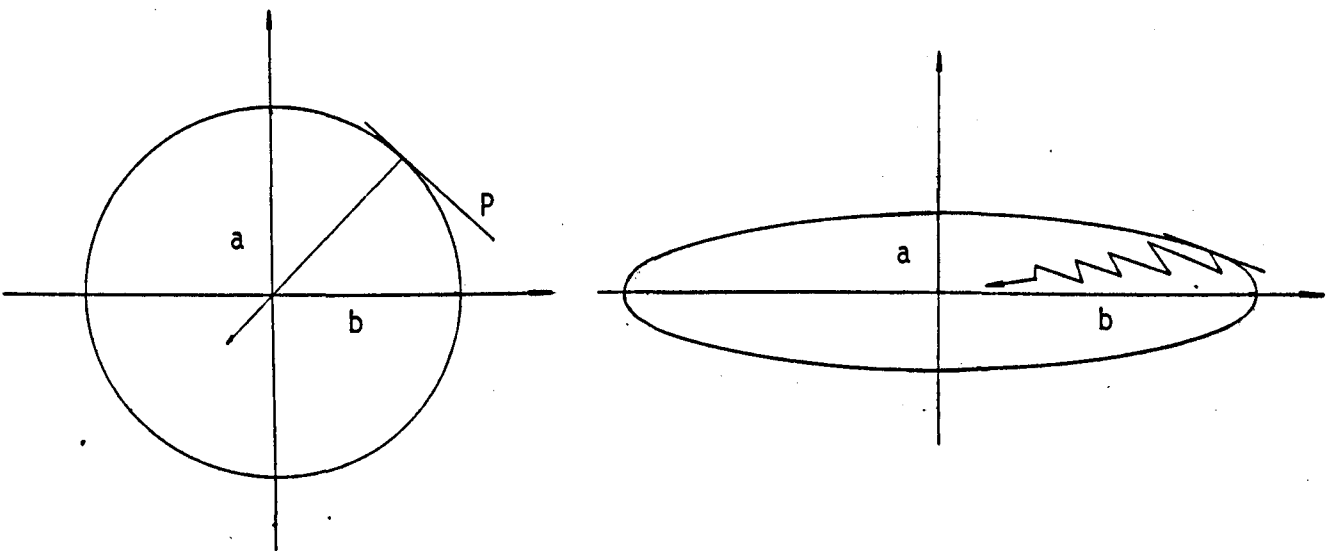
is therefore an inherent property of the system of linear equations and is independent of the method used for the numerical solution.

Ill-conditioned systems can occur when large off-diagonal coefficients exist in the stiffness matrix. This could happen when there are large variations in the elastic modulus or other constants from element to element or when variables are intrinsically different as in the case of mixed forces and moments or displacements and rotations. An inherent ill-conditioning in cable structures has already been discussed in Section 1.1, where due to the peculiar tension distribution big differences in the diagonal terms may occur ; a problem which becomes more acute with the flatness of the network. Also more irregular grids and more variables lead to ill-conditioning, while finer grids and more elements connected to the same node lead to better conditioned systems.

While in the elimination methods, poorly conditioned systems can produce round-off errors without affecting the convergence of the method, in iterative methods the rounding-off errors produced by ill-conditioning can seriously affect convergence.

For a symmetric positive definite matrix the spectral condition number p is defined as the ratio between the largest and the smallest eigenvalue of the matrix

$$p = \frac{\lambda_{\max}}{\lambda_{\min}}$$



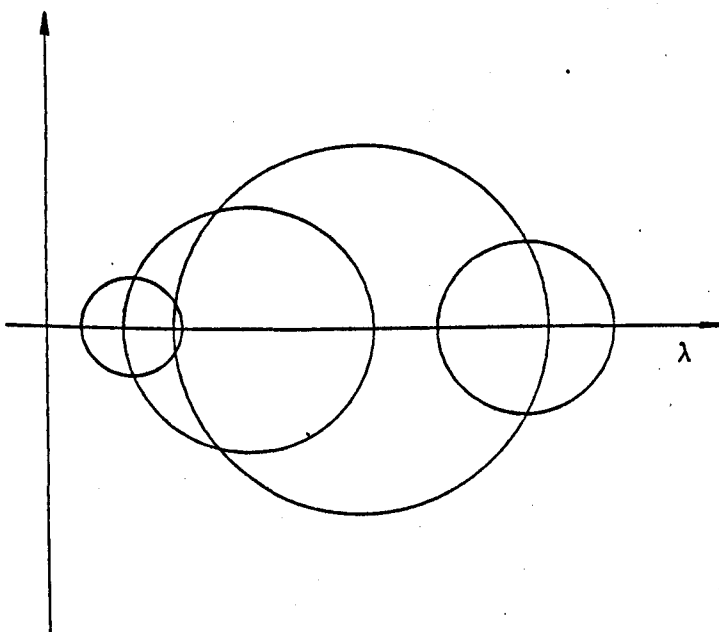
(a) A two dimensional spherical contour

$$b/a = \frac{\lambda_{\max}}{\lambda_{\min}} = 1$$

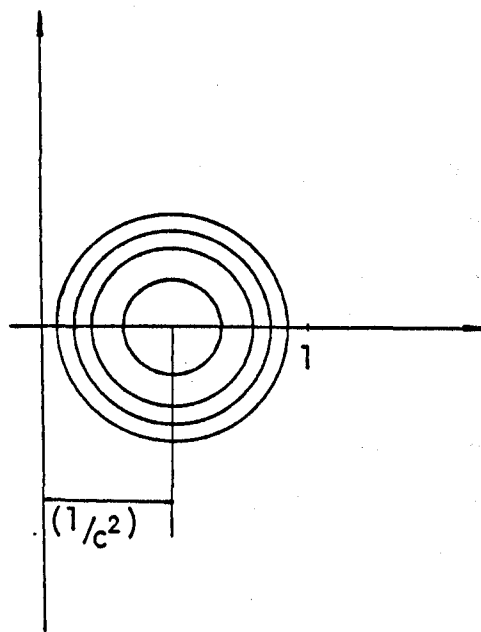
(b) A two dimensional ellipsoid

$$b/a = \frac{\lambda_{\max}}{\lambda_{\min}} > 1$$

Fig. 2.5.



(a) Gerschgorin discs for an unscaled matrix



(b) Gerschgorin discs for a scaled matrix

Fig. 2.6.

- (a) To replace the system of equations by another system with the same solution but with a coefficient matrix A of smaller p -condition number.
- (b) To replace the vector of unknowns x by another vector \bar{x}

$$x = w \cdot \bar{x} \quad (2.39)$$

The first technique, as proposed by Rutishauser [94], is used in Chapter 6 for the conjugate gradient - Tchebycheff method. In practice, finding the optimal matrix w for the second technique is difficult [22]. Several authors [180, 304, 98] have suggested different scaling matrices w . Evans [98,100] preconditioning scheme has been used successfully by Jennings and Malik [157]. It involves the transformation of the original system of equation (2.38) into the system

$$By = d \quad (2.40)$$

where $B = (I - \omega L)^{-1} A (I - \omega L)^{-T}$

$$d = (I - \omega L)^{-1} b \quad (2.41)$$

$$(I - \omega L)^T x = y$$

$$W = (I - \omega L)^{-1}$$

with $A = I - L - L^T$ and ω being an accelerator factor. The disadvantage of the method is that matrix w is not diagonal, and when applied to cable structures where the overall stiffness matrix is not explicitly formulated and stored, a storage scheme should be provided to accommodate the scaling matrix. On the

other hand when the scaling matrix is diagonal the computations are simplified and only one vector space need to be stored.

Gerschgorin's bound theorem guarantees that every eigenvalue λ_i lies in at least one of the discs centered at a_{ii}

and of radii $R_i = \sum_{j \neq i} \|a_{ij}\|$, with a_{ij} being the elements of the stiffness matrix. So the circles of Figure 2.6 indicate the possible range of λ_i . In the unscaled case, the circles are not only large but also centered at widely different points. It is possible to adjust the Gerschgorin disc, for row i of the stiffness matrix, by using either a scaling or a transformation operation which modifies the elements in row and column i .

The scaling technique consists of centering all the discs at a centre point of the λ axis, while the transformation technique consists of reducing the radius R_i of the discs to fit into predetermined bounds by performing the multiplication $A^* = BAB^T$, where B is an off-diagonal matrix.

The following scaling technique has been used widely in many structural problems [112,58]. To minimize a positive definite quadratic form of the potential energy

$$F(x) = \frac{1}{2} x^T A x - x^T b \quad (2.42)$$

operate in the scaled coordinates

$$F(y) = \frac{1}{2} y^T \bar{A} y - y^T \bar{b} \quad (2.43)$$

where

$$\bar{A} = D^T A D, \quad \bar{b} = D^T b \quad (2.44)$$

$$\text{and } d_{ij} = \begin{cases} 0 & i \neq j \\ 1/c\sqrt{a_{ij}} & i = j \end{cases} \quad (2.45)$$

The effect of this transformation is to center all the Gerschgorin discs at the same point, namely $1/c^2$. The location of this point cannot affect the conditioning number since c cancels out in the eigenvalue ratio. It has been shown by Fox and Stanton [112] that when $c = (n)^{\frac{1}{2}}$, where n is the maximum number of non zero elements in any row, the spectral radius of \bar{A} is less than one. A slightly different approach has been suggested by Fried [117] where $c_i = (N_i)^{\frac{1}{2}}$ and N_i is proportional to the norm of the i^{th} row or column. Usually, the number of non zero entries in a row or column is much less than the total number of degrees of freedom, and there is no considerable difference in the norms of different rows. Thus taking $c_i = 1$ is the best workable way of scaling the stiffness matrix.

For nonlinear problems the shapes of constant energy surfaces are not only more complex but could be not even convex. However, Taylors theorem indicates that in the neighbourhood of a relative minimum of the total potential energy surface, having positive definite second variation, the dominant contribution to the potential energy is the matrix of second derivatives :

$$\left[\frac{\partial^2 \pi}{\partial x_i \partial x_j} (x) \right] = \left[\frac{\partial^2}{\partial x_i \partial x_j} (U_2 + U_3 + U_4 - W) \right] \quad (2.46)$$

with elements

$$a_{ij}(x) = A_{ij} + \frac{\partial^2}{\partial x_i \partial x_j} (U_3 + U_4) \quad (2.47)$$

and with W being the total work of the applied loads and U_2 ,

U_3 , U_4 being respectively the quadratic, cubic and quartic terms of the strain energy. Hence it is possible to define scaling for the nonlinear problem as in the linear case. Computational experience has shown that scaling based on the linear matrix A is as good as scaling based on $a_{ij}(x)$ only when the variation in diagonal elements is less than one order of magnitude. Example 1 of the single cable is a characteristic example where $a_{ij}(x)$ is one order of magnitude greater than A_{ij} , while in all other test problems $a_{ij}(x)$ are not very different from A_{ij} .

2.8. Termination Criteria

There are two important questions associated with the termination of any iterative procedure. The first is when does the iteration cease to improve the solution, and the second is how accurate is the calculated solution.

Theoretically, to satisfy equilibrium, the Euclidean norm of the out of balance forces should be zero. Clearly this is the formal requirement for a displacement state to be a minimum. Using finite arithmetic, the chances of the norm being identically zero are non-existent. Therefore, certain tolerances should be imposed as upper limits for the length of the gradient. But even this criterion cannot be unique for all types of problem. The speed at which the gradient will tend to zero will depend on the type of structure and on the initial loading condition.

An appropriate quantity to trace, particularly when using minimization methods, is the total potential energy as it decreases monotonically. But for many cable problems, several successive displacement states may exist which are equal to within only 3 - 4 digits and give the same total potential energy to 6 - 8 digits. In such cases it is impossible to get 5 digits accuracy with a termination criterion based entirely on the total potential energy. There occasionally are cases when the gradient too is not as small as one would like even after the energy is converged to the prescribed accuracy. Also, the adoption of an energy criterion would require additional arithmetic when using relaxation and stiffness methods where the total potential energy is not a byproduct of the iteration process.

The Vector difference criterion

$$\frac{\|x^k - x^{k-1}\|_2}{\|x^k\|_2} \leq \epsilon \quad (2.48)$$

has been frequently used, but it has the disadvantage that it does not give any information as to how accurate the calculated solution is. The relative error norm

$$\frac{\|x^k - x^*\|_2}{\|x^*\|_2} \leq \epsilon \quad (2.49)$$

where x^* is the true solution, has also been used [186], but its practical use is limited only to cases with a known solution.

In order to compare effectively all different iterative methods used in this work, the need of a uniform readily available

and reliable termination criterion was imperative. Since the calculation of the gradient vector is part of any iterative non-linear procedure, and provides all the information required for a convergence test of the method, the following termination criteria were used throughout this work :

$$(a) \quad RNORM = \|R_i\|_2 \leq \epsilon \quad (2.50)$$

$$(b) \quad QUOT = \frac{\|R_i\|_2}{\|F_i\|_2} \leq \epsilon \quad (2.51)$$

$$(c) \quad RNORM - SC = \|R_{SC_i}\|_2 \leq \epsilon \quad (2.52)$$

$$(d) \quad QUOT - SC = \frac{\|R_{SC_i}\|_2}{\|F_i\|_2} \leq \epsilon \quad (2.53)$$

where R_i is the current residual vector, F_i the current load vector and R_{SC_i} is the current scaled residual vector. The value of the specified convergence tolerance, or termination parameter ϵ , varies with the test problem and the termination criterion used.

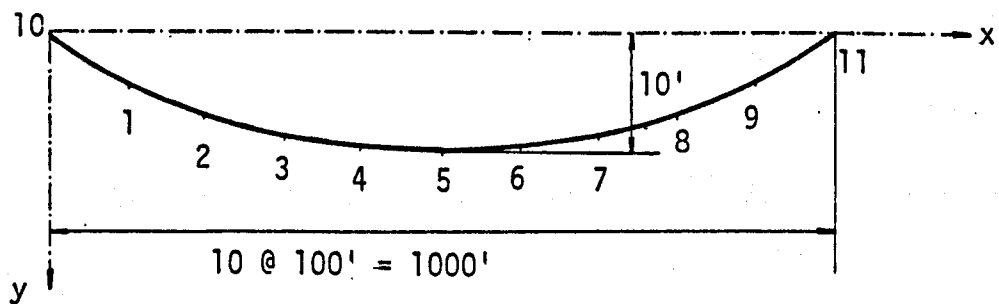
For structures with localised nonlinear behaviour the maximum absolute value of the residuals could also be found and checked against the norm of the applied loads.

$$\frac{|R_i^{\max}|}{\|F_i\|_2} \leq \epsilon_1 \quad (2.54)$$

2.9. Test Problems

CASE STUDY 1 : Ten-member suspension cable

Figure 2.7 shows a $1\frac{1}{8}$ in diameter locked coil strand, spanning 1000 ft., having a cross-sectional area of 0.85 sq. ins. and dead weight of 3.16 lb. per ft. Michalos and Birnstiel [196] originally presented a solution for the cable displacements when an 8.0 kips live load was applied at node 4 in the y-direction. To approximate the weight of the cable, the curved initial position was replaced by 10 straight line segments with dead load concentrated at the intersections. The cable in its initial configuration has a horizontal component of prestress of 4.0 kips. However, in order to test the behaviour of the applied methods for structural mechanisms, the horizontal component of prestress was not taken into account in its initial configuration. This represents a more severe test since in such a case the initial stiffness matrix is singular and cannot be inverted.



$$E = 19,000 \text{ ksi}$$

$$A = 0.85 \text{ sq. in.}$$

Fig. 2.7. Ten member suspension cable, example 1

Joint	X(ft)	Y(ft)	Load (kips)
1	100.0	36.30	0.332
2	200.0	64.30	0.325
3	300.0	84.18	0.320
4	400.0	96.05	8.317
5	500.0	100.00	0.316
6	600.0	96.05	0.317
7	700.0	84.18	0.320
8	800.0	64.30	0.325
9	900.0	36.30	0.332
10	0.0	0.0	0.0
11	1000.0	0.0	0.0

Table 2.1. Initial configuration of example 1

CASE STUDY 2 : Two dimensional counterstressed dual cable structure

The structure shown in Figure 2.8 is symmetrical about the centre line and the horizontal line between the supports. The node points lie on two parabolic curves. Table 2.2 shows the initial configuration.

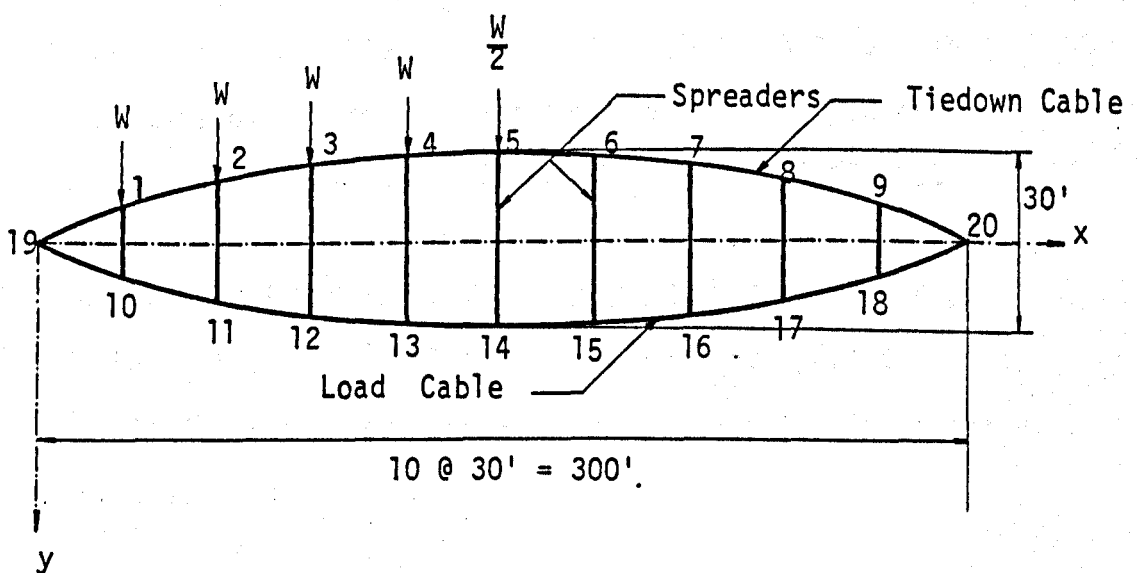


Fig. 2.8. Counterstressed dual cable structure, example 2

Joint	X(ft)	Y(ft)
1	30.0	- 5.4
2	60.0	- 9.6
3	90.0	-12.6
4	120.0	-14.4
5	150.0	-15.0
6	180.0	-14.4
7	210.0	-12.6
8	240.0	- 9.6
9	270.0	- 5.4
19	300.0	0.0
20	0.0	0.0

Table 2.2 Initial configuration of example 2

The following properties were assumed for the structure :

- Area of spreaders = 2.0 sq. in.
- Area of tiedown cable = 1.62 sq. in.
- Area of load cable = 3.24 sq. in.
- Modulus of elasticity of spreaders = 30,000 Ksi
- Modulus of elasticity of cables = 24,000 Ksi

The structure was analysed for a total uniform load of 50.0 kips on the left half of the span. The uniform load was approximated by concentrated loads at the upper nodes ($W = 10.0$ kips). The horizontal component of prestress force was 72.0 kips.

CASE STUDY 3 : Orthogonal hyperbolic paraboloid prestressed net

This example, shown in Figure 2.9, which was originally analysed by Thornton and Birnstiel [282], consists of seven prestressing cables in the y direction and seven suspension cables in the x direction. The cables are all equally spaced and are supported by an assumed rigid frame. The following properties were used :

Area of cables	= 1.0 sq. in.
Modulus of elasticity	= 24,000 Ksi
Horizontal component of prestress force	= 50.0 kips

The z-coordinates of joints of the net, in its initial position, were taken from reference [282] and are shown in Figure 2.9.

The structure was analysed for a dead load of 1.0 kip in the z direction at each node, plus a live load of 14.0 kips in the z direction at node 7.

CASE STUDY 4 : Three dimensional counterstressed dual cable structure

This structure shown in Figure 2.10 was also originally analysed by Thornton and Birnstiel [282]. The following values were used :

Area of cables	= 2.0 sq. in.
Area of hangers	= 0.5 sq. in.
Modulus of elasticity	= 24,000 Ksi
Horizontal component of prestress force	= 100 kips

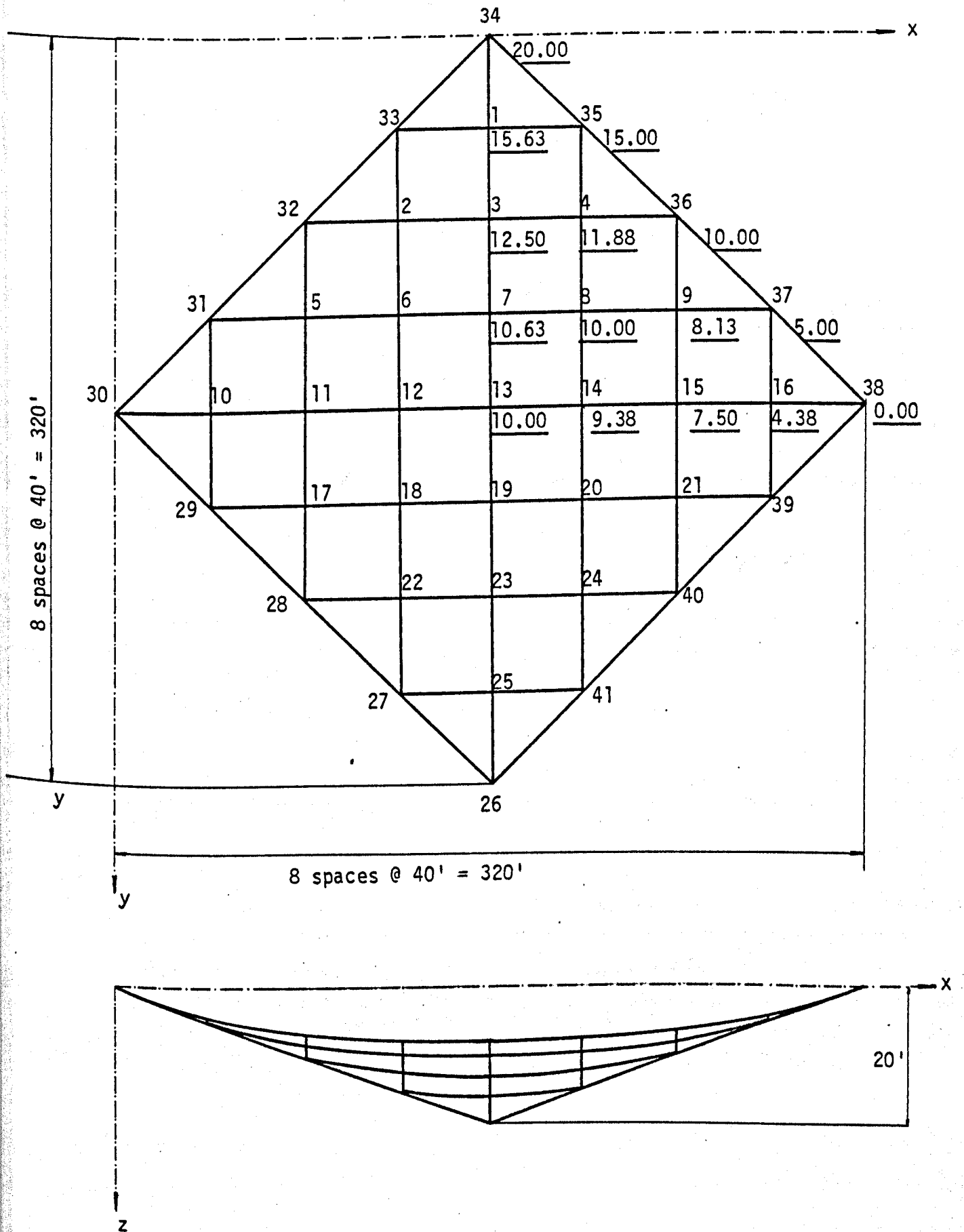


Fig. 2.9 Hyperbolic-paraboloid prestressed net, example 3.

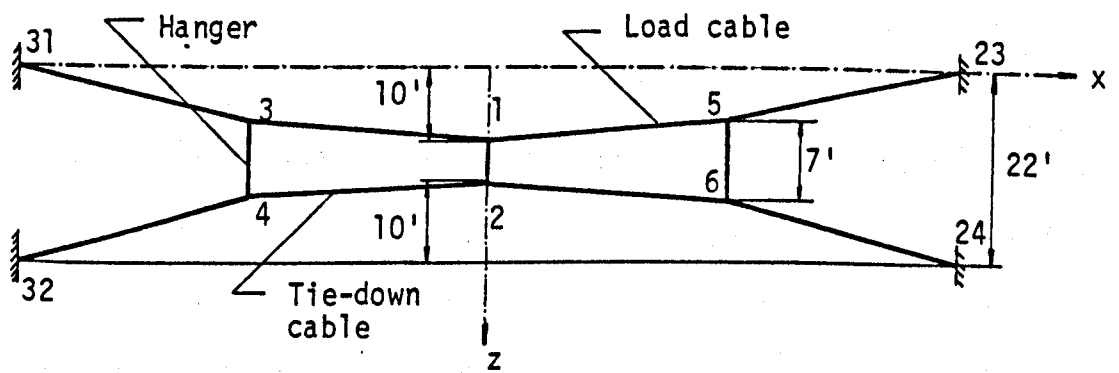
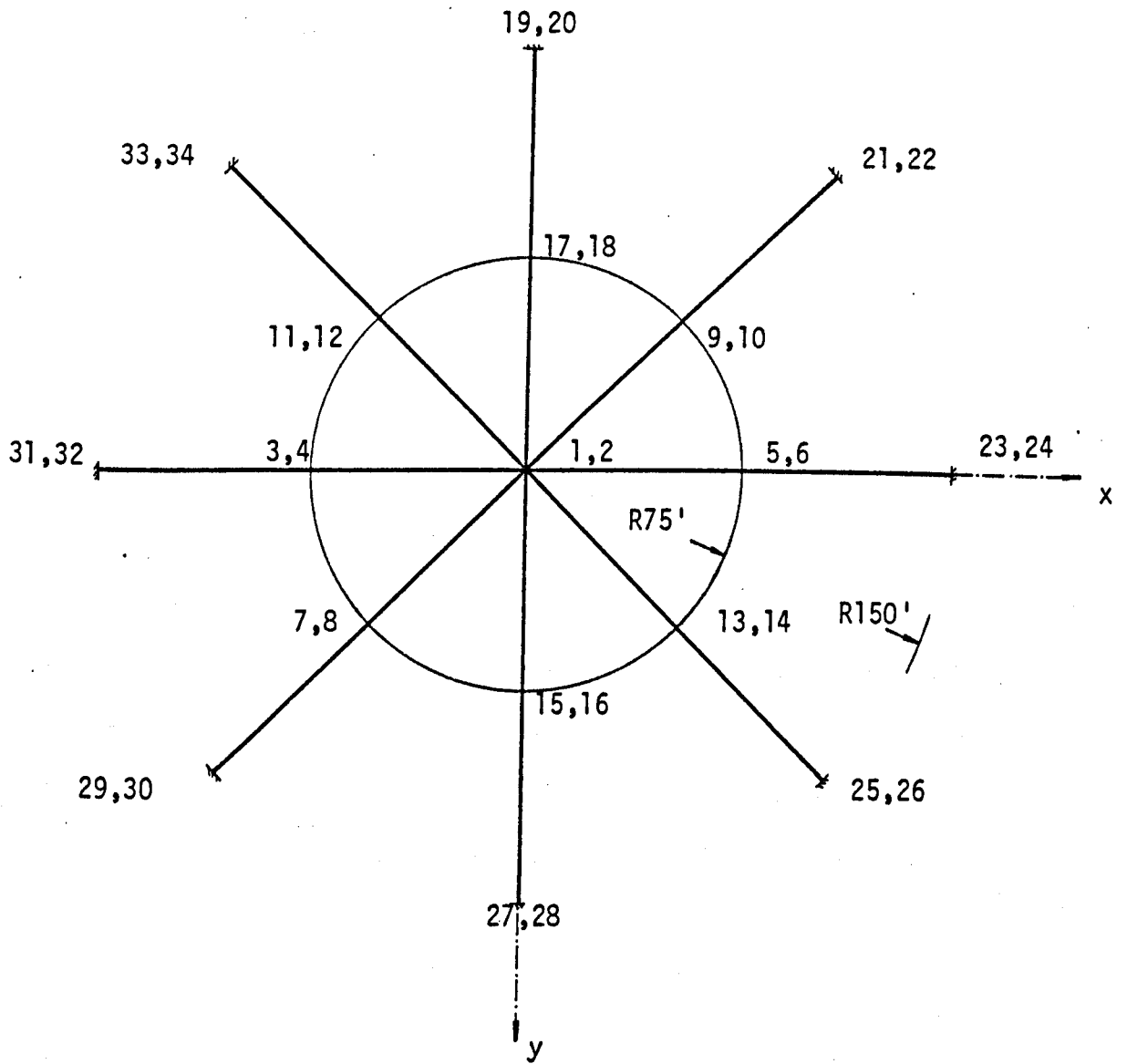


Fig. 2.10 Three dimensional dual cable structure, example 4

The structure was analysed for a vertical load of 50.0 kips applied at joint 5.

CASE STUDY 5 : Large prestressed net

This example is similar in form to the Raleigh Arena and was first analysed by Murray [209]. As shown in Figure 2.11, the orthogonal net is bounded by two intersecting rigid parabolic arches, each rising 30 ft. from the intersection points to the vertex. In each direction the maximum horizontal cable span is 200 ft and the cable spacing is 10 ft. The resulting net has 76 support points and 265 interior nodes. The horizontal component of prestress force, for the prestress cables (y direction) is taken as 100.0 kips and for the suspension cables (x direction) is taken as 40.0 kips.

The following galvanized bridge strands were selected for the full net : all prestressing cables are $1\frac{1}{8}$ in. diameter, the first four suspension cables from the arch intersection are $1\frac{1}{8}$ in. in diameter, the next suspension cable is $2\frac{1}{8}$ in. in diameter and all remaining suspension cables are $2\frac{1}{4}$ in. in diameter. Two load cases were considered : (a) a load of 5.7 kips in the z direction at each node and (b) a load of 54.3 kips in the z direction at node 135, in addition to the 5.7 kips load at each node. Although for these load conditions only half of the structure need be analysed, the methods were applied to the full structure to test them more fully.

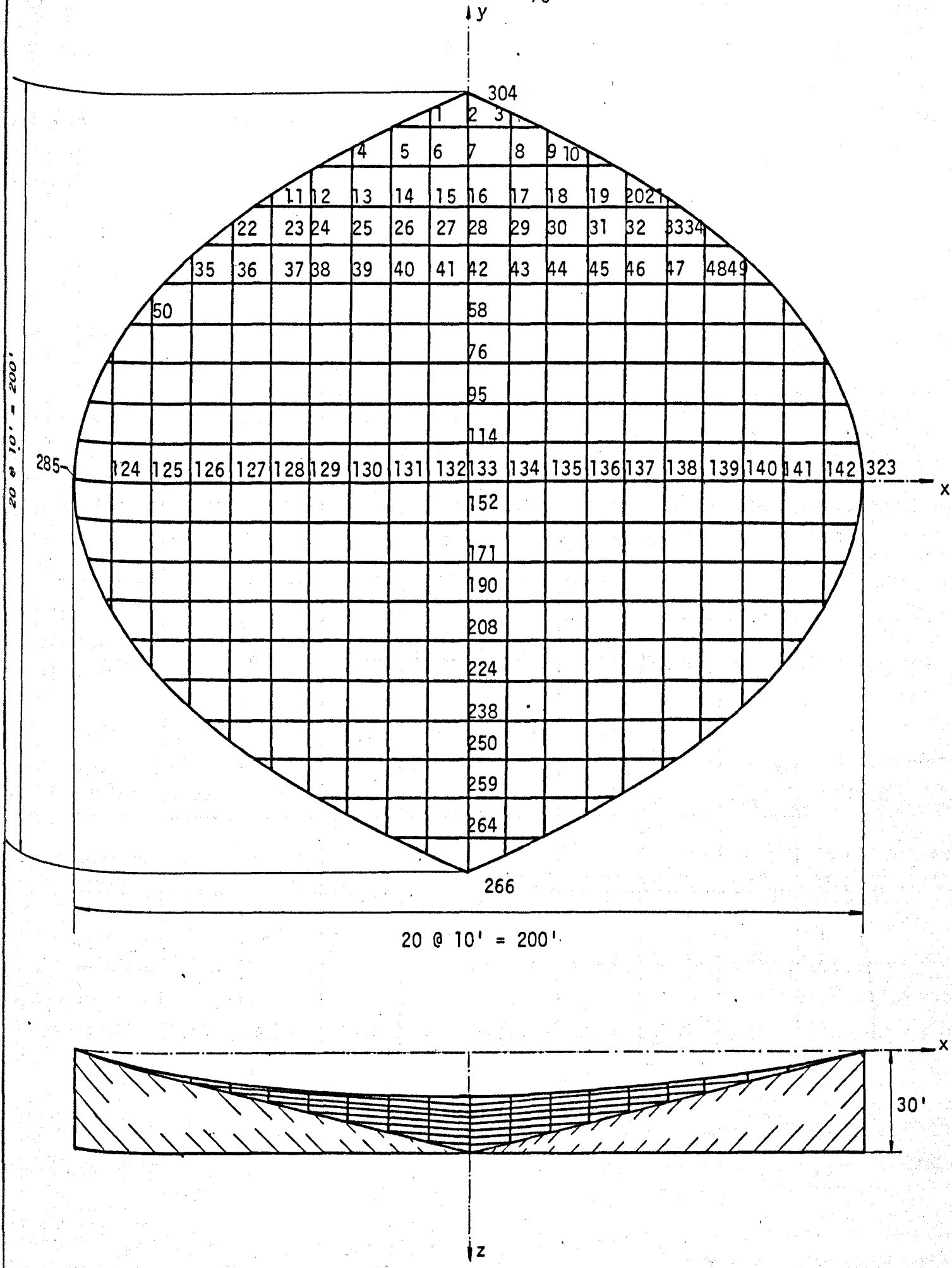


Fig. 2.11 Large prestressed net, example 5

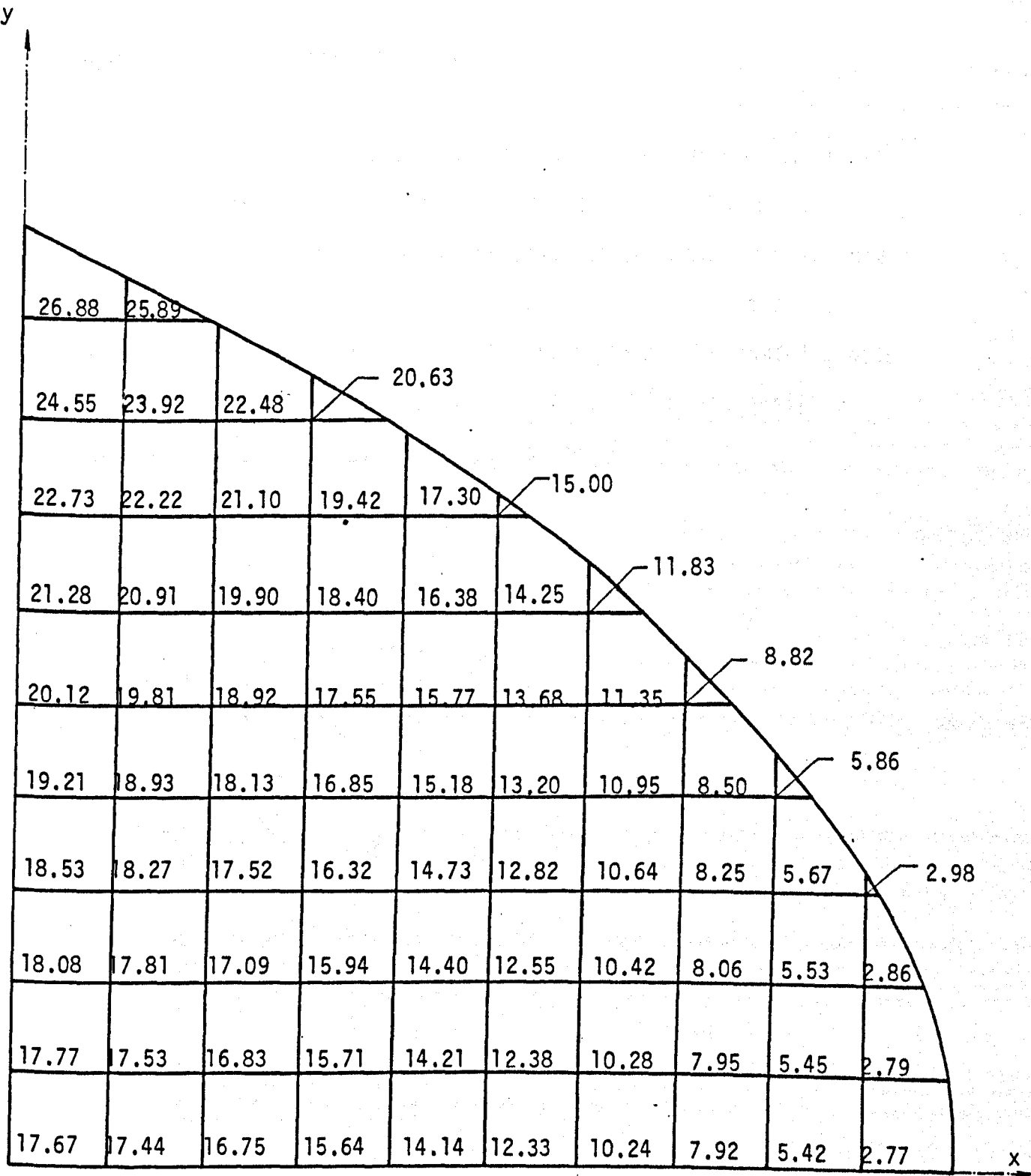


Fig. 2.12 Initial vertical coordinates for example 5

CASE STUDY 6 : Three storey frame

Although this example is not a cable structure, it was included in this study in order to assess the performance of numerical methods of nonlinear analysis for a structure with only slight nonlinearity. All the members of the frame have a cross sectional area of 1.5 sq. in., with the modulus of elasticity being 0.5 Ksi. The structure as shown in Figure 2.13 was analysed for a horizontal load of 0.02 kips at node 6.

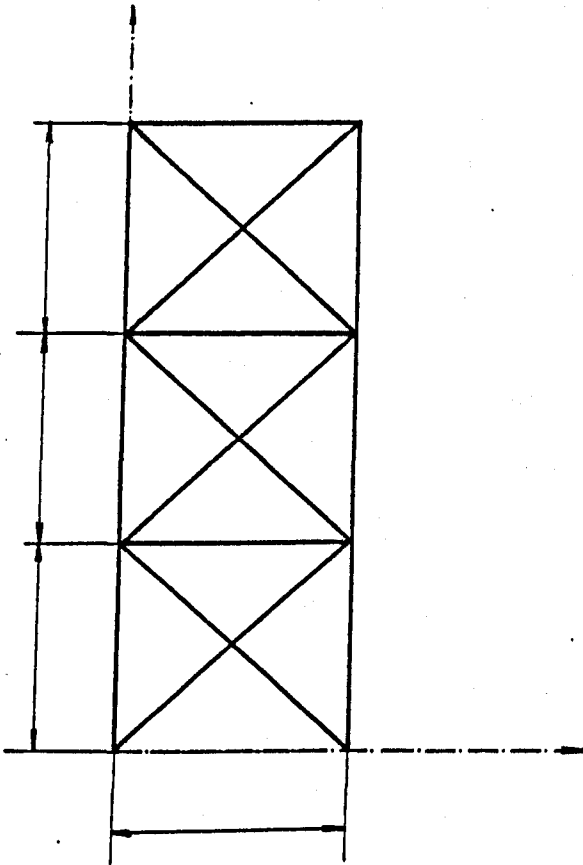


Fig. 2.13 Three storey frame, example 6

CHAPTER 3

GRADIENT METHODS

3.1. Introduction

The expanding use of the finite element method in most branches of structural engineering and other fields of continuum mechanics has given rise to the problem of solving the large algebraic equation systems produced by the discretization procedure. Although elimination methods have been extensively used for the computer solution of large sparse sets of linear simultaneous equations they suffer from the disadvantage that the overall stiffness matrix must be stored in an ordered form which leads to considerable book-keeping as well as to excessive storage requirements due to the "fill-in" that occurs during the decomposition of the matrix. Most of the gradient iterative procedures are, on the contrary, much more efficient with respect to computer storage requirements since only the storage of several N-dimensional vectors is needed.

One of the oldest and best known gradient methods is the method of steepest descent, proposed by Coushy [74] in 1847. In this method the direction ϕ_i of equation (2.9) becomes the negative gradient. The method has several disadvantages which make it impractical for many problems. The rate of convergence depends strongly on the graph of the function. The inefficiency of the method for solving large problems is

characterised geometrically by a zig-zag behaviour caused by the eccentricity of the function contours. A number of schemes have been proposed to overcome the zig-zag difficulty [30, 102, 104]. The main reason for the slow convergence is the fact that each iterative cycle is calculated independently of the others and so no information from previous iterations is stored that may accelerate the convergence.

The most effective gradient techniques are based on the idea of conjugate directions. Two of the most powerful conjugate direction methods are the conjugate gradient method and the variable metric method.

The conjugate gradient method for the solution of a system of linear algebraic equations was developed independently by Hestenes [137] and by Stiefel [137] with the cooperation of J. B. Rosser, G. Forsythe and L. Paige. A more thorough presentation of the method along with the conjugate direction method and related iterative methods was given by Hestenes [138]. Fletcher and Reeves [108] first broadened the area of application of the conjugate gradient method to nonlinear problems by taking the potential energy as a non-quadratic function to be minimized, and later Daniel [82] gave a more general development.

The variable metric method was developed by Davidon [86] and modified by Fletcher and Powell [107]. The method starts with an initial approximation of the inverse stiffness matrix H_0 , and an iterative procedure is established in such a way that as the displacement vector reaches the solution, H_i becomes

the inverse of the stiffness matrix. The method is a very powerful gradient method but has the disadvantage of requiring storage space for half the matrix H and time for its manipulation which, for large problems, become excessive.

3.2. The Conjugate Gradient Algorithm

Denoting by K the global matrix of the discretized continuum, by x the vector of nodal unknowns and by F the vector of the applied loads, the total energy of a linear system could be written

$$E = \frac{1}{2} x^T Kx - xF \quad (3.1)$$

assuming that K is positive definite and symmetric entails that the energy E possesses a minimum at the point where the residual vector

$$\frac{\partial E}{\partial x} = r = Kx - F \quad (3.2)$$

vanishes.

The essence of the conjugate gradient method consists of obtaining a new vector x_{i+1} along a direction p_i at a distance a_i , i.e.

$$x_{i+1} = x_i + a_i p_i \quad (3.3)$$

The direction p_i is pointing to the centre of the energy contour cut by the plane spanned by g_i and p_{i-1} , where the latter is tangent to the contour. Thus as p_{i-1} is tangent to

the contour and p_i points to its centre then

$$p_i^T K p_{i-1} = 0 \quad (3.4)$$

and

$$p_i = -r_{i+1} + \beta_i p_i \quad (3.5)$$

The scalar β is determined by substituting equation (3.5) into equation (3.4) resulting in

$$\beta_i = \frac{r_{i+1}^T K p_i}{p_i^T K p_i} \quad (3.6)$$

The scalar α is fixed by the condition that at the centre of the energy contour, E possesses a minimum with respect to α . Thus

$$\frac{\partial}{\partial \alpha_i} E(x_i + \alpha_i p) = 0 \quad (3.7)$$

and

$$\alpha_i = - \frac{r_i^T p_i}{p_i^T K p_i} \quad (3.8)$$

Other equivalent expressions for α and β may also be formed

$$\alpha_i = \frac{|r_i|^2}{p_i^T K p_i} = \frac{p_i^T r_0}{p_i^T K p_i} \quad (3.9)$$

and

$$\beta_i = \frac{|r_{i+1}|^2}{|r_i|^2} = - \frac{r_{i+1}^T K r_i}{p_i^T K p_i} \quad (3.10)$$

With these formulae the CG algorithm becomes :

$$x_0 = \text{arbitrary}$$

$$r_0 = r(x_0)$$

$$p_0 = - r_0$$

$$\alpha_i = \frac{|r_i|^2}{p_i^T K p_i} \quad (3.11)$$

$$x_{i+1} = x_i + \alpha_i p_i$$

$$r_{i+1} = r_i + \alpha_i K p_i$$

$$\beta_i = \frac{|r_{i+1}|^2}{|r_i|^2}$$

$$p_{i+1} = - r_{i+1} + \beta_i p_i$$

This process is guaranteed, apart from rounding-off errors, to locate the minimum of any quadratic function of N arguments in at most N iterations. For general functions which are not quadratic the process is iterative rather than N -step, and a test for convergence is required. In such cases, as the iterate approaches the minimum the function is more closely quadratic and so convergence is more nearly assured. Furthermore, even in regions remote from the minimum, the conjugate gradient methods, by taking account of the curvature of the function, are best able to deal with complex situations such as the presence

of a long curving valley. The oscillatory behaviour characteristic of methods such as steepest descent is thereby avoided.

In nonlinear problems a closed form solution for the scalar α is not available and a one dimensional linear search along the direction p_i should be applied. The residual vector is replaced by the gradient vector, $g(x)$ and the corresponding recursive expression for the gradient is not valid any more. Other conjugate gradient methods use a two-directional search where the values of α_i and β_i are determined from the minimization of $f(\alpha_i, \beta_i)$. However, quasi-linear problems, that is, problems in which K depends on x , can be efficiently solved with algorithm (3.11) by calculating r anew each cycle and changing in each loop K so as to reflect its dependence on x .

3.3. The Single Variable Search

The single variable search or linear search is the problem of finding the smallest positive root of the directional derivative $p_i^T g(x_i + tp_i)$ for prescribed x_i and p_i , and thus the minimum of $f(x_i + tp_i)$ considered as a function of the scalar t .

In nonlinear applications of the conjugate gradient method the step-length algorithm is a factor that strongly affects the efficiency of the method. In any practical application the time

spent evaluating the function and the gradient may well dominate the time for the whole minimization process. The required computer time depends not only on the total number of iterations, but on the number of cycles in each iteration required for the linear search as well.

The most common routine of the linear search methods is first to evaluate an interval (t_a, t_b) known to contain the minimum of the function $f(t_i)$ along the direction p_i , and then to apply an iterative procedure to approximate the minimum.

3.3.1. Methods for Bracketing the Solution

The object of these methods is to find an initial interval $(0, h)$ where

$$f'(x_i + h p_i) = p_i^T g(x_i + h p_i) > 0 \quad (3.12)$$

Then the minimum is bounded inside this interval since the value of the derivative of the function with respect to h at $h = 0$ is always non-positive.

$$f'(0) = p_i^T g_i \leq 0 \quad (3.13)$$

If inequality (3.12) is not satisfied, then $f'(h)$ is examined at the points $2h, 4h, t_a, t_b$, where t_b is the first of these values at which either $f'(h)$ is non-negative or $f(h)$ has not decreased.

a. Davidon's scheme

This approach was proposed by Davidon [86] and later was modified by Fletcher and Reeves [108]. On the supposition that there is available an estimate, "est", of the value $f(x)$ at the unconstrained minimum and that the function is quadratic in the neighbourhood of the minimum, then

$$f'(0) = \frac{f(t) - f(0)}{t} \quad (3.13)$$

and

$$t = \frac{\text{est} - f(0)}{f'(0)} \quad (3.14)$$

Davidon has taken twice this length $h = 2t$, to obtain a first estimate for the step length. In fact the unconstrained minimum will generally not lie on the direction of p_i , and so h will tend to be larger. Fletcher and Powell [107] suggested the alternative expression

$$h = (p_i^2)^{-\frac{1}{2}} \quad (3.15)$$

if

$$(p_i^2)^{-\frac{1}{2}} < 2t \quad (3.16)$$

b. Stanton's Method

This method for generating the first step size h , in each new direction, was proposed by Stanton [262] and was applied in the nonlinear finite element analysis of plates. The step size is given by

$$h = C_i \|x_i\|_\infty \quad (3.17)$$

where $\|x_i\|_\infty = \max_j |x_j|$, is the infinite norm of the current vector, and C_i is a parameter dependent on the history of all $i-1$ linear searches previously performed.

$$\begin{aligned} C_0 &= 1 \\ C_i &= (2)^{r-1} \left(\frac{1}{2}\right)^S C_{i-1} \end{aligned} \quad (3.18)$$

where r is the number of increments required to bracket the root in the previous iteration and S is the number of decrements required to ensure

$$|g(ta)| > 0.01 |g(tb)| \quad (3.19)$$

The value of S is increased by 1, if the search results in $t_i < ta + 0.1 (tb - ta)$, at iteration i . Within a few iterations the value of C_i is adapted to the space and the bracketing of the root t_i is assured with a minimum effort.

3.3.2. Methods for Approximating the Minimum

The most commonly used methods in structural analysis for approximating a bracketed minimum along a line are

- a. Davidon's method
- b. A regula falsi-bisection algorithm
- c. Fibonacci search

Other methods currently used in other fields of optimization can be found in References [32, 219, 301].

a. Davidon's method

In this method a cubic curve is fitted in the interval (t_a, t_b) and the minimum is approximated by the lowest point of the cubic curve

$$t_e = t_b - \frac{f'(t_a) + w - z}{f'(t_b) - f'(t_a) + 2w} \cdot (t_b - t_a) \quad (3.20)$$

where

$$z = 3 \frac{f(t_a) - f(t_b)}{t_b - t_a} + f'(t_a) + f'(t_b) \quad (3.21)$$

$$w = \pm (z^2 - f'(t_a) \cdot f'(t_b))^{\frac{1}{2}} \quad (3.22)$$

A real value is guaranteed by the problem and the sign of w is chosen so that t_e lies in the interval (t_a, t_b) . If both values of t_e lie in the interval, the one closer to t_a is chosen. If neither of $f(t_a)$ or $f(t_b)$ is less than $f(t_e)$ then t_e is accepted as an estimate of t_1 . Otherwise depending on whether $f'(t_e)$ is positive or negative, the interpolation is repeated over the subinterval (t_a, t_e) or (t_e, t_b) respectively.

b. Regula Falsi-Bisection Algorithm

The most common difficulty encountered in Davidon's method is in satisfying the condition

$$\left| \frac{f'(t_j)}{\|p_j\|_2 \|g(x_i + t_j p_j)\|_2} \right| \leq \epsilon \quad (3.23)$$

Geometrically this is the cosine of the "angle" between p_j and $g(x_i + t_j p_j)$. In other words ϵ is a convergence criterion for accepting t_j as a zero for the directional derivative $f'(t)$. Using Davidon's scheme it will be difficult to find a good approximation when the directional derivative crosses zero with a steep slope.

This method which was first used by Stanton [262] is a combination of the regula-falsi and the bisection techniques. In the bisection algorithm the new approximation is

$$t_j = \frac{(t_a + t_b)}{2} \quad (3.24)$$

and (i) if $f(t_a) \cdot f(t_j) < 0$ t_j replaces t_a

(ii) if $f(t_a) \cdot f(t_j) \geq 0$ t_j replaces t_b

In the rule of false position (regula-falsi) the standard secant formula is adopted

$$t_j = t_a - f'(t_a) \cdot \frac{(t_a - t_b)}{f'(t_a) - f'(t_b)} \quad (3.25)$$

The estimates chosen for the next iteration are t_j and whichever of t_a, t_b give a function value of opposite sign to $f(t_j)$.

The combination of these two procedures gives the following algorithm shown diagrammatically in Figure 3.1.

1. $t_e = t_a - f'(t_a) \left(\frac{t_a - t_b}{f'(t_a) - f'(t_b)} \right)$
2. (i) if $f'(t_e) \cdot f'(t_a) < 0$ $t_a \rightarrow t_e$
 $t_b \rightarrow t_b$

 (ii) if $f'(t_e) \cdot f'(t_a) \geq 0$ $t_a \rightarrow t_a$ (3.26)
 $t_b \rightarrow t_e$
3. $t_e = \frac{1}{2} (t_a + t_b)$
4. Step 2 repeated

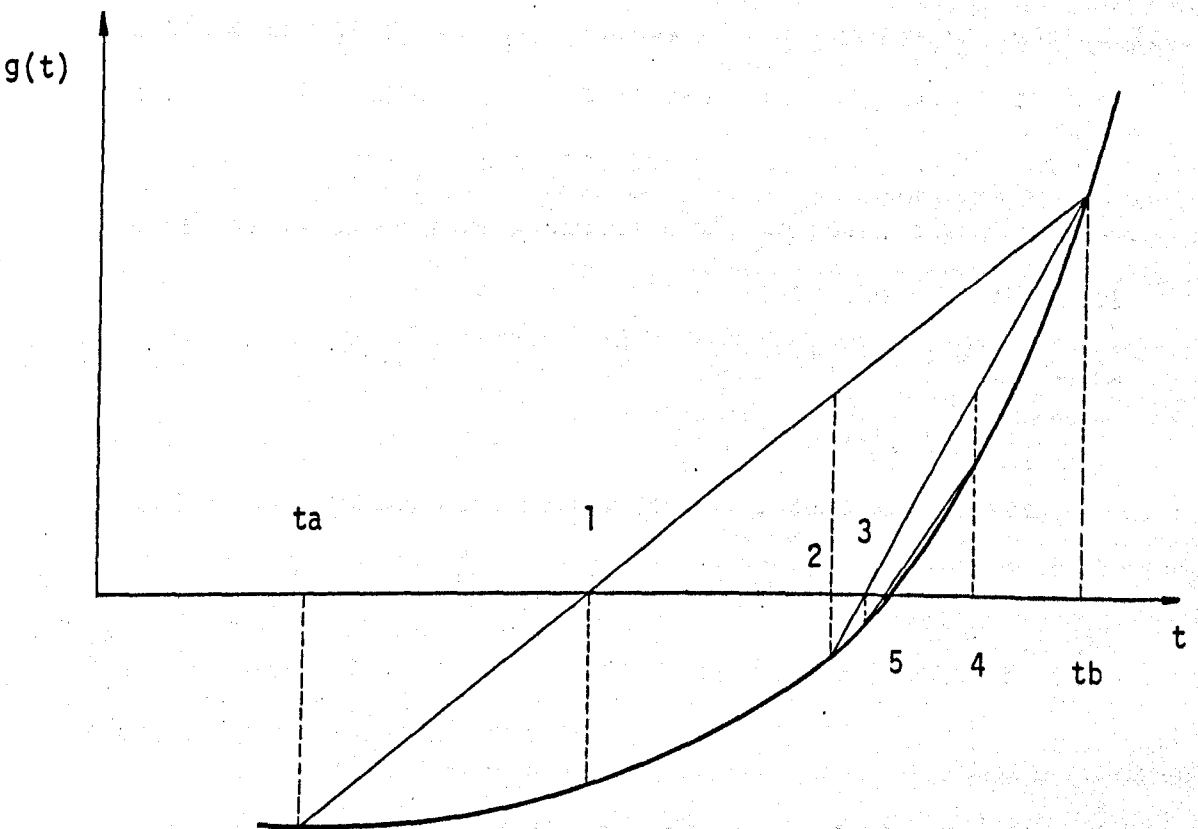


Fig. 3.1 Regula falsi-bisection linear search algorithm

The use of step 3 insures against slow convergence from the regula falsi algorithm, steps 2 and 4 ensure that the interpolation points always to a bracketed root. The flat part of the curve corresponds to a region in which the quadratic term in the function f dominates. As t becomes larger the higher order terms dominate, causing the angle of the curve to become steeper. It is this behaviour that necessitates step 3. The method is assumed to converge when two successive approximations for t are less than a prescribed value.

c. Fibonacci Search

This method was found by Kiefer [178] in 1953. But although this discovery is relatively recent, it has theoretical connections to the work of Fibonacci, a thirteenth century mathematician whose name has been given to the technique. The basic idea of this method is to perform a sequence of two point searches to reduce the uncertainty interval, and to place the search points t_1^K, t_2^K , with $K = 0, 1, \dots$, in such a way that, if, for example, (t_1^0, t_2^0) is the first reduced uncertainty interval, then t_1^0 is used as one of the next search points ; that is, we set $t_2^1 = t_1^0$, and so on. The problem is to select the sequence (t_1^K, t_2^K) in such a way that the decrease in the length of the uncertainty interval is maximal.

The optimal choice of the t_1^K, t_2^K is as follows :

Let

$$T_{K+1} = T_K + T_{K-1}, \quad T_0 = T_1 = 1, \quad K = 1, 2, \dots$$

be the Fibonacci sequence and $N > 0$ the maximum number of two-point searches which are to be performed ; then we use the points

$$\begin{aligned} t_1^{K+1} &= (T_{N-1-K} / T_{N+1-K}) (tb^K - ta^K) + ta^K \\ t_2^{K+1} &= (T_{N-K} / T_{N+1-K}) (tb^K - ta^K) + ta^K \end{aligned} \quad K = 0, 1, \dots, N-2$$

(3.27)

Here $t_a^0 = ta$, $t_b^0 = tb$, and

$$t_a^{K+1} = ta^K, \quad t_b^{K+1} = t_2^{K+1}, \quad \text{if } f(t_1^{K+1}) < f(t_2^{K+1}),$$

(3.28)

$$t_a^{K+1} = t_1^{K+1}, \quad t_b^{K+1} = t_b^K, \quad \text{if } f(t_1^{K+1}) \geq f(t_2^{K+1})$$

For $K = N-1$ (3.27) has to be modified, and if $\epsilon > 0$ is the maximum round-off error in the evaluation of f , set

$$t_1^N = \frac{1}{2} (t_a^{N-1} + t_b^{N-1}) - \epsilon$$

(3.29)

$$t_2^N = \frac{1}{2} (t_a^{N-1} + t_b^{N-1}) + \epsilon$$

If the minimum is required to an accuracy δ , then N must be chosen so that

$$T_N \geq \frac{(t_b^0 - t_a^0)}{\delta - \epsilon} \geq T_{N-1}$$

(3.30)

3.4. Buchholdt's Method

On the assumptions that the law of elastic behaviour is linear and in conformity with the elastic limits, that the loads are applied at the joints, and that the elongations are negligible compared with the initial lengths, Buchholdt et al [48] have shown that the total potential energy of a pin-jointed assembly, free of bending and torsional elements, can be expressed as a fourth order polynomial in the step length t , of the form

$$\phi = C_1 t^4 + C_2 t^3 + C_3 t^2 + C_4 t + C_5 \quad (3.31)$$

The step length that minimizes ϕ along the conjugate direction p_i is given by the smallest positive root of the cubic equation

$$\frac{d\phi}{dt} = 4C_1 t^3 + 3C_2 t^2 + 2C_3 t + C_4 = 0 \quad (3.32)$$

The solution of equation (3.32) can be found either analytically or iteratively using Newton's method.

To evaluate the constants C_1, C_2, C_3, C_4, C_5 , we consider a link m which is attached to joints j and n . If the initial strain energy due to pretension P_m^0 is U_m^0 , then

$$U_m = U_m^0 + P_m^0 e_m + \frac{1}{2} EA e_m^2 / L_m \quad (3.33)$$

is the strain energy of the link with an elongation e_m . The total potential energy is

$$\pi_{i+1} = \sum_{m=1}^m (U_m^0 + P_m^0 e_m + \frac{1}{2} EA e_m^2) - F^T(x^{(k)} + t \quad (k)) \quad (3.34)$$

Let L_m be the initial prestressed length of link j_n , then

$$(L_m + e_m)^2 = \sum_{i=1}^{NDF} ((X_{in} - X_{ij}) + (x_{in} - x_{ij}))^2 \quad (3.35)$$

where X_{ij} ($i = 1, 2, 3$) denotes the initial coordinate of joint j .

Ignoring the second order of smallness equation (3.35) may be written

$$e_m = \sum_i (2 (X_{in} - X_{ij})(x_{in} - x_{ij}) + (x_{in} - x_{ij})^2) / 2L_m \quad (3.36)$$

Writing for brevity

$$X_i = X_{in} - X_{ij}$$

$$x_i = x_{in} - x_{ij}$$

$$p_i = p_{in} - p_{ij}$$

the expression for e_m now becomes

$$e_m = \frac{1}{2L_m} \left[2X_i^T(x_i^{(k)} + t p_i^{(k)}) + (x_i^{(k)} + t p_i^{(k)})^T(x_i^{(k)} + t p_i^{(k)}) \right] \quad (3.37)$$

Substituting equation (3.37) into equation (3.36) we get

$$e_m = \frac{1}{L_{jn}} (\epsilon_1 + \epsilon_2 t + \epsilon_3 t^2) \quad (3.38)$$

where

$$\epsilon_1 = X_i^T(x_i^{(k)}) + (x_i^T(x_i^{(k)})) / 2$$

$$\epsilon_2 = X_i^T(x_i^{(k)}) \cdot p_i^{(k)} + x_i^T(x_i^{(k)}) \cdot p_i^{(k)} \quad (3.39)$$

$$\epsilon_3 = (p_i^T(x_i^{(k)}) \cdot p_i^{(k)}) / 2$$

and finally substituting equation (3.38) into equation (3.34)

we obtain

$$\begin{aligned}
 C_1 &= \sum EA \epsilon_3^2 / 2L_m^3 \\
 C_2 &= \sum EA \epsilon_2 \epsilon_3 / L_m^3 \\
 C_3 &= \sum \left(\frac{p_m^0}{L_m} \epsilon_3 + EA (\epsilon_2^2 + \epsilon_1 \epsilon_3) / 2L_m^3 \right) \quad (3.40) \\
 C_4 &= \sum \left(\frac{p_m^0}{L_m} \epsilon_2 + EA \epsilon_1 \epsilon_2 / L_m^3 \right) - F^T p \\
 C_5 &= \sum \left(U_0 + \frac{p_m^0}{L_m} \epsilon_1 + EA \epsilon_1^2 / 2L_m^3 \right) - F^T x
 \end{aligned}$$

3.5. Extensions of the CG Algorithm

3.5.1. Polak and Ribiere Algorithm

This version of the conjugate gradient algorithm was described by Polak and Ribiere [231] and Poljak [232]. The method originated from an expression proposed by Daniel [83] for the scalar β :

$$\beta_i = - \frac{g_{i+1}^T J(x_{i+1}) \cdot p_i}{p_i^T \cdot J(x_{i-1}) \cdot p_i} \quad (3.41)$$

where $J(x_{i+1})$ is the Jacobian matrix at the point x_{i+1} .

In order to overcome the difficulty of obtaining the Jacobian in each iteration, Polak and Ribiere expressed the

gradient in Taylor series

$$-g_{i+1} = -g_i + t_i J_i' p_i \quad (3.42)$$

where

$$J_i' = \int_0^1 J(x_i + \theta t_i p_i) d\theta \quad (3.43)$$

This development leads to the expression for β_i

$$\beta_i = \frac{g_{i+1}^T g_i}{\|g_i\|^2} - \frac{g_{i+1}^T J_i' p_i}{p_i^T J_i' p_i} \quad \text{or} \quad (3.44)$$

$$\beta_i = \frac{\|g_{i+1}\|^2 - g_{i+1}^T g_i}{\|g_i\|^2} \quad (3.45)$$

3.5.2. Sorenson's Version

Another modification of the Fletcher and Reeves algorithm was proposed by Sorenson [274]. In this version the scalar parameter β_i is evaluated as

$$\beta_i = \frac{\gamma_i^T g_{i+1}}{\gamma_i^T \gamma_i} \quad (3.46)$$

where

$$\gamma_i = g_{i+1} - g_i$$

and
$$\beta_1 = \frac{\|g_2\|^2}{\|g_1\|^2}$$

The expression of equation (3.46) is a product of the orthogonality condition of vectors p_{i+1} and y_i . Takahashi [279] proposed another expression for β which comes from the orthogonality condition

$$g^T(x_{i+2}) p_i = 0$$

3.6. The Memory Gradient Method

Miele and Cantrell [197] introduced a modification of the CG algorithm which performs a two directional search for the determination of the scalars α and β . The algorithm, which they called the memory gradient method, can be stated as follows :

$$x_{i+1} = x_i + \delta x_i \tag{3.47}$$

$$\delta x_i = -\alpha g_i + \beta \delta x_{i-1}$$

in which the scalars α and β are chosen at each step so as to yield the greatest decrease in the function.

The first variation of the function, to first order terms, is given by

$$\delta f(x_i) = g^T(x_i) \delta x_i \tag{3.48}$$

with

$$\delta x_i = x_{i+1} - x_i$$

The greatest decrease in the value of the function is achieved if the first variation (3.48) is minimized. Here, we limit the analysis to those variations δx_i which satisfy the constraint

$$K = (\delta x_i - \beta \delta x_{i-1})^T (\delta x_i - \beta \delta x_{i-1}) \quad (3.49)$$

where K and β are prescribed.

Standard methods of the theory of maxima and minima show that the fundamental function of this problem is the scalar function

$$f = g^T(x_i) \delta x_i + (1/2 \alpha) (\delta x_i - \beta \delta x_{i-1})^T (\delta x_i - \beta \delta x_{i-1}) \quad (3.50)$$

where $1/2 \alpha$ is a constant Lagrange multiplier. The optimum system of variations must be such that

$$G(\delta x_i) = 0 \quad (3.51)$$

where G is the gradient of the function f with respect to the scalar variables $\delta x^1, \dots, \delta x^n$. Equation (3.51) in the light of (3.50) gives the relation

$$\delta x_i = -\alpha g_i + \beta \delta x_{i-1} \quad (3.52)$$

In the case of $\beta = 0$, equation (3.52) reduces to

$$\delta x = -\alpha g_i(x) \quad (3.53)$$

which is the steepest descent method, and for

$$\beta = \frac{\alpha_i g_i^T g_i}{\alpha_{i-1} g_{i-1}^T g_{i-1}} \quad (3.54)$$

equation (3.52) becomes the CG method.

Equation (3.50) can be also written in the form

$$f(\delta x_i) = f(x - \alpha g(x) + \beta \delta x_{i-1}) = F(\alpha, \beta) \quad (3.55)$$

The greatest decrease in the function $F(\alpha, \beta)$ occurs if the parameters α and β satisfy the following necessary conditions :

$$F_{\alpha} = 0, \quad F_{\beta} = 0 \quad (3.56)$$

The main task of the method is to find the optimum values of the parameters α and β , that is, those which satisfy equation (3.56). This search is fully discussed in Reference [67].

Let $\delta\alpha = \alpha - \alpha_0$ and $\delta\beta = \beta - \beta_0$ be the corrections to α and β , starting from arbitrary values α_0, β_0 . Then it is shown in [67] that the following corrections must be employed.

$$\delta\alpha = -\mu(D_1/D_3) \text{ sign}(D_4/D_3), \quad \delta\beta = -\mu(D_2/D_3) \text{ sign}(D_4/D_3) \quad (3.57)$$

where

$$\begin{aligned} D_1 &= F_{\alpha}F_{\beta\beta} - F_{\beta}F_{\alpha\beta} \\ D_2 &= F_{\beta}F_{\alpha\alpha} - F_{\alpha}F_{\alpha\beta} \\ D_3 &= F_{\alpha\alpha}F_{\beta\beta} - F_{\alpha\beta}^2 \\ D_4 &= F_{\alpha}^2 F_{\beta\beta} - 2F_{\alpha}F_{\beta}F_{\alpha\beta} + F_{\beta}^2 F_{\alpha\alpha} \end{aligned} \quad (3.58)$$

and where $F_{\alpha}, F_{\beta}, F_{\alpha\alpha}, F_{\beta\beta}, F_{\alpha\beta}$ are computed at α_0, β_0 , that is, at the point x^0 defined by

$$x^0 = x_j - \alpha_0 g_j + \beta_0 \delta x_{j-1} \quad (3.59)$$

and μ lies in the interval $0 \leq \mu \leq 1$.

The partial derivatives appearing in equations (3.58) can be computed from the expressions

$$F_{\alpha} = -g^T(x^0)g(x_j), \quad F_{\beta} = g^T(x^0) \delta x_{j-1} \quad (3.60)$$

$$F_{\alpha\alpha} = g^T(x_i)H(x^0)g(x_i), \quad F_{\alpha\beta} = -g^T(x_i)H(x^0)\delta x_{i-1},$$

$$F_{\beta\beta} = \delta x_{i-1}^T H(x^0)\delta x_{i-1}$$

Since the matrix H , which is the matrix of the second partial derivatives of F , is not explicitly available, a difference scheme is used to approximate equations (3.60)

$$F_{\alpha\alpha} = (g(x^0 + \epsilon_1 g_i) - g(x^0 - \epsilon_1 g_i))^T \cdot g_i / 2\epsilon_1 \quad (3.61)$$

$$F_{\beta\beta} = (g(x^0 + \epsilon_2 \delta x_{i-1}) - g(x^0 - \epsilon_2 \delta x_{i-1}))^T \cdot \delta x_{i-1} / 2\epsilon_2$$

$$\text{and } F_{\alpha\beta} = (g(x^0 - \epsilon_1 g_i) - g(x^0 + \epsilon_1 g_i))^T \cdot \delta x_{i-1} / 2\epsilon_1$$

$$\text{with } \epsilon_1 = \epsilon / \|g(x_i)\|, \quad \epsilon_2 = \epsilon / \|\delta x_{i-1}\| \quad (3.62)$$

where ϵ is a small number :

The search starts with $\alpha_0 = \beta_0 = 0, \mu = 1$. Then $\delta\alpha, \delta\beta$ are computed from equations (3.57) and then the function F is evaluated at the new points $\alpha = \alpha_0 + \delta\alpha, \beta = \beta_0 + \delta\beta$. If $F(\alpha, \beta) > F(\alpha_0, \beta_0)$ then μ is divided by 2 and new values for α, β are computed until $F(\alpha, \beta) < F(\alpha_0, \beta_0)$. At this stage the final values for α, β become the nominal values for the next search step, and the procedure is repeated until a desired degree of accuracy on α, β is obtained. The starting value for δx is assumed to be zero. When the function is quadratic the convergence of the method has the same characteristics as the original conjugate gradient algorithm.

3.7. The Inversion of a Matrix by the CG Method

When applying the conjugate gradient method to a linear system $Ax = b$, of N equations whose matrix A is symmetric and positive definite, N orthogonal vectors $(g_0, g_1, \dots, g_{N-1})$ and N A -orthogonal vectors $(p_0, p_1, \dots, p_{N-1})$ are established after N iterations. The sequence p is linearly independent and forms a basis.

From the A -orthogonality condition :

$$p_i A p_j \begin{cases} > 0 & i = j \\ = 0 & i \neq j \end{cases} \quad (3.63)$$

one can have after N_{it} iterations, the sequence of vectors p_i forming a matrix $P(N \times N_{it})$ and satisfying the relation

$$P^T A P = D, \quad D_{ij} \begin{cases} = 0 & i \neq j \\ = p_i A p_j & i = j \end{cases} \quad (3.64)$$

As the sequence p is linearly independent, P is non-singular and both sides of equation (3.64) can be inverted yielding the following formula for A^{-1} :

$$A^{-1} = \begin{cases} N-1 & \frac{p_i p_i^T}{p_i^T A p_i} \\ i=0 \end{cases} \quad (3.65)$$

Although the above formula is strictly correct only for N vectors, we regard it as purely iterative so that when convergence

is achieved in less than N iterations the inverse can be very compactly stored in a non-square matrix $P(N \times N_{it})$ where N_{it} is the number of executed iterations.

CHAPTER 4

NUMERICAL STUDIES ON CONJUGATE GRADIENT METHODS

In this chapter, the relative efficiency of a number of conjugate gradient algorithms has been compared for the non-linear analysis of cable structures. The total execution time required to obtain a certain degree of convergence is taken as the basis for the comparison, and not the total number of iterations, since the computer time required to perform one iteration differs from method to method. For this reason all the computer programs have been constructed in the same pattern in order to produce comparable results. All computational work has been carried out on the CDC 7600 computer. Table 4.1 shows the methods used in this chapter and their abbreviated names. The letters "SC" after the abbreviated name of a method means a scaled version of the method, while the symbol "Rn" means that a reinitialization process has been applied to the method with n being the number of reinitializations for each load increment.

4.1. Fletcher and Reeves method (CGFR)

Fletcher and Reeves [108] first modified the linear search proposed by Davidon [86] and applied it to the conjugate

	ABBREVIATED NAME	DESCRIPTION OF THE METHOD
WITHOUT LINEAR SEARCH	CGFRIN	The linear CG algorithm with the residuals and the stiffness matrix being modified after each iteration
	CGFRIP	The same method as above with the product kp_i being obtained as the product kx_i
	CGFRIL	A Newton-Raphson method, with linear solutions obtained from the CG algorithm
	CGFRIK	A Newton-Raphson method, with a conjugate gradient inversion of the stiffness matrix (Section 3.7)
	CGFR	Davidon's linear search as modified by Fletcher and Reeves and Davidon's cubic curve
WITH LINEAR SEARCH	CGST	Stanton's linear search and the regula falsi-bisection algorithm
	CGSR	A combined Stanton-Davidon linear search
	CGMEM	Memory gradient method
	CGBUC	Buchholdt's method
	CGSTPR	Stanton's linear search with Polak and Ribiere's algorithm for β_i
	CGSTSR	Stanton's linear search with Sorenson's algorithm for β_i

Table 4.1 Conjugate gradient computer programs used in Chapter 4

gradient method. The expression proposed for the evaluation of the step length (Eq. 3.14), requires an estimate of the total potential energy at the unconstrained minimum. Such an estimate is not generally known for structural problems. To cope with this difficulty the estimated value at the global minimum was replaced by the value of the total potential energy at the local minimum along the direction p of the previous iteration. Equation 3.14 is now slightly altered in order to give positive values for the step length

$$t = \frac{f_i(0) - f_{i-1}(0)}{f'_i(0)} \quad (4.1)$$

With this alteration, equations (3.14) and (3.15) for bracketing the root were not efficient, and as a result very much computer time was wasted, inside each iteration, until the root was finally bracketed. For this reason the tentative step was taken from 10 up to 100 times of that given by equation (4.1).

When the method was applied to example 1, 10 times the initial estimate produced the fastest convergence, while greater values tended to produce negative values for z , from equation (3.21), which meant that the computed minimum value for the total potential energy lay outside the bracketed interval (t_a, t_b) . In example 3, on the other hand, the best results were obtained with $h = 100.t$.

4.2. Stanton's method (CGST)

Stanton [262] suggested a method for bracketing the minimum potential energy along the direction p_i , and used this method together with the regula falsi-bisection algorithm for the nonlinear analysis of plates. In fact, the bracketing algorithm produced such accurate results that one iteration with the regula falsi-bisection algorithm was enough to locate a workable minimum for the next iteration.

Table 4.2 and Figure 4.1 show the response of the method, when reinitializations are used, for the suspension cable and the hyperbolic paraboloid test problems. With reinitialization, the return to the gradient direction takes place after N iterations, with N being the total number of degrees of freedom.

A reduction of up to 80% on the total number of iterations can be achieved by changing the direction p to g after N iterations. But as Figure 4.1 shows the response of the technique to these two examples is different. The reason for this is that the hyperbolic paraboloid problem has a condition number of 1508, while the free suspended cable has a condition number of 60056. In other words, as example 1 is an ill-conditioned problem, it seems that N iterations for resetting the direction are not enough to alleviate the zig-zag behaviour of p directions, after the introduction of the new direction. In these cases a larger number $N' > N$ should produce better results.

EXAMPLE	Nrein	N _{it}	EXAMPLE	Nrein	N _{it}
CASE STUDY 1 p = 60056	0	1008	CASE STUDY 2 p = 1508	0	1058
	1	894		1	226
	2	616		2	218
	3	625		3	212
	4	638		4	212
	5	640		5	212

RNORM criterion
($\epsilon = 0.1E-07$)

Table 4.2 The effect of reinitialization on the convergence of the CGST method

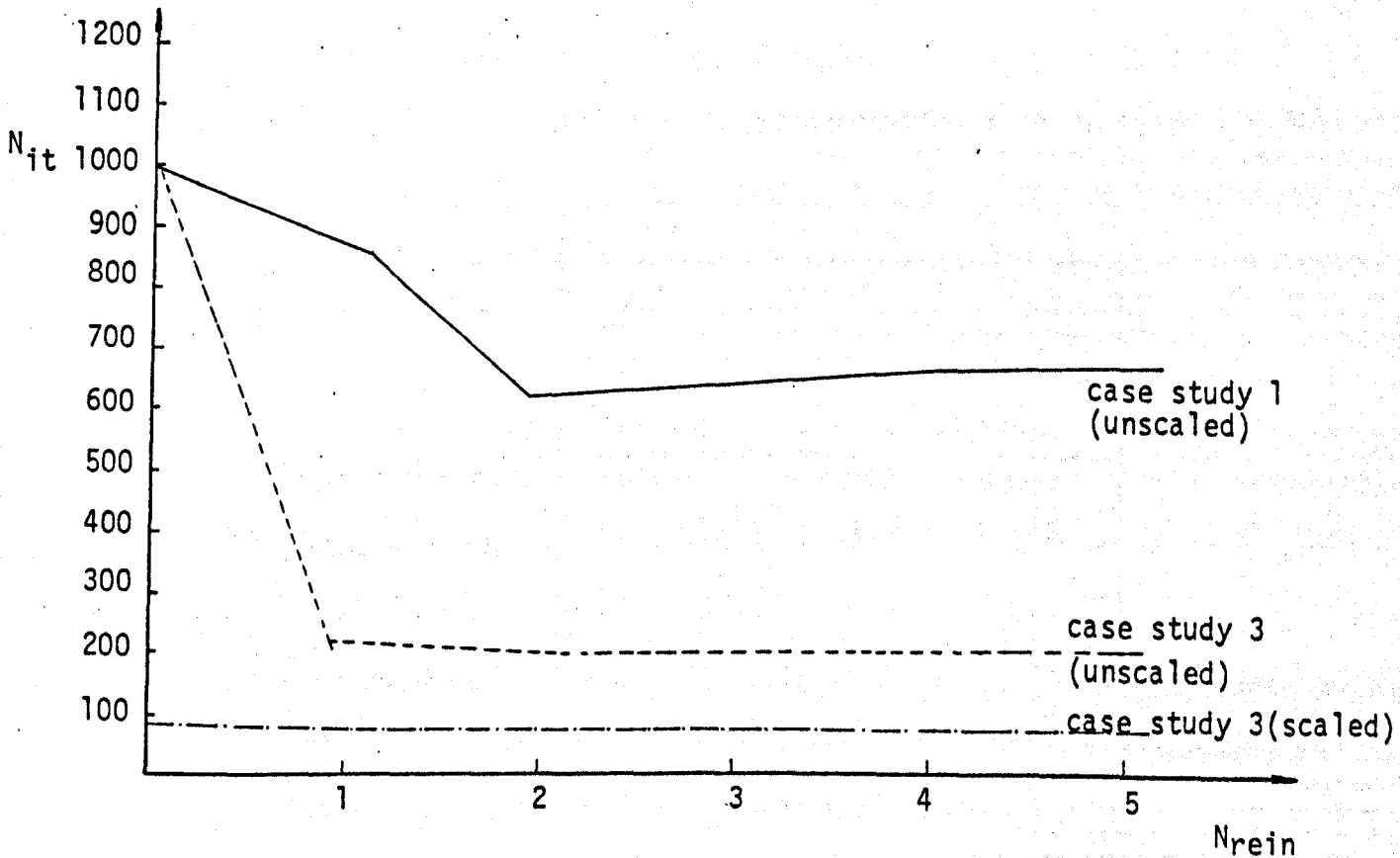


Fig 4.1 Graphical representation of the reinitialization effects for the CGST method

The implementation of the complete regula falsi-bisection algorithm for the linear search could sometimes be time consuming in trying to find an accurate approximation of the root inside the interval (t_a, t_b) . In fact, for most cases, equation (3.25) gives a very good approximation to the minimum root, and a more accurate one has virtually no effect on the overall convergence. This was justified when the method was scaled and applied to example 2. In this case the scaled values for t_b increased by more than 1000 times and the iteration process of the regula falsi-bisection algorithm was abandoned in order to make the method converge in reasonable time. Otherwise too much time was consumed in the effort to achieve convergence to the correct value t in each interval (t_a, t_b) .

Table 4.3 shows the effect of scaling on examples 2, 3 and 4. The improvement on the total execution time is less

EXAMPLE	METHOD	N _{it}	TIME(sec)
CASE STUDY 2	CGST	881	2.067
	CGST-SC	381	1.136
CASE STUDY 3	CGST	1058	5.668
	CGST-SC	90	0.605
CASE STUDY 4 (Members are not allowed to go slack)	CGST-R1	219	0.863
	CGST-SC-R1	158	0.763
CASE STUDY 4 (Members are allowed to go slack)	CGST-R1	1967	6.974
	CGST-SC-R1	221	1.040

Table 4.3. Effect of scaling in CGST method

than the improvement on the total number of iterations in all

cases. This is due to the additional number of operations required in each iteration for scaling operations.

The effect of scaling depends on the type of structure and degree of ill-conditioning as well as the degree of non-linearity of the problem. For examples 2 and 3 the condition numbers before and after scaling are as follows :

EXAMPLE 2	$P_{UNSC} = 12740$	$P_{UNSC} = 7861$
EXAMPLE 3	$P_{SC} = 1508$	$P_{SC} = 55$

For highly nonlinear problems, where there is a great difference in the diagonal terms of the stiffness matrix before and after the application of loads, an updated process must be introduced for the stiffness diagonals. Otherwise the original diagonal terms which are used for scaling, may differ considerably from the current values and have little effect in reducing the condition number of the stiffness matrix. This happened in case study 1 where there is a 10-fold increase of the stiffness matrix after the application of the load.

The effect of reinitialization in effectively scaled systems is less successful than in unscaled systems. This is shown in Figure 4.1 for the scaled hyperbolic paraboloid, where convergence is achieved in almost N iterations.

Two other methods, Polak-Ribiere's algorithm and Sorenson's algorithm with Stanton's linear search, have been studied and compared with the ordinary conjugate gradient method. Table 4.4

indicates that the modification introduced by Polak and Ribieve for the evaluation of the parameter β , gives marginal improvement on the convergence of the method, while the modification proposed by Sorenson has a bad effect on the convergence.

METHOD	N_{it}	TIME (sec)
CGST-SC	84	0.595
CGSTPR-SC	72	0.535
CGSTSR-SC	143	1.046

Table 4.4 Studies of example 3

Table 4.5 shows the performance of the CGST and CGSTPR algorithms for the large prestressed net of example 5.

Termination Parameter	0.1E-00		0.1E-02		0.1E-04		0.1E-06	
	N_{it}	TIME	N_{it}	TIME	N_{it}	TIME	N_{it}	TIME
CGST-SC-R4	170	5.243	433	13.265	634	19.396	851	26.016
CGSTPR-SC-R4	181	6.025	375	12.407	566	18.690	755	24.908

Table 4.5 Convergence of Stanton's algorithm for example 5 with QUOT-SC termination criterion

4.3. Other CG Algorithms

A combination of Stanton's linear search and Fletcher and Reeves' method was proposed. To eliminate the inaccuracy involving equation (3.14) in estimating the value of the total potential energy and the unconstrained minimum, Stanton's

bracketing technique was introduced, while the minimum in the interval (t_a, t_b) was approximated by Davidon's cubic curve. Davidon's fitting curve calculates the minimum in a more direct way, avoiding many iterative steps, as was experienced in the regula falsi-bisection algorithm, particularly for scaled applications of the method.

In the memory gradient method, different values of the parameter ϵ in equations (3.62), ranging from 1.0 to 0.1E-06, were tried in order to monitor how ϵ affects the convergence of the method. It was found that the value of ϵ has almost no effect on the convergence rate of the memory gradient method. However, the required degree of convergence of the parameters α and β , during the two dimensional search, could have a paramount effect on the overall convergence of the method. Figure 4.2 shows the number of iterations required for convergence in case study 1, for different values of the tolerance in the linear search.

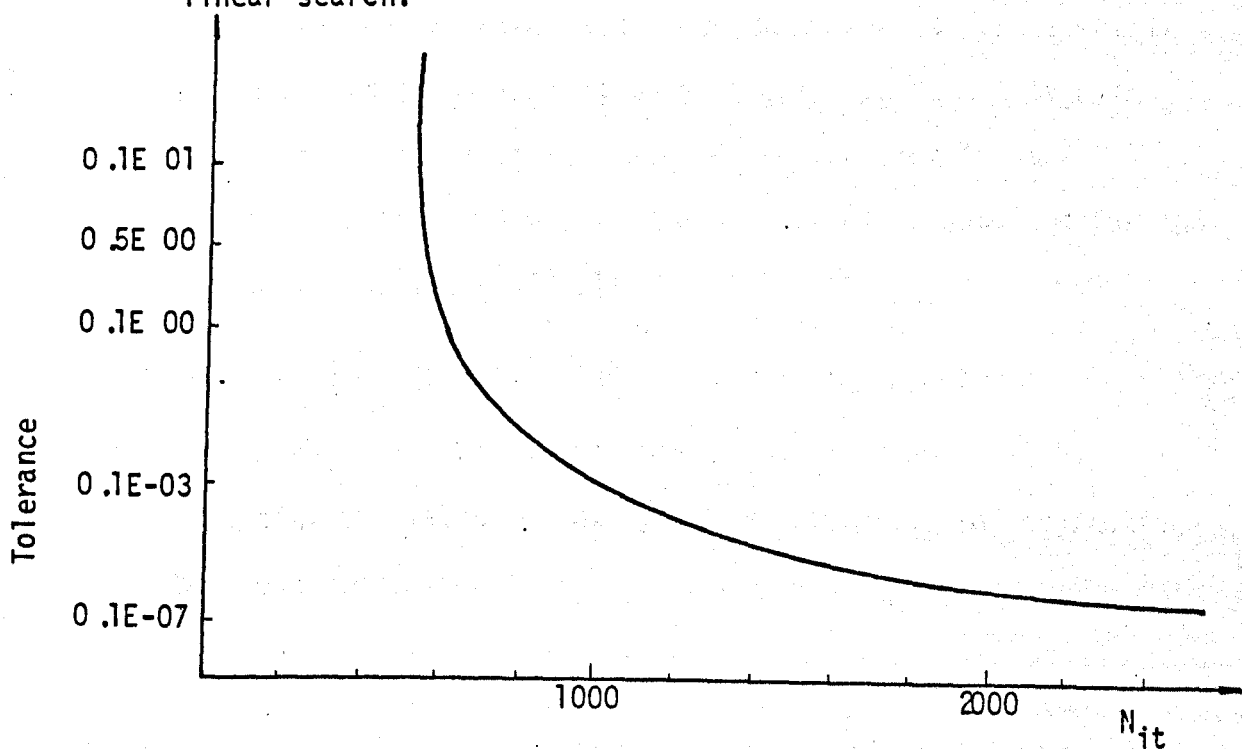


Fig. 4.2 Convergence of the memory method with respect to the value of the tolerance coefficient in the two dimensional search, case study 1

In Buchholdt's method the solution of the third order equation with respect to the step length t (eq. 3.32), was carried out both analytically and iteratively using Newton's method. The results obtained from these two solutions of the cubic equation were identical with respect to the final computed values, the number of iterations, and the required time.

Four other modifications of the conjugate gradient algorithm, without linear search, were applied. The CGFRIN method is the linear conjugate gradient algorithm, but with the residuals being calculated from equations (2.26,2.27) and updating the elemental contributions to the overall stiffness matrix at each iteration. The overall stiffness matrix is not assembled, since the required product Kp is performed at the elemental level and assembly is carried out only on the resulting vector.

The CGFRIP method does not update the stiffness matrix or perform the multiplication of the stiffness matrix with the vector p explicitly. Instead, the product Kp is obtained in the same way as the product Kx is obtained for the evaluation of the residuals :

$$r_i = Kx_i - F \quad (4.2)$$

The product Kp could be obtained from equation (4.2) by replacing the values of x_i by the values of p_i and neglecting the load vector.

The CGFRIL method is an exact linear application of the conjugate gradient method. After the convergence of the method to a residual load vector, the out of balance forces are calculated and the whole process is repeated until the norm of the residual loads converge to a specific tolerance. A modification of this approach is the CGFRIK method, where the linear solution is obtained by inverting the overall stiffness matrix in the way described in Section 3.7. Again there is no need to store the inverse stiffness matrix since the contributions to the product $\bar{A}^{-1}.F$ from every iteration can be computed independently.

The Fibonacci linear search was not included in this comparative study, because Murray [209] has already compared it with Davidon's linear search and has found the latter superior. Another powerful gradient method, the Fletcher and Powell variable metric method, has not been included here. The reason is that it has been shown [209] that although the method is very efficient for small cable problems, it becomes time consuming when applied to large systems with the additional disadvantage of requiring excessive computer storage.

4.4. Comparative Study

Table 4.6, shows the convergence achieved from different conjugate gradient methods when applied to example 1. It is clear from this table that the CGFRIN method, without linear search, is not efficient for the single cable problem which is highly nonlinear. From the methods with linear

METHOD	Nit	TIME(sec)
CGFRIN	495	1.428
CGMEM	115	0.628
CGBUC	510	0.603
CGSR	380	0.475
CGST	321	0.417
CGFR	372	0.535

RNORM
criterion
($\epsilon = 0.013$)

Table 4.6 Studies of example 1

METHOD	CGBUC ($\epsilon = 0.013$)		CGMEM ($\epsilon = 0.1E-07$)		CGST ($\epsilon = 0.1E-07$)	
	X(ft)	Y(ft)	X(ft)	Y(ft)	X(ft)	Y(ft)
1	1.67182	-4.51880	1.67246	-4.52056	1.67247	-4.52056
2	1.37778	-3.01083	1.37581	-3.00356	1.37581	-3.00356
3	-0.31507	4.64347	-0.31428	4.63620	-0.31428	4.63626
4	-2.82102	18.49347	-2.82121	18.49513	-2.82120	18.49515
5	-3.72436	-0.31120	-3.72382	-0.30505	-3.72382	-0.30505
6	-4.86456	-12.71990	-4.86553	-12.72376	-4.86553	-12.72374
7	-5.65333	-18.83940	-5.65376	-18.84064	-5.65376	-18.84067
8	-5.49830	-18.72180	-5.49874	-18.72333	-5.49874	-18.72333
9	-3.81410	-12.44180	-3.81103	-12.42774	-3.81105	-12.42775

Table 4.7 Final displacements of example 1

search, Stanton's algorithm is marginally quicker, while the convergence obtained from the memory gradient method is much in line with the convergence obtained from the other methods.

The final displacements of example 1, without initial prestressing force, are shown in Table 4.7. The results from the CGMEM and CGST methods having the same termination parameter are identical, while those obtained by the CGBUC method are only slightly different despite the big difference in the termination parameter. The CGBUC method on the other hand could not produce better convergence than $RNORM = 0.013$.

Table 4.8 and figure 4.3 show the convergence rates of six different conjugate gradient methods for the counterstressed dual cable structure of example 2, when the "QUOT" termination criterion is applied for all cases. It can be seen that the memory gradient method has an extremely slow rate of convergence, in contrast to the CGFRIN method without linear search which is extremely fast in the first stages. The CGST method produced the smallest residual norm, while Buchholdt's method could not improve beyond $\epsilon = 0.1E-02$.

Table 4.9 and figure 4.4 show the convergence rates of nine different combinations of the conjugate gradient algorithm for the hyperbolic paraboloid structure of example 3. Again the memory gradient method proved extremely slow for this problem. Buchholdt's method produced the fastest convergence up to $\epsilon = 0.1E-02$ and then stopped improving with further iterations.

Termination Parameter ϵ		0.1E-00		0.1E-01		0.1E-02		0.1E-03		0.1E-04		0.1E-05		0.1E-06	
No.	METHOD	N_{it}	TIME	N_{it}	TIME	N_{it}	TIME	N_{it}	TIME	N_{it}	TIME	N_{it}	TIME	N_{it}	TIME
1	CGFRIN	5	0.080	115	0.162	557	0.778	-	-	-	-	-	-	-	-
2	CGMEM	1349	4.473	5655	18.750	-	-	-	-	-	-	-	-	-	-
3	CGFR	103	0.243	186	0.397	271	0.552	414	0.815	636	1.336	-	-	-	-
4	CGSR	249	0.479	379	0.725	526	1.004	685	1.305	-	-	-	-	-	-
5	CGBUC	99	0.196	159	0.314	271	0.536	-	-	-	-	-	-	-	-
6	CGST	92	0.18	173	0.345	285	0.557	368	0.72	442	0.864	525	1.027	618	1.209

Table 4.8 Studies of example 2

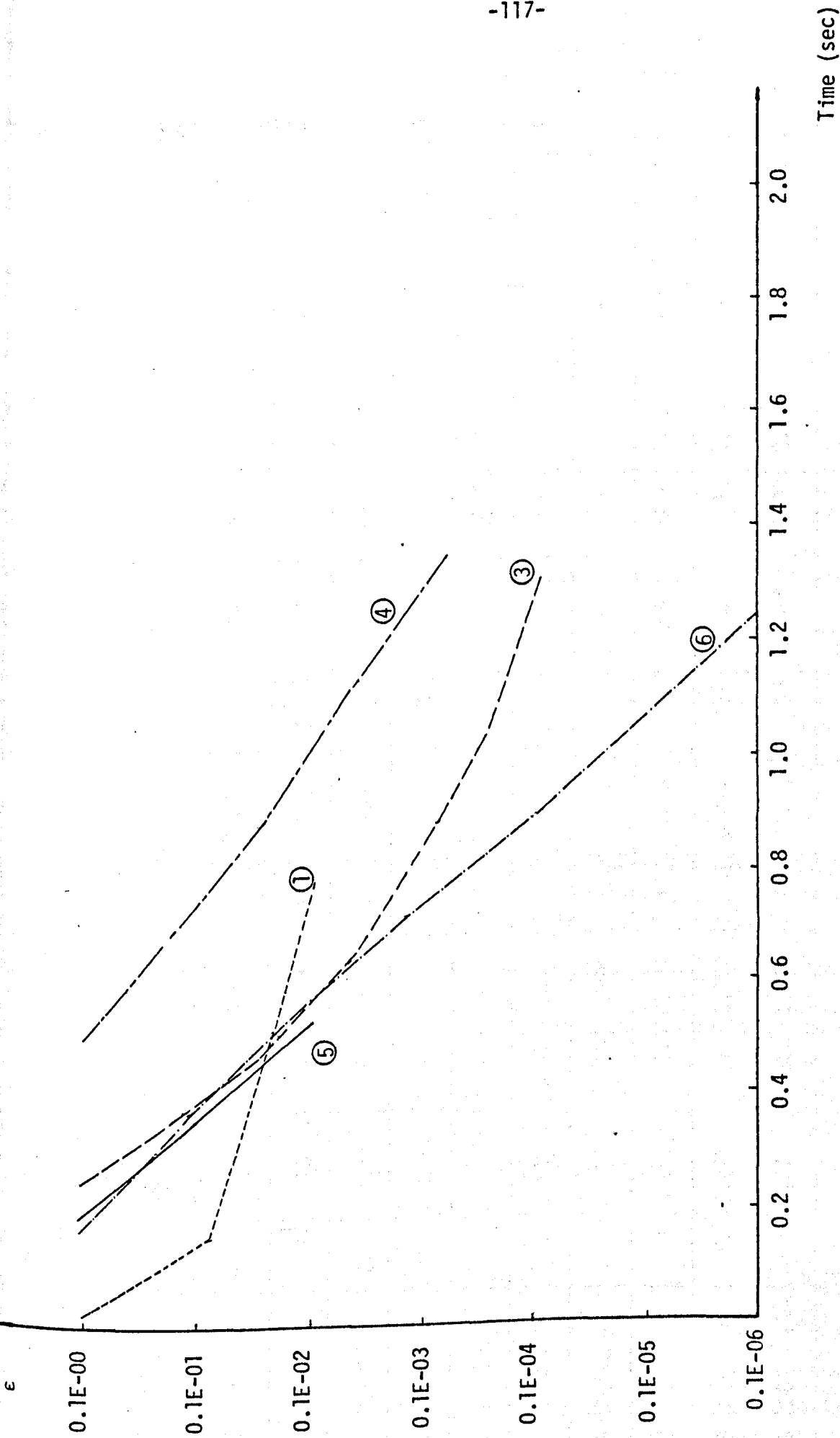


Fig. 4.3. Example 2. Results from Table 4.8

Termination Parameter ϵ		0.1E-00		0.1E-01		0.1E-02		0.1E-03		0.1E-04		0.1E-05		0.1E-06	
METHOD		N_{it}	TIME	N_{it}	TIME	N_{it}	TIME	N_{it}	TIME	N_{it}	TIME	N_{it}	TIME	N_{it}	TIME
1	CGFRIN	35	0.515	65	0.954	100	1.466	255	3.733	-	-	-	-	-	-
2	CGFRIP	292	1.171	527	2.111	7298	29.188	-	-	-	-	-	-	-	-
3	CGFRIL	243	2.190	-	-	-	-	309	2.786	-	-	-	-	367	3.587
4	CGFRIK	-	-	-	-	-	-	-	-	319	6.495	-	-	-	-
5	CGMEM	602	5.242	3977	34.646	-	-	-	-	-	-	-	-	-	-
6	CGBUC	37	0.194	59	0.308	90	0.470	-	-	-	-	-	-	-	-
7	CGFR	51	0.266	77	0.383	126	0.603	201	1.047	240	1.251	423	2.45	765	4.696
8	CGSR	50	0.251	75	0.366	98	0.474	131	0.625	175	0.889	-	-	-	-
9	CGST	180	0.778	308	1.320	430	1.854	556	2.397	683	2.940	809	3.48	935	4.032

Table 4.9 . Studies of example 3

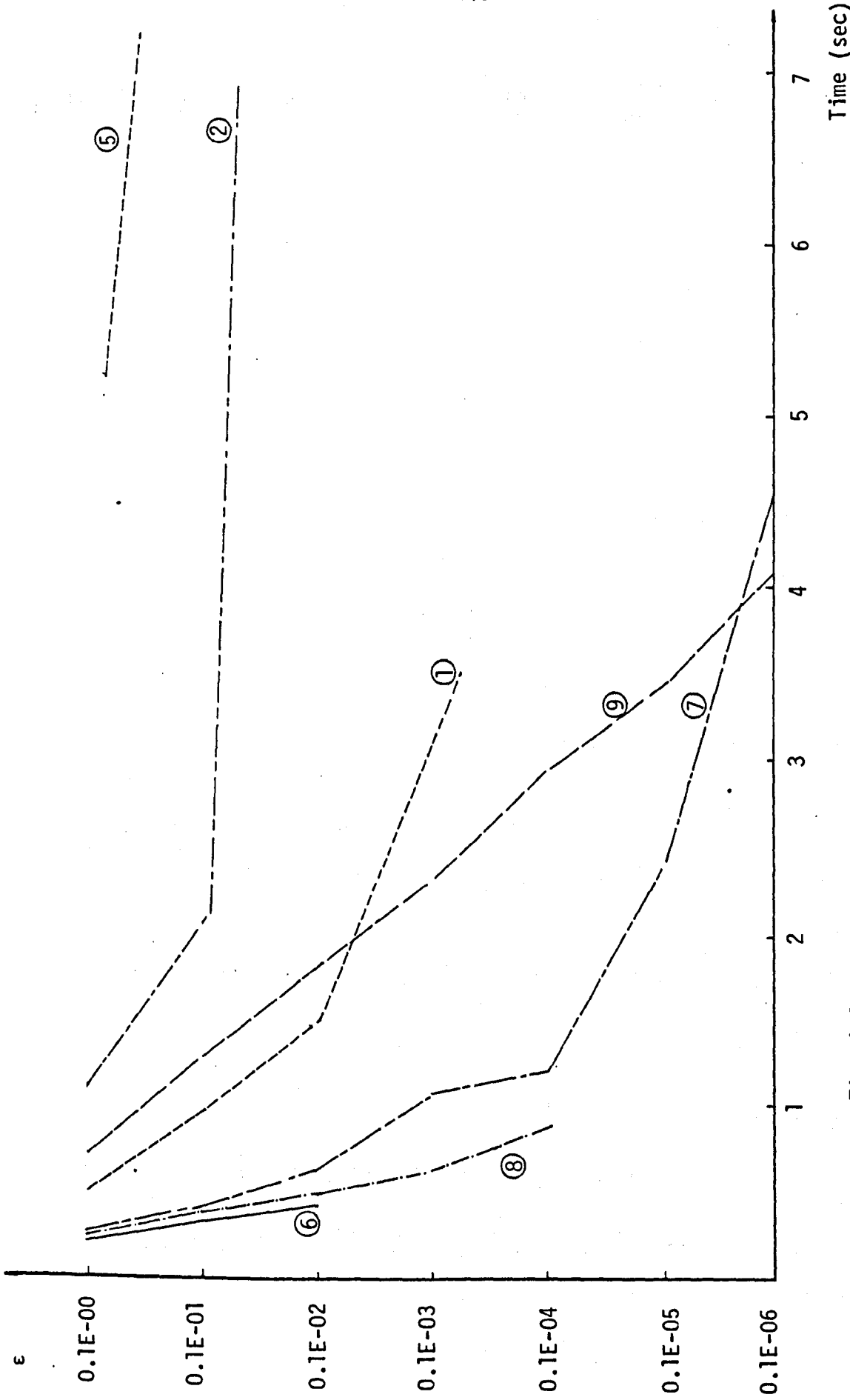


Fig. 4.4. Example 3. Results from Table 4.9

The combination of Stanton's and Davidon's algorithms worked very efficiently up to $\epsilon = 0.1E-04$, while Stanton's and Fletcher and Reeves' methods reached the final termination criterion, with the latter method being considerably faster than the second. Another interesting point is that the CGFRIN without linear search gave very workable results which were better than the CGST method in the first stages.

The final displacements of example 3, using the CGBUC, CGFRIN and CGST methods, are shown in Table 4.10. The results again vary insignificantly between the methods despite the difference in the final termination parameter.

Table 4.11 and figure 4.5 show the convergence rates of the Buchholdt and Stanton methods when scaling and reinitialization processes are applied. It can be seen that when the scaled termination criterion "QUOT-SC" is used the two methods almost coincide up to $\epsilon = 0.1E-03$ and from then on CGBUC ceases improving. But when the unscaled true termination criterion is used Buchholdt's method stops at $\epsilon = 0.1E-1$, while Stanton's method converges up to the final value of ϵ with almost the same rate of convergence as before. We can also see that the reinitialization process has a negligible effect on the CGST-SC method and a marginal effect on the CGBUC-SC method.

Table 4.13 shows that reinitialization every $(N + 1)$ steps for the CGFRIP method, when applied to example 3, did not improve the rate of convergence. The zig-zag behaviour of p

METHOD	CGBUC ($\epsilon = 0.1E-02$)			CGFRIN ($\epsilon = 0.1E-04$)			CGST ($\epsilon = 0.1E-07$)		
node	X(ft)	Y(ft)	Z(ft)	X(ft)	Y(ft)	Z(ft)	X(ft)	Y(ft)	Z(ft)
1	0.00000	-0.02226	0.37720	0.00000	-0.02224	0.37714	0.00000	-0.02224	0.37715
3	0.00000	-0.06530	1.27218	0.00000	-0.06527	1.27194	0.00000	-0.06527	1.27195
4	0.01455	-0.02921	0.73465	0.01456	-0.02921	0.73480	0.01456	-0.02921	0.73478
7	0.00000	-0.08823	3.71902	0.00000	-0.08817	3.71972	0.00000	-0.08818	3.71972
8	-0.01337	-0.04250	1.73505	-0.01335	-0.04251	1.73570	-0.01335	-0.04251	1.73570
13	0.00000	0.00891	1.72688	0.00000	0.00896	1.72772	0.00000	0.00896	1.72772
14	0.01696	-0.01133	1.26586	0.01696	-0.01133	1.26641	0.01696	-0.01133	1.26641
15	0.01576	-0.00190	0.74058	0.01577	-0.00189	0.74087	0.01577	-0.00189	0.74087
19	0.00000	0.02032	1.01835	0.00000	0.02037	1.01936	0.00000	0.0204	1.01935
20	0.01685	0.00536	0.82975	0.01687	0.00538	0.83063	0.01687	0.00538	0.83062
21	0.01854	0.00684	0.46540	0.01855	0.00685	0.4658	0.01855	0.00685	0.46580
23	0.00000	0.01963	0.60678	0.00000	0.01967	0.60745	0.00000	0.0020	0.60744
24	0.00926	0.00930	0.41979	0.00926	0.00933	0.42017	0.00926	0.00933	0.42002
25	0.00000	0.01023	0.25478	0.00000	0.01022	0.25482	0.00000	0.01022	0.25482

Table 4.10. Example 3. Final displacements

Termination Parameter ϵ		0.1E-00		0.1E-01		0.1E-02		0.1E-03		0.1E-04		0.1E-05		0.1E-06	
METHOD		N_{it}	TIME	N_{it}	TIME	N_{it}	TIME	N_{it}	TIME	N_{it}	TIME	N_{it}	TIME	N_{it}	TIME
1	CGBUC-SC QUOT-SC	5	0.040	13	0.104	25	0.201	34	0.272	-	-	-	-	-	-
2	CGST-SC QUOT-SC	5	0.039	15	0.117	28	0.218	36	0.280	45	0.351	52	0.406	66	0.515
3	CGBUC-SC QUOT	14	0.095	307	1.860	-	-	-	-	-	-	-	-	-	-
4	CGST-SC QUOT	19	0.128	32	0.208	40	0.257	47	0.301	58	0.368	69	0.436	78	0.492
5	CGBUC-SC-R3 QUOT	14	0.095	90	0.553	-	-	-	-	-	-	-	-	-	-
6	CGST-SC-R3 QUOT	19	0.127	32	0.208	40	0.257	47	0.301	58	0.369	69	0.437	77	0.486

Table 4.11. Studies of Example 3 .

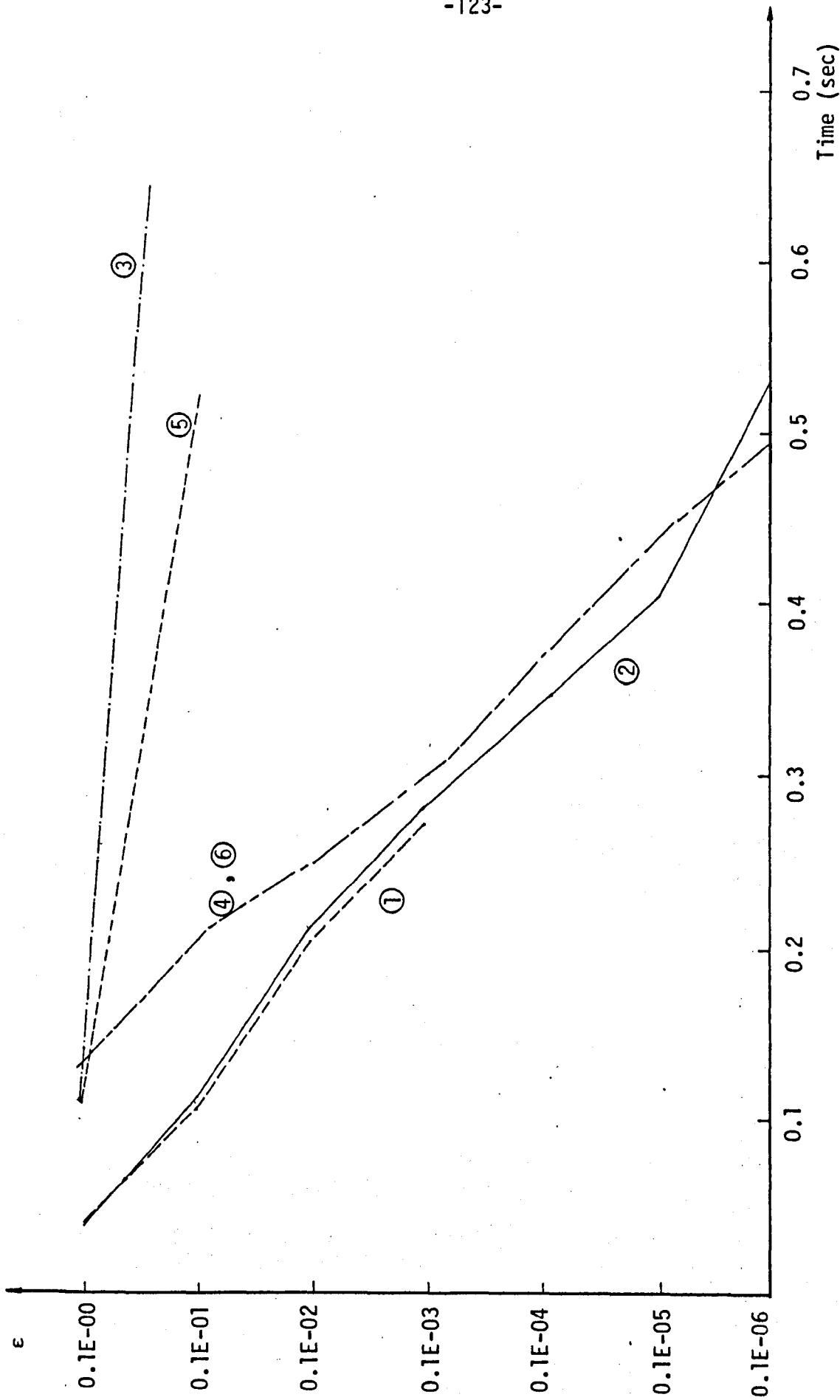


Fig. 4.5 Example 3. Results from Table 4.11.

	CGST (RNORM $\leq 0.1E-07$)		CGBUC (energy criterion)	
Node	X(ft)	Y(ft)	X(ft)	Y(ft)
1	0.23972	1.6334	0.2398	1.6350
2	0.34445	2.54673	0.3445	2.5486
3	0.35334	2.73181	0.3534	2.7343
4	0.30659	2.18763	0.3066	2.1910
5	0.24498	0.91711	0.2449	0.9207
6	0.23247	-0.42154	0.2323	-0.4180
7	0.25872	-1.17735	0.2385	-1.1738
8	0.26617	-1.3540	0.2659	-1.3514
9	0.19825	-0.95792	0.1981	-0.9570
10	-0.29627	1.61924	-0.2965	1.6206
11	-0.39836	2.52976	-0.3986	2.5322
12	-0.37904	2.71777	-0.3793	2.7211
13	-0.31317	2.17708	-0.3134	2.1815
14	-0.27630	0.91038	-0.2764	0.9142
15	-0.29428	-0.42668	-0.2943	-0.4237
16	-0.31057	-1.18405	-0.3105	-1.1810
17	-0.28988	-1.36223	-0.2898	-1.3601
18	-0.1976	-0.96530	-0.1976	-0.9645

Table 4.12 Final displacements, example 2

ϵ \ NSD	0	1	Every (N+1) _{it}
10^{-2}	292	295	372
10^{-3}	527	483	1356
10^{-4}	7298	7291	7942

Table 4.13. Studies on the CGFRIP method, example 3

direction remained unaffected after one reinitialization, while reinitialization after every $N + 1$ steps produced negative results.

4.5. Conclusions

The main objective of this chapter has been to find the most reliable and efficient conjugate gradient method for the nonlinear analysis of cable structures. As was expected, the methods with a step length evaluated from a linear search procedure proved more efficient than the linearised conjugate gradient methods. Only the memory gradient method with a two dimensional linear search gave inferior results to the linearised methods for problems with a relatively large number of degrees of freedom. When applied to small problems the method was competitive with the other methods and could prove even better when applied to optimization problems with only a few variables [67]. However, when the memory method was applied to the special eigenvalue problem (see Chapter 6), where the function is homogenous and the two dimensional search can be performed analytically rather than iteratively, the efficiency of the method was greatly improved.

The linear version of the conjugate gradient algorithm combined with a Newton Raphson iteration technique gave better results than the linearised methods. The current stiffness matrix is inverted on an elemental basis without the need to form and handle the overall stiffness matrix as in the stiffness

approach (see Chapter 8). This method is very straightforward, very easy to program, and combines the advantages of the conjugate gradient algorithm and the Newton Raphson approach.

The second linear conjugate gradient method (CGFRIK) combined with the Newton Raphson approach, gave inferior results to the CGFRIL. One explanation could be that the inversion process generally destroys the sparsity of the matrix and the number of operations is increased. This method could be helpful when the inverse of a matrix is explicitly required. In this case the inverse can be compactly stored in the non square matrix $P(N, N_{it})$, where N_{it} is the number of executed iterations [115].

Of the two remaining linearized methods, the CGFRIN gave the more consistent results. In this method the residuals are updated in each iteration using equations (2.26, 2.27) instead of the recursive relationship of algorithm (3.11). The element stiffness matrices are also updated in each iteration such as to reflect their dependence on x . The method produced acceptable results for problems with moderate non-linearity but when applied to more nonlinear problems the convergence rate worsened and sometimes the method failed to converge. The CGFRIP method does not perform the multiplication $K.p$ explicitly as in the CGFRIN method. Instead, the product $K.p$ is obtained in the same way as the product Kx for the evaluation of the residuals. But although the required time per iteration was reduced by a factor of 4, the overall computer

time was increased. This happened because the approximation involved in the calculation of the product Kp deteriorated the conjugate gradient directions and worsened the zig-zag phenomenon. For this reason the reinitialization process after $(N + 1)$ iterations did not improve convergence. A more positive effect from the reinitialization could have been produced if the reinitializations had taken place after more than $(N + 1)$ iterations.

The initial scaling and reinitialization techniques improved the convergence of the linearized methods, but not to the same extent as in the methods with a linear search algorithm.

The nonlinear conjugate gradient algorithms, with step length algorithms produced almost similar results with the exception, of course, of the memory gradient method. The Fletcher and Reeves algorithm, with the bracketing formula based on an estimate of the value of the total potential energy at the minimum, and with Davidon's cubic curve for evaluating the minimum along the search line, gave very competitive results for bigger values of the termination parameter ϵ . But as ϵ became smaller the rate of convergence deteriorated and the method ceased to become competitive. This phenomenon could be explained by the approximation involved in evaluating the minimum from the cubic curve (eq. 3.21).

The combination of Stanton's bracketing algorithm and Davidon's cubic curve, gave the best results in example 3

and the worst results in example 2. It seems that the same approximations involved in evaluating the local minimum from the cubic curve, affected the convergence of the method in the same way as in the CGFR method for small values of the termination parameter ϵ .

Buchholdt's method proved a very powerful method. It is very easy to program and to implement and has the more simple and straightforward evaluation of the step length. The total potential energy is approximated by a fourth order polynomial with respect to the step length. The required minimum along the p direction is located from the solution of a third order equation produced from the differentiation of the total potential energy expression with respect to the step length. The method has also its limitations in that although there are significant computational advantages in the use of a 4th order polynomial expression for the total potential energy, higher order polynomials may have to be derived for different structural systems.

Another disadvantage of Buchholdt's method is its inability to converge to small values of the termination parameter ϵ . It is this lack of "well-behaviour" of the method that makes the termination, based on the residual norm difficult to obtain for small values of the termination parameter ϵ . The reason for this inability of the method to converge to small ϵ , it is believed, lies in the approximations involved in the evaluation of the parameters C_i of the

fourth order total potential energy polynomial.

Stanton's algorithm for bracketing the solution and the consequent application of the regula falsi-bisection algorithm in the CGST method gave the most consistent results of all the conjugate gradient algorithms employed in this work. The bracketing formula proved very efficient in all the applications of the method and the regula falsi-bisection algorithm needed only a few iterations to approximate the minimum, up to a workable accuracy, along the search line. Sometimes, however, accuracy in the evaluation of the step length could badly affect the convergence of the method (Fig. 4.4). The method has an excellent "well-behaviour" and produced always the same accuracy with the second order Newton Raphson method. It has also been applied to other type of structural problems with very successful results [262] .

CHAPTER 5

RELAXATION METHODS

5.1. Dynamic Relaxation

5.1.1. Historical Development

The method was originally conceived when Day [88] noticed the similarity between the equations of tidal flow he had previously studied with Otter [291] with the equations of damped elastic vibration. The technique of replacing the equations of continuity with the constitutive equations of elasticity, replacing the equation of fluid motion with the equations of motion, and then carrying out a step-by-step integration of the damped elastic oscillations of a structure was called "dynamic relaxation".

The method is based on the fact that a system undergoing damped vibration, excited by a constant force, ultimately comes to rest in the displaced position of static equilibrium of the system under the action of the force. The static solution of structural problems was then regarded as the limiting equilibrium condition of damped structural vibrations.

Newmark [212] had previously commented on the possibility of determining the static behaviour of a structure through a damped dynamic procedure. Later Chaundhury et al [75] and Hussay [224] proposed a damped Newmark method for the static

solution, but the implicit integration scheme of Newmark 's method put the technique at a disadvantage compared with the explicit central difference formulation for dynamic relaxation [185].

The application of dynamic relaxation in the early years of its introduction was almost exclusively associated with the finite difference formulation in space of both the equations of motion and the constitutive relationships. It is in this form that the technique has been applied to the static analysis of a variety of engineering problems together with the implementation of interlacing nets to specify the stress and displacement variables.

Otter [222] applied the method for the stress analysis of a pressure vessel and Otter, Cassel and Hobbs [223] for the analysis of a cylindrical arch dam, using cylindrical polar coordinates. Rushton [248] studied the plane stress problem of tensile loading of a flat plate containing grooves. The small deflection bending analysis of thin plates was examined by Day [89] and Rushton [247], while Cassel et al [69] and Peters [229] studied the application of dynamic relaxation to the analysis of cylindrical shells using full shell equations.

Nonlinear material effects were first included by Holland [140], who examined local stresses in prestressed concrete following a curvilinear stress-strain path up to cracking. Stamenkovic [275] examined a similar problem in a column-slab intersection. The large deflection of plates under transverse

loading has been analysed by Rushton [249, 251] , Cassel and Hobbs [71] , and Tuma and Galletly [288] ; while the combination of material and geometric nonlinearities has been examined by Rushton and Hook [252] . An incremental load procedure has been used by Lowe and Flint [183] to investigate the collapse behaviour of a single span composite bridge. Basu and Dawson [20] analysed rectangular isotropic and orthotropic plates with significant shear deformations.

Finite element spatial idealizations of dynamic relaxation have been less widely used. The first to use this method for the solution of linear simultaneous equations arising from the finite element idealization of plates were Lynch, Kesley and Saxe [185] . Brew and Brotton [38] used dynamic relaxation for the analysis of plane frames subject to large deflections, elastic instability and plasticity. Their formulation employed the explicit nature of the method by omitting the formulation of the overall stiffness matrix. Bunce and Brown [63] also applied the method to the finite deflection analysis of plane frames.

The first application to tension structures with geometrically nonlinear behaviour was published by Day and Bunce [91] . Barnes [12,13] applied the method to the analysis of large cable networks. He also extended dynamic relaxation to the form-finding of networks, membrane and pneumatic structures [14,16] . In the field of optimization of the form of triangulated space structures the method has also been applied successfully by

Barnes [18] for the design of structures subject to a dominant loading, and further developed by Topping [285] to deal with multiple loading and deflection constraints.

It is of interest to note that dynamic relaxation has also been applied to the solution of some transient problems ; i.e. a transient 3-dimensional thermal stress analysis [213] , the response of a beam to a moving load [298] , the dynamic analysis of tension structures [15,315] and a 3-dimensional application to rock mechanics [79] .

5.1.2. Formulation of the Iterative Procedure

The following discussion applies to the solution of a system of linear equations which results from the application of the stiffness method of structural analysis. The system of equations for which a solution is sought is given by

$$Kx = F \quad (5.1)$$

with the solution

$$x^* = K^{-1}F \quad (5.2)$$

In order to achieve this solution by the method of dynamic relaxation, equation (5.1) is transformed into an equation of motion by introducing point masses and viscous damping forces at the nodes

$$M\ddot{x} + C\dot{x} + Kx = F \quad (5.3)$$

where M and C are the mass damping diagonal matrices respectively and the dots indicate differentiation with respect

to time.

Equation (5.3) is then integrated for displacement response under the load F , until the system achieves a steady state equilibrium. Equation (5.3) may now be written using centred finite differences in time as :

$$M \left[\frac{\dot{x}^{k+\frac{1}{2}} - \dot{x}^{k-\frac{1}{2}}}{h} \right] + C \left[\frac{\dot{x}^{k+\frac{1}{2}} + \dot{x}^{k-\frac{1}{2}}}{2} \right] + Kx^k = F \quad (5.4)$$

where superscripts indicate time stations and h is the time step. From equation (5.4) the recurrence equation for the velocities may be expressed as

$$\dot{x}^{k+\frac{1}{2}} = \left[\frac{1}{h} M + \frac{1}{2} C \right]^{-1} \left[\frac{1}{h} M - \frac{1}{2} C \right] \dot{x}^{k-\frac{1}{2}} + \left[\frac{1}{h} M + \frac{1}{2} C \right]^{-1} [F - Kx^k] \quad (5.5)$$

Since equation (5.3) does not have to represent the true dynamic behaviour of the structural system, but is merely a means to arrive at the steady state response of the static solution, the selection of the parameters involving mass, damping and time step is in principle arbitrary. Both mass and damping matrices are assumed to be proportional to the main diagonal terms of K

$$M = \rho D \quad \text{and} \quad C = cD \quad (5.6)$$

with D being the diagonal matrix of the main diagonal terms of K .

Using equation (5.6), equation (5.5) becomes

$$\dot{x}^{k+\frac{1}{2}} = \left[\frac{2 - \frac{ch}{\rho}}{2 + \frac{ch}{\rho}} \right] \dot{x}^{k-\frac{1}{2}} + \left[\frac{\frac{2h}{\rho}}{2 + \frac{ch}{\rho}} \right] D^{-1} [F - Kx^k] \quad (5.7)$$

Using the standard central finite difference form for the relationship between displacements and velocities, the equation for x^{k+1} becomes

$$x^{k+1} = x^k + h \dot{x}^{k+\frac{1}{2}} \quad (5.8)$$

Equations (5.7) and (5.8) represent the iterative process for the finite element formulation in space of dynamic relaxation. Starting with an initial approximation of zero for the displacements and assuming that the velocities at the start of the iteration obey the relationship

$$v_i^{-\frac{1}{2}} = v_i^{\frac{1}{2}} \quad (5.9)$$

calculate the new velocities from equation (5.7) and subsequently from equation (5.8) the new displacements. This iterative process is carried out until both the velocities and the residuals

$$R = F - Kx^k \quad (5.10)$$

reach acceptably small values.

5.1.3. Asymptotic convergence of Dynamic Relaxation

The subsequent analysis is due to Lynch et al [185]

who transformed the iterative process into a standard eigenvalue problem for error vectors and examined quantitatively the convergence of the method.

Any basic iterative method can be expressed as

$$x^{k+1} = H D^{-1} F + (I - H D^{-1} K) x^k \quad (5.11)$$

where H is the characteristic matrix of the iterative method. Subtracting the true solution given by equation (5.2) from equation (5.11) we obtain the relationship between successive error vectors

$$\epsilon^{k+1} = M \epsilon^k \quad (5.12)$$

where

$$\epsilon^k = x^k - x^*$$

$$M = (I - H D^{-1} K)$$

x^* is the true solution vector

Convergence for the purpose of this discussion will refer to the rate at which the error vector decays with each iterative step. If the parameter λ gives this rate, then

$$\epsilon^{k+1} = \lambda \epsilon^k \quad (5.13)$$

and substituting equation (5.13) into equation (5.12) gives

$$[\lambda I - M] \epsilon = 0 \quad (5.14)$$

If M is $N \times N$, there are N eigenvalues λ_i and N associated eigenvectors that control the way in which the error vector

converges to zero. In the complete process only the error mode with the largest modulus λ_i need be considered since this dictates the asymptotic rate of convergence.

Turning now to dynamic relaxation, after substituting equation (5.7) into equation (5.8), the expression for x^{k+1} becomes

$$x^{k+1} = x^k + \alpha(x^k - x^{k-1}) + \gamma [D^{-1}F - D^{-1}K x^k] \quad (5.15)$$

with

$$\alpha = \frac{2 - \frac{ch}{\rho}}{2 + \frac{ch}{\rho}}, \quad \gamma = \frac{\frac{2h^2}{\rho}}{2 + \frac{ch}{\rho}} \quad (5.16)$$

Subtracting the true solution given by equation (5.2) from equation (5.15), gives

$$\epsilon^{k+1} - \epsilon^k = \alpha \epsilon^k - \alpha \epsilon^{k-1} - \gamma B \epsilon^k \quad (5.17)$$

where

$$B = D^{-1}K$$

which can also be written as

$$\epsilon^{k+1} = [\beta I - \gamma B] \epsilon^k - \alpha \epsilon^{k+1} \quad (5.18)$$

with

$$\beta = \alpha + 1$$

Equation (5.13) can also be written as

$$\epsilon^{k+1} = \lambda_{DR} \epsilon^k = \lambda_{DR}^2 \epsilon^{k-1} \quad (5.19)$$

Substituting these relations into equation (5.18), the eigenvalue problem in terms of the error vector can be stated as

$$\left[\left(\frac{\lambda_{DR}^2 - \lambda_{DR}^{\beta + \alpha}}{\lambda_{DR}^\gamma} \right) I + B \right] \epsilon = 0 \quad (5.20)$$

If λ_{iB} denotes the N eigenvalues of B given by

$$[\lambda_B I - B] \epsilon = 0 \quad (5.21)$$

then from equations (5.20) and (5.21) comes the following relation

$$\lambda_{DR}^2 - (\beta - \gamma\lambda_B) \lambda_{DR} + \alpha = 0 \quad (5.22)$$

Therefore the roots of equation (5.22) will be :

(a) Complex conjugate if $\left(\frac{\beta - \gamma\lambda_B}{2} \right) < \alpha$

(b) Two equal roots if $\left(\frac{\beta - \gamma\lambda_B}{2} \right) = \alpha$

(c) Two unequal roots if $\left(\frac{\beta - \gamma\lambda_B}{2} \right) > \alpha$

With complex conjugate roots the modulus λ_{DR} is independent of λ_B and is given by

$$|\lambda_{DR}| = \sqrt{\alpha} = \sqrt{\frac{2 - \frac{ch}{\rho}}{2 + \frac{ch}{\rho}}} \quad (5.23)$$

The roots will be real when

$$\frac{c^2 h^2}{\rho^2} = \frac{\lambda_B h^2}{\rho} \left(4 - \frac{\lambda_B h^2}{\rho} \right) \quad (5.24)$$

While for the two unequal roots the modulus of the larger root is given by

$$|\lambda_{DR}| = \left[\frac{1}{2 + \frac{ch}{\rho}} \left| 2 - \frac{\lambda_B h^2}{\rho} \right| + \sqrt{\frac{\lambda_B^2 h^4}{\rho^2} - \frac{4\lambda_B h^2}{\rho} + \frac{c^2 h^2}{\rho^2}} \right] \quad (5.25)$$

Figures 5.1 and 5.2 show graphically the relation of the largest modulus of λ_{DR} to ch/ρ for constant values of $\lambda_B \frac{h^2}{\rho}$, and to $\lambda_B \frac{h^2}{\rho}$ for constant values of $\frac{ch}{\rho}$ respectively.

5.1.4. Evaluation of the Optimum Iteration Parameters

The optimum parameters are those which give the best asymptotic convergence or the minimum $|\lambda_{DR}|$. Figure 5.3 shows that for a given value of the parameter $\lambda_B \frac{h^2}{\rho}$ the minimum $|\lambda_{DR}|$ is obtained when the roots of equation(5.22) are real and equal. Therefore the value of ch/ρ that gives two equal roots is considered analogous to critical damping.

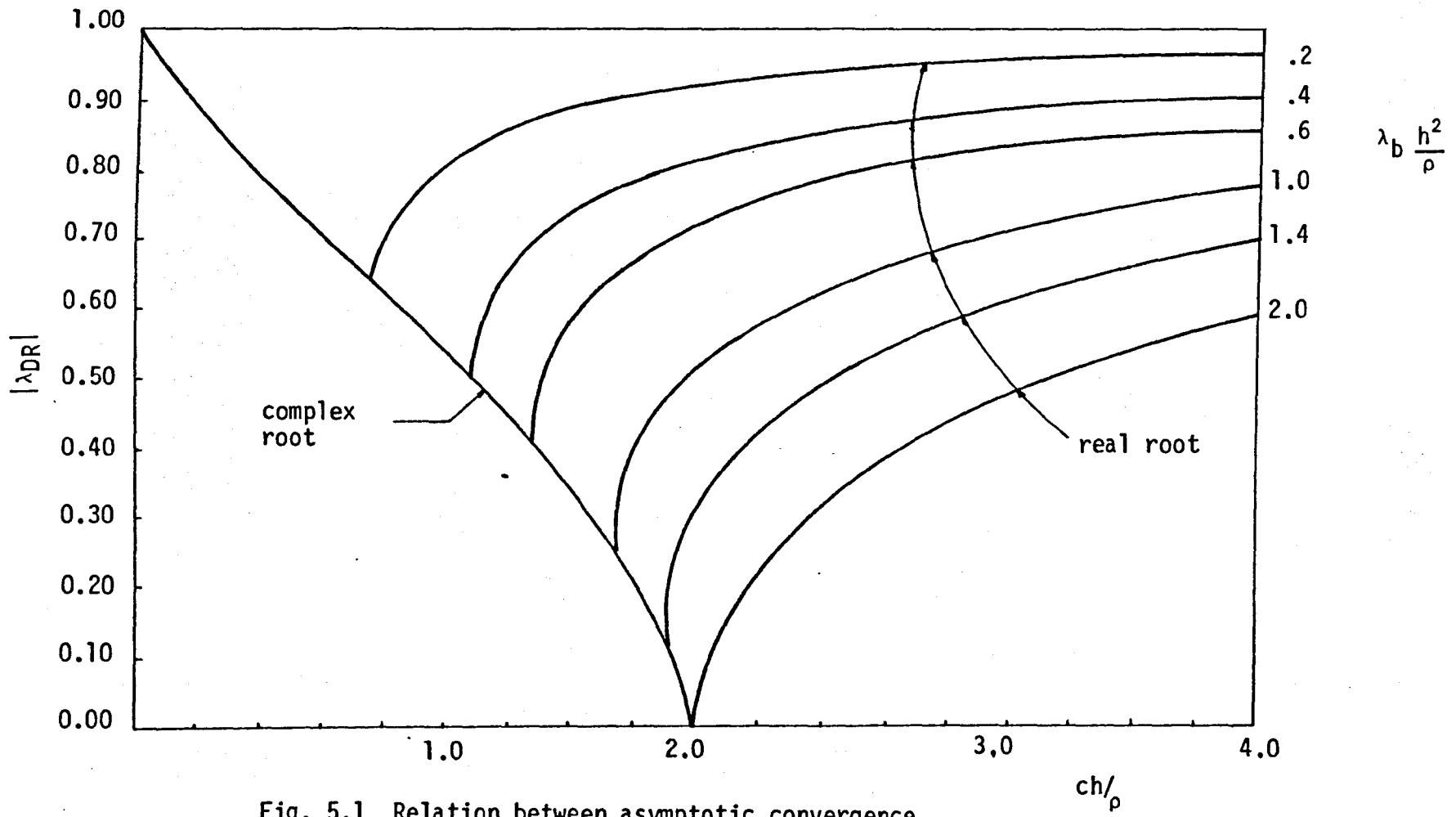


Fig. 5.1 Relation between asymptotic convergence and ch/ρ in dynamic relaxation

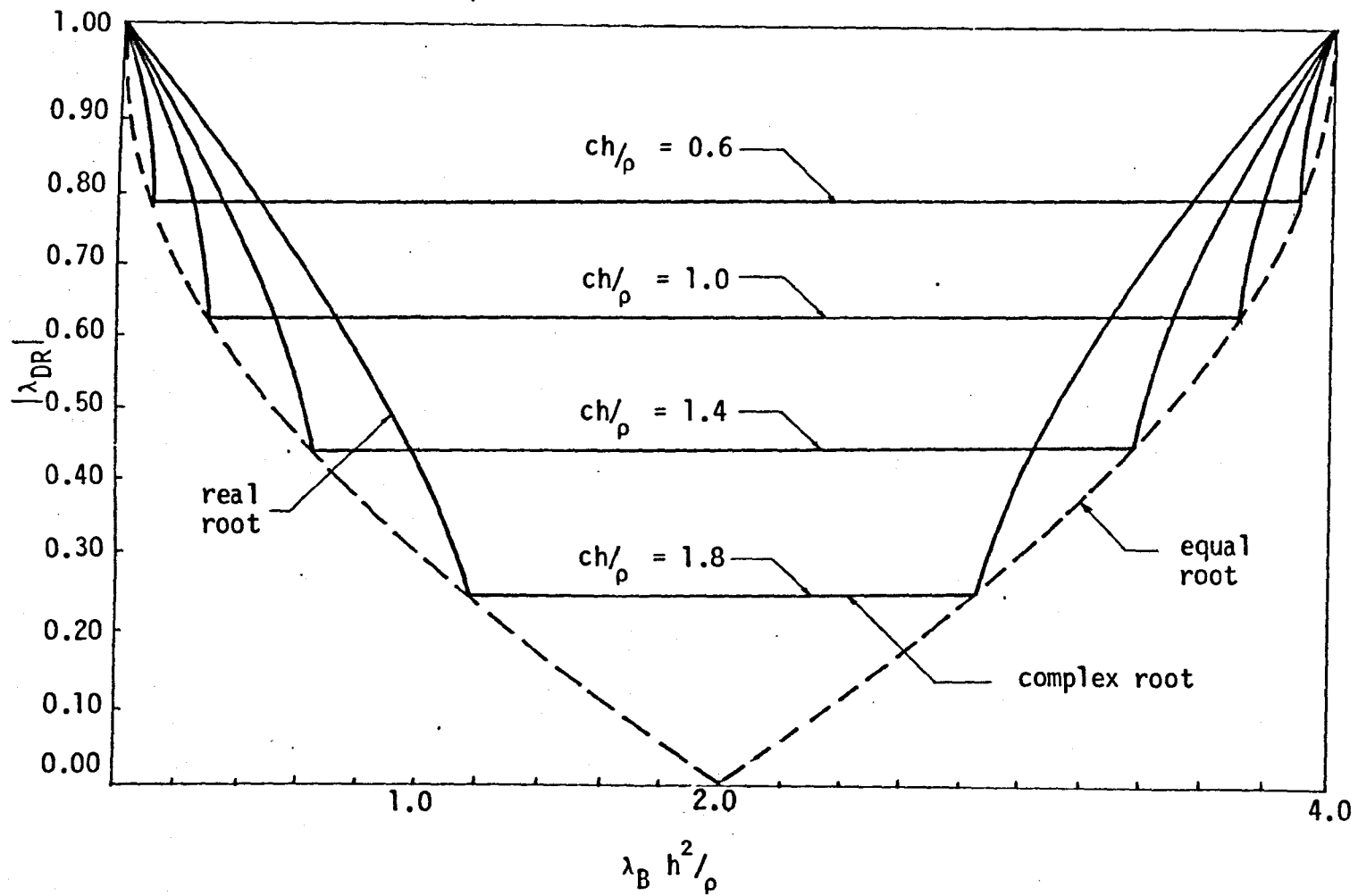


Fig. 5.2 Relation between asymptotic convergence and $\lambda_B h^2 / \rho$ in dynamic relaxation

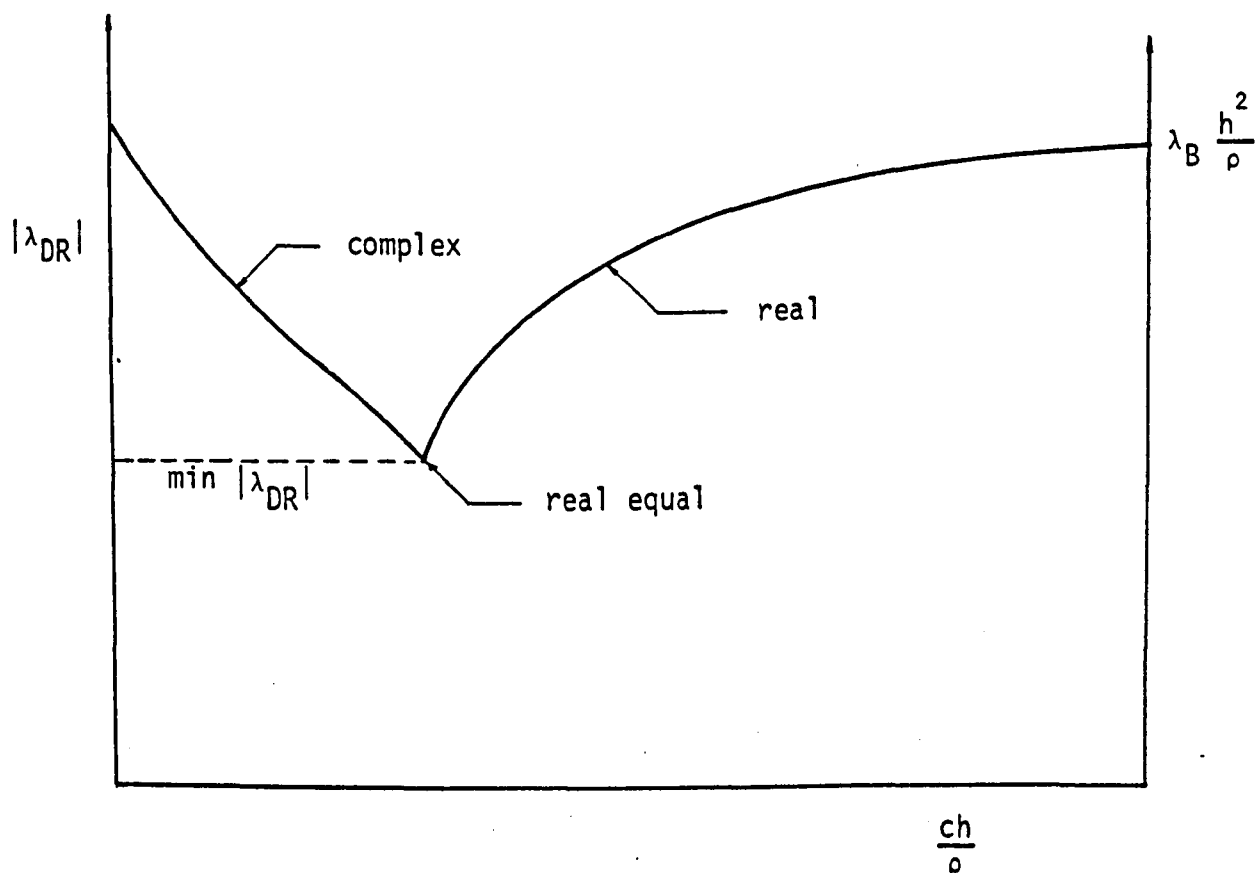


Fig. 5.3. Graphical representation of the critical damping

Figure 5.2 shows that the two equal roots are symmetrical about the ordinate where $\lambda_B \frac{h^2}{\rho}$ is equal to 2.0, and also that they are associated with the lowest and highest eigenvalues of B. So the optimum parameter $\frac{h^2}{\rho}$ is chosen in order to make the two parameters $\lambda_{B \max} \frac{h^2}{\rho}$ and $\lambda_{B \min} \frac{h^2}{\rho}$ symmetrical about the ordinate 2.0. This is achieved by the expression,

$$\left(\frac{h^2}{\rho}\right)_{\text{opt}} = \frac{4.0}{\lambda_{B \text{ max}} + \lambda_{B \text{ min}}} \quad (5.26)$$

Then using equation (5.26), equation (5.24) will give the optimum parameter ch/ρ as

$$\left(\frac{ch}{\rho}\right)_{\text{opt}} = \frac{4\sqrt{\lambda_{B \text{ max}} - \lambda_{B \text{ min}}}}{\lambda_{B \text{ max}} + \lambda_{B \text{ min}}} \quad (5.27)$$

This strategy will guarantee that all error modes are decaying at exactly the same rate.

The optimum convergence achievable in the dynamic relaxation iteration can be expressed by substituting the optimum value of ch/ρ given by equation (5.27) into equation (5.23)

$$\left|\lambda_{\text{DR}}\right|_{\text{opt}} = \left|\frac{\sqrt{p} - 1}{\sqrt{p} + 1}\right| \quad (5.28)$$

where $p = \frac{\lambda_{\text{max}}}{\lambda_{\text{min}}}$, is the condition number of B.

5.1.5. Stability of Dynamic Relaxation

Instability in any iterative method will occur when the largest modulus λ_i of equation (5.14) is greater than one. In this case the magnitude of at least one error mode is being increased each cycle. The number of cycles required for manifestation of an instability in the process, will depend on how many other nodes have moduli greater than one and the initial magnitudes of those error modes.

From Figure 5.1 one can see that whatever the value of the parameter ch/ρ the modulus of λ_{DR} is always less than one. Referring to Figure 5.2, instability will occur when the parameter h^2/ρ is chosen so that $\lambda_{Bmax} h^2/\rho > 4.0$. To avoid instability λ_{Bmin} must always be an upper bound of the eigenvalues of the current or tangent modified stiffness matrix $B = D^{-1}K$. This will ensure that the actual maximum eigenvalue times h^2/ρ will in fact be less than 4.0 for stability, and that the associated root, although now complex, will be very close in magnitude to the optimum of two equal real roots.

Another way to avoid instability would be to reduce the time increment by using a percentage of the original h , or to use a larger coefficient ρ . In such cases again the product of the maximum eigenvalue times h^2/ρ will be less than 4.0.

The estimation of the minimum eigenvalue does not affect the stability of the method (Figure 5.2.). For reasons of convergence only it is desirable that λ_{min} should be smaller than the actual one. Again by referring to Figure 5.2. it can be seen that, from the point of view of convergence, this adjustment makes the associated root of the iterative procedure complex but close in magnitude to the optimal two equal roots.

5.2. Methods with Three Term Recursion Formulae

S. Frankel [114] was probably the first to propose a recursion formula for relaxation which makes use of the predecessors of x^k . He called this method "second order Richardson process".

The general form of a 3-term recursion formulae is given by

$$x_{k+1} = x_k + \Delta x_k \tag{5.29}$$

$$\Delta x_k = \frac{1}{q_k} (-R_k + e_{k-1} \Delta x_{k-1}), \quad k = 0, 1, 2, \dots$$

with $e_{k-1} = 0$ for $k = 0$

$$\text{and } R_{k+1} = Kx_{k+1} - F \tag{5.30}$$

The q_k and e_{k-1} are the relaxation coefficients - they are characteristic of the method.

A flow diagram is given in Figure 5.4 which is valid for all the 3-term recursion formulae methods.

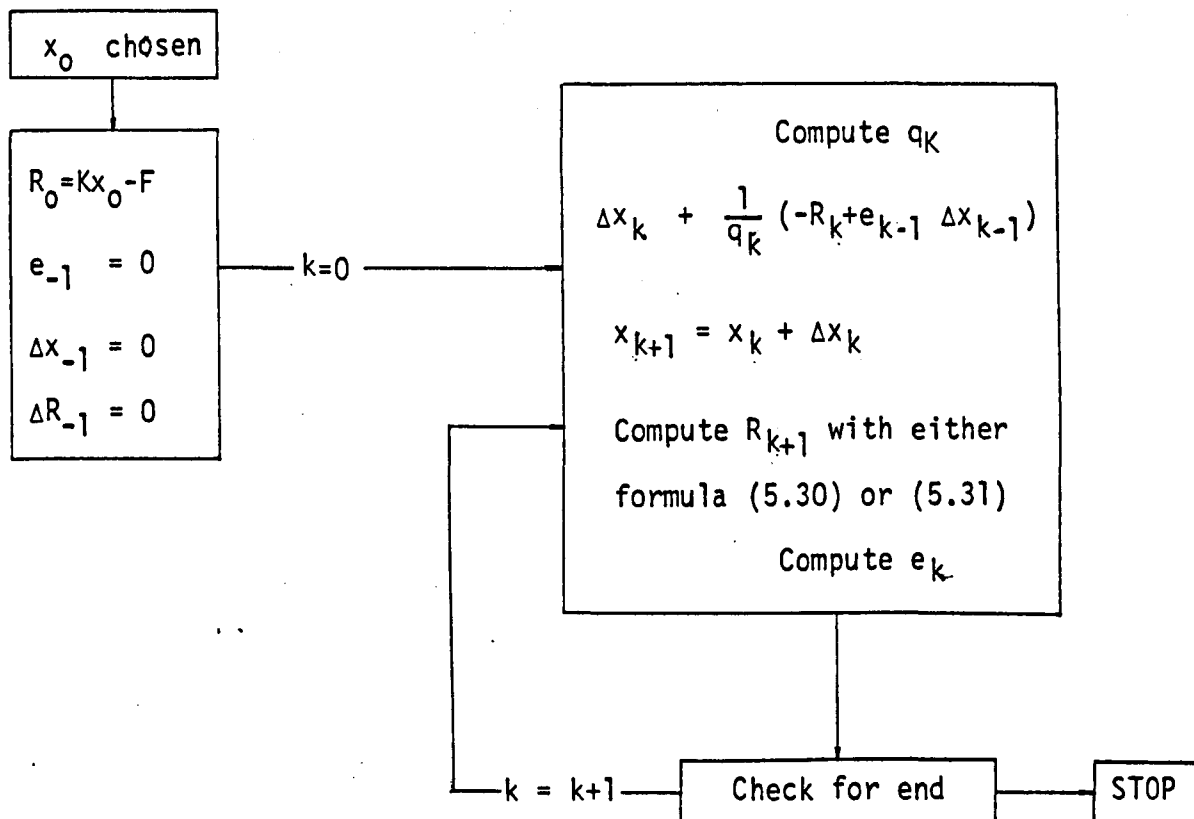


Fig. 5.4. Flow-diagram for general three term iterative method

The residuals can be computed either from equation (5.30) or, in linear cases, recursively by

$$R_{k+1} = R_k + \Delta R_k \quad (5.31)$$

$$\Delta R_k = \frac{1}{q_k} (-KR_k + e_{k-1} \Delta R_{k-1})$$

Frankel's method uses the following values for the parameters q and e

$$q_0 = \frac{a+b}{2}, \quad e_{-1} = 0 \quad \text{for } k = 0$$

(5.32)

$$q_k = \left(\frac{\sqrt{a} + \sqrt{b}}{2}\right)^2, \quad e_{k-1} = \left(\frac{\sqrt{a} - \sqrt{b}}{2}\right)^2 \quad \text{for } k > 0$$

where a, b are upper and lower bounds of the eigenvalues of matrix K .

Flanders and Shortley [106] proposed the following choice for the parameters q and e :

$$q_0 = \frac{a+b}{2}, \quad e_{-1} = 0 \quad \text{for } k = 0$$

$$q_k = \frac{b-a}{4} \frac{\cosh[(k+1)\omega]}{\cosh(k\omega)} = \frac{b-a}{4} \frac{t_{k+1}}{t_k} \quad \text{for } k > 0 \quad (5.33)$$

$$e_{k-1} = \frac{b-a}{4} \frac{\cosh[(k-1)\omega]}{\cosh(k\omega)} = \frac{b-a}{4} \frac{t_{k-1}}{t_k}$$

where

$$\cosh \omega = \frac{b+a}{b-a}$$

and

$$t_k = T_k(f(0)) \quad (5.34)$$

with T_k denoting the Tchebycheff polynomial of the first kind of degree k , and

$$f(z) = \frac{b+a}{b-a} - 2 \frac{z}{b-a} \quad (5.35)$$

Equations (5.33) for large k can be written as

$$\lim_K q_k = \left(\frac{\sqrt{b} + \sqrt{a}}{2} \right)^2, \quad \lim_K e_k = \left(\frac{\sqrt{a} - \sqrt{b}}{2} \right)^2 \quad (5.36)$$

Young [311] optimized a semi-iterative method given by Varga [294] in terms of the minimum and maximum eigenvalues of the iteration matrix based on the use of Tchebycheff polynomials. If the iterative method is given by

$$x_{k+1} = Gx_k + K \quad (5.37)$$

with $K = (I - G)K^{-1}F$

then

$$x_{k+1} = \omega_{k+1} \left[\omega_0(Gx_k + K) + (1 - \omega_0)x_k \right] + (1 - \omega_{k+1})x_{k-1} \quad (5.38)$$

where

$$\omega_0 = \frac{2}{2 - M(G) - m(G)} \quad (5.39)$$

$$\omega_1 = 1$$

$$\omega_2 = \frac{2z^2}{2z^2 - 1} \quad (5.40)$$

$$\omega_{k+1} = \left(1 - \frac{1}{4z^2} \omega_k \right)^{-1} \quad K = 2, 3 \dots$$

with

$$z = \frac{2 - M(G) - m(G)}{M(G) - m(G)}$$

and $M(G)$ being the maximum eigenvalue and $m(G)$ the minimum eigenvalue of G . Young called this method Jacobi semi-iterative method.

In the sequel, the methods listed under this Chapter will, for obvious reasons, be called Tchebycheff methods.

5.3. Relation Between Dynamic Relaxation and Tchebycheff Methods

The general 3-term recursion formula given by equations (5.29) can be also written as

$$x_{k+1} - x_k = -\frac{R_k}{q_k} + \frac{e_{k-1}}{q_k} (x_k - x_{k-1}) \quad \text{or}$$

$$x_{k+1} - x_{k-1} = \frac{1}{q_k} (-R_k + e_{k-1} \Delta x_{k-1}) + x_k - x_{k-1} \quad \text{or}$$

$$x_{k+1} - x_{k-1} = -\frac{R_k}{q_k} + \left(\frac{e_{k-1}}{q_k} + 1\right) (x_k - x_{k-1}) \quad (5.41)$$

The recursive equation (5.7) for dynamic relaxation can be written in terms of increments of displacements as

$$\Delta x_k = \frac{\left(1 - \frac{ch}{\rho}\right)}{\left(1 + \frac{ch}{\rho}\right)} \Delta x_{k-1} + \frac{h^2}{\left(1 + \frac{ch}{\rho}\right)} [F - Kx_k] D^{-1} \quad (5.42)$$

Substituting equations (5.26) and (5.27) into equation (5.42)

$$\Delta x_k = \frac{1 - \frac{2\sqrt{a \cdot b}}{(a+b)}}{1 + \frac{2\sqrt{a \cdot b}}{(a+b)}} \Delta x_{k-1} - \frac{\frac{4}{(a+b)}}{1 + \frac{2\sqrt{ab}}{(a+b)}} D^{-1} R_k \quad \text{or}$$

$$\Delta x_k = \frac{(\sqrt{a} - \sqrt{b})^2}{(\sqrt{a} + \sqrt{b})^2} \Delta x_{k-1} - \frac{4}{(\sqrt{a} + \sqrt{b})^2} D^{-1} R_k \quad (5.43)$$

The unscaled version of equation (5.43), with $M = \rho I$ and $C = cI$ instead of equations (5.6) can be written as follows

$$\Delta x_k = \frac{(\sqrt{a} - \sqrt{b})^2}{(\sqrt{a} + \sqrt{b})^2} \Delta x_{k-1} - \frac{4}{(\sqrt{a} + \sqrt{b})^2} R_k \quad (5.44)$$

with a and b this time being bounds to the maximum and minimum eigenvalue of K .

A comparison of equations (5.41) and (5.44), shows that dynamic relaxation is a 3-term recursive formula with

$$\frac{1}{q_k} = \frac{4}{(\sqrt{a} + \sqrt{b})^2} \quad \text{and} \quad \frac{e_{k-1}}{q_k} = \frac{(\sqrt{a} - \sqrt{b})^2}{(\sqrt{a} + \sqrt{b})^2} \quad \text{or}$$

$$q_k = \left(\frac{\sqrt{a} + \sqrt{b}}{2} \right)^2 \quad \text{and} \quad e_{k-1} = \left(\frac{\sqrt{a} - \sqrt{b}}{2} \right)^2 \quad (5.45)$$

which are exactly the values for the iteration parameters of Frankel's method.

Following the same procedure, the relationships between the parameters of the 3-term recursive formulae and Jacobi semi-iterative method are as follows:

$$\frac{1}{q_k} = \omega_{k+1} \omega_0 \quad \text{and} \quad \frac{e_{k-1}}{q_k} + 1 = \omega_{k+1} \quad \text{or}$$

$$q_k = \frac{1}{\omega_{k+1} \cdot \omega_0} \quad \text{and} \quad e_{k-1} = \frac{(\omega_{k+1} - 1)}{\omega_{k+1} \cdot \omega_0} \quad (5.46)$$

With the iteration matrix being equal to $I - K$

$$M(G) = 1 - b \quad \text{and} \quad m(G) = 1 - a \quad (5.47)$$

and subsequently

$$\omega_0 = \frac{2}{a + b} \quad \text{and} \quad z = \frac{a + b}{a - b} \quad (5.48)$$

5.4. Relation Between Conjugate Gradient and Tchebycheff Methods

The recursive relationships of the conjugate gradient method can be written as

$$x_{k+1} = x_k + t_k p_k \quad (5.49)$$

$$p_k = -R_{k+1} + \beta_k p_k$$

with

$$p_k = \frac{(x_{k+1} - x_k)}{t_k}, \quad p_{k-1} = \frac{(x_k - x_{k-1})}{t_{k-1}} \quad (5.50)$$

Combining equations (5.50) and (5.49) we obtain

$$(x_{k+1} - x_k) / t_k = -R_k + \beta_{k-1} (x_k - x_{k-1}) / t_{k-1} \quad \text{or}$$

$$x_{k+1} - x_k = -R_k t_k + \beta_{k-1} \frac{t_k}{t_{k-1}} (x_k - x_{k-1}) \quad \text{or}$$

$$x_{k+1} - x_{k-1} = -R_k t_k + \left(\beta_{k-1} \frac{t_k}{t_{k-1}} + 1 \right) (x_k - x_{k-1}) \quad (5.51)$$

Equation (5.51) has the same form as the general 3-term recursive formula of equation (5.41) with the following correspondence between the iteration parameters

$$t_k = \frac{1}{q_k} \quad \text{and} \quad \beta_{k-1} = \frac{e_{k-1}}{q_{k-1}} \quad (5.52)$$

From the development of the last two sections we can draw the conclusion that dynamic relaxation, Frankel's method, Tchebycheff method and conjugate gradient method may all be regarded as belonging to the same category of iterative methods, namely the "3-term recursive formulae".

5.5. The Residual Polynomial

For any of the methods discussed in Section (5.4) we have

$$x_{k+1} = x_k + \sum_{j=0}^k c_{k,j} R_j \quad (k = 0, 1, 2, \dots) \quad (5.53)$$

with $c_k, k \neq 0$. By multiplication with K we obtain

$$R_{k+1} = R_k + \sum_{j=0}^k c_{k,j} K R_j \quad (k = 0, 1, 2, \dots) \quad (5.54)$$

Equation (5.54) can also be written [94] as

$$R_k = S_k(K)R_0 \quad (5.55)$$

Where the $S_k(\lambda)$ are polynomials of degree K and they are called the residual polynomials of the iterative method. The $S_k(\lambda)$ obey the recursion formula

$$S_{k+1}(\lambda) = S_k(\lambda) + \lambda \sum_{j=0}^k c_{k,j} S_j(\lambda) \quad (5.56)$$

with

$$S_0(\lambda) \equiv 1 \quad \text{and} \quad R_k(0) = 1 \quad \text{for all } k.$$

The most important property of the residual polynomials is that they allow estimates for the length of the error vector of the k -th approximant :

$$x_k - K^{-1}F$$

which are otherwise difficult to obtain. For this purpose we consider the spectral decomposition of the error vector of x_0 :

$$x_0 - K^{-1}F = \sum_{j=1}^N c_j u_j \quad (5.57)$$

where u_j are eigenvectors to the N eigenvalues $\lambda(j = 1, 2, \dots, N)$ of the matrix K . Then

$$x_k - K^{-1}F = K^{-1}R_k = S_k(K) \sum_{j=1}^N c_j u_j = \sum_{j=1}^N c_j S_k(\lambda_j) u_j \quad (5.58)$$

which may be expressed as follows : After k steps of an iterative method with residual polynomials $S_k(\lambda)$, the contribution of any eigenvalue to the error vector is reduced to the $S_k(\lambda_j)$ - fold of its original value. Therefore, in order to obtain optimal convergence, and if an interval $a \leq \lambda \leq b$ with

$a > 0$ containing all eigenvalues is known, then the best procedure would be to choose S such that $S_k(\lambda) \rightarrow 0$ as fast as possible for all λ 's in (a,b) .

5.6. The Conjugate Gradient - Tchebycheff Method

Considering the original linear system

$$Kx+b = 0 \tag{5.59}$$

being multiplied by $B = K^{-1} [I - S(K)]$, where $S(\lambda)$ is a polynomial with $S(0) = 1$. Then the original system (5.59) is transformed into

$$K^*x + \beta = 0 \tag{5.60}$$

where

$$K^* = I - S(K)$$

$$\beta = K^{-1} [I - S(K)] b$$

Let us now proceed to the solution of equation (5.60) starting with an initial approximation ξ_0 , and compute the residuals first

$$\rho_0 = K^*\xi_0 + \beta \tag{5.61}$$

But the matrix K^* is not explicitly known and neither is the product $K^*\xi_0$. In order to evaluate the residual ρ_0 we solve the original system (5.59) with another iterative method called the inner method, starting with $x_0 = \xi_0$, then

$$R_0 = K\xi_0 + b \quad (5.62)$$

and according to equation (5.55)

$$\begin{aligned} R_m &= S_m(K) R_0 \\ &= S_m(K) (K\xi_0 + b) \end{aligned} \quad (5.62)$$

where $S_m(K)$ is the m^{th} residual polynomial of the inner method, so that

$$S_m(K) = I - K^*$$

Hence

$$R_0 - R_m = K^*(K\xi_0 + b) \quad (5.63)$$

$$\begin{aligned} x_0 - x_m &= K^{-1}K^*(K\xi_0 + b) \\ &= K\xi_0 + \beta = \rho_0 \end{aligned} \quad (5.64)$$

Therefore after m -steps of the inner method for the solution of $Kx+b = 0$ with the initial approximant $x_0 = \xi_0$, the residual of the modified system (5.60) is given by

$$\rho_0 = x_0 - x_m \quad (5.65)$$

Furthermore, we have to compute for every step of the outer method, which operates into the modified system (5.60), the coefficients q_k and e_k according to the iterative method used and the new residuals.

In the linear case the residuals can be computed by

$$\rho_{k+1} = \rho_k + \Delta\rho_k \quad (5.66)$$

where

$$\Delta\rho_k = \frac{1}{q_k} (-K\rho_k + e_{k-1} \Delta\rho_{k-1})$$

and the new approximant by

$$\xi_{k+1} = \xi_k + \Delta\xi_k$$

$$\text{where } \Delta\xi_k = \frac{1}{q_k} (-\rho_k + e_k + \Delta\xi_{k-1}) \quad (5.67)$$

Equation (5.66) requires the product $K\rho_k$ which again is not explicitly available. This may be done by solving the system $Kx + \rho_k = 0$ with the inner method, beginning with the initial approximant $x_0 = 0$. Doing so, we get

$$R_0 = K x_0 + \rho_k = \rho_k \quad (5.68)$$

$$R_m = S_m(K)R_0 = S_m(K)\rho_k \quad (5.69)$$

Therefore, combining equations (5.68) and (5.69)

$$\begin{aligned} R_0 - R_m &= [I - S_m(K)] \rho_k \\ &= K^* \rho_k \end{aligned}$$

The residual polynomial $S_m(\lambda)$ generated by the inner method as well as the integer m , must be strictly the same for the computation of ρ_0 and all $K\rho_k$. Therefore methods like the conjugate gradient for which the coefficients q_k and

e_k depend on the choice of the initial vector x_0 , can not be used as inner methods. Furthermore, the matrix $K^* = I - S(K)$ must be positive definite, which means that $S(\lambda) < 1$ for all $\lambda = \lambda_i$. For the Tchebycheff methods this condition is automatically fulfilled, provided b is an upper bound for the eigenvalues of K and also $a > 0$.

The above limitations are sufficient to define the choice of the inner and outer methods as follows :

Conjugate gradient method as outer method
a Tchebycheff method as inner method

Figure 5.5 (after Engeli et al [94]) shows the range of the eigenvalues before and after the transformation using the method of Flanders and Shortley as inner method.

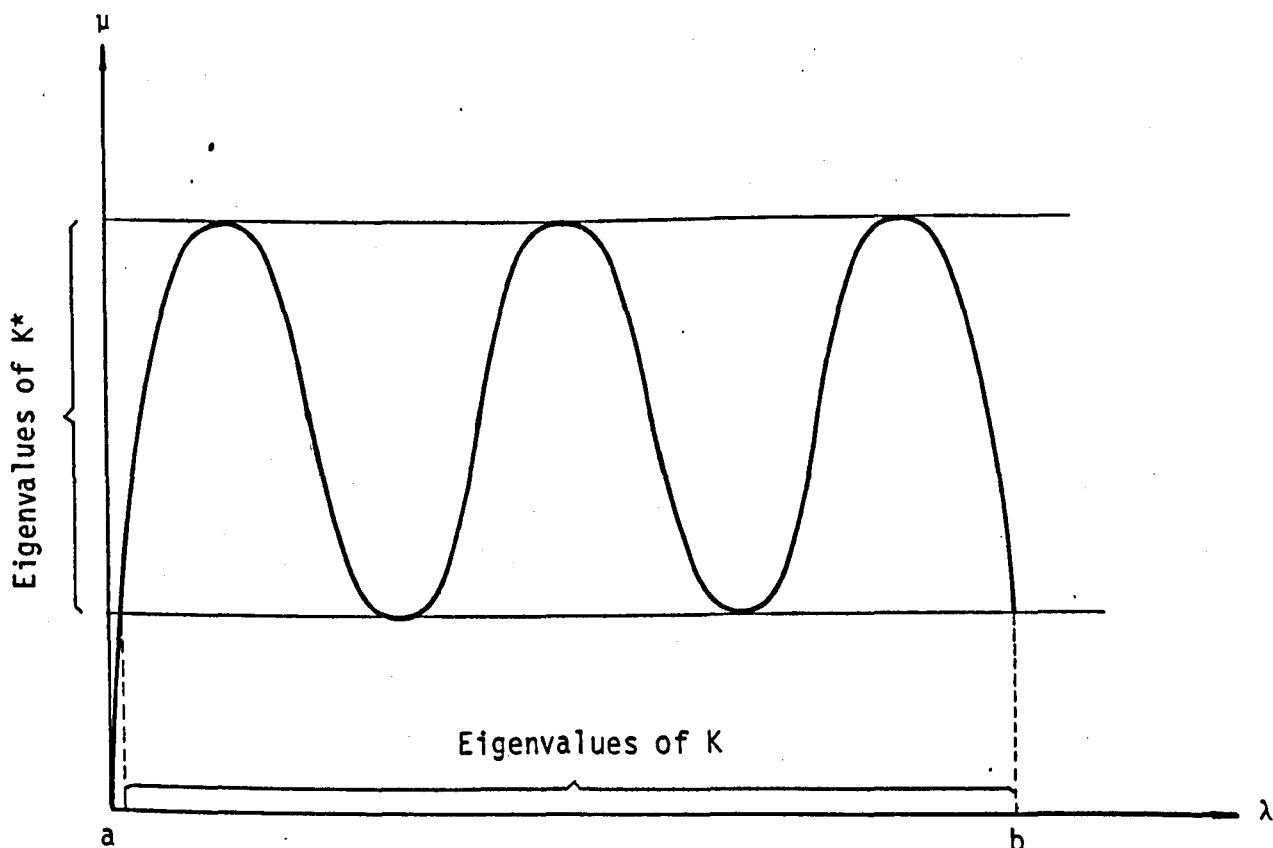


Fig. 5.5. Spectral transformation for the conjugate gradient - Tchebycheff method

In nonlinear cases equation (5.66) for the evaluation of the residuals is no longer valid. For this reason the whole process for the evaluation of ρ_0 must be repeated after each iteration of the outer method, in order to have estimates for the residuals ρ_i . The flow diagram of the conjugate gradient - Tchebyscheff method is shown in Figure 5.6.

5.7. Assessment of the Dynamic Relaxation Parameters

The majority of dynamic relaxation parameters were performed in the unscaled version of equation (5.7)

$$\ddot{x}^{k+\frac{1}{2}} = \frac{(1 - Q/2)}{(1 + Q/2)} \ddot{x}^{k-\frac{1}{2}} - \frac{h}{(1 + Q/2)} R^k \quad (5.71)$$

where

$$Q = \frac{ch}{M_i}$$

The stability of the method was ensured when the time increment was less than a certain critical value. For finite difference idealizations Otter, Cassel and Hobbs [223] used a stability criterion proposed by Forsythe and Wasow [316] .

$$h \leq \frac{1}{d} \left(\frac{1}{(\Delta x_1)^2} + \dots + \frac{1}{(\Delta x_k)^2} \right)^{-\frac{1}{2}} \quad (5.72)$$

where d denotes the faster velocity of either the pressure or shear wave, and $\Delta x_1, \dots, \Delta x_n$ are the mesh lengths in the coordinate directions.

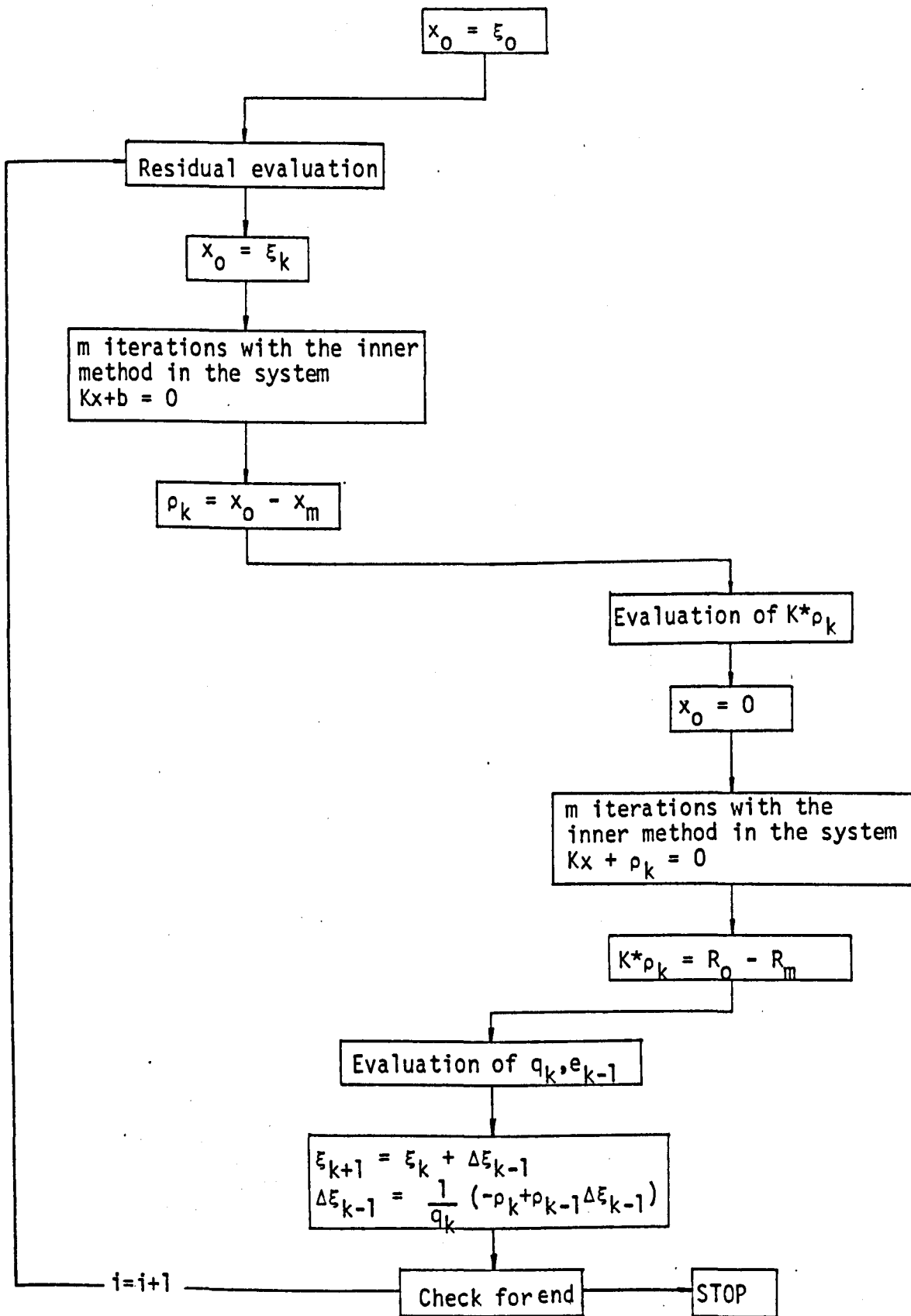


Fig. 5.6 Flow diagram for the conjugate gradient Tchebycheff method

Barnes [13] has introduced bounds for the time increment, using finite element idealizations, as follows

$$\sqrt{\frac{2M_i}{S_i}} \leq h \text{ crit} \leq \sqrt{\frac{4M_i}{S_i}} \quad (5.73)$$

where S_i is the direct stiffness (or leading diagonal component) relative only to adjacent nodes.

Cassel and Hobbs [71] proposed another expression for the critical time increment derived from the direct comparison of dynamic relaxation with Frankel's method

$$h^2 \leq \frac{4M_i}{a + b} \leq \frac{4M_i}{b_G} \quad (5.74)$$

where b_G is an upper bound of the sum $(a + b)$, usually taken from the Gershgorin bound theorem.

The evaluation of critical damping has always produced some difficulties because it involves the evaluation of the minimum eigenvalue or the fundamental frequency of the structure which is not easily obtainable. The critical damping can be expressed as

$$K \text{ crit} = \frac{4\sqrt{ab}}{a + b} \quad (5.75)$$

which for $a \ll b$ can be written as

$$K \text{ crit} = 4\sqrt{\frac{a}{b}} = 4 \frac{f \text{ min}}{f \text{ max}}$$

where $f \text{ min}$ and $f \text{ max}$ are the minimum and maximum frequencies of the structure respectively.

An alternative expression for the critical time increment is

$$h_{crit} = \frac{1}{\pi f_{max}}$$

which makes the critical damping parameter

$$K_{crit} = 4 \pi f_{min} h_{crit} \quad (5.76)$$

proportional to the fundamental frequency times the critical time increment. This expression agrees with the optimum value of K based on the dynamic heuristic of critically damping the fundamental mode (Rushton [247]). The structure then is allowed to vibrate in a trial run with zero damping until a periodic response of the deflections or the total kinetic energy is observed which yields the fundamental frequency.

This procedure has the disadvantage of the uncertainty involved in knowing "a priori" the required running time with zero damping in order to develop a periodic response. Sometimes the number of iterations for the trial run needed to develop a periodic response exceeded the number of iterations required for the solution itself [71].

To avoid trial runs Lynch, Kelsey and Saxe [185] proposed an ongoing alteration of the iteration parameters. Starting with a rough estimate for the damping parameter, when a check on the curvatures of the deflection vector norms for each coordinate direction indicated that the process was overdamped, a change in parameter was made. Similarly changes were made each time an alteration in the sign of a displacement

norm indicated underdamped behaviour. The amount of adjustments to be made in the parameters h^2/ρ and ch/ρ , once the need for it has been determined, was largely dictated by how accurate the estimate of the minimum eigenvalue was considered to be.

The process proposed by Lynch et al was used for linear plane stress problems and conclusions were uncertain to the extent that large adjustments could take the parameters beyond their optimum values and give inferior convergence to that of analyses using constant parameters in the correct region.

5.8. "A Priori " Evaluation of Dynamic Relaxation Parameters

For the evaluation of the required bounds to the minimum and maximum eigenvalues of the iteration matrix one of the methods to be discussed in Chapter 6 could very easily be employed. When the iteration matrix is the stiffness matrix K then the application of special eigenvalue methods is straightforward. But in the case which the scaled version of the dynamic relaxation, given by equation (5.7) is used, then a modification should be made to the iteration matrix B .

As all the methods to be discussed in Chapter 6 operate much more easily and efficiently in symmetric matrices, we transform the non-symmetric iteration matrix $B = D^{-1}K$ to a

symmetric one by multiplying the original equation (5.3) by $D^{-\frac{1}{2}}$

$$M D^{-\frac{1}{2}} \ddot{x} + CD^{-\frac{1}{2}} \dot{x} + D^{-\frac{1}{2}} Kx = D^{-\frac{1}{2}} F \quad (5.77)$$

which after substituting the values of M and C from equations (5.6) we obtain

$$\rho D^{\frac{1}{2}} \ddot{x} + cD^{\frac{1}{2}} \dot{x} + D^{-\frac{1}{2}} Kx = D^{-\frac{1}{2}} F \quad (5.78)$$

If in the above equation we replace vector x by another vector x' such as

$$x' = D^{\frac{1}{2}} x, \quad \dot{x}' = D^{\frac{1}{2}} \dot{x} \quad \text{and} \quad \ddot{x}' = D^{\frac{1}{2}} \ddot{x}$$

then equation (5.78) becomes

$$\begin{aligned} \rho \ddot{x}' + c \dot{x}' + D^{-\frac{1}{2}} K D^{-\frac{1}{2}} x' &= D^{-\frac{1}{2}} F \quad \text{or} \\ \rho \ddot{x}' + c \dot{x}' + K' x' &= D^{-\frac{1}{2}} F \end{aligned} \quad (5.78)$$

Equation (5.78) is equivalent to equation (5.7) but the iteration matrix B is symmetric and given by

$$B = K' = D^{-\frac{1}{2}} K D^{-\frac{1}{2}} \quad (5.79)$$

However, as an alternative to an "a priori" evaluation of the iteration parameters of dynamic relaxation, an ongoing process has been developed by the author in the next section, which proved to be very efficient for the nonlinear problems that have been investigated in this work.

5.9. Automatic Adjustment of the Dynamic Relaxation Parameters

In nonlinear structures and in particular in cable structures the need for an ongoing process for the adjustment of the parameters of dynamic relaxation becomes of paramount importance. The initial estimated values for the minimum and maximum eigenvalues from one of the methods to be described in Chapter 6 are no longer valid as the iteration process continues up to the final configuration of the structure. Large changes in the eigenvalues of the stiffness matrix could lead either to very slow convergence or more frequently particularly for cable structures, to divergence of the method.

In the majority of problems concerning the analysis of cable structures the maximum eigenvalue becomes greater as the structure deforms under the application of the external loads. This is a characteristic of stiffening systems. When the maximum eigenvalue becomes greater than the estimated bound then instability occurs.

An upper bound for the maximum eigenvalue may be determined from the Gershgorin theorem, which states that

$$|\lambda_B \max| \leq \max_i \sum_{j=1}^N |K_{ij}| \quad (5.80)$$

where K_{ij} are the elements of the stiffness matrix. This evaluation can be performed very easily at any stage of the iteration process.

Therefore, starting with an initial value for $\lambda_B \max$ from equation (5.80), a new estimation is obtained either by reapplying equation (5.80) with the current values of the stiffness components K_{ij} , or by increasing the previous value of $\lambda_B \max$ by a certain amount, according to the degree of nonlinearity of the structure, when a check on the curvatures of the deflection vector norm or the velocity norm indicate an oscillatory behaviour.

After establishing $\lambda_B \max$, and if the iteration parameters h^2/ρ and ch/ρ are so chosen that the λ_{DR} associated with $\lambda_B \min$ is real and given by equation (5.25) then this value of λ_{DR} is the dominant eigenvalue of the iteration process and can be estimated as follows : Equation (5.12) which is

$$\epsilon^{k+1} = M \epsilon^k$$

may be written as

$$\dot{x}^{k+1} - x^* = M(x^k - x^*) \quad (5.81)$$

or similarly

$$x^k - x^* = M(x^{k-1} - x^*) \quad (5.82)$$

where x^* is the exact solution-vector. Subtracting equation (5.82) from equation (5.81) gives

$$x^{k+1} - x^* = M(x^k - x^{k-1}) \quad (5.83)$$

The above equation represents the same eigenvalue

problem as that given by equation (5.13) , with the difference that it is in terms of successive correction vectors rather than error vectors. A series of approximations to the dominant eigenvalue λ_{DR} can be obtained by calculating the quotient

$$\lambda_{DR} = \frac{|x^{k+1} - x^k|}{|x^k - x^{k-1}|} \quad (5.84)$$

When the quantity given by equation (5.81) has converged to a relative constant value, it means that the dominant eigenvalue is the minimum eigenvalue and is given by the solution of equation (5.22) with respect to λ_B .

$$\lambda_B = - \frac{\lambda_{DR}^2 - \lambda_{DR} \beta + \alpha}{\lambda_{DR} \gamma} \quad (5.85)$$

The above estimate of λ_B min can then be used in equations (5.26) and (5.27) to evaluate the optimum iterations parameters.

When the initial estimate of λ_B min is greater than the actual minimum eigenvalue, then the dominant eigenvalue given by equation (5.84) will correspond to a real root of equation (5.22) and subsequently will give a real value of the estimated minimum eigenvalue of equation (5.85). If, however, the initial estimate of λ_B min is much less than the actual minimum eigenvalue then the dominant eigenvalue will correspond to a complex conjugate root of equation (5.22) and subsequently

equation (5.85) will produce a complex root for λ_B min. This situation can be very easily avoided by increasing the initial estimate by a certain factor when a complex root for λ_B min is detected. This procedure is repeated until a real root for the estimated minimum eigenvalue is calculated from equation (5.85).

Two very important parameters to watch in any iterative method are the current convergence rate and the optimum convergence rate. Engeli et al [94] introduced the convergence quotient for the Tchebycheff methods as

$$e^{-\omega} = \frac{\sqrt{b} - \sqrt{a}}{\sqrt{b} + \sqrt{a}} \quad (5.86)$$

which is the same expression given by Lynch et al [185] for the asymptotic convergence of dynamic relaxation, given by equation (5.23), as

$$|\lambda_{DR}| = \sqrt{\frac{1 - ch/\rho}{1 + ch/\rho}} \quad (5.87)$$

The optimum convergence rate is given by the value of the parameter ω

$$\omega = -\ln \left(\frac{\sqrt{b} - \sqrt{a}}{\sqrt{b} + \sqrt{a}} \right) = -\ln |\lambda_{DR}| \quad (5.88)$$

On the other hand the expression $-\ln(\lambda_{DR})$, with λ_{DR} given by equation (5.84), is a measure of the current convergence rate of the method. Thus, the value

$$Q^k = \frac{-\ln(\lambda DR)}{\omega} \quad (5.89)$$

is an estimate of the ratio of current to optimal convergence rates.

If during the iteration process the value of Q^k becomes greater than one, this means that the current convergence rate is greater than the optimal. This automatically suggests that an instability process has started to develop in the method. In such cases the iterations are continued without changing the iteration parameters to those with the possibility of inducing an instability effect in the method. A flow diagram of the whole process discussed in this Section is shown in Figure 5.7.

6.10. The Use of Kinetic Damping

Cundall [80] examining the application of explicit integration methods to problems in geomechanics, suggested that the kinetic energy of the structure be constantly monitored, and that when an energy peak is detected all the current velocities to be set to zero. For a system oscillating in one mode, this state of stress would be the static equilibrium position, which coincides with a peak of the total kinetic energy curve. However, for practical problems with many degrees of freedom, the process must be repeated through further peaks,

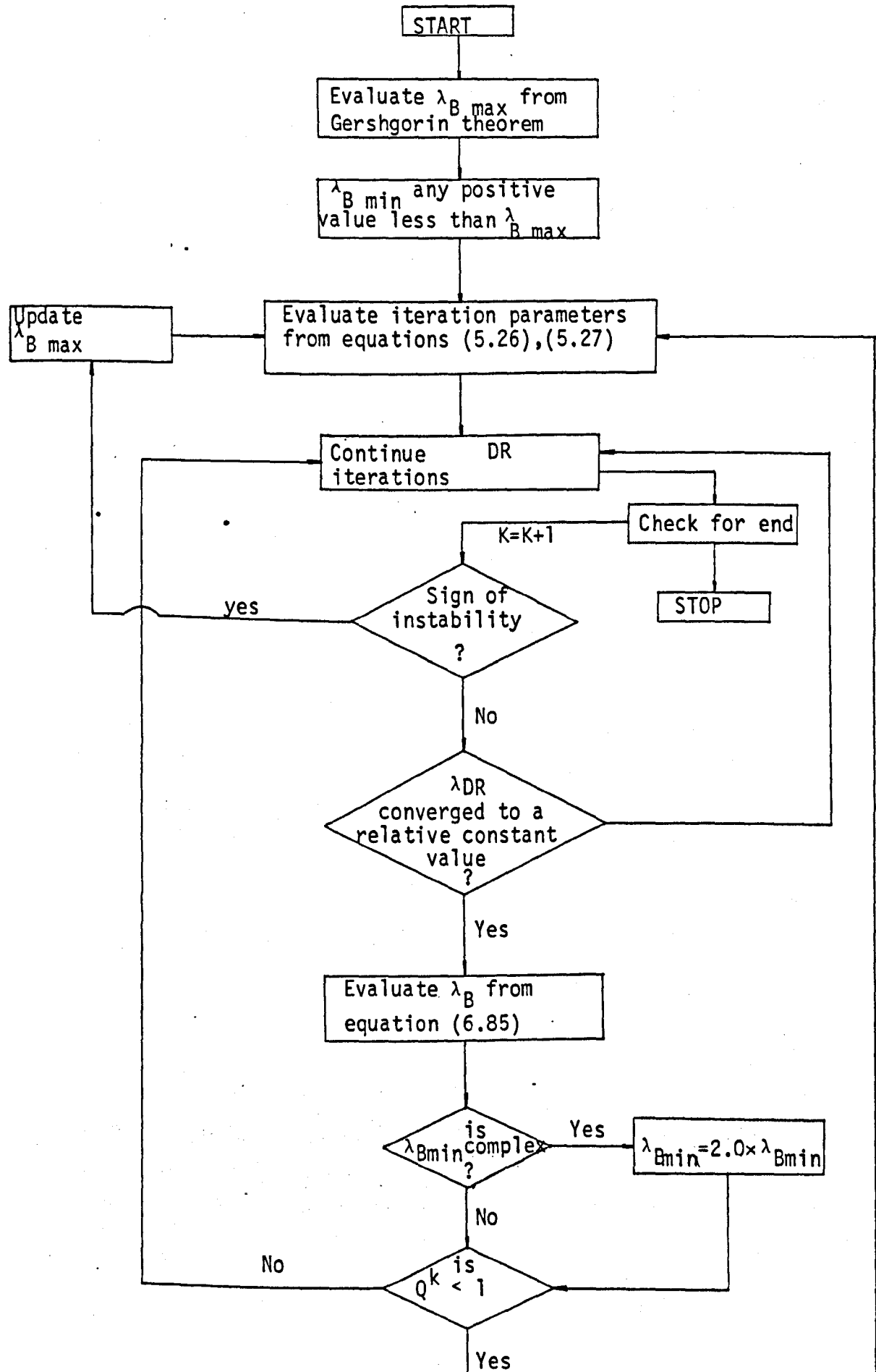


Fig. 5.7 Flow diagram for automatic adjustment of dynamic relaxation parameters

eliminating the kinetic energy for all the modes, until the required degree of accuracy is obtained.

Using this method the viscous damping coefficient of equation (5.3) is neglected and the original equation of motion becomes

$$M\ddot{x} + Kx = F \quad (5.90)$$

Integrating equation (5.90) in the same way as equation (6.3) we get

$$\dot{x}^{k+\frac{1}{2}} = \dot{x}^{k-\frac{1}{2}} + \frac{h}{\rho} D^{-1} R^k \quad (5.91)$$

and

$$x^{k+1} = x^k + \frac{h^2}{\rho} D^{-1} R^k \quad (5.92)$$

Following the same process as in Section 5.1.4. , the optimum value for h^2/ρ is

$$\begin{aligned} \left(\frac{h^2}{\rho}\right)_{\text{opt}} &= \frac{4.0}{\lambda_{B\text{min}} + \lambda_{B\text{max}}} \quad (5.93) \\ &= \frac{4.0}{b_G} \end{aligned}$$

Here again, the sum of $\lambda_B \text{ min}$ and $\lambda_B \text{ max}$ is replaced by the Gershgorin bound b_G .

When the time increment is kept constant throughout the iteration process, an energy peak could be detected at each successive time step, and in this case the structure

is oscillating about the equilibrium state with a constant frequency. To overcome this difficulty, the time step is reduced to half of its current value every time an energy peak is detected until the iteration process returns to its normal convergence. Once this has been achieved the time increment is reset to its original value.

A flow chart of the method is shown in Figure 5.8.

5.11. Successive Overrelaxation

Varga [294] lists the three basic iterative methods as the point Jacobi, Gauss-Seidel and successive overrelaxation.

A general form of the basic iterative method is

$$x^{k+1} - x^k = H [C - Bx^k] \quad (5.94)$$

with the following notation

point Jacobi	$H = I$
Gauss-Seidel	$H = (I + L)^{-1}$
Successive overrelaxation	$H = \omega(I + \omega L)^{-1}$

where

$$B = D^{-1}K$$

$$C = D^{-1}F$$

and ω is a relaxation parameter

Equation (5.94) may be alternatively expressed in the following form

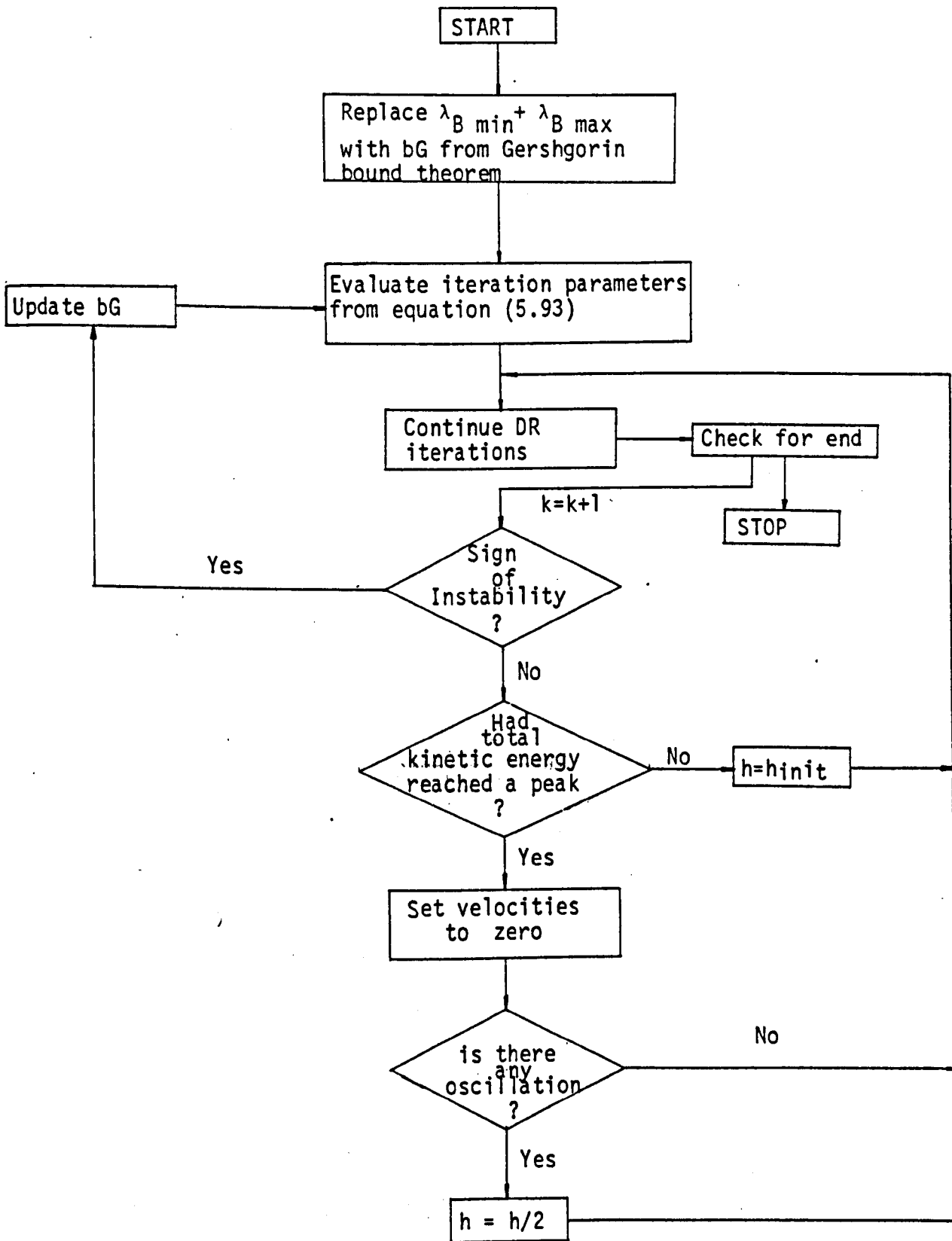


Fig. 5.8. Flow short for the dynamic relaxation with kinetic damping

$$x^{k+1} = HC + (I - HB) x^k \quad \text{or}$$

$$x^{k+1} = HC + Mx^k \tag{5.95}$$

with matrix M being the characteristic matrix of the iterative method.

The asymptotic convergence of the above methods may be obtained in the same way as in dynamic relaxation. The comparison of the asymptotic rate of convergence between the methods is valid only when the system of equations have a coefficient matrix which possesses the property "A" or is tridiagonal, because only under this assumption it is possible to obtain explicitly the asymptotic convergence for the successive overrelaxation method.

$ \lambda_{PJ} = \frac{p-1}{p+1}$	$ \lambda_{DR} = \frac{\sqrt{p-1}}{\sqrt{p+1}}$
$ \lambda_{GS} = \left(\frac{p-1}{p+1}\right)^2$	$ \lambda_{SOR} = \left(\frac{\sqrt{p-1}}{\sqrt{p+1}}\right)^2$

Table 5.1 Asymptotic convergence rates for four iterative methods

Table 5.1 shows that successive overrelaxation is twice as fast as dynamic relaxation and that the same relationship exists between Gauss-Seidel and point Jacobi methods.

The original linear system of equations $Kx = F$ can be also expressed as

$$\sum_{j=1}^N K_{ij} x_j = f_i \quad 1 \leq i \leq N \quad (5.96)$$

Using the above expression, for the case of the successive overrelaxation method, equation (5.94) can be expressed as :

$$K_{ii}x_i^{k+1} = K_{ii}x_i^k + \omega \left[- \sum_{j=1}^{i-1} K_{ij}x_j^{k+1} - \sum_{j=i+1}^N K_{ij}x_j^k + f_i - K_{ij}x_i^k \right] \quad (5.97)$$

Equation (5.97) is slightly modified in order to be applied to the nonlinear analysis of cable structures. If we add and subtract from the right hand side the sum

$$\sum_{j=1}^{i-1} K_{ij}x_j^k$$

then equation (5.97) becomes

$$K_{ii}x_i^{k+1} = K_{ii}x_i^k + \omega \left[- \sum_{j=1}^{i-1} K_{ij}(x_j^{k+1} - x_j^k) - \sum_{j=i+1}^N K_{ij}x_j^k + f_i - K_{ii}x_i^k - \sum_{j=1}^{i-1} K_{ij}x_j^k \right] \quad \text{or}$$

$$x_i^{k+1} = x_i^k + \frac{\omega}{K_{ii}} \left[- \sum_{j=1}^{i-1} K_{ij}(x_j^{k+1} - x_j^k) + R^k \right] \quad (5.98)$$

where R^k is the current residual $R^k = F - Kx^k$.

Equation (5.98) reduces to the Gauss-Seidel iteration method when $\omega = 1$.

5.12. The Successive Overrelaxation Parameter

Unfortunately, there is no algebraic expression available for the optimum parameter (ω_{opt}) when the iteration matrix does not possess the property "A". For this special case Young [310] proposed an expression which Lynch et al [185] also produced using a standard eigenvalue analysis. It can be shown that when

$$\omega = \omega_{opt} = \frac{2}{1 + \sqrt{1 - \lambda_{pJ}^2 \max}} \quad (5.99)$$

where

$$\lambda_{pJ} = 1 - \lambda_B$$

all the eigenvalues of the successive overrelaxation method have the same modulus. The optimum convergence rate is then given by

$$\begin{aligned} |\lambda_{SOR}| = \omega_{opt} - 1 &= \frac{1 - \sqrt{1 - \lambda_{pJ}^2 \max}}{1 + \sqrt{1 + \lambda_{pJ}^2 \max}} \\ &= \left(\frac{\sqrt{p}-1}{\sqrt{p}+1} \right)^2 \end{aligned} \quad (5.100)$$

Equation (5.99) automatically imposes a limitation to the

parameter $|\lambda_{PJ}|$ of being less than one, which in turn requires that

$$0 < \lambda_B < 2 \quad (5.101)$$

If $\omega < \omega_{opt}$, then λ_{SOR} is a real eigenvalue of the iteration matrix

$$M = [D - \omega L]^{-1} [(1 - \omega)D + \omega U] \quad (5.102)$$

where $K = D - L - U$

and satisfies the relationship [310]:

$$\lambda_{PJ}^2 \max = (\lambda_{SOR \max} + \omega - 1)^2 / (\omega^2 \lambda_{SOR \max}) \quad (5.103)$$

Schwarz [257] has shown that for general cases with matrices not possessing property "A" and for linear analyses, successive overrelaxation always converges provided the relaxation parameter is given by

$$0 < \omega < 2$$

5.13. Automatic Adjustment of the SOR Parameter

In what follows it was assumed that K is a consistently ordered 2-cyclic matrix. Hageman and Porching [132] have suggested the following algorithm.

If $\delta^k = x^k - x^{k-1}$ and $\epsilon^k = x^k - x^*$ denote the difference and the error vectors respectively, then for linear K

$$\delta^{k+1} = M \delta^k \quad (5.104)$$

$$\epsilon^{k+1} = M \epsilon^k \quad (5.105)$$

$$\epsilon^k = (M-I)^{-1} \delta^{k+1} \quad (5.106)$$

Moreover, if $\omega < \omega_{opt}$, the power iterative eigenvalue process (5.104) is convergent so that

$$\lim_{k \rightarrow \infty} \frac{\|\delta^{k+1}\|}{\|\delta^k\|} = \rho(M) \quad (5.107)$$

where $\rho(M)$ is the spectral radius of M .

Thus for $\omega < \omega_{opt}$ it is natural to consider

$$q^k = \frac{\|\delta^k\|}{\|\delta^{k-1}\|} \quad (5.108)$$

as an approximation to $\rho(M)$. Then using equations (5.99) and (5.103), estimates for $\lambda_{pJ}^2 \max$ and ω_N , the new value for ω , are given by

$$\bar{\lambda}_{pJ} \max = (q^k + \omega - 1)^2 / (\omega^2 q^k) \quad (5.109)$$

and

$$\omega_N = \frac{2}{1 + \sqrt{1 - \bar{\lambda}_{pJ}^2 \max}} \quad (5.110)$$

The optimum convergence rate in this case is $-\ln(\omega - 1)$ and the current convergence rate is $-\ln(q^k)$.

Here again, as in the case of dynamic relaxation the updating of ω takes place when q^k converges to a relatively constant value and the quotient

$$Q^k = - \ln(q^k) / - \ln(\omega - 1) \quad (5.111)$$

is less than one.

Carre [68] has proposed another algorithm for the evaluation of the optimum parameter. The strategy he employs is given below :

- (a) Do 1 iteration using $\omega = 1.0$
- (b) Do 12 iterations using $\omega = 1.375$. At the end of these 12 iterations compute a new ω , say ω_c , using equations (6.109) and (6.110).
- (c) Do 12 iterations using $\omega = \omega_c - (2 - \omega_c) / 4.0$. At the end of 12 iterations compute a new ω_c using again equations (6.109) and (6.110). Let $\Delta\omega_c$ be the arithmetic difference between this ω_c and the previous one. If $\Delta\omega_c / (2 - \omega_c) \leq 0.05$, go to step (d) and if $\Delta\omega_c / (2 - \omega_c) > 0.05$ repeat step (c).
- (d) Do subsequent SOR iterations with $\omega = \omega_c$.

5.14. Application of the Successive Overrelaxation Method to Cable Structures

As we can see from equation (5.38) the successive over-

relaxation method is not an un-coupled iterative method as are the Tchebycheff and conjugate gradient methods.

Members of the stiffness matrix exist in the right hand side of the equation and this creates some difficulties in non-linear applications of the method. In structures with large nonlinearities the stiffness matrix is recalculated after a certain number of iterations and new stiffness coefficients are introduced in equation (5.98). On the other hand, there is no need to store the overall stiffness matrix. Since only the product of members of the matrix and the displacement vector is needed, the overall stiffness is stored in four or six rows depending on the number of degrees of freedom.

Then a special number is assigned to each stiffness coefficient, corresponding to each node of the structure, and each time a multiplication of a stiffness coefficient with a displacement is needed the correct coefficient is allocated using this reference number.

In the next Chapter a number of iterative methods for the solution of the minimum and maximum eigenvalues of the stiffness matrix have been developed and compared. The purpose of this study is to select an efficient method, with the minimum execution time and using the minimum computer storage, to produce reasonable estimates for the extreme eigenvalues of the stiffness matrices of cable structures. These estimates can then be used for an "a priori" evaluation of the dynamic relaxation parameters.

CHAPTER 6

THE SPECIAL EIGENVALUE PROBLEM

6.1. Introduction

The special eigenvalue problem consists in determining one or a few eigenvalues of a matrix A and the eigenvectors belonging to them, in contrast to the complete eigenvalue problem where all the eigenvalues are required. The special eigenvalue problem arises in quantum mechanics or stress analysis, where some values of λ are required for which

$$Ax = \lambda x \quad (6.1)$$

has no trivial solutions. In stress analysis problems particularly, bounds for the eigenvalues are needed not only in the Tchebycheff methods but also in stability and vibration problems.

Methods like Jacobi, Givens and Householder are suitable for the complete eigenvalue problem while all methods for solving the special eigenvalue problem are pure iterative methods. For large sparse matrices it is preferable from the point of view of computational effort and storage requirements to apply the iterative methods, rather than the transformation methods, when only several eigenvalues are required.

Iterative methods can be divided into two categories.

Those in the first category are based on the assumption that there exists a basis of N -eigenvectors which spans the N -dimensional space. Starting with a certain vector, generally arbitrary, an infinite sequence of vectors is constructed such that, in this process, one eigenvector predominates more and more and converges directionally to the individual eigenvector .

Methods of the second category are based on the external properties of eigenvalues and are applicable only to symmetric matrices. Methods based on this idea give a sequence of vectors which best realise the maximum or minimum of the Rayleigh quotient

$$f(x) = \frac{x^T A x}{x^T x} \quad (6.2)$$

which is equal to an eigenvalue when x is the corresponding eigenvector. From the first category the power method and from the second category the methods of steepest descent, conjugate gradient and coordinate relaxation are examined and compared in this Chapter.

Combinations of the above methods with other iterative algorithms have been used in the past for solving the special eigenvalue problem. Engeli et al [94] used a combination of the Tchebycheff or gradient method and the QD-algorithm. Mollman [205] used a matrix iteration method for the calculation of the maximum eigenvalue. For the calculation of the minimum eigenvalue he used the same procedure but for the

reciprocal matrix A^{-1} . The maximum eigenvalue in this case corresponds to the reciprocal of the minimum eigenvalue of A . He also developed a simple approximate formulae for the minimum and maximum eigenvalues for certain types of matrices.

Recently, in several studies [214, 246, 258] the coordinate relaxation method has been generalized by analogy with the successive overrelaxation method, and in [257] a theoretical treatment of the analogy between the asymptotic convergence of these two methods has been developed. But optimum convergence can only be achieved when the matrix A has property "A".

6.2. The Power Method

This method is the simplest iterative process for solving the special eigenvalue problem. It is also described as the direct iteration method by Fox [111] and as the intensification method by Allen [3].

On the assumption that the elements of the matrices under consideration are real, there exists a basis of eigenvectors x_i belonging to the eigenvalues λ_i arrayed in order of decreasing moduli, where $|\lambda_1| > |\lambda_2|$ but some of the rest may be equal to each other. An arbitrary vector y_0 can then be written in terms of eigenvectors as

$$y_0 = a_1x_1 + a_2x_2 + \dots + a_kx_k \quad (6.3)$$

$$= \lambda_1 \frac{1 + b_2 d_2^{k+1} + b_3 d_3^{k+1} + \dots + b_n d_n^{k+1}}{1 + b_2 d_2^k + b_3 d_3^k + \dots + b_n d_n^k} \quad (6.8)$$

where $b_i = c_i/c_1$, $d_i = \lambda_i/\lambda_1$

For k sufficiently large, equation (6.8) can be simplified, by deleting higher order terms, to the following expression

$$\frac{y_{k+1}}{y_k} = \lambda_1 \quad (6.9)$$

The rate of convergence of the process is determined by the magnitude of the ratio $|\lambda_2|/|\lambda_1|$ and may be slow if this ratio is close to one. If there is a number of independent eigenvectors corresponding to the dominant eigenvalue the rate of convergence in this case is determined by the magnitude of the ratio $|\lambda_{r+1}|/|\lambda_1|$ where

$$|\lambda_1| = |\lambda_2| = \dots = |\lambda_r| > |\lambda_{r+1}| \geq \dots \geq |\lambda_n|$$

The choice of the initial vector y_0 could affect convergence when the resulting coefficient a_1 is equal to zero or very close to zero. In this case the predominant element will be one depending on λ_2 (if $a_2 \neq 0$) but then, after several iterations and due to rounding-off errors, the element depending on λ_1 shows up.

6.2.1. Improving the Convergence of the Power Method

The eigenvalues μ_i of the matrix $B = A - pI$ are

connected with the eigenvalues μ_i of the matrix A by the relationship

$$\lambda_i = \mu_i + p \tag{6.10}$$

If p is chosen appropriately, convergence to an eigenvector may be accelerated by applying the power method to the matrix B. Such a variation of the power method is called the power method with translation.

From Figure 6.1 we can see that, by choosing the value of p appropriately, either $\lambda_1 - p$ or $\lambda_n - p$ can be the dominant eigenvalue. For convergence to x_1 the optimum value of p is $\frac{1}{2}(\lambda_2 + \lambda_n)$, while the optimum choice of p

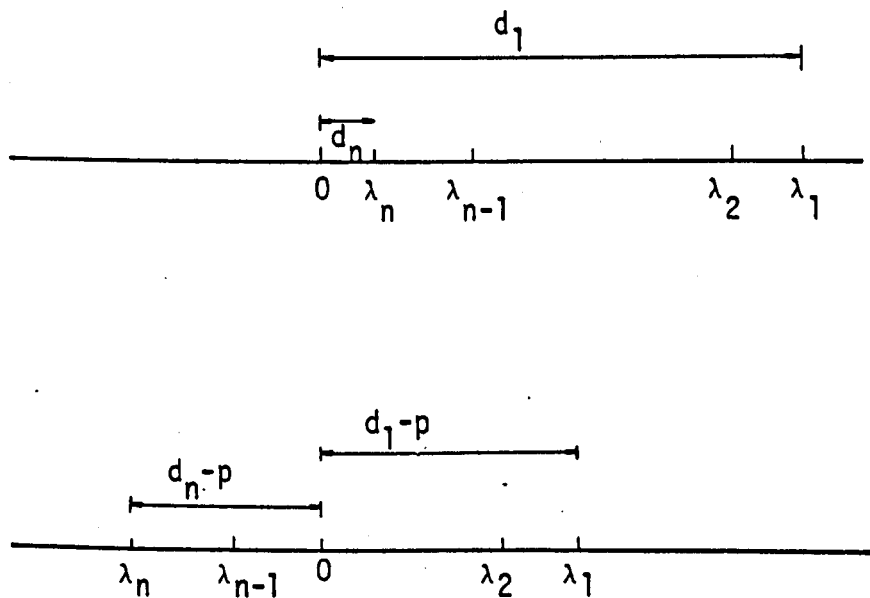


Fig. 6.1. One dimensional plot of the eigenvalues before and after the shift of the origin.

for convergence to x_n is $p = \frac{1}{2}(\lambda_1 + \lambda_{n-1})$. Of course these considerations have only theoretical value since the eigenvalues are not known "a priori". The convergence could be very slow even if the optimum values for p were chosen in cases where $|\lambda_{n-1} - \lambda_n| \ll |\lambda_1 - \lambda_n|$ or

$$|\lambda_2 - \lambda_1| \ll |\lambda_1 - \lambda_n| .$$

Another improvement on the convergence of the power method can be achieved by using the scalar product

$$\frac{(A^k y_0, A^T k z_0)}{(A^{k-1} y_0, A^T k z_0)} \quad (6.11)$$

where $y_0 = a_1 x_1 + \dots + a_n x_n$

$$z_0 = b_1 v_1 + \dots + b_n v_n$$

to approximate the largest eigenvalue.

The use of the scalar product can reduce the number of iterative steps necessary to determine λ_1 by almost half.

In the case of A being symmetric, $z_0 = y_0$ and λ_1 is given by

$$\lambda_1 = \frac{(A^k y_0, A^k y_0)}{(A^{k-1} y_0, A^k y_0)} \quad (6.12)$$

6.3. The Method of Steepest Descent

The problem of finding the algebraically largest λ_1 or the algebraically smallest λ_n , is connected with the problem of maximizing or minimizing the Rayleigh quotient

$$f(x) = \frac{x^T A x}{x^T x} \quad (6.13)$$

with the readily evaluated derivative

$$g(x) = 2(Ax - f(x).x) / x^T x \quad (6.14)$$

The method of steepest descent looks in the direction of the gradient g_i for finding a better approximation x_{i+1} to the previous local minimum x_i , which minimizes the function in this direction. Let

$$x_{i+1} = x_i + \alpha_i g_i \quad (6.15)$$

be the expression for the new approximation. Substituting the value of x_{i+1} in equation (6.13), and after some algebra we find that

$$f(x_{i+1}) = f(x_i) + \frac{2\alpha_i t_o^2 + \alpha_i^2 t_o^2 f(g_i)}{1 + \alpha_i^2 t_o^2} \quad (6.16)$$

$$\text{where } t_o^2 = \frac{g_i^T g_i}{x_i^T x_i}$$

The change $\delta f(x_i)$ is given by

$$\delta f(x_i) = f(x_{i+1}) - f(x_i) = \frac{2\alpha_i - \alpha_i S_0}{1 + \alpha_i^2 t_o^2} t_o^2 \quad (6.17)$$

where $S_0 = f(x_i) - f(g_i)$

After equating the derivative of $\delta f(x_i)$ with respect to the step length α_i to zero we obtain the quadratic equation

$$\alpha_i^2 t_0^2 + \alpha_i S_0 - 1 = 0 \quad (6.18)$$

with the two roots

$$\alpha_1 = \frac{-S_0 + (S_0^2 + 4t_0^2)^{\frac{1}{2}}}{2 t_0^2}$$

$$\alpha_2 = \frac{-S_0 - (S_0^2 + 4t_0^2)^{\frac{1}{2}}}{2 t_0^2} \quad (6.19)$$

corresponding respectively to the search for the maximal and minimal $f(x)$.

6.4. The Method of Conjugate Gradients

The conjugate gradient method for the evaluation of eigenvalues was first used by Hestenes and Karush [136] and later has been applied with or without modifications by many investigators [34,113,116,120,121,123]. In this method the next approximation to the eigenvector x_{i+1} is sought along the vector p_i such that

$$x_{i+1} = x_i + \alpha_i p_i \quad (6.20)$$

with α_i being fixed by the condition that $f(x_{i+1})$ attains a minimum or a maximum along p_i . The search direction p_i itself

is generated recursively by

$$p_i = g_i + \beta_{i-1} p_{i-1} \quad (6.21)$$

$$\text{with } \beta_{i-1} = \frac{g_i^T g_i}{g_{i-1}^T g_{i-1}}$$

The best approximation of the Rayleigh quotient along p_i is realized by the roots of α_i that satisfy the equation

$$\frac{\partial f(x_i + \alpha_i p_i)}{\partial \alpha_i} = 0 \quad (6.22)$$

An explicit formula can be generated by substituting the values of x_i and p_i obtained from equations (6.20) and (6.21) into equation (6.22). After some algebra the resulting quadratic equation with respect to α has the form

$$\alpha^2 (abd - c) + \alpha ad + 1 = 0 \quad (6.23)$$

with the two roots

$$\alpha_1 = -2 / (ad + \sqrt{\Delta}) \quad (6.24a)$$

$$\Delta = a^2 d^2 - 4(abd - c)$$

$$\alpha_2 = 2 / (-ad + \sqrt{\Delta}) \quad (6.24b)$$

where

$$a = \frac{p_i^T p_i}{g_i^T g_i}$$

$$b = \frac{p_i^T x_i}{x_i^T x_i}$$

$$c = \frac{p_i^T p_i}{x_i^T x_i}$$

$$d = \frac{p_i^T A p_i}{p_i^T p_i} - \frac{x_i^T A x_i}{x_i^T x_i} \quad (6.25)$$

corresponding respectively to the search for the minimal (α_1) and the maximal (α_2) $f(x)$.

The conjugate gradient algorithm for the minimum or maximum eigenvalue of a symmetric matrix A is as follows :

$$\text{Start : } x_0, f(x_0) = \frac{x_0^T A x_0}{x_0^T x_0}$$

$$g(x_0) = 2(A x_0 - f(x_0)x_0) / (x_0^T x_0), p_0 = g_0$$

Iterate :

$$\alpha_i = \frac{-2}{+} \left(\frac{+}{-} a_i d_i + \sqrt{\Delta_i} \right)$$

$$x_{i+1} = x_i + \alpha_i p_i$$

$$f(x_{i+1}) = (x_{i+1}^T A x_{i+1}) / (x_{i+1}^T x_{i+1}) \quad (6.26)$$

$$g(x_{i+1}) = 2(A x_{i+1} - f(x_{i+1})x_{i+1}) / (x_{i+1}^T x_{i+1})$$

$$\beta_i = (g_{i+1}^T g_i) / (g_i^T g_i)$$

$$p_{i+1} = g_{i+1} + \beta_i p_i$$

with

$$a_i = \frac{p_i^T p_i}{g_i^T g_i}, \quad b_i = \frac{p_i^T x_i}{x_i^T x_i}, \quad c_i = \frac{p_i^T p_i}{x_i^T x_i}$$

$$d_i = \frac{p_i^T A p_i}{p_i^T p_i} - \frac{x_i^T A x_i}{x_i^T x_i}, \quad \Delta = a_i^2 d_i^2 - 4(a_i b_i d_i - c_i)$$

and x_0 being an arbitrary initial approximation to the required eigenvector.

6.5. Optimization of the Conjugate Gradient Algorithm

6.5.1. Fried's Method

A different evaluation of β_j can be derived from the condition that $f(x)$ is minimized not only with respect to α_j but also with respect to β_j . This in fact is the basic idea of the memory gradient method previously discussed in Chapter 3. This time an explicit expression can be obtained from the minimization of the Rayleigh quotient with respect to β_j .

Minimum Eigenvalue

Substituting α_j from equation (5.24a) into

$$\delta f(x_j) = \frac{g_j^T g_j}{x_j^T x_j} \frac{\alpha_j d_j \alpha_j^2 + 2\alpha_j}{1 + 2b_j \alpha_j + c_j \alpha_j^2} \quad (6.27)$$

gives

$$\delta f(x) = \frac{g_j^T g_j}{x_j^T x_j} \frac{\alpha_j}{1 + b_j \alpha_j} \quad (6.28)$$

The best change in the function with respect to β_j is obtained from

$$\partial \delta f(x_j) / \partial \beta_j = 0 \quad (6.29)$$

which leads to

$$\alpha_j - \alpha_j^2 b_j = 0 \quad (6.30)$$

where $()' = \frac{\partial}{\partial \beta_i}$

According to equation (6.24a), α_1 can be written

$$\alpha_1 = -2/F, \quad F_i = a_i d_i + \sqrt{\Delta_i}$$

and equation (5.30) is reduced to

$$F'_i - 2b'_i = 0 \quad (6.31)$$

The expression for the parameter F can be simplified, after neglecting c_i , into

$$F_i = a_i d_i + (a_i^2 d_i^2 - 4a_i b_i d_i)^{\frac{1}{2}} \quad (6.32)$$

Expanding the square root in the above equation and retaining only the first order terms, F is further simplified to

$$F_i = 2(a_i d_i - b_i) \quad (6.33)$$

Now equation (6.31) becomes

$$a_i' d_i + a_i d_i' - 2b'_i = 0 \quad (6.34)$$

Substituting the values for a_i , d_i , b_i from equations (6.25), and taking the derivatives with respect to β_i , equation (6.34) yields the following value for the scalar parameter β_i .

$$\beta_{i-1} = - (p_{i-1}^T (A-f_i) g_i - g_i^T g_i p_{i-1}^T x_i / x_i^T x_i) / p_{i-1}^T (A-f_i) g_i \quad (6.35)$$

Neglecting the term $(x_{i+1} - x_i)^T x_i$ equation (6.35) reduces to

$$\beta_{i-1} = - p_{i-1}^T (A-f_i) g_i / p_{i-1}^T (A-f_i) p_{i-1} \quad (6.36)$$

By neglecting some additional first order terms, the above equation can be degenerated into the equation

$$\beta_{i-1} = \frac{g_i^T g_i}{g_{i-1}^T g_{i-1}} \quad (6.37)$$

Maximum Eigenvalue

Substituting α_2 from equation (6.24b) into equation (6.30) results in

$$F'_i + 2b'_i = 0 \quad (6.38)$$

and the corresponding equation (6.34) for the case of the maximum eigenvalue is

$$\frac{b'_i}{a'_i d'_i} (a'_i d'_i + a_i d'_i) - 2b'_i = 0 \quad (6.39)$$

which unfortunately does not give an explicit expression for β_{i-1} as in equation (6.35). But after neglecting some terms β_{i-1} can be approximated by equation (6.36).

6.5.2. Geradin's Method

This algorithm relies upon the generation of a set of H-conjugate gradients, with H representing the Hessian matrix of the local second order derivatives of the function. Quadratic convergence is guaranteed in the neighbourhood of the eigensolution, by analogy to the conjugate gradient method when applied to quadratic functions. The importance of this method is that the H-conjugate directions can be computed without physically building up the H matrix.

The value of β_i is evaluated from the orthogonality condition

$$p_{i+1}^T H p_i = 0 \quad (6.40)$$

with

$$H = \frac{\partial^2 f}{\partial x_i \partial x_j} \quad (6.41)$$

From equations (6.40) and (6.41) it follows that the orthogonalization parameter is given by

$$\beta_i = \frac{g_{i+1}^T H p_i}{p_i^T H p_i} \quad (6.42)$$

By referring to its definition, the local Hessian matrix can be written as

$$H = \frac{2}{x_{i+1}^T x_{i+1}} (A - f_{i+1} - x_{i+1}^T g_{i+1} - g_{i+1}^T x_{i+1}) \quad (6.43)$$

Substituting the expression for the Hessian matrix into equation (6.42) and taking into account that

$$\frac{\partial f(x_i + \alpha_i p_i)}{\partial \alpha_i} = g_{i+1}^T p_i = 0 \quad (6.44)$$

the orthogonalization parameter reduces to

$$\beta_i = \frac{g_{i+1}^T (A - f_{i+1}) p_i - g_{i+1}^T g_{i+1} (x_{i+1}^T p_i)}{p_i^T (A - f_{i+1}) p_i} \quad (6.45)$$

6.6. Convergence and Initial Approximation

The problem of minimizing the Rayleigh quotient is somewhat of an exception to that of a function with a well

defined minimum in that the Rayleigh quotient has no unique minimum point. Owing to the homogeneous form of the Rayleigh quotient, its value remains constant at all points lying in any given line in N-dimensional space passing through the origin. Hence there is one redundant degree of freedom, which causes the Hessian matrix to be singular in the neighbourhood of an eigenvector, and so the minimization algorithm cannot utilize to the full the property of the quadratic convergence.

In order to overcome this uncertainty which surrounds the function around the minimum Bradbury and Fletcher [34] reduced the number of variables by one so as to remove the redundant degree of freedom. The vectors x_i are restrained to lie on a convex surface containing the origin, typically the "unit-sphere" of any vector norm of x_i . Obvious possibilities would include the Euclidean (L_2) norm with unit sphere $x^T x = 1$, the sum (L_1) norm ($\sum |x_i| = 1$), and the maximum (L_∞) norm ($\max_i |x_i| = 1$). The simplest way of doing the transformation is to use the maximum norm where the convex surface becomes an intersection of planes producing a hypercube having $2N$ faces with variables directly related to the elements of x_i .

Posing the problem in this way, it becomes important that a good starting value is found in order to avoid wasting unnecessary time in trying to find the appropriate face of the hypercube upon which to minimize the function. A convenient initial starting point is one of the unit vectors e_i . Then the Rayleigh quotient at e_i is given by

$$f(e_i) = \frac{e_i^T A e_i}{e_i^T e_i} = a_{ii} \quad (6.46)$$

where a_{ii} is the i -th diagonal element of A . The gradient vector is given by

$$g(e_i) = 2(a_i - f(e_i)) \quad (6.47)$$

where a_i is the i -th column vector of A . Hence the e_i which is chosen as a starting point is that which corresponds to the minimum or maximum (depending on the search for the minimum or maximum eigenvalue) of the diagonal elements a_{ii} . If it happens that the minimum element a_{ii} is the same for more than one i , then e_i is chosen as that for which the modulus of the gradient is largest to ensure that with the first step the minimization procedure makes the fastest descent towards the minimum. When matrix A is diagonally scaled with $a_{ii} = 1$ then the maximum gradient is the criterion for choosing e_i .

Using this method proposed by Bradbury and Fletcher, the elements of x_i are examined at each iteration and normalized by the appropriate scalar which reduces the element of largest absolute value to unity. However, Geradin's procedure avoids this artificial normalization because of the explicit implementation of the Hessian matrix with the conjugate directions building up without referring to the length of the vectors x_i .

The product Ax_{i+1} can be calculated recursively, instead of carrying out the multiplication at each iteration, from the relationship

$$Ax_{i+1} = Ax_i + \alpha_i A p_i \quad (6.48)$$

It is advisable however to compute this directly every so often so as to prevent the domination of rounding-off errors, particularly with ill-conditioned problems.

6.7. Gershgorin Theorem

Gershgorin in his original paper in 1931, proved that all eigenvalues of a matrix A were less in modulus than any norm of the same matrix. Estimates using the first and second norms are especially convenient, since they are simply expressed by the matrix elements.

Let $A = (a_{ij})$ be a matrix with arbitrary complex elements, then all the eigenvalues of this matrix are located in a region D which is the union of the circles

$$|\lambda - a_{ii}| \leq R_i \quad (i = 1, \dots, N) \quad (6.49)$$

where

$$R_i = \sum_{\substack{j=1 \\ j \neq i}}^N |a_{ij}|$$

or

$$|\lambda| \leq |a_{ii}| + R_i \quad (6.50)$$

$$\leq \sum_{i=1}^N |a_{ij}|$$

6.8. Coordinate Relaxation

The coordinate relaxation was proposed by Faddeev and Faddeeva [101] and recently has been used by many authors [25, 141, 163, 258, 263] .

In this method, which is also called the method of alternative directions, the search direction w is taken successively as the different base vectors e_m , with $m = 1, \dots, N$. The new estimate x_{i+1} is now given by

$$x_{i+1} = x_i + \alpha_i w_i . \quad (6.51)$$

$$\text{with } w_i = (0, 0, \dots, 1, 0)^T$$

The optimum value for α will be obtained, as in the case of the gradient methods, by minimizing the Rayleigh quotient with respect to α . This procedure yields the same quadratic equation as before

$$a\alpha^2 + b\alpha + c = 0 \quad (6.52)$$

where

$$a = (x^T w)(w^T A w) - (w^T w)(x^T A w) / (x^T x)$$

$$b = (w^T A w) - (w^T w) \cdot f(x) \quad (6.53)$$

$$c = (w^T A w) - (x^T w) f(x)$$

As w is one of the base vectors e_m , equations (5.53) become

$$a = (a_{mm} x_m - d_m) / (x^T x)$$

$$b = a_{mm} - f(x) \quad (6.54)$$

$$c = d_m - f(x)x_m$$

where

a_{mm} is the m-th diagonal term of A

x_m is the m-th term of the vector x

d_m is the m-th term of the vector Ax

The Rayleigh quotient is found recursively from

$$f_{i+1} = f_i + (b.a + 2c) \alpha / (x^T x)^{i+1} \quad (6.55)$$

$$\text{with } (x^T x)^{i+1} = (x^T x)^i + (2x_m + \alpha) \alpha \quad (6.56)$$

6.9. Numerical Studies

For the purpose of this study the computer programs shown in Table 6.1 were developed. Their efficiency in calculating the minimum and maximum eigenvalues of the stiffness matrices of examples 2 and 3 was studied and compared. The matrices were initially scaled. The letter "B" after the abbreviated name of a method means that the Bradbury and Fletcher orthogonalization process is applied in each iteration of the method. The following difference error termination criterion has been used throughout this section :

$$\frac{|\lambda^k - \lambda^{k-1}|}{|\lambda^k|} \leq \epsilon \quad (6.57)$$

Abbreviated name	Explanation
EIGP	Power method
EIGSD	Steepest descent method
EIGFR1	Fried's method with equation (6.36) for the evaluation of β
EIGFR2	Fried's method with equation (6.35) for the evaluation of β
EIGCG	Conjugate gradient algorithm
EIGGER	Geradin's algorithm
EIGCR	Coordinate relaxation method

Table 6.1 Computer programs for the special eigenvalue problem

Table 6.2 and Figure 6.2 show the number of iterations and the total execution time required for the evaluation of the minimum eigenvalue of example 2. The steepest descent method was applied with a relaxation coefficient $\gamma = 0.6$, while the power method was applied without translation. From Figure 6.2 we can see that the EIGCG and EIGGER methods gave almost identical results. They converged very quickly up to the value of the termination parameter $\epsilon = 0.1E-03$ and then they produced slower convergence. The EIGFR2 with the Bradbury

Termination Parameter ϵ		0.1E-00		0.1E-01		0.1E-02		0.1E-03		0.1E-04		0.1E-05		0.1E-06	
Number	Method	N_{it}	TIME	N_{it}	TIME	N_{it}	TIME	N_{it}	TIME	N_{it}	TIME	N_{it}	TIME	N_{it}	TIME
1	EIGSD ($\beta = 0.6$)	5	0.012	26	0.06	33	0.074	43	0.097	557	1.257	764	1.725	1070	2.416
2	EIGCR	20	0.030	36	0.055	48	0.074	62	0.095	4367	6.707	14876	22.850	16854	25.88
3	EIGFR1	4	0.005	67	0.09	95	0.127	123	0.165	13455	17.99	17784	23.78	22032	29.50
4	EIGFR2	6	0.014	6	0.014	28	0.07	104	0.256	151	0.372	247	0.608	526	1.296
5	EIGFR2B	6	0.010	13	0.022	58	0.096	96	0.159	109	0.180	120	0.199	144	0.239
6	EIGCG	10	0.016	11	0.017	13	0.020	17	0.026	165	0.254	191	0.297	205	0.319
7	EIGCGB	2	0.016	3	0.024	4	0.032	693	5.492	1302	9.995	1372	10.32	1442	11.429
8	EIGGER	10	0.017	12	0.020	17	0.029	19	0.023	146	0.251	156	0.268	177	0.305

Table 6.2 Numerical studies for the minimum eigenvalue of example 2

Termination Parameter ϵ		0.1E-00		0.1E-01		0.1E-02		0.1E-03		0.1E-04		0.1E-05		0.1E-06	
Number	Method	N_{it}	TIME	N_{it}	TIME	N_{it}	TIME	N_{it}	TIME	N_{it}	TIME	N_{it}	TIME	N_{it}	TIME
1	EIGP	5	0.006	9	0.01	17	0.02	36	0.06	55	0.070	74	0.094	96	0.122
2	EIGSD ($\beta = 0.6$)	5	0.012	7	0.016	13	0.029	17	0.038	21	0.047	27	0.061	33	0.075
3	EIGCR	2	0.003	4	0.006	8	0.012	19	0.029	54	0.083	86	0.132	118	0.181
4	EIGFR1	4	0.007	6	0.01	13	0.02	23	0.038	32	0.052	42	0.07	55	0.09
5	EIGFR1B	2	0.003	6	0.01	8	0.013	27	0.045	45	0.075	63	0.10	81	0.134
6	EIGCG	4	0.006	6	0.093	9	0.014	12	0.019	14	0.022	16	0.025	23	0.036
7	EIGCGB	2	0.016	3	0.024	4	0.032	5	0.040	6	0.048	135	1.077	136	1.078
8	EIGGER	2	0.003	8	0.014	10	0.017	13	0.022	15	0.026	18	0.030	25	0.043

Table 6.3 Numerical studies for the maximum eigenvalue of example 2

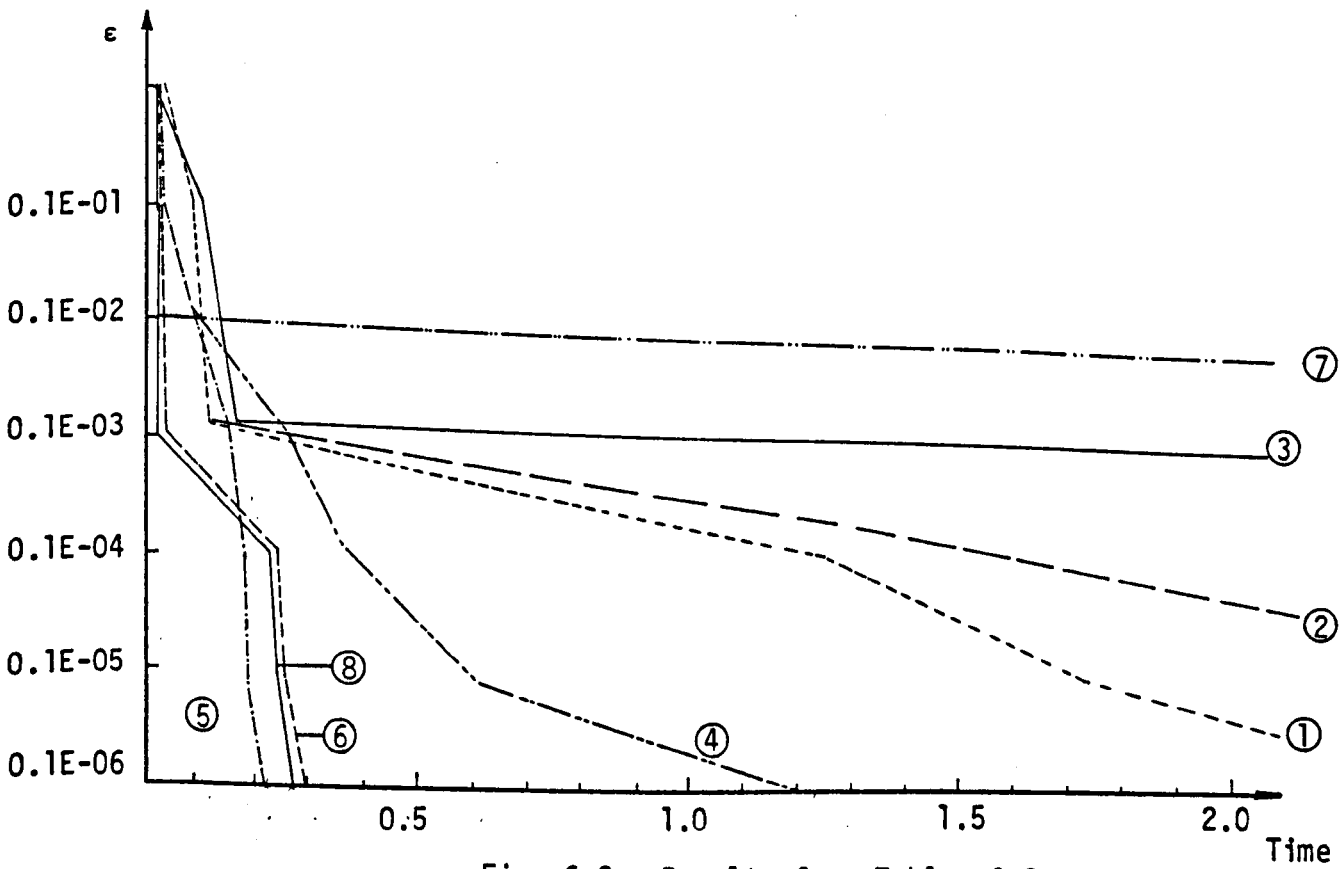


Fig. 6.2 Results from Table 6.2

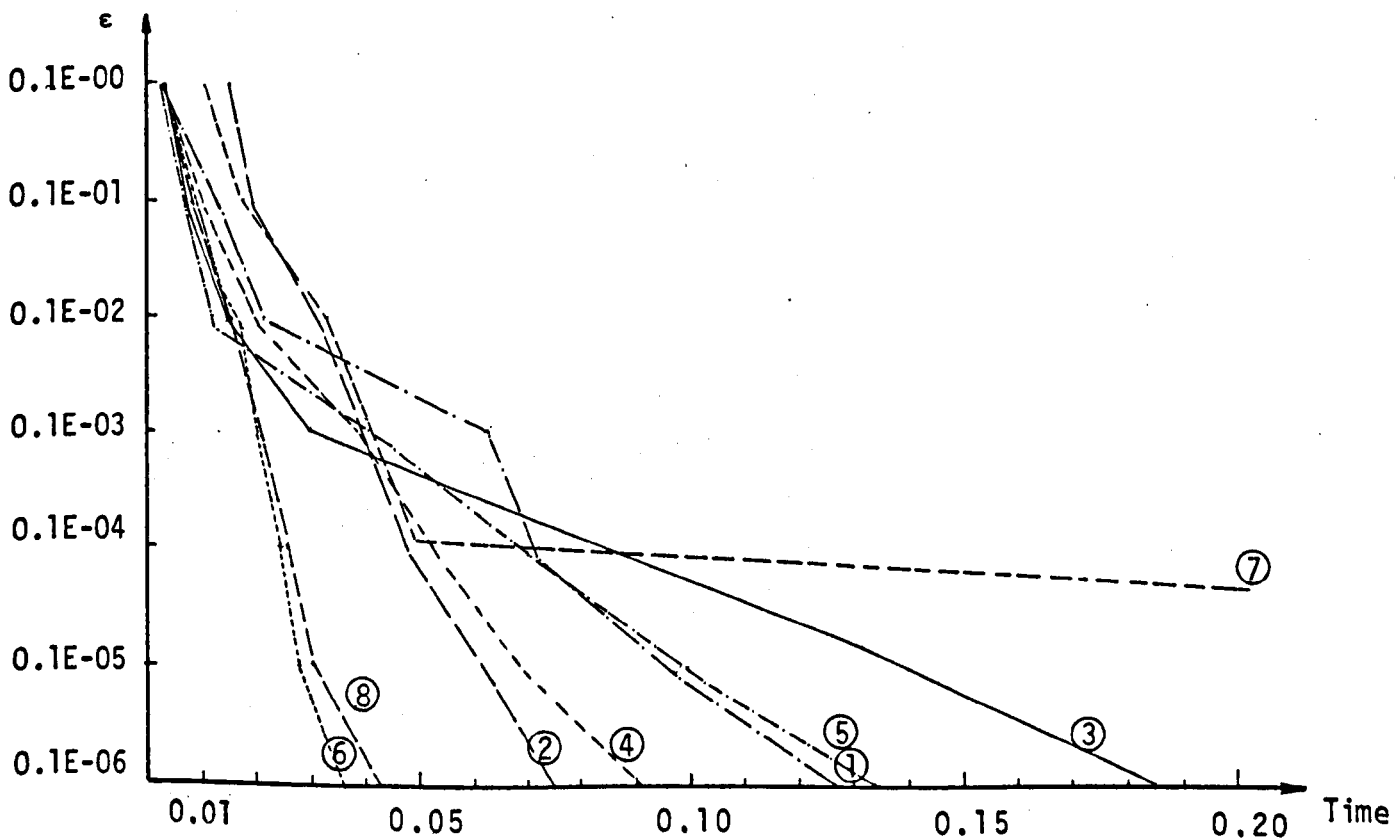


Fig. 6.3 Results from Table 6.3

and Fletcher orthogonalization technique produced better convergence after the value of $\epsilon = 0.1E-04$.

Figure 6.3 demonstrates that the simple conjugate gradient method is the fastest method for the evaluation of the maximum eigenvalue of the scaled stiffness matrix of example 2. Geradin's algorithm gave very close results to EIGCG, while the Bradbury and Fletcher orthogonalization algorithm, as applied to EIGCG method, produced the slowest convergence rate. In Table 6.4 and Figure 6.4, the convergence rates of the methods are demonstrated for the evaluation of the minimum eigenvalue, while in Table 6.5 and Figure 6.5 the same studies are performed for the maximum eigenvalue of the scaled stiffness matrix of example 3.

In all the above examples the initial estimate of the vector x was taken as $x_i^0 = 1.0$, $i = 1, \dots, N$. Different starting values, ranging from $x_i^0 = 10$ up to $x_i^0 = 10,000$, were tried in order to study the degree of dependence of the convergence rates, as well as the accuracy of the final results, on the initial starting value. All methods, except EIGFRI, remained unaffected by these changes of the initial vector. The EIGFRI produced slower convergence only for the minimum eigenvalue of example 2 and also converged to a different minimum from the true one.

Table 6.6 shows the improvement in the convergence rate of the steepest descent method when a relaxation parameter is

Termination Parameter ϵ		0.1E-00		0.1E-01		0.1E-02		0.1E-03		0.1E-04		0.1E-05		0.1E-06	
Number	Method	N_{it}	TIME	N_{it}	TIME	N_{it}	TIME	N_{it}	TIME	N_{it}	TIME	N_{it}	TIME	N_{it}	TIME
1	EIGSD ($\beta = 0.6$)	5	0.042	16	0.136	34	0.289	47	0.399	53	0.450	70	0.594	94	0.798
2	EIGCR	5	0.027	18	0.096	28	0.149	39	0.208	52	0.277	65	0.347	1820	9.707
3	EIGFR1	5	0.028	25	0.142	55	0.400	90	0.505	125	0.701	161	0.903	203	1.138
4	EIGFR2	6	0.033	15	0.085	19	0.107	23	0.130	26	0.147	29	0.162	61	0.349
5	EIGFR2B	8	0.053	14	0.093	16	0.106	23	0.152	27	0.176	30	0.197	34	0.224
6	EIGCG	7	0.039	15	0.084	18	0.101	23	0.129	26	0.146	30	0.168	67	0.376
7	EIGCGB	7	0.046	13	0.086	15	0.099	22	0.145	26	0.171	31	0.204	33	0.217
8	EIGGER	7	0.039	15	0.084	18	0.101	23	0.129	26	0.146	32	0.179	63	0.352

Table 6.4 Numerical studies for the minimum eigenvalue of example 3

Termination Parameter ϵ		0.1E-00		0.1E-01		0.1E-02		0.1E-03		0.1E-04		0.1E-05		0.1E-06	
Number	Method	N_{it}	TIME	N_{it}	TIME	N_{it}	TIME	N_{it}	TIME	N_{it}	TIME	N_{it}	TIME	N_{it}	TIME
1	EIGP	5	0.014	8	0.038	15	0.072	23	0.110	31	0.149	40	0.192	52	0.250
2	EIGSD ($\beta = 0.6$)	4	0.035	7	0.061	11	0.096	15	0.131	20	0.174	24	0.201	981	8.538
3	EIGCR	3	0.016	4	0.021	5	0.027	17	0.091	38	0.203	60	0.320	512	2.730
4	EIGFR1	3	0.018	6	0.034	10	0.056	14	0.079	19	0.107	23	0.151	981	6.451
5	EIGFR1B	2	0.019	4	0.038	8	0.075	14	0.132	20	0.241	26	0.245	335	3.151
6	EIGCG	3	0.017	5	0.028	7	0.039	8	0.045	11	0.062	12	0.067	32	0.179
7	EIGCGB	2	0.013	3	0.018	5	0.033	11	0.068	13	0.086	14	0.092	33	0.217
8	EIGGER	2	0.011	7	0.039	9	0.050	10	0.056	12	0.067	13	0.073	33	0.185

Table 6.5 Numerical Studies for the maximum eigenvalue of example 3

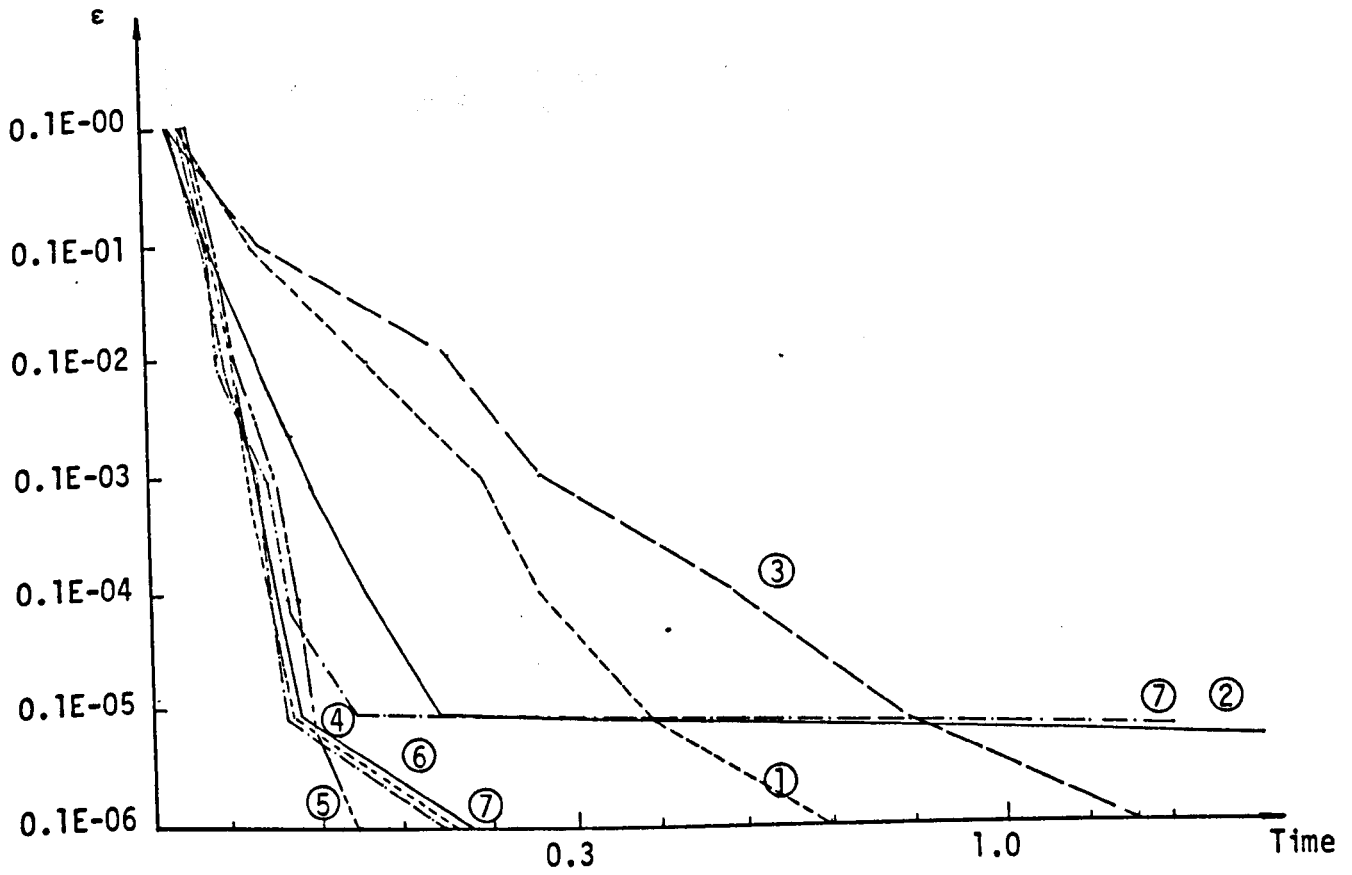


Fig. 6.4. Results from Table 6.4.

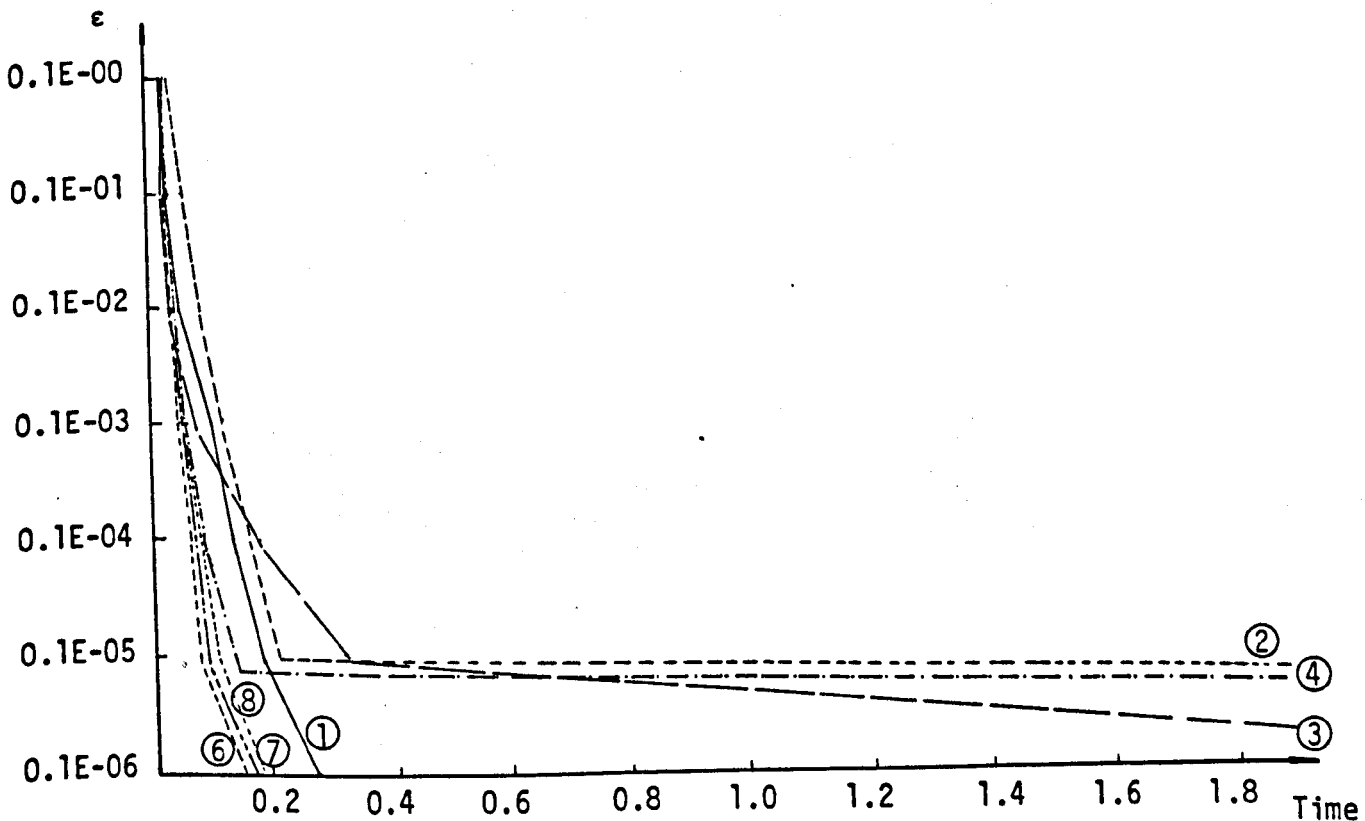


Fig. 6.5. Results from Table 6.5.

used each time a new approximation to the final eigenvector is calculated. Tables 6.7 and 6.8 show the convergence of the methods to the true minimum eigenvalues of examples 2 and 3. The number of iterations required to achieve convergence up to 2, 4 and 6 significant decimal digits to the true values are demonstrated.

Finally, Table 6.9 indicates the difference in the convergence rates achieved when the simplified residual

$$r_i = Ax - f(x).x \quad (6.57)$$

is used, instead of the gradient vector given by equation 6.14. We can see that this simplification has no effect on the steepest descent method, but has significantly reduced the convergence of the conjugate gradient algorithms.

6.10. Conclusions

The power method, as applied in this study, without shifting, produced very satisfactory results for the evaluation of the maximum eigenvalue. For the evaluation of the minimum eigenvalue however, the value of the shifting parameter p should be properly chosen so as to make the minimum eigenvalue the dominant one. And since there is no formula for an "a priori" evaluation of the proper shifting parameter, a slight misjudgment in the value of p could produce another eigenvalue.

The method of coordinate relaxation or alternating



Termination Parameter ϵ		0.1E-000	0.1E-01	0.1E-020	0.1E-03	0.1E-04	0.1E-05	0.1E-06
λ min 	$\beta = 1.0$	5	68	96	124	13460	-	-
	$\beta = 0.6$	5	26	33	43	557	764	1070
λ min 	$\beta = 1.0$	6	26	58	94	130	168	211
	$\beta = 0.6$	5	16	34	47	53	170	94

Table 6.6. EIGSD with and without relaxation parameter

Method	$n_q = 2$	$n_q = 4$	$n_q = 6$	Final eigenvalue
EIGSD	557	1070	10509	0.27362566E-03
EIGCR	14876	16854	20806	0.27362565E-03
EIGFR1	13455	22032	34749	0.27362566E-03
EIGFR2B	96	120	170	0.27362565E-03
EIGCG	165	191	248	0.27362565E-03
EIGGER	146	156	177	0.27362565E-03
EIGFR2	104	247	1092	0.27362565E-03
EIGCGB	1302	1372	1480	0.27362565E-03

Table 6.7 Convergence study for the minimum eigenvalue of example 2

Method	$n_q = 2$	$n_q = 4$	$n_q = 6$	Final Eigenvalue
EIGSD	34	473	2751	0.51127477E-01
EIGCR	28	11108	-	0.51129449E-01
EIGFR1	55	-	-	0.51164060E-01
EIGFR2	15	61	128	0.51127473E-01
EIGFR2B	14	-	-	0.51201473E-01
EIGCG	13	-	-	0.51201473E-01
EIGCGB	15	67	67	0.51127473E-01
EIGGER	15	63	100	0.51127473E-01

Table 6.8 Convergence study for the minimum eigenvalue of example 3

Termination Parameter		0.1E-00	0.1E-01	0.1E-02	0.1E-03	0.1E-04	0.1E-05	0.1E-06
EIGSD ($\beta = 1.0$)	r_i	5	68	96	124	13460	-	-
	g_i	5	68	96	124	13460	-	-
EIGCG	r_i	10	11	13	19	255	279	314
	g_i	10	11	13	17	165	191	205
EIGGER	r_i	6	17	22	25	333	395	461
	g_i	10	12	17	19	146	156	177

Table 6.9 Convergence to the minimum eigenvalue of example 2 for different gradient vectors

directions produced better results in the evaluation of the maximum eigenvalue than for the minimum eigenvalue. While in all cases the convergence rate was inferior to that of the conjugate gradient method.

From the gradient methods, the method of steepest descent, as was expected, produced the slower convergence. Despite the significant improvement in the convergence when the proper relaxation coefficient is used, the total execution time could be up to 50 times more than the required time for convergence of the conjugate gradient method.

The modifications proposed by Fried in the evaluation of the scalar parameter β , did not produce the expected results. The implementation of the expression for β given by equation (6.35) gave better results than the simplified expression given by equation (6.36), but in both cases the final convergence obtained was slower than that obtained by the simple conjugate gradient algorithm. The use of the Bradbury and Fletcher orthogonalization process improved only the convergence of the EIGFR2 method, and did not produce at all competitive results when applied to the EIGCG.

The method proposed by Geradin and the simple conjugate gradient algorithm gave almost identical results. Both methods proved to be the fastest in the evaluation of the minimum and maximum eigenvalues of the stiffness matrices for the examples considered in this work. The convergence characteristics of the methods remained unaffected by the value of the first

approximation of the eigenvector x . The evaluation of the minimum eigenvalue proved more time consuming than the evaluation of the maximum eigenvalue. The reason for this is that the ratio $\lambda_{n-1} / \lambda_n$ is much closer to unity than the ratio λ_2 / λ_1 .

Finally, the main conclusion from the work carried out in this Chapter is that when the minimum and maximum eigenvalues of a stiffness matrix are required, the simple conjugate gradient algorithm, and the modified algorithm proposed by Geradin, give the most consistent and accurate results in the minimum execution time. These methods could be very easily incorporated in the "a priori" evaluation of the iteration parameters for the Tchebycheff method. The additional storage requirements are negligible while the additional execution time remains around 10% of the total execution time (see Chapter 7).

CHAPTER 7

NUMERICAL STUDIES ON RELAXATION METHODS

In this Chapter, as in Chapter 4, comparisons have been made of the relative efficiencies of the relaxation methods discussed in Chapter 5 as applied to nonlinear analysis of cable structures. All computer programs have been written with similar processes to allow effective comparisons to be made on the basis of the total execution time required to obtain convergence. Here again the number of iterations are not a reliable measure for comparison since the execution time for each iteration varies from method to method.

All computational work has been carried out on the CDC 7600 computer. Table 7.1 shows the methods used in this Chapter and their abbreviated names.

7.1. Dynamic Relaxation Method

The method of dynamic relaxation as developed in Chapter 5 was applied to stiffening structures. The minimum and maximum eigenvalues of the matrix B have been calculated by applying Geradin's algorithm as discussed in Chapter 6. The procedure for obtaining the extreme eigenvalues in this way needs almost no extra storage since it is separate from the main dynamic relaxation algorithm and the same space vectors can be utilized twice.

	Abbreviated name	Description of the method
Dynamic relaxation methods	DRGR	DR with Geradin's algorithm for finding the extreme eigenvalues
	DRGRFS	DR with Flanders and Shortley parameters and Geradin's algorithm for the extreme eigenvalues
	DRGRYN	DR with Young's parameters and Geradin's algorithm for the extreme eigenvalues
	DRAUT	DR with automatic adjustment of the iteration parameters
	DRKR	DR with the use of kinetic damping and a residual criterion to avoid divergence
	DRKV	DR with kinetic damping and a velocity criterion to avoid divergence
	CGTCH	A combined conjugate gradient algorithm and the DRAUT method
Successive overrelaxation methods	SORNL	SOR with the stiffness matrix being reset in each iteration
	SORES	SOR with the stiffness matrix being constant and resetting only the residuals
	SORESC	SOR with Carre algorithm for the parameter ω and resetting only the residuals
	SORESH	SOR with Hageman algorithm for the parameter ω and resetting only the residuals

Table 7.1 Relaxation methods used in Chapter 7

After obtaining the minimum and maximum eigenvalues, the iteration parameters of damping, mass and time step may be evaluated from equations (5.26) and (5.27). From these equations we can see that one of the three dynamic relaxation parameters is superfluous, since there are only two equations and three unknown parameters to be determined. To overcome this interdependence the time step h was chosen to be unity and then the other two parameters are evaluated from

$$\rho_{opt} = \frac{1}{4} (\lambda_{B \min} + \lambda_{B \max}) \quad (7.1)$$

$$c_{opt} = \sqrt{\lambda_{B \min} \cdot \lambda_{B \max}} \quad (7.2)$$

The method was first applied to the three storey frame of example 6. Although this problem is not a cable structure, the application of dynamic relaxation for the nonlinear solution of this structure was very helpful for understanding the behaviour of the method when applied to stiffening structures with small nonlinearities. The values of the minimum and maximum eigenvalues of the scaled stiffness matrix of example 6, before and after the application of the horizontal load at node 6, are shown in Table 7.2 .

When the iteration parameters were evaluated from the minimum and maximum eigenvalues of the original stiffness matrix before the application of the load, an oscillatory behaviour of the structure about its equilibrium form was observed, without any sign of convergence to the static solution. The method was

then applied for the linear solution and reached the specified

	Minimum eigenvalue	Maximum eigenvalue	Condition number
Initial configuration	0.10772E-01	2.195794	204
Final configuration	0.11679E-01	2.21229	190

Table 7.2. Eigenvalue analysis of example 6

convergence in 131 iterations. This indicated that the increase in the maximum eigenvalue from 2.195794 to 2.21229 after the application of the load, which was not taken into account in the evaluation of the iteration parameters, produced this non-convergence effect. A bigger increase in the maximum eigenvalue would have caused the method to diverge.

There are two ways to cope with an increasing maximum eigenvalue during the application of the loads. The first is to recompute the maximum eigenvalue when the convergence of the method deteriorates, using the current values of the elemental stiffness matrices. The second is to modify "a priori" the relaxation parameters to allow for an increase of the maximum eigenvalue as the iteration process continues. The scale of this modification depends on the degree of nonlinearity of the problem.

The first approach could be time consuming since the whole process of calculating the maximum eigenvalue must be repeated each time the convergence rate deteriorates. The second process, on the other hand, is more straight forward, since an increase in the iteration parameter ρ or a reduced value for the time step h , could alleviate the effects of the stiffening behaviour of the structure.

For an increase of 20% in the initial value of the parameter ρ , in example 6, the dynamic relaxation method converged in 166 iterations, while a 70% increase in the value of ρ resulted in convergence at 510 iterations.

Example 2, of the counterstressed dual cable structure was also studied. Two load cases were considered :

Load case "A" $w = 10.0$ kips

Load case "B" $w = 50.0$ kips

Table 7.6 shows the eigenvalue analysis of the scaled stiffness matrix of this example. It is very interesting to see how the condition matrix is reduced with increased loading.

After calculating the minimum and maximum eigenvalues of the unstiffened matrix and applying dynamic relaxation with iteration parameters obtained from the initial estimates of the extreme eigenvalues, the method produced a very slow convergence. But with a slight increase in the value of the parameter ρ (see Table 7.7), the method converged rapidly. This 1% increase in the value of ρ was enough to ensure that the actual maximum eigenvalue,

METHOD	DRGR	DRGRFS	DRGRYN
Number of iterations	166	156	156
Time (sec)	0.182	0.180	0.179

$$\rho = 1.20 \times \rho_0$$

RNORM criterion
($\epsilon = 0.1E-07$)

Table 7.3. Studies of example 6

Nodes	x(ft)	y(ft)
1	0.20863	0.1333
2	0.20889	0.1334
3	0.63210	0.21359
4	0.6296	-0.21307
5	1.14767	0.23747
6	1.17154	-0.24253

Table 7.4 Linear displacements of example 6

Nodes	x(ft)	y(ft)
1	0.212108	0.11846
2	0.18981	-0.1313
3	0.61971	0.15602
4	0.57633	-0.2373
5	1.0974	0.12122
6	1.07172	-0.3118

Table 7.5 Final displacements of example 6

	Minimum Eigenvalue	Maximum Eigenvalue	Condition Number
Initial configuration	0.27363E-03	2.15050	7860
After loading condition "A" (w = 10 kips)	0.5791E-03	2.16674	3741
After loading condition "B" (w = 50 kips)	0.11887E-02	2.25858	1900

Table 7.6 Eigenvalue analysis of example 2

Values of "ρ"	$\rho = 1.0\rho_0$	$\rho = 1.01\rho_0$	$\rho = 1.05\rho_0$	$\rho = 1.10\rho_0$	$\rho = 1.2\rho_0$
Number of iterations	after 5400 no convergence	1402	1427	1730	2543

RNORM criterion ($\epsilon=0.1E-07$)

Table 7.7 Studies of example 2 with DRGR. Load case "A"

ϵ	Values of h	1.00	0.985	0.98	0.95	0.90	0.85
	0.1E-03	-	879	885	918	1354	1725
0.1E-07	-	-	-	5425	2395	3130	

RNORM criterion ($\epsilon=0.1E-07$)

Table 7.8 Studies of example 2 with DRGR. Load case "A"

after the application of the loads, times h^2/ρ , will in fact be less than 4.0 for stability. Table 7.7 also indicates that as we increase the value of ρ the convergence deteriorates since we are moving away from the current minimum and maximum eigenvalues.

Table 7.8 shows the effect on the convergence obtained, not by increasing the value of ρ as before, but by decreasing the value of the time increment h . A decrease in the time step will again ensure that the actual current maximum eigenvalue times h^2/ρ will be less than 4.0. Time steps close to unity produced better convergence, for bigger values of the termination parameter ϵ , than time steps less than one, but failed to converge for values of the termination parameter around $0.1E-07$. The value of $h = 0.90$, although slower in the beginning, gave in the end the best convergence results.

Comparing the two Tables 7.7 and 7.8 we can draw the conclusion that, from the point of view of convergence, it is better to increase the value of the density parameter ρ than to decrease the time step. When the structure was subjected to the load case "B"; a bigger increase in the value of the parameter ρ was necessary to eliminate the effect of the increase of the maximum eigenvalue during the application of loads. As Table 7.9 indicates, the best result was obtained when the original value of ρ was increased by 14%.

The conjugate gradient algorithm, for the evaluation of the

minimum and maximum eigenvalues of example 2, required only 30 iterations for both eigenvalues to converge to a termination parameter $\epsilon = 0.1E-03$, and the whole process was performed in 0.162 seconds which is about 10% of the total execution time. The required time for the evaluation of the extreme eigenvalues can be further reduced by introducing a six vector representation of the overall stiffness matrix, similar to the one used for the successive overrelaxation method. Then as the overall matrix coefficients are readily available there will be no need to recalculate the elemental stiffness matrices in each conjugate gradient iteration.

In Table 7.10 there is a comparison of dynamic relaxation with iteration coefficients given by Frankel's method and also by the Flanders and Shortley method. The two methods gave almost the same results, with the Flanders and Shortley method converging in a fewer number of iterations, while Frankel's method was slightly better in terms of the total execution time. This suggests that using constant iteration parameters throughout the iteration process required a greater number of iterations but less computer time due to less arithmetic. The use of Young's iteration parameters gave exactly the same results as those of Flanders and Shortley which indicates that the algorithm given by Young for the iteration parameters is the same as that of Flanders and Shortley but with different notation.

When the dynamic relaxation, with an "a priori" evaluation of the iteration parameters, was applied to the single cable of example 1, the iterative procedure diverged for a great number of combinations of the parameters h and ρ . As Table 7.11 indicates,

Value of "ρ"	1.0ρ ₀	1.01ρ ₀	1.20ρ ₀	1.30ρ ₀	1.40ρ ₀
Number of iterations	Divergence	Divergence	5488	5355	5262
Value of -ρ-	1.42	1.46	1.50	1.60	2.0
Number of iterations	3620	5375	3933	3530	2120

RNORM
criterion
(ε=0.1E-07)

Table 7.9 Studies of example 2. Load case 'B'

	Minimum Eigenvalue	Maximum Eigenvalue	Condition Number
Initial configuration	0.6158E-04	3.937957	64000
After the application of loads	0.29026E-03	17.43234	60000

Table 7.11 Eigenvalue analysis of example 1 with pretension

Termination Parameter	0.1E-00		0.1E-02		0.1E-04		0.1E-06		0.1E-08	
	N _{it}	TIME	N _{it}	TIME	N _{it}	TIME	N _{it}	TIME	N _{it}	TIME
DRGR	269	0.249	840	0.771	1398	1.282	1956	1792	2529	2316
DRGRFS	258	0.412	828	0.955	1387	1.488	1945	2021	2509	2559

Table 7.10 Studies of example 2. Load case 'A'

there is a big increase in the maximum eigenvalue for this problem, namely from 3.937957 to 17.4323, before and after the application of the load respectively. Only a very small time step or a big increase in ρ will safeguard convergence for this problem. But under these conditions the convergence of the method would be very slow. The same difficulty of nonconvergence was encountered when the method was applied to the hyperbolic paraboloid of example 3.

7.2. Automatic Adjustment of Dynamic Relaxation Parameters

The automatic adjustment method for the dynamic relaxation parameters, as developed in Section 5.9 was applied to various structures. In order to calculate the iteration parameters the minimum and maximum eigenvalues of the matrix B should first be defined. In the majority of the applications the method was applied in its scaled form with $B = D^{-\frac{1}{2}} K D^{-\frac{1}{2}}$. When no scaling transformations were used, the letters "UNSC" follow the abbreviated name of the method.

Table 7.12 shows the required number of iterations for convergence, with different values of the estimated minimum eigenvalue, when the estimated maximum eigenvalue remained constant. We can see that even after a one hundred-fold increase in the value of the estimated minimum eigenvalue, compared with the actual one, the convergence of the method did not seem to be

λ_{\min}	0.02	0.05	0.1	0.2	0.4	0.6	1.0
N_{it}	183	210	164	145	145	143	203

Table 7.12 Studies of example 6 with DRAUT

$\lambda_{\max} = 2.22$
 RNORM criterion
 ($\epsilon = 0.1E-07$)

N_{it}	λ_{\min}	λ_{\max}	q_{ϵ}
127	1.0	2.22	0.01
144	0.02	2.22	0.01
128	0.02	2.22	0.0001
123	0.02	1.80	0.01
121	0.1	1.80	0.001
119	0.1	2.40	0.001
98	0.1	2.22	0.001
128	0.001	2.22	0.001

RNORM criterion
 ($\epsilon = 0.1E-07$)

Table 7.13 Studies of example 6 with DRAUT

affected.

The value of q_ϵ in Table 7.13 is the difference between two successive values of the asymptotic convergence rate (eq. 5.84) required in order to proceed with another evaluation of the iteration parameters. It is apparent from Table 7.13, that for example 6, despite the different combinations in the values of q_ϵ , λ_{\max} and λ_{\min} , the number of iterations required for convergence was little affected. The method can handle not only arbitrary estimations of the minimum eigenvalue but also incorrect estimations of the maximum eigenvalue. One very easily obtained starting value for λ_{\max} is given by the Gershgorin bound theorem. An over-estimated value for λ_{\max} will safeguard against divergence but will slow down the convergence rate, while an underestimation of λ_{\max} will soon lead to instability of the method.

In stiffening structures, as indeed are the majority of cable structures, even if a bound for the maximum eigenvalue is obtained from the Gershgorin theorem, the true current maximum eigenvalue may often become greater than the estimated bound. In such cases the method will start to oscillate around the equilibrium state and eventually this will lead to divergence of the method. When such an oscillatory behaviour is detected, the estimation for λ_{\max} is updated to prevent divergence of the method. The updating process may be done either by repeating the algorithm for obtaining a new bound from the Gershgorin theorem, or by increasing the existing value by a certain factor.

N_{it}	λ_{min}	λ_{max}	q_{ϵ}
759	0.1	2.8736	0.0001
609	0.1	2.8736	0.00001
711	0.01	2.8736	0.00001
801	10.0	2.8736	0.00001
729	0.1	1.0	0.00001

RNORM criterion
($\epsilon = 0.1E-05$)

Table 7.14 Studies of example 2 with DRAUT. Load case "A"

N_{it}	λ_{min}	λ_{max}	q_{ϵ}
888	0.10	2.8736	0.0001
941	10.0	2.8736	0.0001
530	0.10	2.60	0.001
688	0.10	2.60	0.0001
511	0.10	2.60	0.00001
533	0.10	1.80	0.00001
592	0.10	1.70	0.00001
569	0.10	1.50	0.00001
654	0.10	1.20	0.00001
560	0.1	1.0	0.00001

RNORM criterion
($\epsilon = 0.1E-05$)

Table 7.15 Studies of example 2 with DRAUT. Load case "B"

Tables 7.14 and 7.15 show the dependence of the convergence on different combinations of λ_{\min} , λ_{\max} and q_e for the counterstressed dual cable structure of example 2. The number of iterations required for convergence fluctuated only moderately, even for the extreme combinations of the above parameters. In load case "A" the difference in the final number of iterations was 20% when initial and terminal values of the iteration parameter $\lambda_{B \min}$ differed by 1000%. Variations in convergence rates for different initial estimates of λ_{\max} were also small.

The estimated minimum eigenvalue during the course of the iterative process is not always an approximation to the actual current minimum eigenvalue. This difference sometimes could be quite substantial without affecting the convergence rate to the same degree. This could be explained by the fact that the process used ensures that the estimated minimum eigenvalue combined with the estimated maximum eigenvalue will produce a better pair of iteration parameters ρ and c , than the current actual minimum eigenvalue and the estimated maximum one.

Smaller initial estimates for λ_{\max} , as can be seen from Table 7.15, produced better convergence. This happened because smaller values for λ_{\max} create underdamped behaviour which accelerates the convergence in the early stages. The value of the parameter q_e also does not seem to have any profound effect on the convergence of the method.

In the studies carried out in this Chapter the oscillating

behaviour of the iterative process, that develops when the actual current eigenvalue becomes greater than the estimated one, was detected by monitoring the norm of the residuals in each iteration.

7.3. Kinetic Damping

In this version of the dynamic relaxation method, there is no need to evaluate the minimum eigenvalue of the stiffness matrix. Only an upper bound for the summation of the minimum and maximum eigenvalue is required to obtain the iteration parameters. The Gershgorin bound again provides a good approximation for this sum, since the minimum eigenvalue is always very small compared with the value of the maximum eigenvalue and will usually be less than the amount by which λ_{\max} obtained from the Gershgorin theorem is overestimated.

Two versions of the method were studied, which differ only in the way in which the oscillatory behaviour is detected when the estimated λ_{\max} becomes smaller than the actual one. The DRKV method uses a velocity criterion and the DRKR method uses a residual criterion. The parameter p_k controls the difference by which two successive velocity vector norms are allowed to differ. When this tolerance is exceeded, the parameter GER which is the sum of λ_{\max} and λ_{\min} is increased by a factor m . In the DRKR method, on the other hand, GER is increased when

N_{it}	GER	NUNCE	p_k	m	n
1045	2.80	1	-	-	
1039	2.60	5	0.01	1.05	
1148	2.40	5	0.01	1.05	
divergence	2.40	1	0.1	1.10	
993	2.15	5	0.01	1.05	
913	2.15	10	0.01	1.10	
1031	2.15	10	0.001	1.05	
divergence	2.15	10	0.1	1.10	
1284	2.15	10	0.0001	1.05	
968	2.6	5		1.10	2.0
1031	2.40	5		1.10	2.0
1076	2.40	10		1.10	2.0
982	2.15	5		1.10	2.0
1077	2.15	5		1.05	2.0

RNORM
criterion
($\epsilon = 0.1E-07$)

NUNCE controls the number of iterations to check for instability
 q_ϵ is for the V difference criterion
n is for the RNORM criterion
m is the multiplication parameter for ($\lambda_{max} + \lambda_{min}$)
GER = $\lambda_{max} + \lambda_{min}$

Table 7.16 Studies of example 2 with DRKV and DRKR.
Load case "A"

the current norm of the residuals is greater than the norm of the residuals at the start of the iterations times a safety parameter n .

Table 7.16 shows the convergence achieved by these two methods as applied to load case "A" of example 2. When the value of p_k is comparatively large then instability can occur, but otherwise the final number of iterations remains approximately the same. The parameter NUNCE controls the number of iterations for which the criterion for increasing the value of GER is not operational. As we can see from Table 7.16, for this particular example, this parameter does not affect significantly the behaviour of the method.

From Table 7.17 it is interesting to see how the value of the parameter NUNCE can affect the convergence of the method for problems with greater nonlinearities such as example 2 with load case "B". For NUNCE = 5 and $p_k = 0.01$ the method diverged, and only when p_k was reduced to 0.001 did the method converge. The selection of these parameters proved to be very sensitive in the dynamic relaxation method with kinetic damping for problems with increased nonlinearities. Example 1 is a characteristic problem with strong nonlinearities and Table 7.18 indicates that these control parameters needed even more careful selection to ensure convergence of the method.

7.4. The Conjugate Gradient -Tchebycheff Method

As explained in Section 5.6, where the theory of the method

N_{it}	GER	NUNCE	P_k	n	m
1008	2.60	1	0.01		1.05
1019	2.40	1	0.01		1.05
842	2.15	1	0.01		1.10
divergence	2.15	5	0.01		1.05
divergence	2.15	5	0.1		1.10
853	2.15	5	0.001		1.10
850	2.15	5	0.0001		1.10
826	2.40	10		2.0	1.10
849	2.40	10		3.0	1.10
907	2.40	20		2.0	1.10

RNORM
criterion
($\epsilon = 0.1E-07$)

Table 7.17 Studies of example 2 with DRKV and DRKR. Load case "B"

N_{it}	GER	NUNCE	P_k	n	m
1619	4.50	2		10.0	1.20
1977	4.50	2		5.0	1.10
divergence	4.50	3		5.0	1.10
1573	4.50	3		10.0	1.20
divergence	4.50	1	0.001		1.10
very slow convergence	4.50	5	0.001		1.30
1706	4.50	5	0.05		1.20
1595	4.50	5	0.01		1.20

RNORM
criterion
($\epsilon = 0.1E-07$)

Table 7.18 Studies of example 1 with DRKV and DRKR

was outlined, dynamic relaxation was chosen as inner method, the conjugate gradient algorithm as outer method. In the applications of the method in this Chapter a smoothing process was also applied. The purpose of the smoothing process is to eliminate the contributions of the eigenvalues to the error vector which are greater than the estimated minimum eigenvalue used during the smoothing process. Theoretically this implies that when the method is applied to linear problems, a Tchebycheff relaxation, with initial estimates λ_{sm} , λ_{max} for the minimum and maximum eigenvalues, will eliminate after a number of iterations all the contributions to the error vector of the eigenvalues $\lambda_i > \lambda_{sm}$. In other words only the remaining contributions of the eigenvalues $\lambda_i < \lambda_{sm}$ are essential. If the eigenvalues λ of the matrix K are then transformed into the eigenvalues μ of the matrix K^* by means of the inner method, the new system $K^*x + \beta = 0$ has as many contributions from the eigenvalues as the old system $Kx+b = 0$, which can be eliminated with n^* conjugate gradient steps of the outer method ; n^* being the remaining number of eigenvalues.

In Table 7.19 the following notations are used :

- NSMOOT : number of DR iterations carried out for smoothing
- MIT : number of steps of the inner method
- λ_{max} : maximum eigenvalue used for smoothing and for the main iteration process
- λ_{sm} : minimum eigenvalue used for smoothing
- λ_{min} : minimum eigenvalue for the inner method

NSMOOT	MIT	λ_{\max}	λ_{sm}	λ_{\min}	NUH	N_{it}	TIME (sec)
-	300	GER	10.0	0.98	4	2400	1.726
-	100	"	0.1	0.1			very slow convergence
-	50	"	0.1	0.1			divergence
100	50	"	1.0	0.1			divergence
200	50	"	0.1	0.01			very slow convergence
200	50	"	0.1	0.1	43	4500	3.767
200	100	"	0.01	0.01	22	4600	3.827
200	50	"	1.0	0.1	31	3300	2.762
200	40	"	1.0	0.1			very slow convergence
200	25	"	1.0	0.1			very slow convergence
400	50	"	1.0	0.1	43	4700	3.939

GER = 0.1297E+05

RNORM-SC
criterion

($\epsilon = 0.1E-05$)

Table 7.19 Studies of example 2 with CGTCH. Load case "A"

- NUH : number of steps for the outer method
- N_{it} : total number of DR iterations
- GER : the value for λ_{max} obtained from the Gershgorin theorem and for the unscaled stiffness method.

7.5. Successive Overrelaxation Method

Four different versions of the successive overrelaxation method were studied in this Section. The SORNL, which resets the elemental matrices in each iteration. The SORES, which resets only the residuals in each iteration, with the stiffness matrix being held constant during the iterations. The SORESC, which incorporates the Carre algorithm for an automatic adjustment of the relaxation parameter ω , and resets only the residuals as SORES. And, finally, the SORESH, which incorporates an algorithm proposed by Hageman for the calculation of the relaxation parameter during the course of the iterations.

Figures 7.1, 7.2 and 7.3 show the convergence rate of SORNL and SORES for different values of the parameter ω . One characteristic aspect of all four examples is that convergence deteriorates abruptly as soon as the relaxation parameter ω becomes slightly larger than a critical optimum value. From Figure 7.3 it can also be seen that although the number of iterations are almost the same for the two methods, the required time is almost double for the SORNL method.

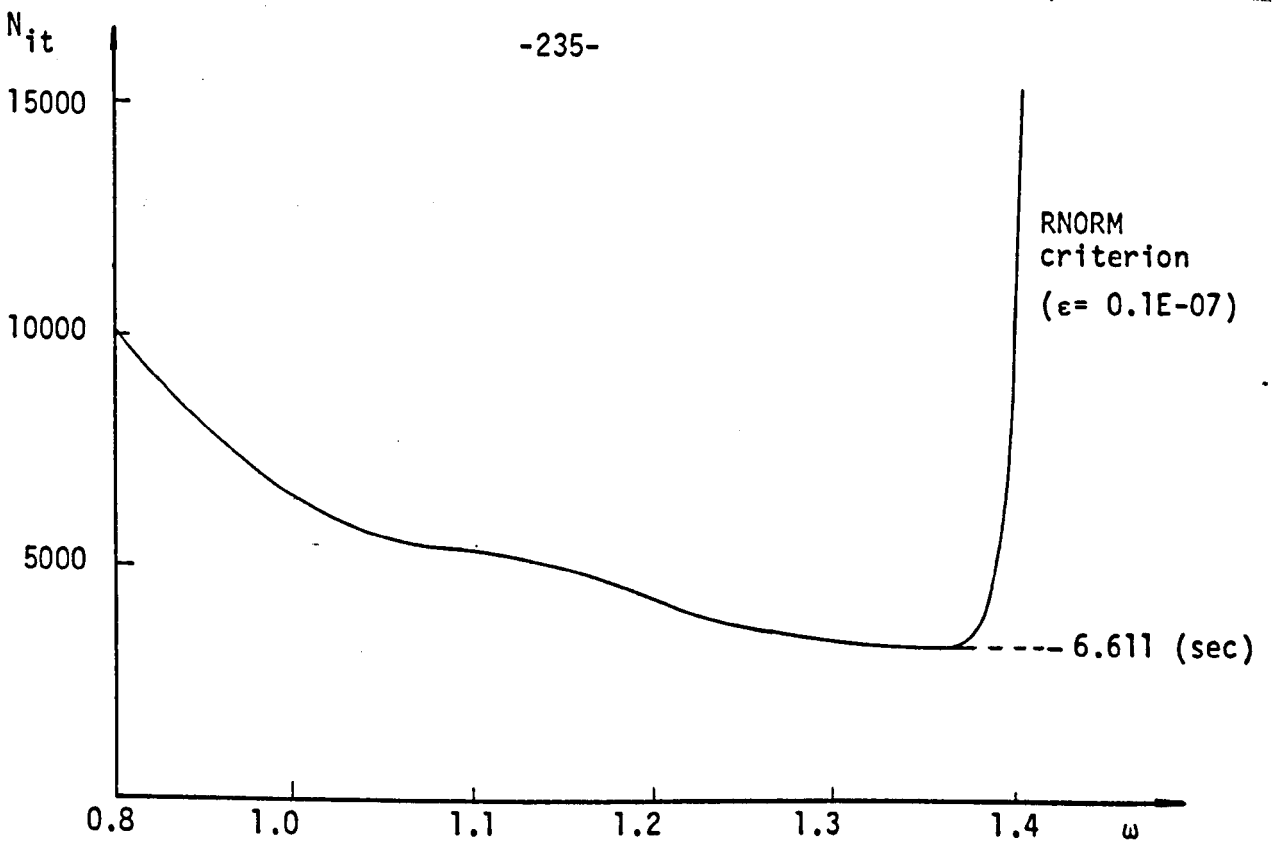


Fig. 7.1 Convergence of SORNL with different relaxation parameters ω (example 1)

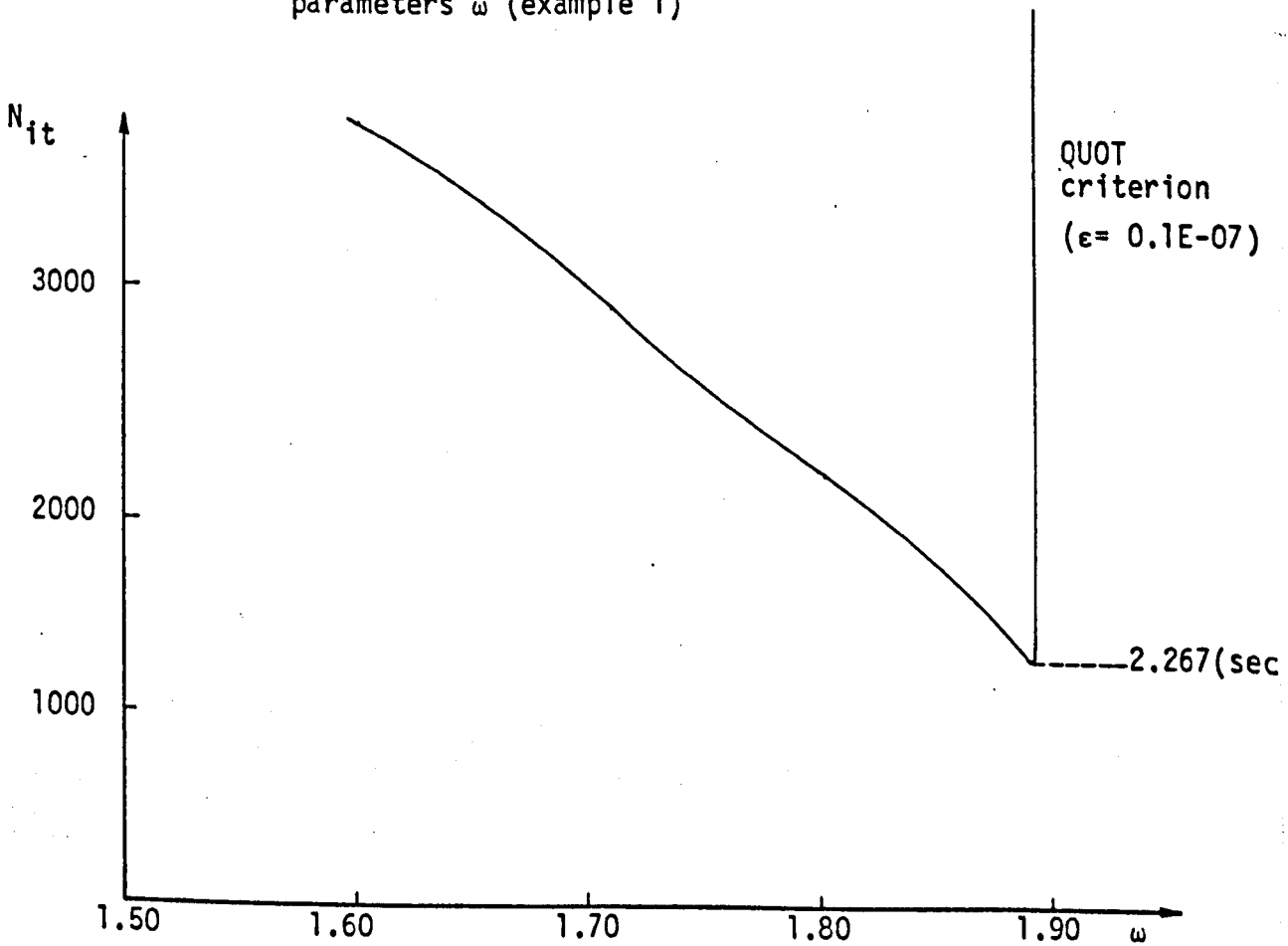


Fig. 7.2 Convergence of SORES with different relaxation parameter ω (example 2, load case "A")

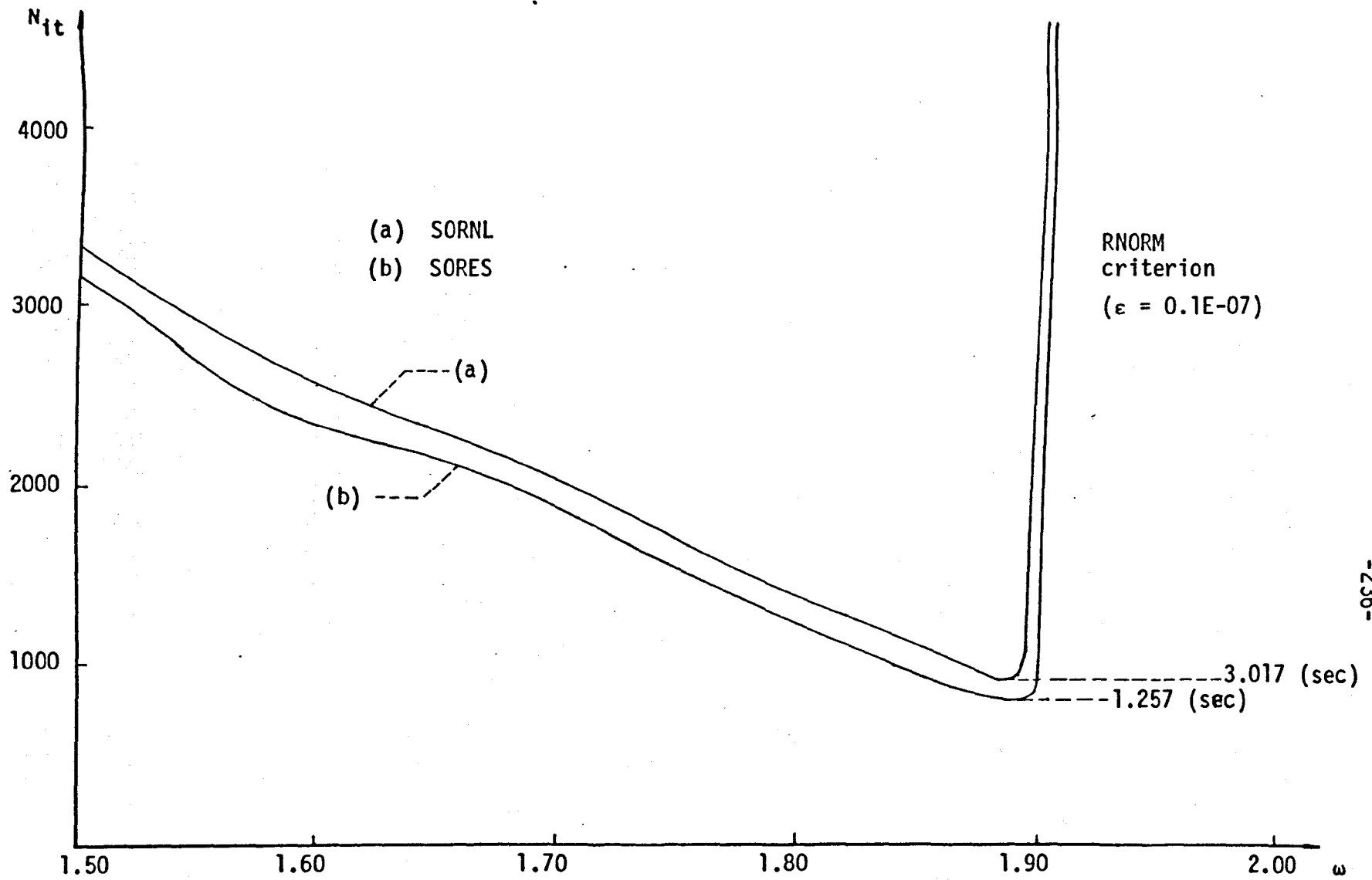


Fig. 7.3. Convergence of SORNL and SORES with different relaxation parameters ω (example 2. Load case "B")

7.6. Comparative Study

Table 7.21 shows the convergence of three versions of the dynamic relaxation method as applied to the three storey frame of example 6. From this Table we can see that although the minimum and maximum eigenvalue remained almost unchanged, the method based on an initial estimate of these parameters produced slower convergence than the method based on automatic adjustment of the iteration parameters. The third method which incorporates the concept of kinetic damping produced slower results than the DRAUT method.

In Table 7.22 and Figure 7.4 there is a study of the convergence rates of all the methods discussed in this Chapter when applied to the counterstressed dual cable structure of example 2. The DRAUT method gave the best results while the two kinetic damping methods produced almost the same convergence rate. The dynamic relaxation method without adjustment of the parameters gave similar results to the kinetic damping methods. The convergence of the conjugate gradient - Tchebycheff method, after the termination parameter ϵ reached $0.1E-02$, ceased improving.

The successive overrelaxation methods with Carre and Hageman automatic adjustment algorithms for the relaxation parameter ω , produced similar results, with the SORESC being better in the first stages. Both methods used an initial estimate for the relaxation parameter of $\omega = 1.0$. The SORES and SORNL methods are presented with their best convergence rate, attained after trial runs with different relaxation parameters (Figures 7.2 and

Node	Load case "A"		Load case "B"	
	x(ft)	y(ft)	x(ft)	y(ft)
1	0.2397	1.63401	0.439126	4.15053
2	0.34445	2.54673	0.66100	6.62475
3	0.35334	2.73182	0.70366	7.39906
4	0.30659	2.18763	0.606863	6.47541
5	0.24498	0.917106	0.41298	3.87625
6	0.232473	-0.42154	0.302996	1.0010
7	0.25872	-1.17735	0.327158	-0.80661
8	0.266174	-1.35397	0.36329	-1.56638
9	0.198245	-0.95792	0.29278	-1.2912
10	-0.296272	1.61923	-0.83604	4.06646
11	-0.39836	2.52976	-1.10475	6.52831
12	-0.379036	2.71777	-1.01949	7.32034
13	-0.313168	2.17708	-0.805840	6.41824
14	-0.276256	0.91038	-0.69037	3.8443
15	-0.294284	-0.42668	-0.70810	0.98336
16	-0.31057	-1.18405	-0.69480	-0.827187
17	-0.28988	-1.3622	-0.60319	-1.59060
18	-0.19761	-0.96529	-0.38682	-1.3125

Table 7.20 Final displacements of example 2

METHOD	N_{it}	TIME (sec)
DRGR	166	0.182
DRAUT	98	0.129
DRKV	180	0.190

RNORM criterion
($\epsilon = 0.1E-07$)

Table 7.21 Comparative study of example 6

Termination Parameter		0.1E-00		0.1E-01		0.1E-02		0.1E-03		0.1E-04		0.1E-05		0.1E-06	
Number	Method	N _{it}	TIME	N _{it}	TIME	N _{it}	TIME	N _{it}	TIME	N _{it}	TIME	N _{it}	TIME	N _{it}	TIME
1	DRGR	152	0.140	317	0.276	472	0.405	634	0.540	792	0.675	950	0.81	1108	0.945
2	DRAUT	140	0.129	195	0.175	321	0.280	368	0.32	495	0.425	539	0.463	672	0.573
3	DRAUT-UNSC	135	0.115	266	0.219	471	0.384	574	0.467	681	0.558	754	0.615	913	0.742
4	DRKR	155	0.135	380	0.316	477	0.396	632	0.524	781	0.644	935	0.770	1081	0.889
5	DRKR-UNSC	73	0.168	144	0.324	247	0.526	320	0.671	434	0.895	504	1.035	597	1.217
6	DRKV	259	0.272	334	0.345	446	0.451	561	0.558	684	0.676	791	0.775	868	0.848
7	CGTCH	600	0.413	700	0.496	1000	0.825	12900	10.589	-	-	-	-	-	-
8	SORNL	413	1.273	627	1.931	839	2.588	1052	3.242	1265	3.902	1478	4.560	1691	5.216
9	SORES	419	0.651	636	0.994	853	1.331	1069	1.669	1286	1.987	1503	2.346	1719	2.682
10	SORESC	411	0.643	617	0.964	821	1.282	1026	1.602	1230	1.92	1435	2.240	1639	2.558
11	SORESH	368	0.575	536	0.837	692	1.081	916	1.429	1228	1.915	1528	2.382	1828	2.848

Table 7.22 Comparative study of example 2. Load case "A" (QUOT criterion)

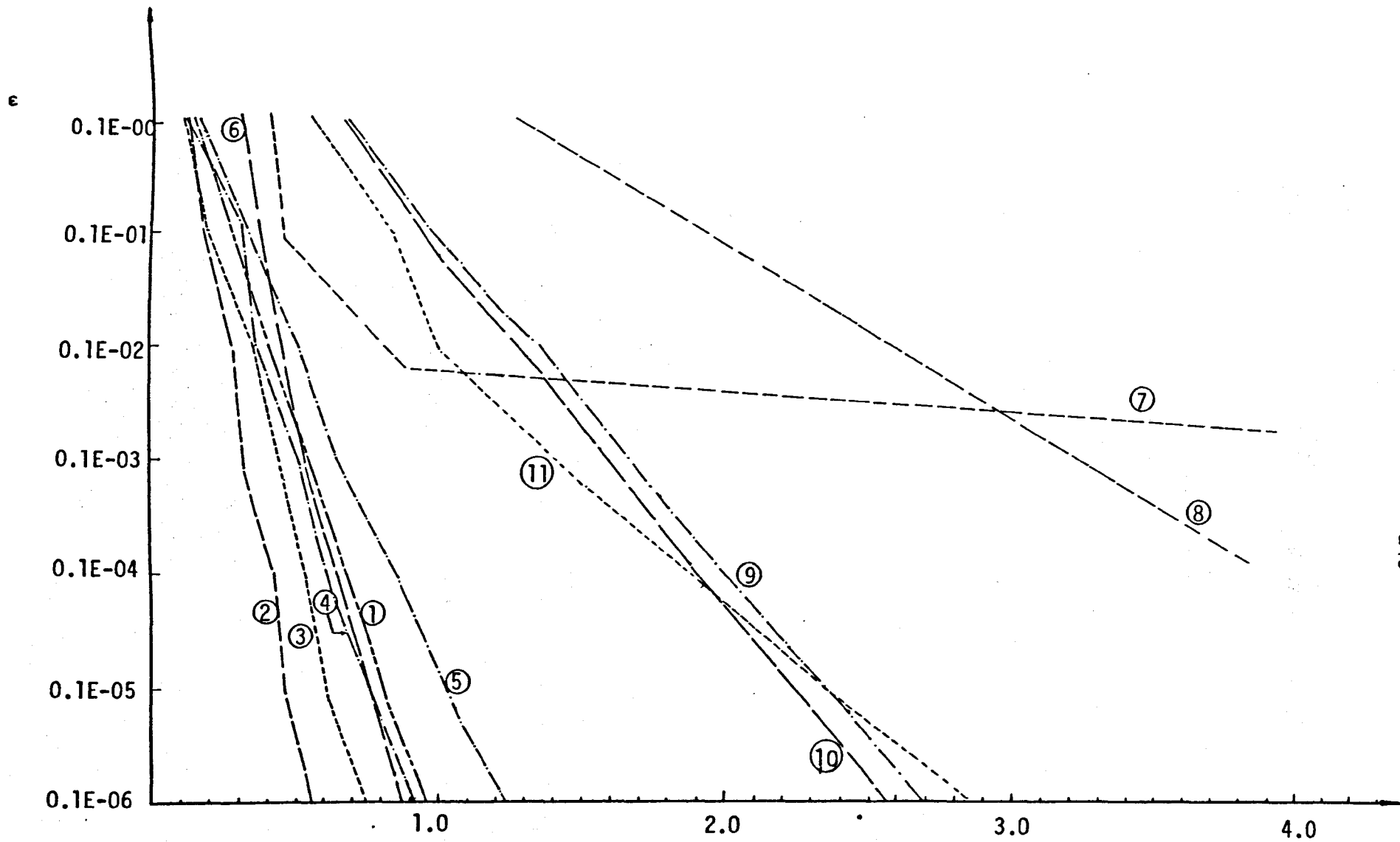


Fig. 7.4 Example 2, results from Table 7.22. Load case "A"

Time (sec)

7.3). It can be seen that the re-evaluation of the stiffness matrix in SORNL, although not affecting the final number of iterations, increased considerably the execution time. One interesting aspect is that the automatic adjustment methods for the evaluation of the parameter ω gave better results than those given when the relaxation parameter remained constant at its optimum value.

Table 7.23 and Figure 7.5 show the convergence rates obtained when the methods were applied to the hyperbolic paraboloid of example 3. Again the dynamic relaxation with automatic adjustment of the parameters, produced the best convergence. The DRKV with the velocity criterion gave better results than the DRKR with the residual criterion. This is something that was expected, since a change in the velocity norm is more indicative of instability than a change in the residual norm. The DRGR and SORNL gave very slow convergence, while the SORES type methods, with fixed and automatic adjustment for the relaxation parameter ω , diverged. This means that the initial values for the coefficients of the stiffness matrix which were used throughout the iterations, should be updated at regular intervals to cope with the changing configuration of the structure.

7.7. Conclusions

The successive overrelaxation method has rarely been applied to the nonlinear analysis of structures with finite element

Termination Paramater		0.1E-00		0.1E-01		0.1E-02		0.1E-03		0.1E-04		0.1E-05		0.1E-06	
Number	Method	N _{it}	TIME	N _{it}	TIME	N _{it}	TIME	N _{it}	TIME	N _{it}	TIME	N _{it}	TIME	N _{it}	TIME
1	DRAUT	20	0.069	40	0.111	56	0.144	71	0.175	84	0.203	96	0.228	107	0.251
2	DRKR	56	0.161	101	0.265	148	0.372	194	0.476	229	0.559	276	0.663	309	0.740
3	DRKR-UNSC	73	0.188	144	0.360	247	0.585	320	0.746	434	0.994	504	1.151	597	1.352
4	DRKV	36	0.126	59	0.186	85	0.253	102	0.298	130	0.368	153	0.427	175	0.484
5	CGTCH	-	-	-	-	-	-	-	-	-	-	-	-	500	0.903

Table 7.23 Comparative study of example 3 (QUOT criterion)

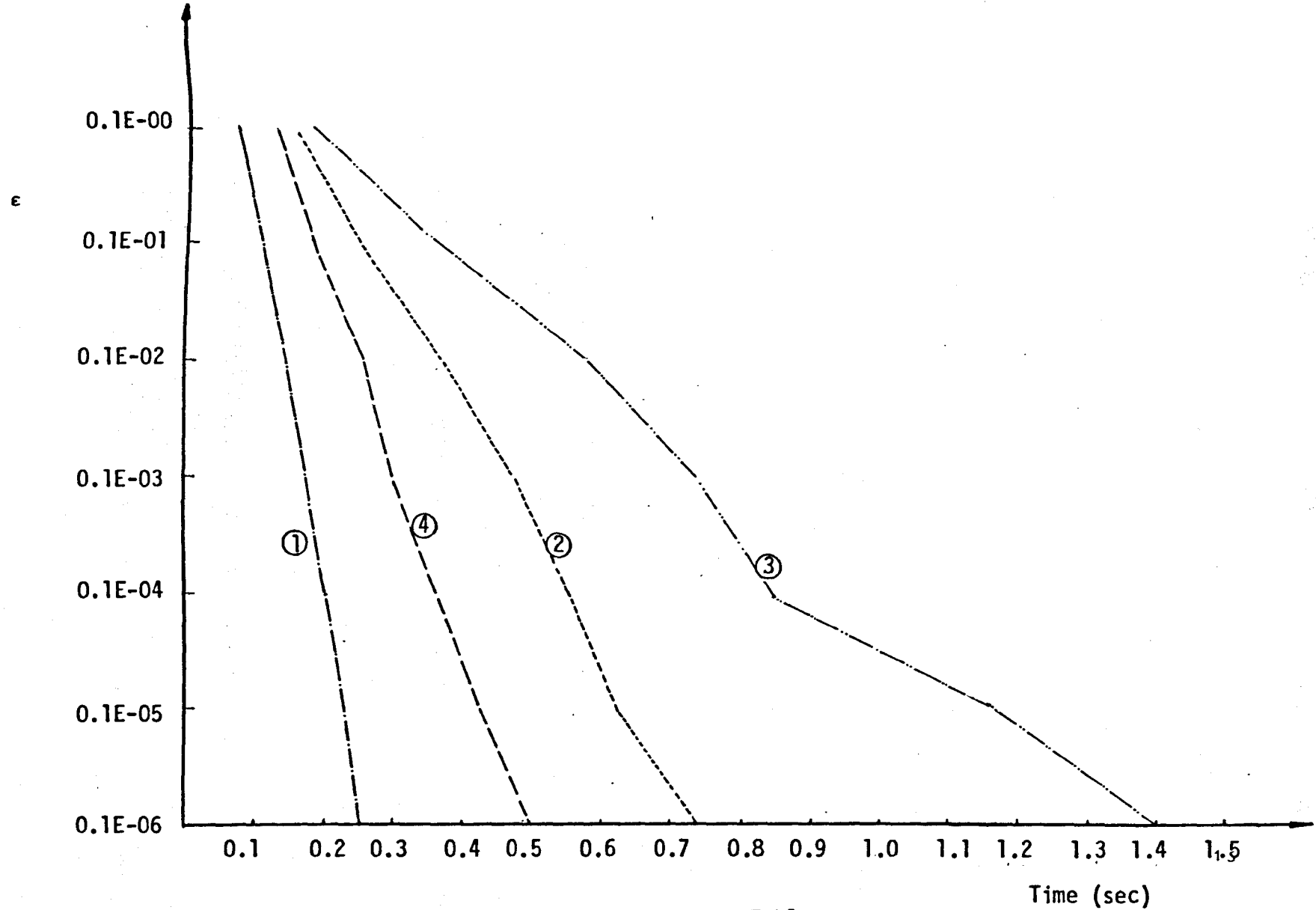


Fig. 7.5 Example 3, Results from Table 7.23

idealizations. The reason is that unless the coefficient matrix has certain properties, there is no available explicit formula for the optimum value of the relaxation parameter ω . By using the ongoing processes, proposed for linear cases and with matrices with property "A", by Carre and Hageman some of the disadvantages of the method have been overcome. Although it can not be claimed that the relaxation parameter produced by these two algorithms will lead always to a convergent method, at least when a solution can be obtained, the convergence of the method with these two ongoing processes is better than the optimum convergence of the method with constant relaxation parameter ω_{opt} .

The convergence rates of the successive overrelaxation methods on the other hand, remained much slower than the convergence rates obtained by the dynamic relaxation methods. This means that the theoretical convergence rates of Table 5.1 are strictly applicable only to tridiagonal matrices and do not represent the behaviour of the methods for general matrices. Another disadvantage of the successive overrelaxation method is the need to form the (6×6) diagonal submatrices of the overall stiffness matrix and then provide a suitable storage scheme.

The combination of the conjugate gradient and Tchebycheff methods did not produce the expected results. The method, for small values of the parameter MIT (number of steps for the inner method) suddenly diverged after a constant number of iterations

for all cases. Also divergence occurred when no smoothing process was used. The method seems to have these difficulties because the only way to apply it to nonlinear systems is to employ a linear evaluation for the step length in the conjugate gradient method. Any attempt to apply a nonlinear step length algorithm will involve enormous computational work. The method still can be useful for extremely ill-conditioned problems as could be the case with cable structures supported by flexible boundaries.

The dynamic relaxation method with an "a priori" evaluation of the minimum and maximum eigenvalues gave very competitive results when applied to structures with moderate nonlinearity. But when applied to structures with significant nonlinearities, the iteration parameters have to be altered to avoid instability and this reduces the convergence rate of the method. The method employed for the evaluation of the minimum and maximum eigenvalues produced very fast and accurate estimates without the need of any additional storage. The time required for the "a priori" evaluation of the extreme eigenvalues was about 10% of the whole execution time for the problems studied in this Chapter.

The concept of kinetic damping simplifies the method to the evaluation only of a bound for the maximum eigenvalue. This estimate could be obtained using the Gershgorin bound theorem. The method thus has the advantage that it can be applied very easily, with only one parameter to be checked against the possibility of divergence when the method is applied to

stiffening systems. Of the two criteria used to check oscillatory behaviour during the iteration process, the velocity criterion gave more stable and faster results. Even in the extreme non-linear case of the single cable of example 1, the velocity criterion incorporated very reliably the changes in the current maximum eigenvalue during the application of the loading.

The method which produced the best results in terms of number of iterations and total execution time, was the dynamic relaxation with automatic adjustment of the iteration parameters. The maximum eigenvalue is obtained from Gershgorin theorem, while a first estimate of the minimum eigenvalue can be any positive number less than the estimated maximum eigenvalue. After a few iterations a new estimate of the minimum eigenvalue is obtained, not necessarily a close approximation to the true minimum eigenvalue, which in conjunction with the maximum eigenvalue produces the best rate of convergence. This process will allow for any change of the current minimum eigenvalue during the application of the loads, while a stability criterion similar to those used in the kinetic damping applications, will safeguard against any change of the current maximum eigenvalue capable of inducing divergence of the iterative process.

On the basis of the results obtained so far and the experience gained from the computational studies carried out in this work, dynamic relaxation with automatic adjustment of the relaxation parameters gave the most stable and rapid results of all the relaxation methods discussed in this Chapter. The

method did not fail to converge with almost any possible combination of the iteration parameters. In the opinion of the author this method could be very effective for the analysis of nonlinear structures.

CHAPTER 8

STIFFNESS METHODS

8.1. Linear Equation Systems

8.1.1. Introduction

The majority of problems in structural analysis require, at some stage, the solution of a set of linear equations. In linear structural analysis programs, 20% to 50% of the total execution time may be required to solve the set of linear equations, depending on the size of the problem and the amount of peripheral processing involved. However, in nonlinear static or dynamic problems, with the need for partial or complete reanalysis for each load increment or iteration inside the load increment or time step, up to 80% of the total execution time may be spent in the solution of equations. Consequently, an efficient equation solving routine will reduce considerably the computer storage requirements and the total execution time required for the convergence to a nonlinear solution.

The analysis of structures can be represented by the solution of sets of simultaneous equations with either forces or displacements as unknowns. The latter method, known as the "stiffness approach", is more easily adapted to computer analysis and has, therefore, been accepted by most writers of structural problems.

The stiffness method of structural analysis is represented

in matrix form by

$$Kx = F \quad (8.1)$$

in which F and x are the applied load vector and the displacement vector and K is the stiffness matrix of the structure. For cable problems the stiffness matrix is, in most cases, sparse, banded and symmetric. If K is not symmetric, it can be made so by multiplying both sides of equation (8.1) by the transpose of K .

Two main direct methods of solution best incorporate the properties of the stiffness matrix, namely the Gaussian approach and the Choleski approach. According to the theorem of Klynyev and Kokovkin-Scherback [168], no method using rational operations for a dense matrix of coefficients can make fewer operations than Gauss elimination. Therefore, most effort has been directed toward recognising the distribution of the non-zero elements of the coefficient matrix and taking advantage of that distribution to reduce the number of calculations.

Banded solutions are very efficient when the zero elements inside the bandwidth are kept to a minimum. This can be achieved if nodal points are numbered such that the maximum nodal point difference within any one element is kept as small as possible. Ideally suited for such a numbering are unbranched or chain structures, such as continuous beam or folded plate structures and also building frames, bridge structures and some cable structures.

For most regular shaped structures, the optimum numbering of nodal points is straightforward. For complex structures, however, the problem of minimizing the bandwidth usually becomes very difficult. Programs have been developed, especially for this purpose, which automatically renumber the nodes in order to minimize as much as possible the bandwidth of the stiffness matrix [244, 303]. These reordering programs themselves consume considerable computer time and their use should be restricted to very large equation systems.

All band solutions have in common that zero coefficients below non-zero elements in the overall stiffness matrix will become non-zero during the elimination process, thus coupling eventually all degrees of freedom within the wave front while it travels along the longitudinal axis of the structure. Therefore, banded solutions will often not represent the optimum solution with regard to the required number of operations. However, the ease of assembling process, input-output handling, and the very simple book-keeping process, make these techniques very popular.

When a matrix is not effectively banded and has a large proportion of zero elements, then by storing only the non-zero elements, machine store and time may be reduced significantly. Sparse matrix routines are necessarily more complex than standard matrix routines, but once developed provide a useful tool for the computer analysis of structures. Problems of large size

can be accommodated within the main store of a computer without recourse to submatrix techniques or magnetic tapes. They also allow full flexibility as regards joints and member numbering. The use of sparse matrix routines as opposed to standard matrix routines was found [155] to be more economical in computing cost for all but the smallest structural frames.

There are numerous other computational techniques for the solution of linear equations. Among the most effective are the "partitioning methods", the static condensation and the substructuring methods, the "frontal solutions", the "skyline method" and the Grout reduction. It is not the purpose of this work to discuss these methods, further details can be found in References [81, 145, 192, 194, 195] .

A compact storage scheme, which has been developed by Jennings [153], and a half banded method, have been used in this study to provide an alternative comparison to the gradient and relaxation methods already discussed.

8.1.2. Jennings' Compact Storage Scheme for the Solution of Symmetric Linear Simultaneous Equations

This method is a direct solution method using a non-standard form of storage for the matrix of left-hand side coefficients. The method is as versatile as a sparse matrix storage scheme in dealing with arbitrary patterns of non-zero elements, while at

the same time retaining most of the simplicity inherent in the method of direct solution when using a diagonal band storage scheme.

The storage scheme adopted for matrix K is to store the elements below the leading diagonal in sequence by rows, but with all elements preceding the first non-zero element in each row left out. This sequence is stored in a one dimensional array called the main sequence. In addition an address sequence is used to locate the position of the leading diagonal elements within the main sequence. It will be noted that, when solved by elimination and back substitution without row or column interchange, all the buildup of non-zero elements will occur within the elements stored in the main sequence.

The reduction process is best illustrated by considering a set of four simultaneous equations. After the first two equations have been reduced so that their leading diagonal coefficients are unity, the equations appear as follows :

$$\begin{array}{ccccc} 1 & K_{12}^{**} & K_{13}^{**} & K_{14}^{**} & f_1^{**} \\ & 1 & K_{23}^{**} & K_{24}^{**} & f_2^{**} \\ K_{31} & K_{32} & K_{33} & K_{34} & f_3 \\ K_{41} & K_{42} & K_{43} & K_{44} & f_4 \end{array} \quad (8.2)$$

The third equation is then reduced by making

$$\begin{aligned}
 K_{31}^* &= K_{31} \\
 K_{32}^* &= K_{32} - K_{31}^* K_{12}^{**} \\
 K_{33}^* &= K_{33} - K_{31}^* K_{13}^{**} - K_{32}^* K_{23}^{**} \\
 &\cdot \quad \cdot \quad \cdot \quad \cdot \quad \cdot \quad \cdot \quad \cdot \quad \cdot \quad \cdot \quad \cdot \\
 f_3^* &= f_3 - K_{31}^* f_1^{**} - K_{32}^* f_2^{**}
 \end{aligned}
 \tag{8.3}$$

and then putting

$$\begin{aligned}
 K_{34}^{**} &= K_{34}^* / K_{33}^* \\
 &\cdot \\
 &\cdot \\
 f_3^{**} &= f_3^* / K_{33}^*
 \end{aligned}
 \tag{8.4}$$

The sequence of arithmetic operations can be summarised by the flow diagram shown in Figure 8.1. The column number of the first element in row i has been designated r_i , and r is the greatest of r_i and r_j , where r_j is the column number of the first element in row j . A set of temporary stores are used which are designated c . The maximum number of elements in the c array equals the largest number of elements stored for any row of matrix K . The back substitution process is illustrated by the flow diagram of Figure 8.2.

Figure 8.3 shows diagrammatically the elements stored for the elimination and compact store elimination schemes. The elimination of a row, say DE , is performed by the simple elimination method by referring to the elements within the triangle EFJ , while for the compact store elimination, by referring only to the elements

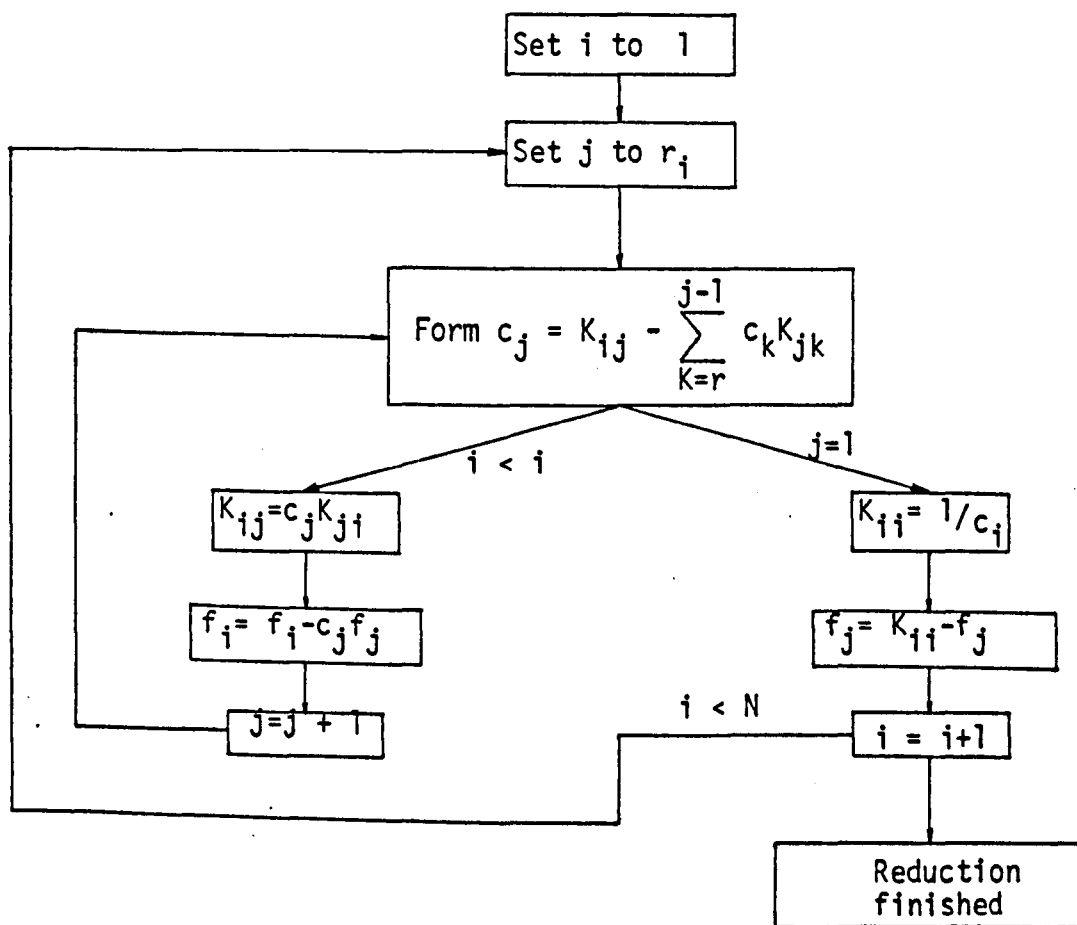


Fig. 8.1 Reduction process of the compact store elimination scheme

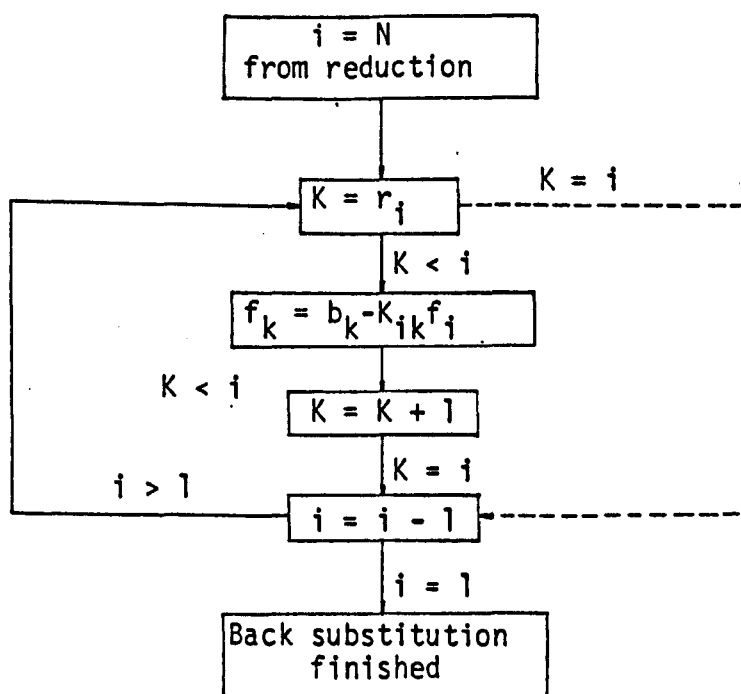


Fig. 8.2 Back substitution of the compact store elimination scheme

of the triangle EDG.

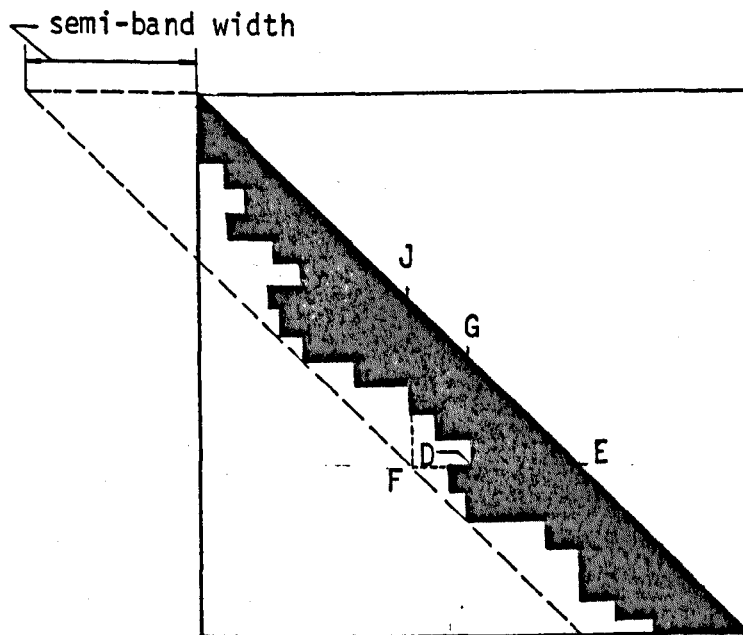


Fig. 8.3. Storage layout for the elimination and compact store elimination schemes

8.2. Non Linear Equation Systems

8.2.1. Introduction

Nonlinear behaviour in structural systems is usually classified into one of the following three categories -

- (a) geometric nonlinearity, which arises from nonlinear terms

in the kinematic equations, (b) material nonlinearity, which arises from nonlinearities in the constitutive equations, and (c) combined geometric and material nonlinearity. Computationally, the mathematical techniques that can be used successfully to treat one type of nonlinearity are, with modifications, generally applicable to other types of nonlinearity. With the exception, perhaps, in problems of stability or of cyclic loading of inelastic elements.

The direct stiffness method of structural analysis was first extended to the analysis of geometrically nonlinear problems by Turner, Dill, Martin and Melosh [289]. In that paper, the problem of large deflections but small strains, is analysed as a sequence of linear problems, using an incremental analysis procedure. Geometric stiffness matrices are derived for pin-jointed bar and triangular plane stress elements. This approach was further elaborated by Argyris [5].

Since then a great number of investigators have studied and developed nonlinear solution techniques. Comprehensive reviews of such solution techniques have been discussed in References [19], [218], [284].

A method of classifying the various techniques concerns the manner in which the force unbalance is treated. A set of displacements which exactly satisfies the equations of equilibrium will give rise to no force unbalance. The force unbalance vector is a measure of the deviation from a true state of equilibrium and is analytically defined as

$$r = -Kx + F \quad (8.2)$$

where

K = the global stiffness matrix

x = nodal displacement vector

F = generalized force vector

If the load is applied incrementally, then the total load at any point may be represented as a function of a load parameter, p , and a normalized load vector \bar{P} ; thus, the generalized force vector is written

$$F = p \cdot \bar{P} \quad (8.3)$$

As the load is incremented, only the value of the load parameter changes. Hence the displacements may also be interpreted as being a function of the load parameter. Differentiation of equation (8.2) with respect to the load parameter p , yields

$$\dot{r} = -K\dot{x} + \bar{P} \quad (8.4)$$

where the dot indicates differentiation with respect to p .

The second derivative of the force unbalance may be obtained from equation (8.4) as

$$\ddot{r} = -K\ddot{x} \quad (8.5)$$

The use of equations (8.2), (8.3) and (8.4), provides an effective basis for classifying the solution techniques employed in non-linear analyses.

The first class of solution procedures seek to exactly satisfy the equations of equilibrium and are, therefore, of the class $r = 0$. These techniques generally seek the equilibrium displacement state at each load level by iterating until a specified level of accuracy is attained. Successive approximations,

Newton Raphson techniques and direct minimization of the total potential energy, comprise the most popular methods in this class.

The second class of solution procedures seek to minimize the force unbalance by requiring a zero value for the path derivative of the force unbalance. This class is characterized by the expression $\dot{r} = 0$. The incremental stiffness procedure and the static perturbation method are typical procedures of this class. These techniques have the tendency to "drift" from the exact equilibrium path (see Figures 8.13 and 8.14). This "drifting" tendency, resulting from errors propagated from successive steps, has created the third class of solution procedures which improve the incremental procedures.

Self-correcting solution procedures seek to correct the deviation from the equilibrium in each load increment. First and second order procedures representing combinations of equations (8.4) and (8.5) have been developed and employed.

The most popular solution procedures for the nonlinear analysis of cable structures, where geometric nonlinearities are predominant, have been of the class $r = 0$. At each load step these techniques generally require an initial estimate of the displacement vector, which usually is the linear solution vector, and then seek through an iterative process to satisfy the equations of equilibrium. Incremental stiffness methods have been applied less frequently in the analysis of cable structures, while the perturbation method has been applied only once by Aizawa, Tanaka

and Tsubota [2] . Second and third classes of solution procedure are better suited to material nonlinearities and general path dependent problems.

8.2.2. Newton Raphson Type Methods

The Newton Raphson method is one of the most popular methods of solution in nonlinear analysis. The wide applicability of the method is evidenced by the inclusion of this technique in virtually all numerical analysis text books.

For an appropriate displacement vector x and the applied load vector F , the unbalance in nodal force corresponding to the i -th co-ordinate may be written

$$r_i(x) = -K_{ij}x_j + F_i \quad 1 \leq i \leq N \quad (8.6)$$

A Taylor's series expression of the force unbalance about the point x yields the following expression for the force unbalance at an adjacent displacement state $(x + \Delta x)$.

$$r_i(x + \Delta x) = r_i(x) + \frac{\partial r_i(x)}{\partial x_j} \Delta x_j + O [(\Delta x)^2] \quad (8.7)$$

The conventional Newton Raphson procedure retains only the first two terms in the Taylor expansion. In addition it is assumed that the unbalance in the nodal forces corresponding to the displacement $(x + \Delta x)$ is zero. These assumptions reduce equation (8.7) to the following

$$-\frac{\partial r_i(x)}{\partial x_j} x_j = r_i(x) \quad (8.8)$$

The partial derivatives in equation (8.8) may be obtained by

differentiating the force unbalance defined in equation (8.6). For each degree of freedom a relation may be obtained in the form

$$K_{ij} \Delta x_j = r_i(x) \quad (8.9)$$

which in matrix notation may be written as

$$K_L^n (\Delta x)^{n+1} = r(x)^n \quad (8.10)$$

where K_L is the linear or tangent stiffness matrix, and n is the number of executed iterations.

The tangent stiffness matrix is composed of two parts :

$$K_L = K_E + K_G \quad (8.11)$$

in which K_E is the same as that obtained in the classical theory for linear elastic structures and K_G is the geometric stiffness matrix. The stiffness matrix k_E is associated with the deformations of an element and k_G is associated with the changes in geometry of the element with the element considered as a rigid body.

Equation (8.10) is then solved to determine an improved displacement vector

$$x_{n+1} = x_n + (\Delta x)_{n+1} \quad (8.12)$$

Diagrammatically, the procedure is illustrated in Figures (8.4a) and (8.4b), for a stiffening and a softening single degree of freedom system.

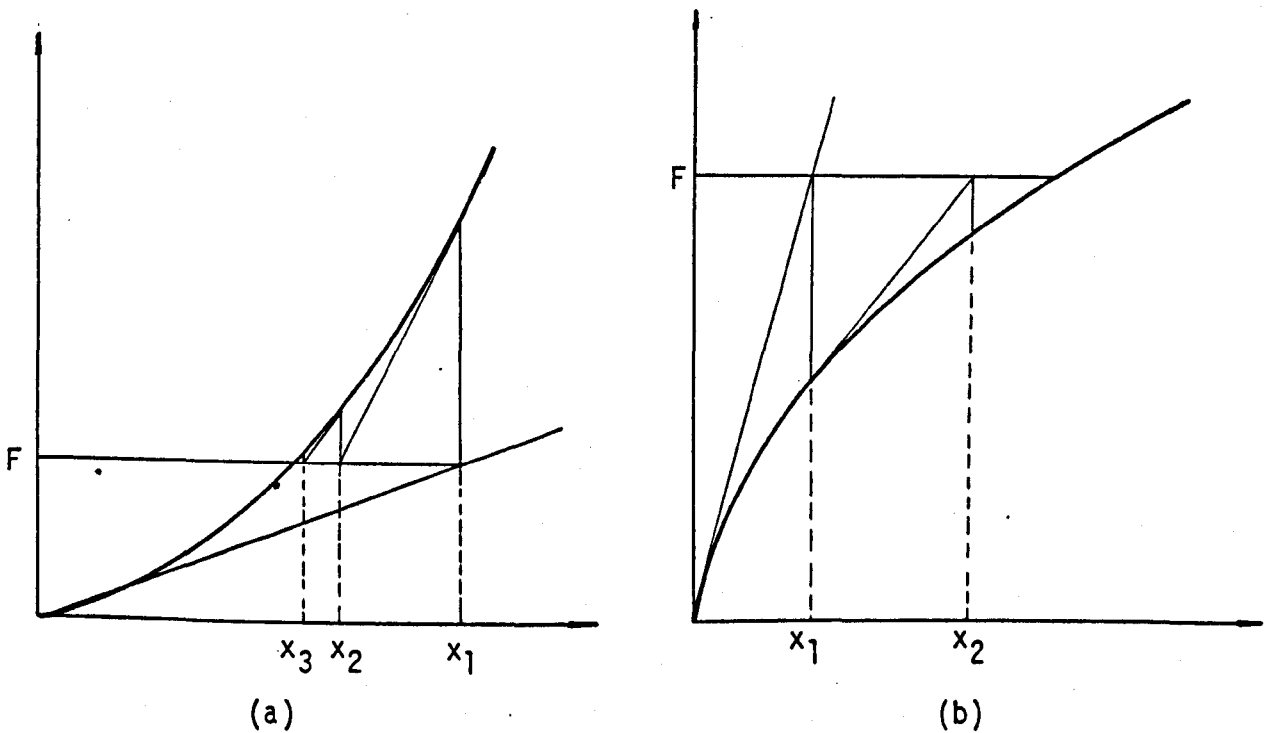


Fig. 8.4. Newton Raphson approach for stiffening and softening type of structures

This procedure is one of the most highly utilized techniques in geometrically nonlinear structural analysis ; on the other hand, the results obtained with this method in plasticity analyses have been less successful. The most significant drawback associated with the Newton Raphson method is the large amount of computational effort required to compute and invert (or solve) at each cycle the coefficient matrix.

For this reason when dealing with structures which are not highly nonlinear a "modified Newton Raphson" method is employed. In this method the stiffness matrix is formed and inverted only once. Equation (8.10) now becomes

$$K_0 (\Delta x)^{n+1} = r(x)^n \quad (8.13)$$

The above process for stiffening and softening systems respectively is represented in Figures (8.5a) and (8.5b)

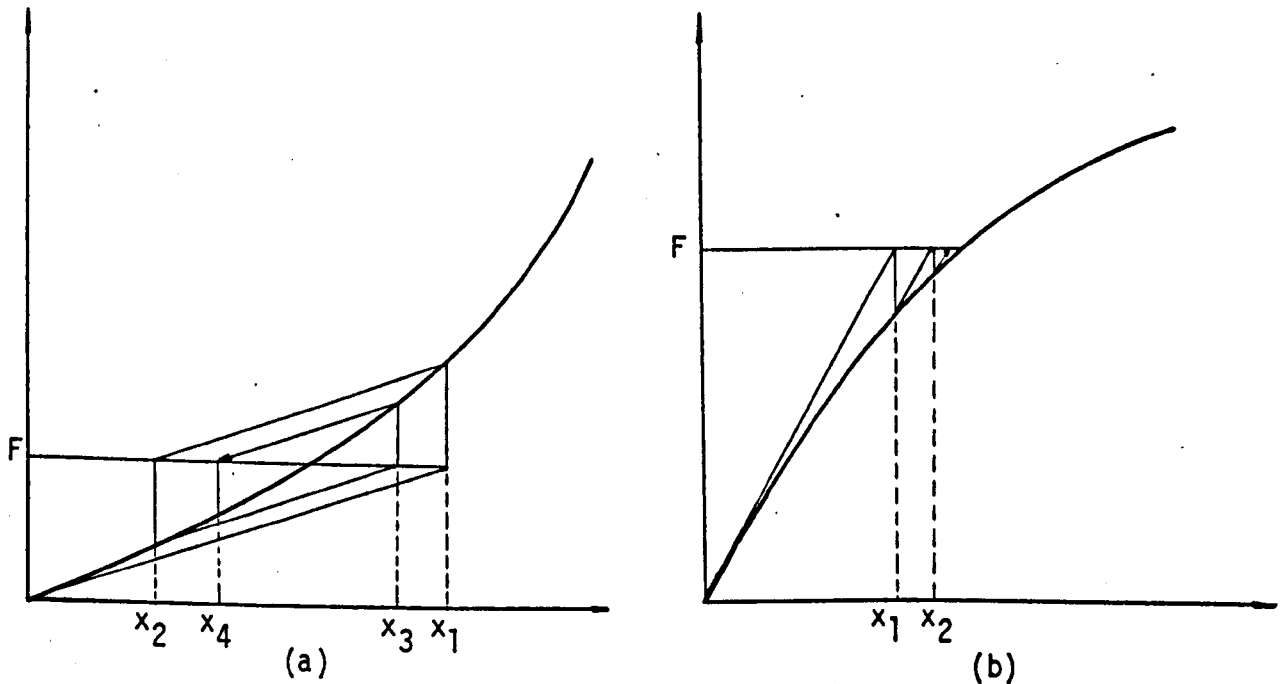


Fig. 8.5. Modified Newton Raphson approach for stiffening and softening type of structures

It can be seen from Figure 8.5b, that for geometrically softening systems, the process should always converge. For stiffening systems, however, if the initial out of balance force is too large and the structure is highly nonlinear, the method may diverge, as shown in Figure 8.6.

Mollman and Mortensen [200] found that for prestressed networks the modified Newton Raphson method, which they called

"simplified Newton Raphson", converged for small applied loads but diverged when the loads became larger. To overcome this difficulty, they suggested the use of a modified geometric stiffness in conjunction with an amended expression for the residual forces.

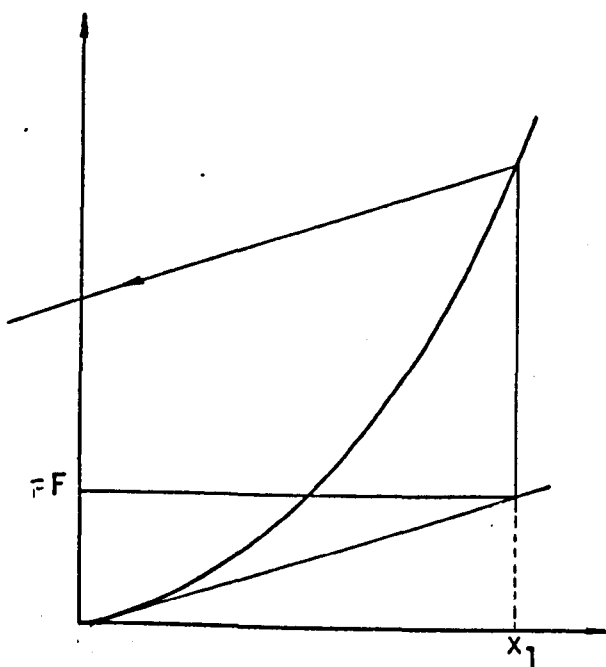


Fig. 8.6.

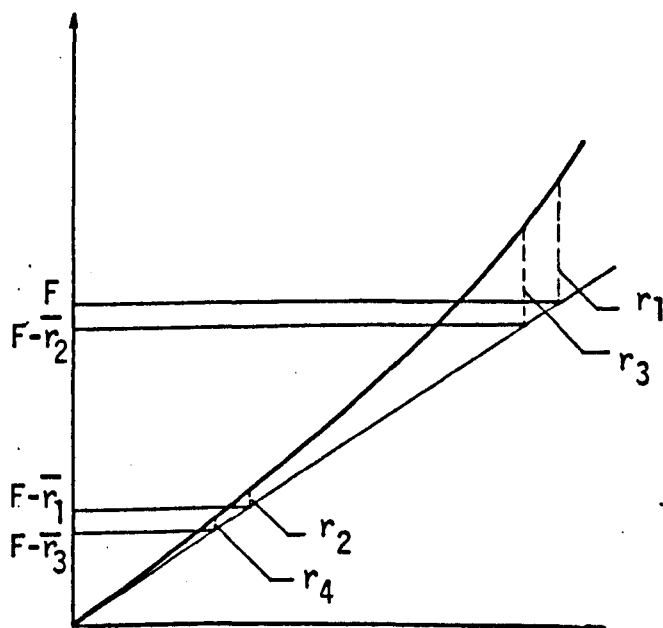


Fig. 8.7.

In total displacement form, the modified Newton Raphson process is illustrated in Figure 8.7, where \bar{r}_i stands for the absolute value of the residual force at the i -th iteration.

Krishna [173] found that an improved convergence could be obtained by using the iteration formula :

$$x^{n+1} = K_0^{-1} \left[F + \frac{1}{2} (r^n + r^{n-1}) \right] \quad (8.14)$$

However, when the applied loads are large in comparison to the prestress, the results may become only slowly convergent and render the method uneconomical.

In an effort to combine the advantages of the Newton Raphson and the modified Newton Raphson, a combined approach may be used, as shown diagrammatically in Figure 8.8. In this method the coefficient matrix is held constant and is updated after several iterations each time.

Another form of total displacement iterative procedure, applied to cable and truss structures by Baron and Venkatesan [19], is the secant stiffness method, in which the following iterative scheme is used for obtaining the solution :

$$F = K_S^n x^{n+1} \quad (8.15)$$

where K_S^n is the secant stiffness method given by

$$K_S^n = K_L + K_{NL}^n \quad (8.16)$$

and K_L is the linear matrix given by equation (8.11) and K_{NL} is a nonlinear function of the displacements. This iterative scheme is illustrated in Figure 8.9.

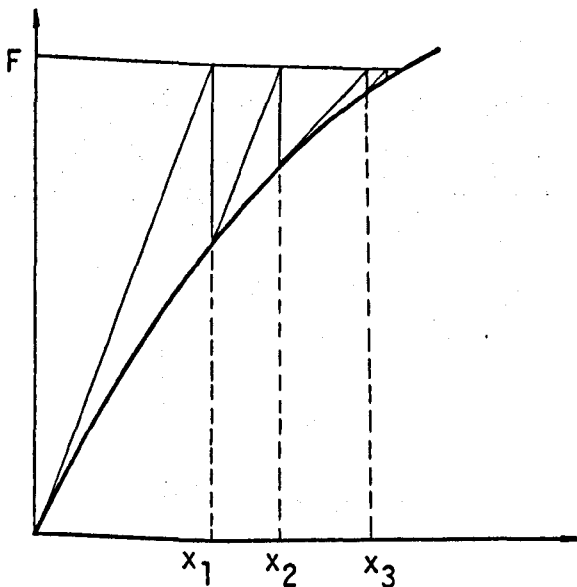


Fig. 8.8

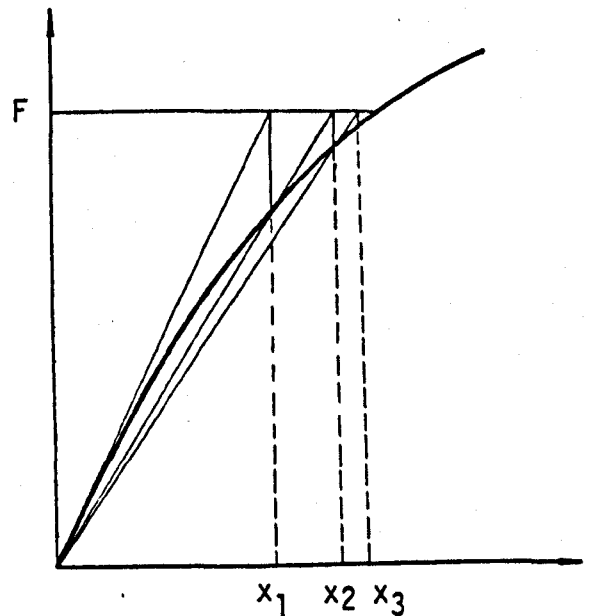


Fig. 8.9

For highly nonlinear cable net problems the equilibrium load based on a linearised solution may be so different from the applied load that convergence may be very slow. For this reason new iterative techniques based on the Newton Raphson method have been proposed in an effort to scale down the overestimated displacements. Kar and Okazaki [166] have modified the linearized displacements by the ratio of the largest applied load in any cycle of iteration, to its corresponding equilibrium load calculated on the basis of the linearised solution. The use of the largest applied load is based on the assumption that it has the greatest overall effect on the behaviour of the net (see Figure 8.10 which represents the load displacement curve of a joint with the largest applied load). The linearised equations (line OB) yield displacement x_1 corresponding to the applied load F . Displacement x_1 is now multiplied by the ratio of F to \bar{F}_1 and x_1 is scaled down to x_1' , which is smaller than the correct displacement. The equilibrium load is now \bar{F}_2 , and the residual load $\bar{\bar{F}}$. The next iteration is continued with the initial estimate being x_1' .

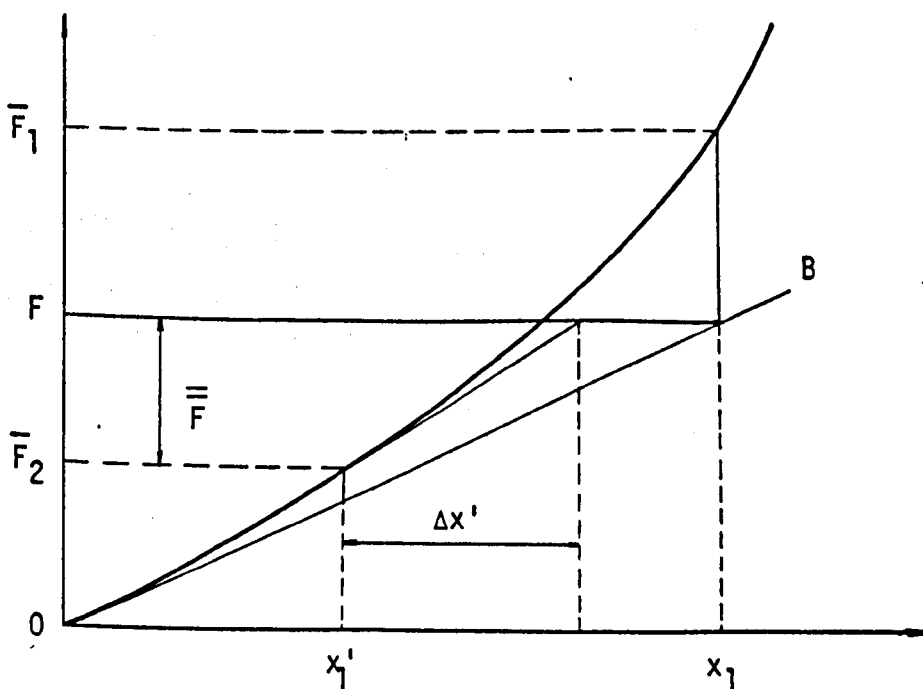


Fig. 8.10

8.2.3. Incremental Stiffness Procedure

In the incremental stiffness procedure the load is applied as a sequence of sufficiently small increments so that the structure can be assumed to respond linearly within each increment. In this manner the incremental technique solves a sequence of linear problems wherein the stiffness properties are recomputed for each load increment. The incremental technique therefore seeks, without iteration, to march the load deflection path.

The development of the recurrence relations for the incremental stiffness method begins with the assumption that the first derivative of the force unbalance with respect to the generalized load parameter p is zero. This assumption allows equation (8.4) to be written at the start of the $(m+1)$ -th load increment as

$$K \dot{x}_m = \bar{P} \quad (8.17)$$

The recursive relations rely upon the use of Euler forward difference approximation of the displacement derivative \dot{x} .

$$\dot{x}_m = \frac{1}{\delta p} (x_{m+1} - x_m) \quad (8.18)$$

Direct substitution of equation (8.18) into equation (8.17) yields the recursion relations applicable in the incremental stiffness method :

$$K \Delta x_{n+1} = \delta p \cdot \bar{P} = \Delta F \quad (8.19)$$

Improved results, at the expense of additional computation, can be obtained by taking the tangent stiffness not at the beginning but near the mid-point of each increment, corresponding to a second order Runge-Kutta procedure [129]. Bergan and Soreide [27] suggested a method for automatic computation of the size of the load increment which uses large increments in linear regions but smaller increments with increasing nonlinearity.

To avoid the "drifting" tendency of the incremental stiffness procedure (Figure 8.13), self-correcting procedures have been used. The simplest self-correcting method is to add the current force residuals to the next load increment. This corresponds to one cycle of Newton Raphson iteration, followed by a simple Euler increment in which the gradient is used as for the Newton Raphson iteration. Improved accuracy is obtained by carrying out several iterations for each level of loading. The tangent stiffness may either be held constant during iterations within each load step or may be reset at each iteration; the latter corresponding with the Newton-Raphson procedure. A flow diagram for an incremental Newton Raphson method is shown in Figure 8.11.

8.2.4. The Perturbation Method

The perturbation method is another solution procedure of the class $\dot{r} = 0$ which is currently receiving considerable attention. The method bears its name from the fact that its purpose is to determine the response of the systems under the constraint

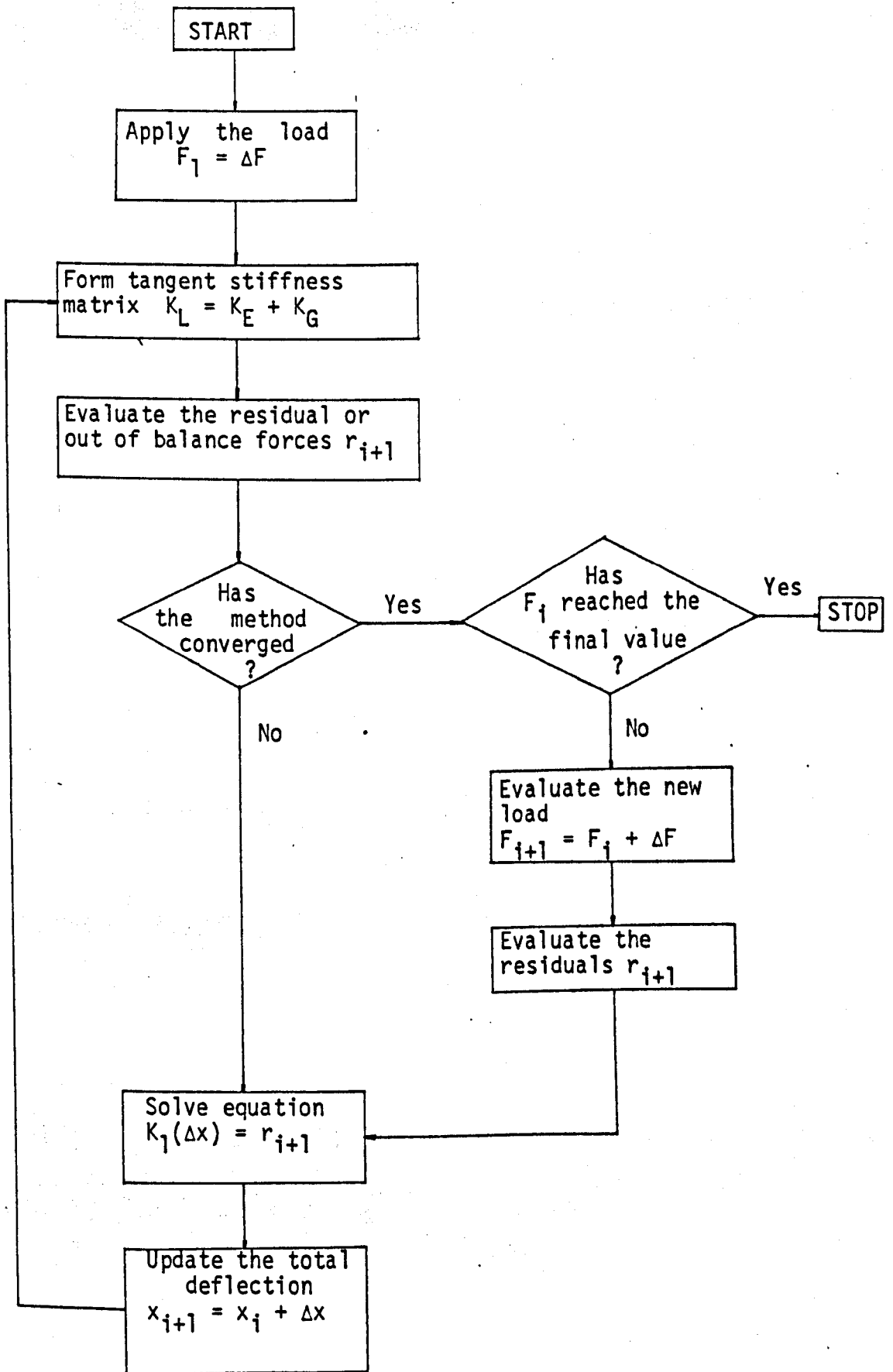


Fig. 8.11 Flow chart for the incremental Newton Raphson method

of equilibrium, when one of the parameters of the system is mathematically perturbed from a known value.

Defining X_i ($i = 1, 2, \dots, N$) to be the generalized displacement coordinates and Λ to be the single generalized loading parameter, which we assume to be independent of the displacements, the r -th algebraic equation may then be written

$$Q_r(X_i, \Lambda) = K_{rj}X_j + K_{rjk}X_jX_k + K_{rjkl}X_jX_kX_l + \dots + \Lambda F_r = 0 \quad (8.20)$$

where K_{rj} , K_{rjk} , \dots , are the constant coefficients of the linear, quadratic \dots , terms respectively, in the r -th equation.

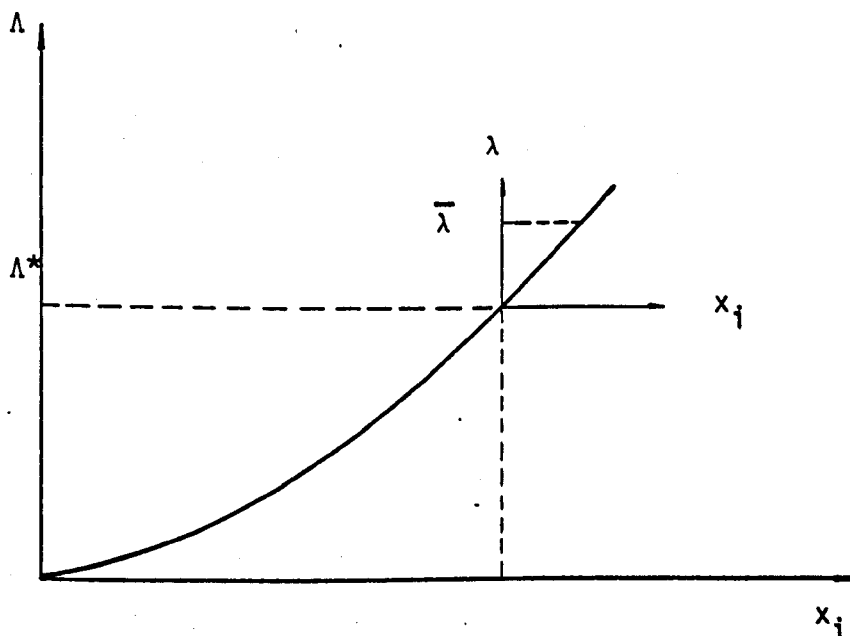


Fig. 8.12 Perturbation axis

Assuming now that at some set of values X_i^* , F^* , equations of type (8.20) are completely satisfied, we may write

$$X_i = X_i^* + x_i, \quad \Lambda = \Lambda^* + \lambda \quad (8.21)$$

and equation (8.20) becomes

$$Q_r [X_i^* + x_i, \Lambda^* + \lambda] = 0 \quad \text{or} \quad (8.22)$$

$$K_{rj}(x_j^* + x_j) + K_{rjk}(X_j^* + x_j)(X_k^* + x_k) + K_{rjkl} \cdot (X_j^* + x_j) \cdot$$

$$(X_k^* + x_k) (X_l^* + x_l) + (\Lambda^* + \lambda)F_r = 0 \quad (8.23)$$

These equations, because of the conditions at X_i^* and F^* , reduce to

$$\begin{aligned} &K_{rj}x_j + K_{rjk} (X_j^*x_k + X_k^*x_j + x_jx_k) + \\ &K_{rjkl} (X_j^* X_k x_l + X_j^* X_l^* x_k + X_k^* X_l^* x_j + \\ &X_j^* x_k x_l + X_k^* x_j x_l + X_l^* x_j x_k + x_j x_k x_l) + \\ &\lambda F_r = 0 \end{aligned} \quad (8.24)$$

Equation (8.24) may also be written as follows

$$K_{rj}^* x_j + K_{rjk}^* x_j x_k + K_{rjkl}^* x_j x_k x_l + \dots + \lambda F_r^* = 0 \quad (8.25)$$

where

$$K_{rj}^* = K_{rj} + (K_{rjk} + K_{rkj})X_k^* + (K_{rjkl} + K_{rlej} + K_{rklej})X_k^* X_l^*$$

$$K_{rjk}^* = K_{rjk} + (K_{rjkl} + K_{rlej} + K_{rklej}) X_l^*$$

$$K_{rjkl}^* = K_{rjkl}$$

$$F_r^* = F_r$$

Introducing a continuous parameter s , which defines progress along the equilibrium path x_i, λ , obtained from the satisfaction of equations (8.24), we write the co-ordinates in parametric form as follows

$$x_j = x_j(s) \quad , \quad \lambda = \lambda(s) \quad (8.26)$$

$$x_j(0) = 0 \quad , \quad \lambda(0) = 0$$

Accordingly, equation (8.25) is written as

$$K_{rj}^* x_j(s) + K_{rjk}^* x_j(s) x_k(s) + K_{rjkl}^* x_j(s) x_k(s) x_l(s) + \dots + \lambda(s) F_r^* = 0 \quad (8.27)$$

Expansion of expressions (8.26) into Taylor series gives

$$x_j(s) = x_j(0) + \dot{x}_j(0)s + \frac{1}{2} \ddot{x}_j(0) s^2 + \frac{1}{6} \dddot{x}_j(0) s^3 + \dots \quad (a) \quad (8.28)$$

$$\lambda(s) = \lambda(0) + \dot{\lambda}(0)s + \frac{1}{2} \ddot{\lambda}(0) s^2 + \frac{1}{6} \dddot{\lambda}(0) s^3 + \dots \quad (b)$$

Introducing the expressions (8.28) into equation (8.27), and then equating the coefficients for the terms of s of each order to zero, the following equations are obtained :

$$K_{rj}^* \dot{x}_j(0) + F_r^* \dot{\lambda}(0) = 0 \quad (a)$$

$$K_{rj}^* \ddot{x}_j(0) + K_{rjk}^* (2\dot{x}_j(0)\dot{x}_k(0)) + F_r^* \ddot{\lambda}(0) = 0 \quad (b)$$

$$K_{rj}^* \dddot{x}_j(0) + K_{rjk}^* (3\ddot{x}_j(0)\dot{x}_k(0) + 3\dot{x}_j(0)\ddot{x}_k(0)) + K_{rjkl}^* (6\dot{x}_j(0)\dot{x}_k(0)\dot{x}_l(0)) + F_r^* \dddot{\lambda}(0) = 0 \quad (c) \quad (8.29)$$

Equations (8.29) constitute the basic equations of the perturbation method. As parameter s can be selected as either a displacement or a load. If λ is selected as parameter s , then from equation (8.29a) the displacement vector x_i is obtained and after substituting these values in equation (8.29b), using the same inverse matrix, \ddot{x}_i is obtained. From the same process, $\ddot{\ddot{x}}_i$ is successively obtained, and so on. Introduction of these values into equation (8.28a) and addition of the increments to the present value of X_i^* , provides a new point on the equilibrium path.

The higher order terms which exist in the equations of the perturbation method, make the technique well suited for studying stability problems and for tracing the postbuckled path for snap-through buckling problems the perturbation method is very advantageous since, by using a displacement parameter as an independent variable with one equilibrium point along the path corresponding to each displacement state, there is no need for interchanging the role of dependent and independent variables as is necessary in the Newton Raphson method.

The perturbation method on the other hand, when applied to highly nonlinear problems, has the tendency to "drift" from the true equilibrium path (see Figure 8.14). The drifting is the result of accumulation of errors at succeeding load steps and both the size of the load step and the number of terms retained in the Taylor's series influence the amount of drifting.

To overcome this drawback correcting procedures have been proposed which are implemented after a certain number of increments of the independent variable.

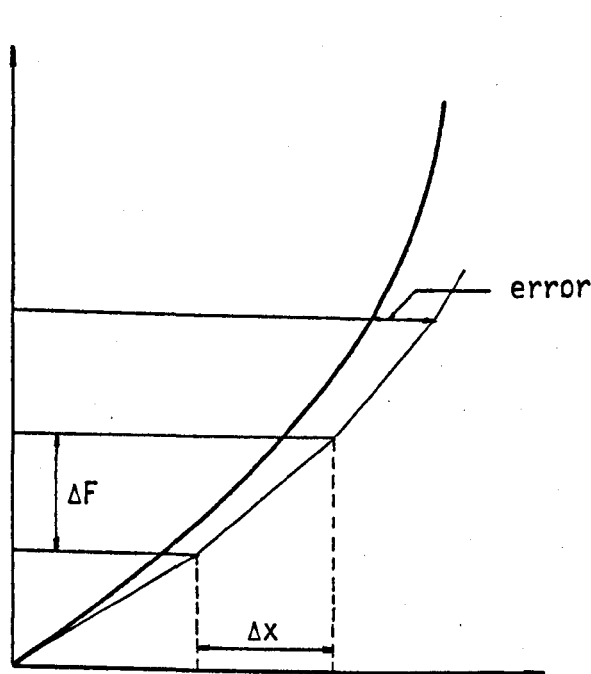


Fig. 8.13 Incremental stiffness procedure

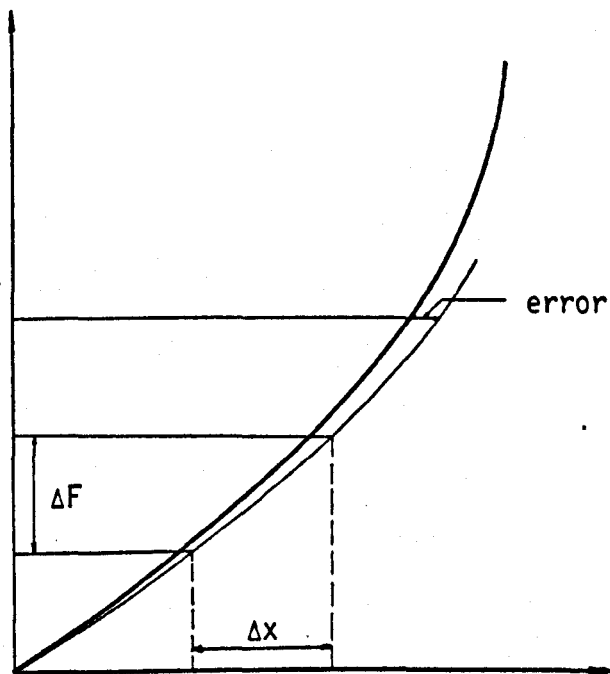


Fig. 8.14 Perturbation method

CHAPTER 9

COMPARATIVE STUDY

For the purpose of this study two stiffness method computer programs have been written, in addition to the programs developed in Chapters 4 and 7. Both stiffness programs utilize the Newton Raphson iteration method to approach the nonlinear solution and the Gauss elimination method to invert the tangent stiffness matrix in each iteration. The only difference between them is the way in which the overall stiffness matrix is stored. The first method, with the abbreviated description NTRA, stores the stiffness matrix in a semi-bandwidth form, while the second method, with the abbreviated description NTRAJE, uses the single array compact store technique proposed by Jennings [153]. To avoid unnecessary repetitions only the methods with the best convergence rates from the gradient and relaxation techniques have been included in this Chapter.

9.1. Example 1 : Suspension Cable

This example, with no initial prestress, has a singular stiffness matrix in its unstressed configuration. In order to solve this problem with the stiffness method, which requires the solution of the stiffness equations in each Newton Raphson iteration, it was assumed that one node was fixed during the first

solution stage. In this way the singularity was removed and subsequently the node was released after the first iteration. The rate of convergence, for this particular problem, was not affected by the choice of the fixed node.

From Table 9.1 it is apparent that the stiffness method with Newton Raphson iterations is a very effective technique for this problem. The semi-bandwidth of the stiffness matrix is only 4 and the required time for the Gauss elimination was kept to a minimum. The total number of Newton Raphson iterations required to reduce the residual norm below the value of $\epsilon=0.1E-07$ was 15, which reflects a highly nonlinear problem.

Of the explicit methods, the conjugate gradient method with Stanton's linear search and dynamic relaxation with kinetic damping gave similar results, while the Fletcher and Reeves method produced better convergence.

Table 9.2 shows the final displacements obtained from three different solution techniques, namely the stiffness method, the conjugate gradient method and the dynamic relaxation method. The results up to six decimal digits are identical.

9.2. Example 2 : Counterstressed Dual Cable

This is also a problem with very small bandwidth and the overall stiffness matrix has a minimum number of zero elements inside the bandwidth. This structure of the stiffness matrix

Method	CGST-R2	CGFR-R2	DRKV	NTRA	RNORM criterion ($\epsilon = 0.1E-07$)
TIME (sec)	0.541	0.325	0.757	0.035	

Table 9.1 Comparison of the results of example 1

Node	X(ft)	Y(ft)	RNORM criterion ($\epsilon = 0.1E-07$)
1	1.672465	-4.520561	
2	1.375813	-3.003561	
3	-0.314281	4.636210	
4	-2.821189	18.495134	
5	-3.723775	-0.305051	
6	-4.865523	12.723695	
7	-5.653763	18.840667	
8	-5.498690	18.723332	
9	-3.811004	12.427658	

Table 9.2 Final displacements of example 1

helps the banded elimination method to converge faster than the compact elimination method. The additional computational work to avoid the zero elements makes the compact store elimination slower (Table 9.3).

The dynamic relaxation method with automatic adjustment of the iteration parameters produced the fastest convergence rate of all the explicit methods. The conjugate gradient Stanton algorithm and dynamic relaxation with kinetic damping gave similar results. The final displacements were again identical up to six decimal digits for all the methods when the termination criterion for the residual norm was $\epsilon = 0.1E-07$.

Method	CGST-SC-R3	DRAUT	DRKR	NTRA	NTRAJE
TIME (sec)	0.905	0.725	0.960	0.105	0.145

RNORM
criterion
($\epsilon=0.1E-07$)

Table 9.3 Comparison of the results of example 2

9.3. Example 3 : Orthogonal Hyperbolic Paraboloid Prestressed Net

This example has a minimum semi-bandwidth of 20, and a relatively small number of zero elements inside the bandwidth.

From Table 9.4 it can be seen that the compact store elimination method, by utilizing a better storage during the elimination process, converged one and a half times faster than the semi-bandwidth elimination ; both methods requiring 8 iterations for the residual norm to converge to the prescribed accuracy of $\epsilon = 0.1E-07$.

For this problem the dynamic relaxation method with automatic adjustment of the iteration parameters gave very close results to the NTRAJE method and better convergence than the NTRA method. The use of kinetic damping in dynamic relaxation, produced better results than the conjugate gradient method, but is still very much slower than the DRAUT method. Again there was no difference in the final displacements given by any of the methods and, as Table 9.5 indicates, there were only moderate differences between the utilization of the initial and current length of members in the evaluation of the direction cosines.

9.4. Example 4 : Three Dimensional Counterstressed Dual Cable Structure

Two separate cases have been considered for this example. The first with members are not allowed to go slack ; while in the second they are allowed to slacken. This is done in order to test the performance of the methods as the problem

Method	CGST-SC	DRAUT	DRKV	NTRA	NTRAJE
TIME (sec)	0.527	0.385	0.705	0.439	0.285

RNORM
criterion
($\epsilon = 0.1E-07$)

Table 9.4 Comparison of the results of example 3

Node	(L)			(L + e)		
	X(ft)	Y(ft)	Z(ft)	X(ft)	Y(ft)	Z(ft)
1	0.00000	-0.02224	0.37715	0.00000	-0.02221	0.37663
3	0.00000	-0.06527	1.27195	0.00000	-0.06517	1.27006
4	0.01456	-0.02921	0.73478	0.01453	-0.02917	0.73361
7	0.00000	-0.08818	3.71970	0.00000	-0.08811	3.71562
8	-0.01335	-0.04251	1.73570	-0.01335	-0.04247	1.73318
13	0.00000	0.00896	1.72772	0.00000	0.00891	1.725056
14	0.01696	-0.01133	1.26641	0.01693	-0.011317	1.264236
15	0.01577	-0.00189	0.74087	0.01574	-0.00189	0.73960
19	0.00000	0.02042	1.01935	0.00000	0.02031	1.017685
20	0.01687	0.00538	0.83062	0.01684	0.00536	0.829270
21	0.01855	0.00685	0.46580	0.01852	0.00684	0.465067
23	0.00000	0.00204	0.60744	0.00000	0.00196	0.606579
24	0.09264	0.00933	0.42002	0.09250	0.00929	0.419562
25	0.00000	0.01021	0.25482	0.00000	0.01022	0.254537

Table 9.5 Final displacements of example 3 with the use of initial and current lengths of the members

becomes path-dependent.

The two idealizations are realized as follows : In the first case, if the tension force of a member becomes compression during the application of the loading, the member behaves like a strut with the same elastic properties as the cables. While in the second case, when a member goes into compression, it ceases to exist structurally and makes no contribution to the overall stiffness matrix until, and if, the compression force becomes tension again in the course of the loading.

This example has a minimum semi-bandwidth of 45 and a considerable number of zero elements inside the bandwidth. Table 9.6 shows the required execution time for convergence of the methods when the members are not allowed to go slack. The difference between the NTRAJE and NTRA methods indicates how powerful the compact store elimination technique can be when zero elements exist inside the bandwidth of a stiffness matrix. The scaled conjugate gradient Stanton algorithm with reinitialization was slightly better than the DRAUT and NTRA methods. Table 9.7 shows that the final displacements computed from the use of initial and current lengths of members are coincident up to 3 decimal digits.

Table 9.7 shows the convergence characteristics of four explicit methods when members are allowed to go slack. The dynamic relaxation with automatic adjustment of the iteration parameters produced the best convergence rate up to a value of

Method	CGST-SC-R3	DRAUT	NTRA	NTRAJE	RNORM criterion ($\epsilon = 0.1E-07$)
TIME (sec)	0.795	0.828	0.801	0.268	

Table 9.6 Comparison of the results of example 4 when members are not allowed to go slack

Node	(L)			(L + e)		
	X(ft)	Y(ft)	Z(ft)	X(ft)	Y(ft)	Z(ft)
1	0.164736	0.0	0.475925	0.164766	0.0	0.474025
2	-0.032838	0.0	0.461649	-0.032977	0.0	0.459742
3	0.115575	0.0	-0.347401	0.115673	0.0	-0.34920
4	-0.045448	0.0	-0.348642	-0.045610	0.0	-0.350443
5	0.404194	0.0	4.766360	0.403711	0.0	4.759345
6	-0.309451	0.0	4.723101	-0.309165	0.0	4.716172
7	0.092036	-0.026263	-0.236304	0.092087	-0.026310	-0.237732
8	-0.019702	0.0277931	-0.236950	-0.019806	0.027854	-0.23838
13	0.087448	0.027540	0.452892	0.087487	0.027600	0.453229
14	-0.022280	-0.024580	0.451256	-0.022384	-0.024621	0.451589
15	0.063114	-0.036705	0.072992	0.063137	-0.036700	0.072472
16	0.054805	0.024074	0.072747	0.054264	0.024132	0.072227

Table 9.7a Final displacements of example 4 without slackening of the members

the termination parameter $\epsilon = 0.5E-04$. Beyond this value of the termination parameter, the scaled conjugate gradient algorithm, with reinitialization and with Stanton's algorithm for the evaluation of the step length and Polak-Ribieve's algorithm for β_i , produced better results. It is once again very interesting to see how the reinitialization process can dramatically affect the convergence of the conjugate gradient method as indicated by the methods 1 and 2 of Table 9.7. Figure 9.1 shows a plot of the required time versus the value of the termination parameter for the methods used in Table 9.7.

Figures 9.2 and 9.3 show plots of the displacements of node 5 versus the number of iterations of the conjugate gradient and the dynamic relaxation methods as they converge towards the final equilibrium position. In the CGST method the convergence to the final displacements, in the first few iterations, is very rapid. Then the displacement curve intersects the equilibrium line several times before the final convergence. The pattern of the DRAUT displacement curves is different. The convergence in the beginning is very slow due to the initially arbitrary chosen value for the minimum eigenvalue. After several iterations the minimum eigenvalue is adjusted, the iteration parameters are automatically optimized and the slope of the curves become steeper. Several intersections with the equilibrium line are also witnessed with the DRAUT method.

The difference between these two methods is that the curves

	Termination Parameter	0.1E-00		0.1E-02		0.1E-03		0.1E-04	
		N _{it}	TIME	N _{it}	TIME	N _{it}	TIME	N _{it}	TIME
1	CGST	3741	13.230	13208	46.713	-	-	-	-
2	CGST-R3	111	0.413	235	0.873	351	1.289	446	1.628
3	CGSTPR-SC - R3	52	0.256	113	0.517	141	0.640	189	0.847
4	DRAUT	73	0.118	280	0.395	499	0.702	701	0.975

QUOT
criterion
($\epsilon = 0.1E-07$)

Table 9.7 Convergence studies of example 5, when members are allowed to go slack

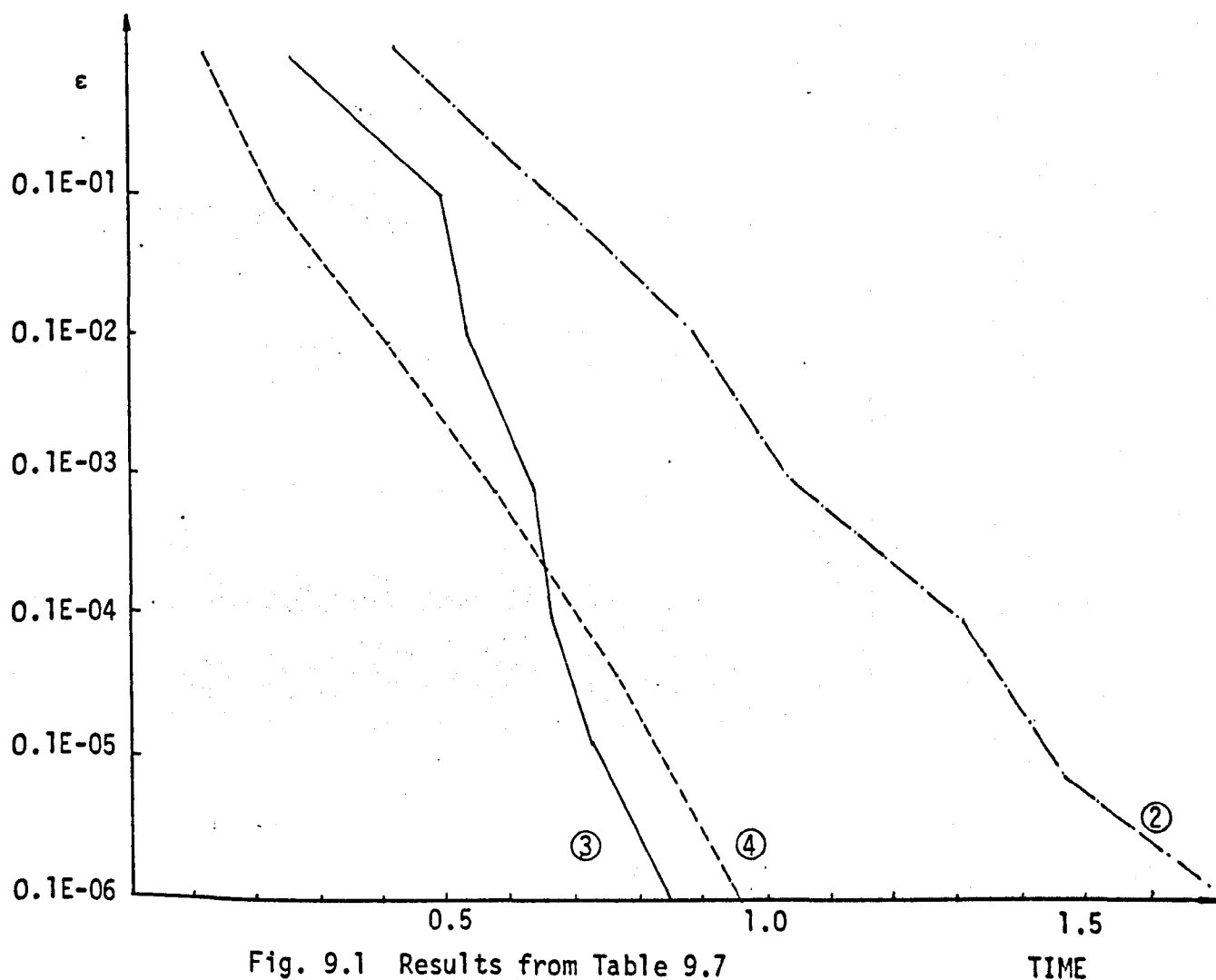


Fig. 9.1 Results from Table 9.7

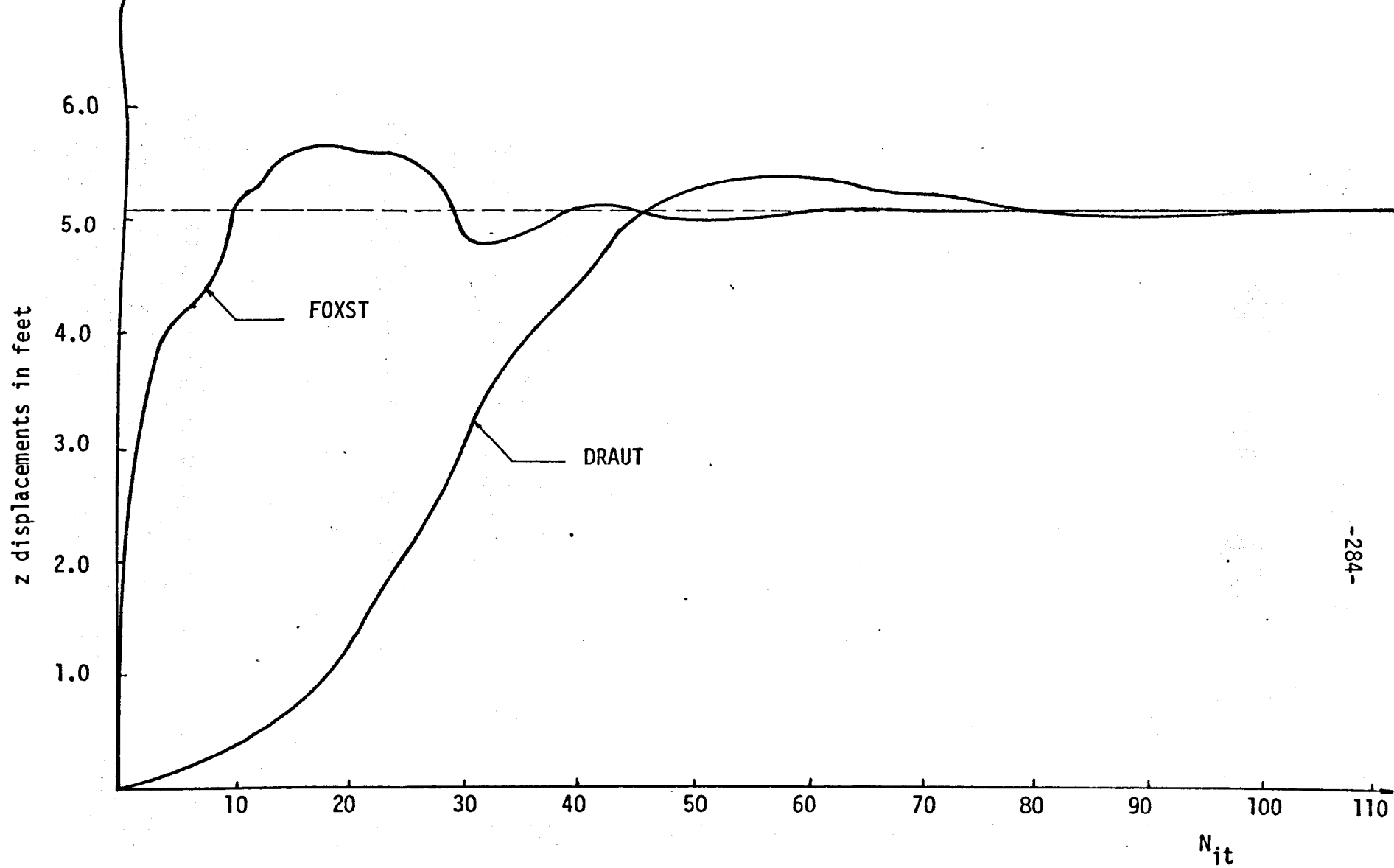


Fig. 9.2 Convergence of vertical deflections of point 5 versus the iteration index N_{it} , for example 4

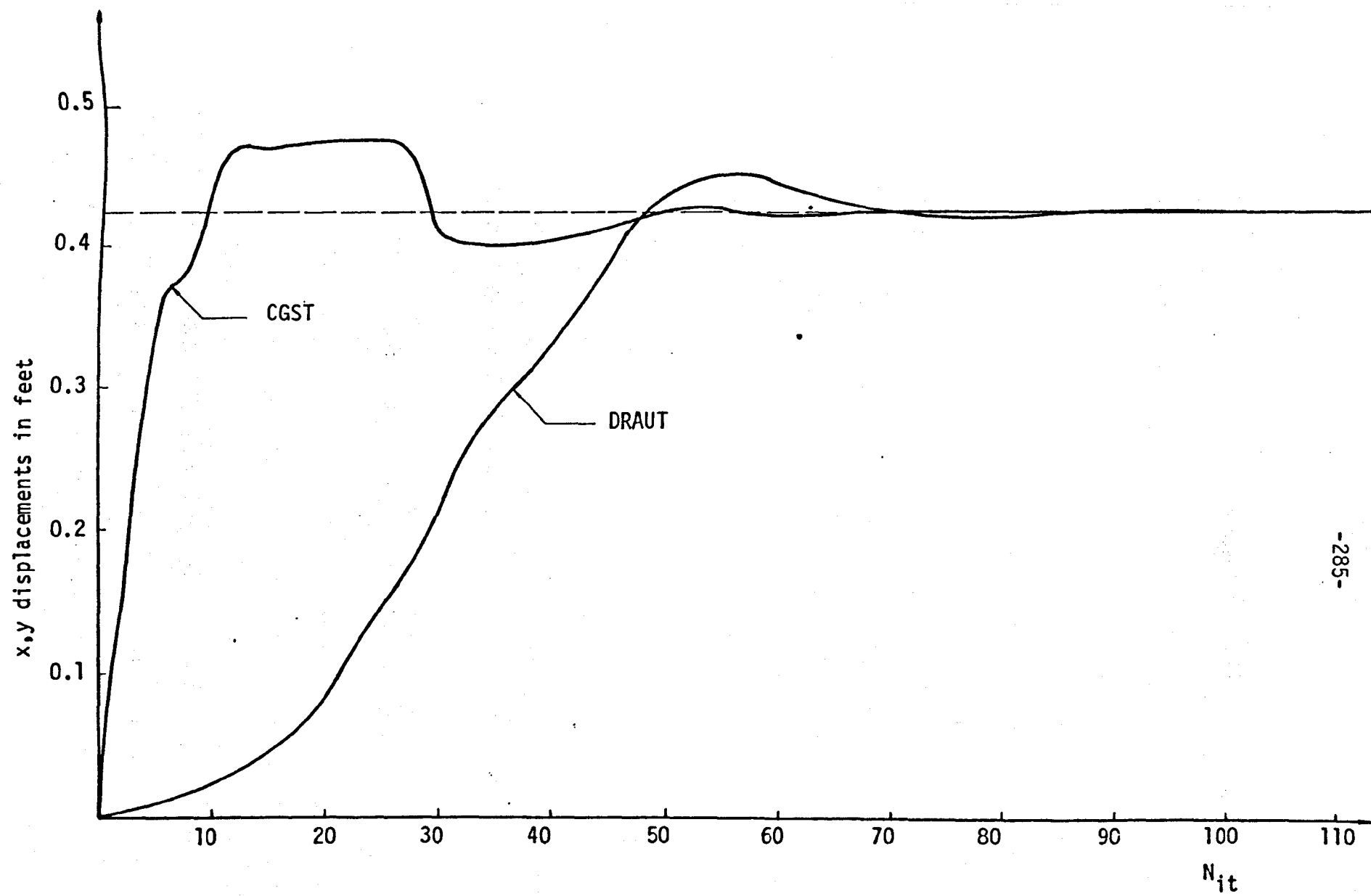


Fig.9.3 Convergence of horizontal deflections of point 5 versus the iteration index N_{it} , for example 4

of the dynamic relaxation are generally smoother than those of the conjugate gradient method. Also the curve patterns of the DRAUT are controllable with properly chosen iteration parameters. A reduced value for the damping parameter will result in an underdamped behaviour with many maximum and minimum points of the displacement curves, while an increased value for the damping parameter will result in overdamped behaviour, with almost no intersection with the equilibrium line until final convergence is achieved. This is an advantage of the dynamic relaxation method when there is a possibility of a structure changing its shape by jumping into a displacement state different than its true final equilibrium position. Theoretically only the overdamped dynamic relaxation can guarantee convergence in such cases of path dependency, unless an incremental load procedure is used. However, in this example, although path dependent, the conjugate gradient method converged with no difficulty to the correct solution in one load increment.

Table 9.8 shows the final displacements when the stiffness method with one load increment ($ND = 1$) and ten load increments ($ND = 10$) is used. The results are identical but the difference in execution time is enormous. The reason why, for this particular example, one load increment gave the correct results lies in the fact that the overestimated displacements from the first Newton Raphson iteration did not produce any change in the shape of the structure that could affect the final equilibrium position. But even if there is a danger of the overestimated displacements affecting the final convergence, relaxation parameters can be

Node	ND = 1			ND = 10		
	x(ft)	y(ft)	z(ft)	x(ft)	y(ft)	z(ft)
1	0.185309	0.000000	0.388612	0.185309	0.000000	0.388612
2	-0.050104	0.000000	0.369847	-0.050104	0.000000	0.369847
3	0.130813	0.000000	-0.446669	0.130813	0.000000	-0.446669
4	-0.059434	0.000000	-0.448668	-0.059434	0.000000	-0.448668
5	0.434223	0.000000	5.076456	0.434223	0.000000	5.076456
6	-0.190508	0.000000	2.674305	-0.190508	0.000000	2.674305
7	0.103382	-0.030160	-0.313677	0.103382	-0.030160	-0.313677
8	-0.028544	0.033033	-0.314759	-0.028544	0.033033	-0.314759
13	0.099290	0.034502	0.518698	0.099290	0.034502	0.518698
14	-0.033738	-0.029887	0.516515	-0.033738	-0.029887	0.516515
15	0.069450	-0.002975	0.058943	0.069450	-0.002975	0.058943
16	0.000734	0.001981	0.058599	0.000734	0.001981	0.058599
TIME (sec) NTRA	0.853			4.938		

RNORM criterion ($\epsilon = 0.1E-07$)

Table 9.8 Final displacements of example 4, when members are allowed to go slack

CGSTPR-SC-R3	DRAUT	NTRA (ND=1)	NTRA (ND= 5)	NTRAJE(ND=1)	NTRAJE(ND=5)
0.951	1.170	0.783	2.806	0.286	1.029

RNORM criterion ($\epsilon = 0.1E-07$)

Table 9.9 Comparative study of example 4, when members are allowed to go slack

introduced to improve the convergence behaviour of the Newton Raphson method. Such a modified Newton Raphson method has been proposed by Krishna [173].

9.5. Example 5 : Large Prestressed Net

A study of a large net, similar in form to the Raleigh Arena of Raleigh, North Carolina, USA, was undertaken to gain computational experience with full scale structures. The whole net has 795 degrees of freedom and a minimum semi-bandwidth of 57.

In this case the required time for convergence and the computer cost of the methods were compared. For the particular CDC7700 computer used at the University of London (FTN compiler), the computer cost is calculated from the following formula :

$$\text{Cost Units} = \frac{1}{100} \left[5 \times \text{Jobtime} + \frac{\text{SCM}}{2} + \frac{\text{LCM}}{10} + \frac{\text{IO}}{100} + \frac{\text{RMS}}{2} + 10 \right]$$

where SCM : small core memory
LCM : large core memory
IO : input-output
RMS : rotating mass storage

Table 9.10, shows the required execution time and cost of the methods for the analysis of the structure subject to a uniform vertical loading of 5.7 kips at each node. In terms of time and cost the NTRAJE method is superior to all other methods.

Method	CGSTPR-SC-R4	DRAUT	NTRA	NTRAJE
Jobtime (sec)	23.198	62.565	24.894	6.039
Cost Units	3.398	7.874	5.210	1.344

QUOT
criterion
($\epsilon = 0.1E-07$)

Table 9.10 Comparison of the results of example 5

Node	Load case"A"	Load case"B"
	z (ft)	z (ft)
2	0.026794	0.022331
7	0.145567	0.139752
16	0.22422	0.218434
28	0.240625	0.238113
42	0.163309	0.165789
58	0.130001	0.145559
76	0.132967	0.175635
95	0.11562	0.209897
114	0.149361	0.332285
133	0.158639	0.444077
124	0.436706	0.324995
125	0.723866	0.530664
126	0.871011	0.620545
127	0.888021	0.630362
128	0.806744	0.514549
129	0.662937	0.391268
130	0.475930	0.258729
131	0.310584	0.189179
132	0.192953	0.227784

Table 9.11 Final vertical displacements at selected nodal points of example 5

The conjugate gradient method produced much better results than the dynamic relaxation and the NTRA methods. The dynamic relaxation method could have produced better results if the criterion for adjusting the minimum eigenvalue had been selected more efficiently. For the purpose of this study, the large core memory of the computer was utilized for both stiffness methods in order to accommodate the storage requirements of the overall stiffness matrix.

Table 9.11 shows the final vertical displacements at selected nodal points for two load cases. Again the results obtained were coincident up to the sixth decimal digit for all the methods applied. The "QUOT" termination criterion was less than $\epsilon = 0.1E-07$.

9.6. Conclusions

When there are no storage limitations, the Newton Raphson method in conjunction with the Gauss elimination method can provide a very powerful technique to cope with almost any degree of nonlinearity in cable structures. The compact store elimination method as proposed by Jennings can work very efficiently even in small problems with a moderate number of zero elements inside the bandwidth of the overall stiffness method. Only in the extreme case of the single cable of example 1, where there are no zero elements inside the bandwidth, did the semi-bandwidth elimination method give better results. In some cases, as in example 5, the difference could be up to five times in favour of

the compact store elimination scheme. There is also no doubt that the results obtained from the Newton Raphson method could be further improved by the use of accelerating parameters.

The dynamic relaxation with automatic adjustment of the iteration parameters, as was developed in Chapter 5, proved a very successful method, particularly for the hyperbolic paraboloid of example 3, where it almost reached the convergence rate obtained by the NTRAJE method. In the other examples, except in the large net, the results obtained from the three explicit methods, namely CGST, DRAUT and DRKV, were very similar to each other.

In the study of the path dependent problem of example 4, when members are allowed to go slack, dynamic relaxation proved more stable as far as the fluctuations of the displacements around the equilibrium line were concerned, but gave less favourable results in terms of total execution time than the scaled conjugate gradient method with reinitialization. The Newton Raphson method gave the correct results even when the load of 50.0 kips at node 5 was applied in one increment. The possibility of members going slack was checked in each Newton Raphson iteration and the geometry of the structure was modified accordingly. The application of the load in increments did not accelerate the convergence.

In path dependent problems, as in example 4 when members may slack during the application of the loading there is always a danger when applying a non-incremental Newton Raphson method, that the structure may jump into another configuration and produce erroneous results. When the load is not applied in

increments, only the dynamic relaxation method with an effective combination of the iteration parameters can guarantee convergence to the correct solution.

The study of the large net revealed that, provided there are enough storage facilities available in the computer, the compact store elimination scheme is the quickest method, though the conjugate gradient method, as applied in this Chapter, proved a very competitive technique.

The real advantage of the explicit methods, as applied to the elastic analysis of cable structures, is that they can produce an effective alternative to the stiffness Newton Raphson methods when there are limitations in the core store available.

The use of discs or magnetic tapes, which is another alternative when direct access store is not available, has however not been considered in this study. And an interesting comparison would be to test the efficiency of the stiffness methods when auxiliary storage facilities are used.

CHAPTER 10

ULTIMATE LOAD ANALYSIS

10.1. Introduction

The majority of publications which deal with the analysis of cable structures have considered the effects of finite deformations but have not studied the ultimate load capacity of these structures. Only the papers presented by Greenberg [129], Jonatowski and Birnstiel [160], Murray and Willems [210] and Saafan [253], have included both the material and geometric nonlinearities. And it was only recently that a complete inelastic analysis, with different stress-strain curves during loading and unloading of the members, was carried out by Jonatowski [161]. However, the inclusion of the nonlinear stress-strain relationships in studying the behaviour of cable structures is fully justified by the fact that only up to about 50% of their breaking strength do the cables exhibit linear stress-strain characteristics.

Another form of material nonlinearity, which may or may not be connected with nonlinear stress-strain relationships is the "slackening" of the cables. A common assumption in the analysis of tension structures, particularly in the early publications, has been that the structure is initially prestressed sufficiently to preclude any change in configuration under the application of loads [271, 92, 46]. Algorithms based on this assumption are limited to rather special cases and, in fact, can produce

erroneous results since no means is provided to determine whether the selected prestress is adequate.

In the following study, the problem of studying the inelastic response of a cable structure is path-dependent and incremental load analysis in conjunction with total potential energy minimization techniques and Newton Raphson stiffness procedures have been used. The deformation response of the structure is traced as the loading is increased from the initial state to the ultimate carrying capacity. The criterion adopted to determine ultimate load carrying capacity is the breaking strength of a cable element rather than excessive deflections which may make an actual structure unusable.

10.2. Mathematical Formulation

The cables used for unstiffened cable supported structures are usually either wire rope or wire strand. Wire strand is an arrangement of wires laid helically about a center wire to produce a symmetrical section. Wire rope consists of many strands laid helically around a core composed of a strand or another wire rope.

The elongation of wire rope or wire strand depends on the combination of two effects : the Strength of the steel itself, and the "construction looseness". The first effect may be elastic or inelastic, while the second is always nonelastic. Only the elastic strength is fully recoverable. The "constructional

looseness" depends upon the size of the strand, the equipment used in the manufacturing process and the arrangement of the wires.

Ramberg and Osgood [241] suggested the representation of complete stress-strain curves by a single expression using three parameters

$$\epsilon = \frac{\sigma}{E} + \left(\frac{\sigma}{B}\right)^n \quad (10.1)$$

in which n and B are constants determined for the particular material, E is the slope of the initial portion of the curve and ϵ and σ are unit strain and unit stress respectively. Since, in the displacement method of analysis, the strains are first calculated and then from the stress-strain relationships the stresses, equation (10.1) must be solved for stresses in terms of strains. This can not be done analytically and Newton's iterative method should be employed.

Greenberg [129] proposed an alternative expression for the stress-strain curve.

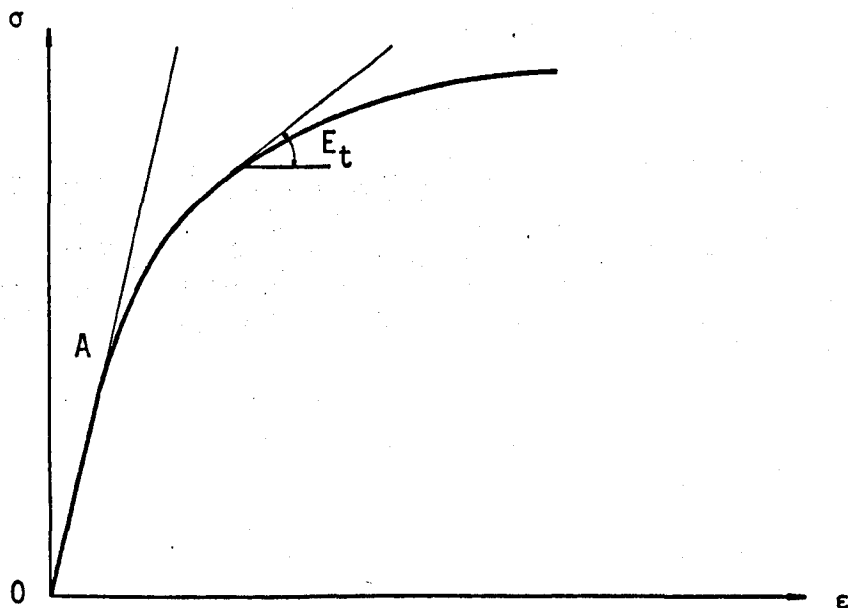


Fig. 10.1 Greenberg's stress-strain curve

When $0 < E \leq \epsilon_e$

$$\sigma = E \cdot \epsilon$$

When $\epsilon_e < E \leq \epsilon_{ult}$

$$\sigma = \sigma_e + \sigma_0 \left[1 - \left(1 - \frac{\epsilon - \epsilon_e}{\epsilon_0} \right)^m \right] \quad (10.2)$$

$$E_t = \sigma_0 \left[\frac{m}{\epsilon_0} \left(1 - \frac{\epsilon - \epsilon_e}{\epsilon_0} \right)^{m-1} \right] \quad (10.3)$$

$$\epsilon = \epsilon_e + \epsilon_0 \left[\left(1 - \frac{\sigma - \sigma_e}{\sigma_0} \right)^{1/m} - 1 \right] \quad (10.4)$$

with

$$m = \frac{\epsilon_0 E}{\sigma_0} \quad \text{and} \quad \sigma_0 = \sigma_{ult} - \sigma_e$$

$$\epsilon_0 = \epsilon_{ult} - \epsilon_e$$

Finally Jonatowski and Birnstiel [160] proposed a stress-strain relationship given by the expression :

$$\sigma = \frac{E\epsilon}{\left[1 + \left| \frac{E\epsilon}{B} \right|^n \right]^{1/n}} \quad (10.5)$$

in which B is a constant equal to or slightly greater than the ultimate stress, σ_{ult} , of the material, and n is a constant defining the shape of the stress-strain relationship. Based on equation (10.5), the tensile force in a member may be computed from

$$p = \frac{EA(L - \bar{L}_0)}{g \bar{L}_0} \quad (10.6)$$

$$\text{where } g = \left[1 + \left| \frac{E(L - \bar{L}_0)}{\bar{L}_0 B} \right|^n \right]^{1/n} \quad (10.7)$$

The term \bar{L}_0 in equations (10.6) and (10.7) is the unstrained length of the cable member, which is not the same as the initial length, and L is the current length. Assuming that the initial configuration of the structure is known, the unstrained length is given by

$$\bar{L}_0 = \frac{L_0}{1 + \frac{P_0}{EA} \left[1 + \left| \frac{E(L - L_0)}{\bar{L}_0 B} \right|^n \right]^{1/n}} \quad (10.8)$$

in which P_0 is the initial prestress in the member and L_0 is the length of the member in its initial configuration. Equation (10.8) is nonlinear and a Newton's iterative procedure has been used to determine \bar{L}_0 . A good starting value may be obtained from the expression

$$\bar{L}_0 = \frac{L_0}{1 + \frac{P_0}{EA}} \quad (10.9)$$

Equation (10.5) must be used only when the cable members are being stressed by increasing tensile loads because of the presence of the quantity g which results from the nonlinear stress-strain relationship. If, however, the member is unloaded then the unit stress is given by

$$\sigma = E\varepsilon - [E\varepsilon_a - \sigma_a] \quad (10.10)$$

where ε_a and σ_a are the unit strain and unit stress at the start of unloading.

It should be noted that cables cannot resist compressive forces. If, therefore, during the analysis the cable member force, P , becomes negative, it will be assumed that the member ceases to exist structurally, and if during the subsequent loading the member strain ϵ satisfies

$$\epsilon \geq \epsilon_a - \sigma_a/E \quad (10.11)$$

then the member is restored. Figure (10.2) shows diagrammatically the loading and unloading paths, with the following stress-

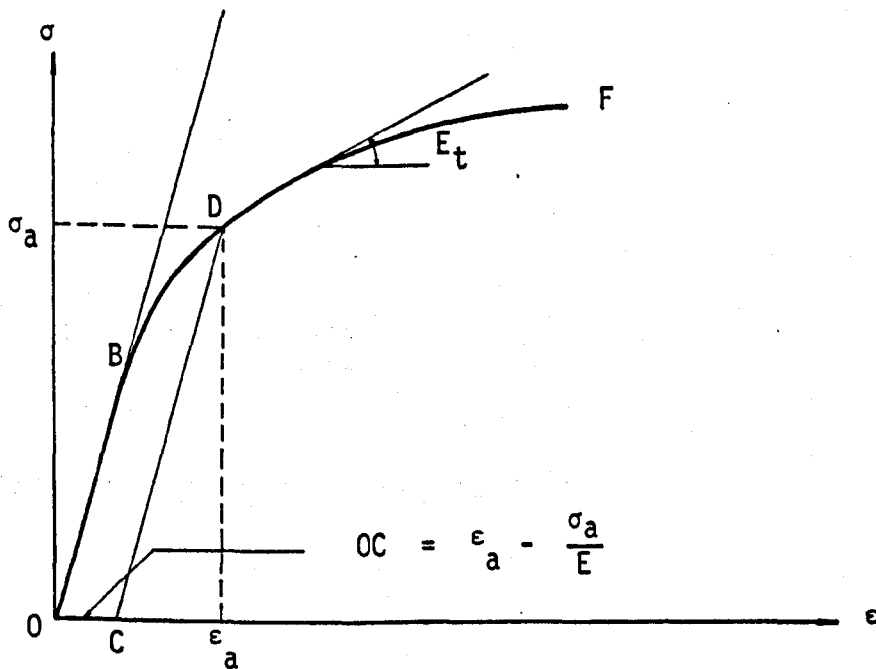


Fig. 10.2 Jonatowski's stress strain curve

strain expressions :

(a) OB portion : $\sigma = \epsilon E$ (10.12)

$$(b) \text{ BF portion : } \sigma = \frac{E\epsilon}{\left[1 + \left|\frac{E\epsilon}{B}\right|^n\right]^{1/n}} \quad (10.13)$$

$$(c) \text{ CD portion : } \sigma = E\epsilon - (E\epsilon_a - \epsilon_a) \quad (10.14)$$

For the purpose of the subsequent studies the Jonatowski and Birnstiel expression for the stress-strain relationship is used with provision for the members to follow a different stress-strain curve when unloading. The constants n and B assumed for the numerical studies carried out in this Chapter are listed in Table 10.1.

Material	E(Ksi)	n	B	$\epsilon_n(i_n/i_n)$	$\sigma_n(Ksi)$
Structural rope	21500	2.7	214	0.032	210.7
Structural strand	30000	1.7	226	0.062	222.4

Table 10.1 Cable material properties

10.3. Non Linear Solution Techniques for Ultimate Load Analysis

Two different solution procedures have been developed and compared for the study of the ultimate load analysis of cable structures. The conjugate gradient method with Stanton's linear

search and the Newton Raphson method in conjunction with the semi-bandwidth elimination and compact storage elimination schemes. Figure 10.3 shows the flow charts for these two methods.

10.4. Numerical Studies

The numerical procedure described in the previous Section has been used to study the deformation response of the structures of examples 3 and 4. Throughout this Section several symbols have been used with the following notation :

ND : is the load increment at the joint with the maximum load

Ec : means that the slope of the stress-strain curve remains unchanged inside the load increment

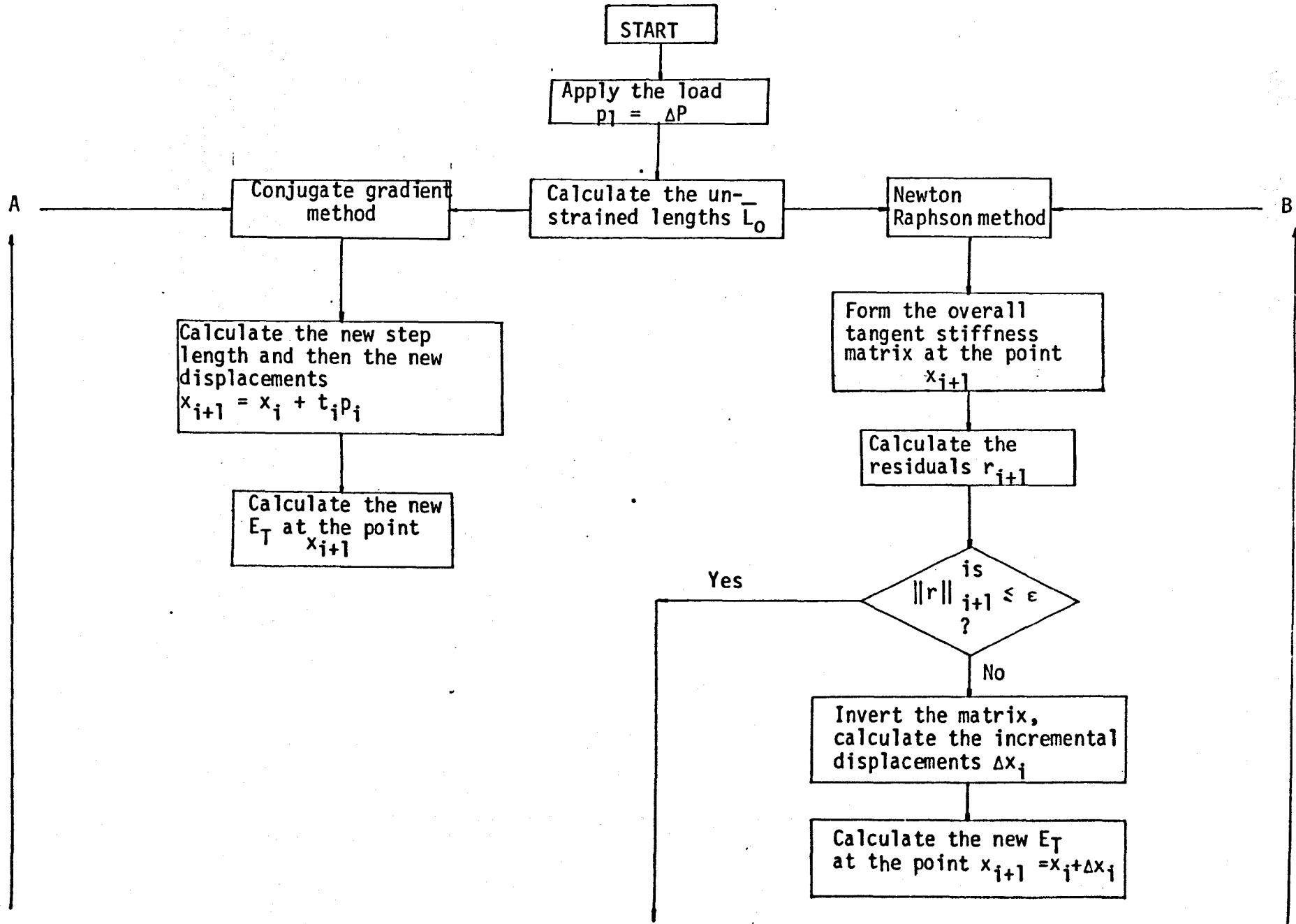
Ev : means that the stress-strain slope is changing in each Newton Raphson or conjugate gradient iteration inside the load increment

e : is the termination parameter for the residual norm at each load increment

The ultimate load condition is quoted as the maximum nodal load at the load increment prior to detection of a ruptured cable.

10.4.1. Example 3 : Hyperbolic Paraboloid

For the purpose of this inelastic analysis it was assumed



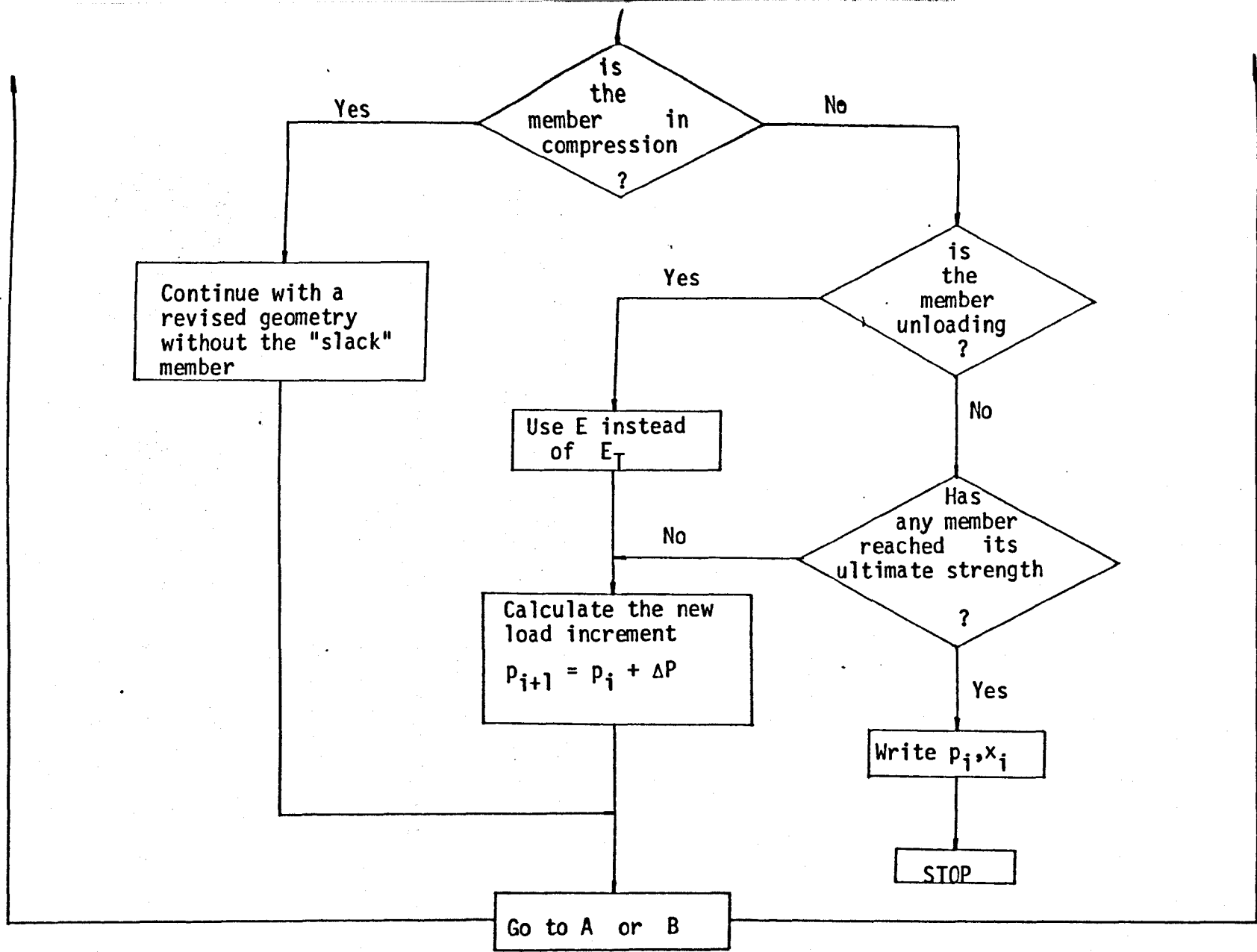


Fig. 10.3 Flow chart for ultimate load methods

that the cables are structural ropes with material properties shown in Figure 10.1. The area of cables and the horizontal component of prestress force have been also modified from the structure originally analysed with elastic behaviour, as follows :

Area of cables = 0.479 sq. in.

Horizontal component of prestress = 40.0 Kips

An increasing vertical load, P , is applied at joint 7 and vertical loads of $0.1P$ at all other joints.

Table 10.2 shows the vertical displacements at joint 7 for every 10 Kips increase of the load P , as well as the ultimate load obtained with different values of the parameter ND and different combinations of the parameters E_c and E_v . The predicted ultimate load for the two cases with $ND = 0.1$ is the same, but there is a difference when $ND = 10$. The displacements obtained when a constant slope (E_c) in each load increment is used, are underestimated and this results in a late rupture of the first member of the structure, thus giving a higher ultimate load. The ultimate carrying capacity with $ND = 10$ and E_v is on the safe side, while there is little difference in the ultimate load obtained using ND values of 1.0 and 0.1. The first cables to rupture were 6-7 and 7-8.

Table 10.3 shows the required execution time before rupture of a member occurs, for different combinations of the parameters and stiffness methods. The use of a small value for e can affect

Vertical load at node 7	ND = 0.1		ND = 1	ND = 10	
	E_C	E_V	E_V	E_C	E_V
10	4.24199	4.26175	4.25286	3.95760	4.26517
20	7.75548	7.75477	7.73335	7.31354	7.75094
30	10.74736	10.72126	10.71655	10.04310	10.74604
40	13.39360	13.39989	13.38683	12.50944	13.41409
50	15.78863	15.7877	15.81350	14.80250	15.83482
60	18.02118	18.09396	18.05416	16.95630	18.07294
70	20.13936	20.14513	20.22246	18.99241	20.24374
80	22.16867	22.21968	22.26165	20.97225	22.2886
Ultimate load at node 7	81.9	81.9	82.0	90.0	80.0

Table 10.2 Vertical displacements in feet at joint 7 of example 3 (stiffness method)

NTRA	NTRAJE	NTRAJE	NTRAJE	NTRA	NTRAJE	NTRAJE	NTRAJE	NTRAJE
e=0.1E-01	e=0.1E-01	e=0.1E-01	e=0.1E-04	e=0.1E-01	e=0.1E-01	e=0.1E-04	e=0.1E-01	e=0.1E-01
$E_V, ND=10$	$E_C, ND=10$	$E_V, ND=10$	$E_V, ND=10$	$E_V, ND=1$	$E_V, ND=1$	$E_V, ND=1$	$E_C, ND=0.1$	$E_V, ND=0.1$
3.161	0.935	1.578	12.525	10.323	5.634	57.008	30.045	30.706

Table 10.3 Final execution time in seconds for example 3

Vertical load at node 7	CGST	CGST-SC	CGST-SC	CGST-SC-R3	CGST-SC-R3
	e = 0.1E-01	e =0.1E-01	e =0.1E-01	e =0.1E-01	e =0.1E-04
	E_c	E_c	E_v	E_v	E_v
10	3.99615	3.99541	4.26509	4.26509	4.26515
20	7.31418	7.64274	7.75391	7.75391	7.75417
30	10.02916	10.04113	10.75963	10.76116	10.76127
40	12.49789	12.50649	13.44270	13.44515	13.44626
50	14.78469	14.79839	15.88006	15.88018	15.88362
60	16.94306	16.95352	18.13569	18.138453	18.13888
70	18.98062	18.99105	20.25835	20.25921	20.25991
80	20.92444	20.93327	22.29379	22.30235	20.29985
Ultimate load at node 7	90.0	90.0	80.0	80.0	80.0
Final time (sec)	7.737	3.732	2.302	2.153	6.882

Table 10.4 Studies of example 3 with the conjugate gradient method (ND = 10)

Vertical load at node 7	ND = 0.1	ND = 1	ND = 10
	E_v	E_v	E_v
10	4.26310	4.26474	4.26509
20	7.73356	7.76507	7.75417
30	10.73923	10.77001	10.76127
40	13.40564	13.45280	13.44626
50	15.78951	15.88759	15.88362
60	18.05616	18.13456	18.13888
70	20.14055	20.25537	20.25991
80	22.20136	22.29536	22.29985
Ultimate load at node 7	81.9	81.0	80.0
Final time	62.902	9.185	6.882

Table 10.5 Studies of example 3 with CGST

significantly the execution time but improves only marginally the computed displacements. Table 10.4 shows the displacements, the ultimate load and the execution time obtained with different combinations of the conjugate gradient method, when $ND = 10$ while in Table 10.5 the same study is performed with different values of the parameter ND . The calculated displacements are different, when the method is applied with scaling or reinitialization, from those obtained with the unscaled version. These discrepancies underline the path dependency of the problem with the different paths of scaled or reinitialized and unscaled displacements leading to different equilibrium positions.

Tables 10.6 and 10.7 show the final displacements at the ultimate loading capacity of the structure for the conjugate gradient and Newton Raphson methods when different load increments are used. While in Figure 10.4 plots are shown of the load P versus the displacements at nodes 7 and 8.

10.4.2. Example 4 : Three Dimensional Counterstressed Dual Cable Structure

This example was also modified for studying its ultimate carrying capacity. The main cables were assumed to be structural strands with a cross-sectional area of 0.614 sq. in., and the vertical ties were structural ropes with a cross-sectional area of 0.479 sq. in. The material properties for the cables and ties are listed in Table 10.1. The following vertical loads were applied to the structure : P at joint 5, $0.875P$ at joint 9,

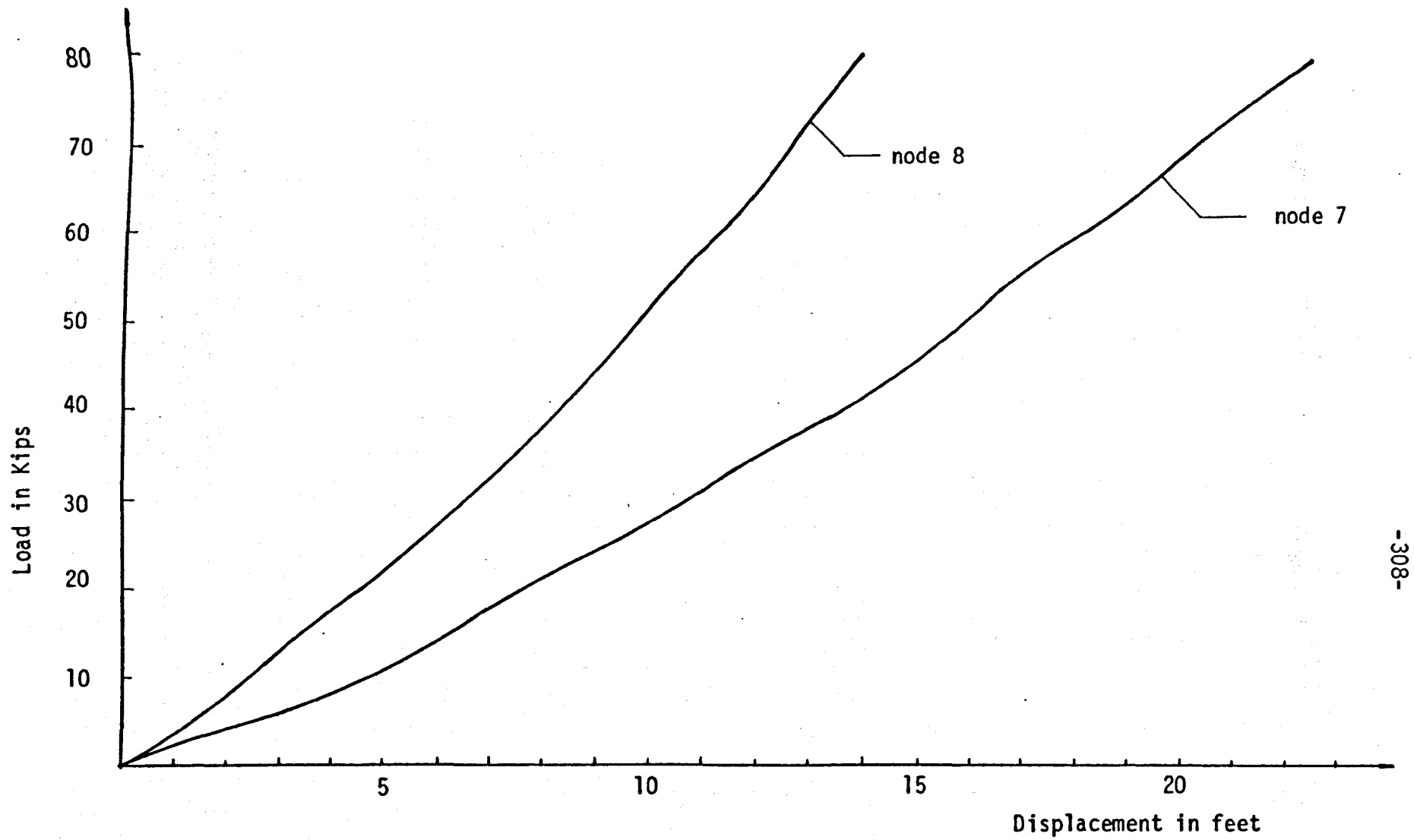


Fig. 10.4 Load-displacement curves for example 3

Node	ND = 10			ND = 1.0			ND = 0.1		
	x(ft)	y(ft)	z(ft)	x(ft)	y(ft)	z(ft)	x(ft)	y(ft)	z(ft)
1	0.00000	-0.42306	3.62564	0.00000	-0.43372	3.69734	0.00000	-0.43088	3.67836
2	-0.26768	-0.02745	6.67736	-0.27118	-0.02190	6.80378	-0.26830	-0.02334	6.76968
3	0.00000	-0.57817	10.51443	0.00000	-0.58667	10.72100	0.00000	-0.58457	10.66486
5	-0.04441	0.13751	6.63159	-0.04661	0.14394	6.73472	-0.05054	0.14219	6.70696
6	-0.01066	0.19733	13.67535	-0.025838	0.20841	13.88799	-0.03775	0.20525	13.82913
7	0.00000	0.36035	22.28860	0.00000	0.37823	22.65543	0.00000	0.37348	22.55793
10	-0.04982	0.00027	3.39802	-0.04824	0.00028	3.45310	-0.04884	0.00028	3.43914
11	-0.23653	0.04338	8.12140	-0.23834	0.04477	8.25662	-0.23797	0.04436	8.22117
12	-0.26126	0.16911	12.61955	-0.26560	0.17434	12.84025	-0.26454	0.17267	12.78121
13	0.00000	0.81501	15.47902	0.00000	0.83642	15.76132	0.00000	0.83088	15.68519
17	-0.32554	-0.00352	5.33017	-0.33140	-0.05718	5.42406	-0.32931	-0.00514	5.39920
18	-0.31356	0.18438	9.38308	-0.32048	0.18696	9.55689	-0.31823	0.18612	9.51015
19	0.00000	0.78303	11.14103	0.00000	0.80122	11.35238	0.00000	0.79651	11.29530
22	-0.21783	0.15366	4.91892	-0.22394	0.15553	5.01221	-0.22224	0.15496	4.98706
23	0.00000	0.63518	6.87346	0.00000	0.64979	7.00483	0.00000	0.64600	6.96955
25	0.00000	0.36210	2.88360	0.00000	0.37098	2.93664	0.00000	0.36867	2.92299

Table 10.6 Final displacements of example 3 with NTRAJE

Node	ND = 10			ND = 1			ND = 0.1 (NTRAJE)		
	x(ft)	y(ft)	z(ft)	x(ft)	y(ft)	z(ft)	x(ft)	y(ft)	z(ft)
1	0.00000	-0.48421	4.01692	0.00000	-0.43133	3.66425	0.00000	-0.43088	3.67836
2	-0.27241	0.06767	7.37222	-0.26264	-0.02412	6.75178	-0.26830	-0.02334	6.76968
3	0.00000	-0.63004	11.65692	0.00000	-0.58556	10.64857	0.00000	-0.58457	10.66486
5	-0.05566	0.17307	7.16803	-0.05417	0.14119	6.69154	-0.05054	0.14219	6.70696
6	-0.07869	0.25771	14.80210	-0.05263	0.20118	13.78314	-0.03775	0.20525	13.82913
7	0.00000	0.43780	24.28967	0.00000	0.36167	22.50597	0.00000	0.37348	22.55793
10	-0.03599	0.00034	3.67330	-0.04877	0.00026	3.43382	-0.04884	0.00028	3.43914
11	-0.23942	0.05109	8.82245	-0.23575	0.04364	8.20474	-0.23797	0.04436	8.29117
12	-0.28082	0.19785	13.78716	-0.26205	0.16849	12.75460	-0.26454	0.17267	12.78121
13	0.00000	0.90651	16.98877	0.00000	0.81742	15.64655	0.00000	0.83088	15.68519
17	-0.34296	-0.01492	5.81684	-0.324321	-0.00510	5.38971	-0.32931	-0.00514	5.39920
18	-0.34209	0.19920	10.29730	-0.31413	0.18341	9.48691	-0.31823	0.18612	9.51015
19	0.00000	0.85990	12.26146	0.00000	0.78444	11.26977	0.00000	0.79651	11.29530
22	-0.25014	0.16362	5.41355	-0.22056	0.15396	4.97545	-0.22224	0.15496	4.98706
23	0.00000	0.69848	7.56273	0.00000	0.63672	6.95071	0.00000	0.64600	6.96955
25	0.00000	0.40157	3.14885	0.00000	0.36312	2.91223	0.00000	0.36867	2.92299

Table 10.7 Final displacements of example 3 with CGST-SC

0.750P at joint 17, 0.625P at joint 11, 0.500P at joint 3,
0.375P at joint 7, 0.250P at joint 15, 0.125P at joint 13.

Table 10.8 shows the vertical displacements and the ultimate load at node 5 for different combinations of the stiffness method. Table 10.9 gives the required execution time, before a ruptured member appears, for different combinations of the parameters and Newton Raphson methods. Once again the use of constant values for the modulus of elasticity throughout each load increment overestimated the ultimate carrying capacity of the structure.

Tables 10.10 and 10.11 give the vertical displacements and the ultimate load at node 5, as well as the total execution time for different combinations of the conjugate gradient method. Tables 10.12 and 10.13 show the final displacement at selected nodal points for the conjugate gradient and Newton Raphson methods at the ultimate carrying capacity of the structure. One can see how different can be the final values of the displacements for different values of the load increments.

In Tables 10.14 and 10.15 are presented the loading histories of the members that have gone slack during the application of the loading, given respectively by the Newton Raphson and conjugate gradient methods. In both cases the member that first ruptured was 5-23. The conjugate gradient method predicted slightly better the correct performance of the members when the load P was increased 1 kip at a time.

Vertical Load at node 5	ND = 0.1		ND = 1.0		ND = 10
	E_c	E_v	E_c	E_v	E_v
10	2.41252	2.41472	2.39098	2.43682	2.59929
20	5.60118	5.62262	5.54152	5.65589	5.20629
30	8.98219	9.02511	8.85622	9.03039	9.18704
40	12.36196	12.40020	12.15370	12.43782	12.56704
50	15.96439	15.99864	15.60599	16.03201	16.1351
60	19.90857	19.94751	19.30661	21.02599	20.0377
Ultimate Load at node 5	64.1	63.9	70.0	64.0	60.0

(e = 0.1E-01)

Table 10.8 Vertical displacements, in feet, at joint 5, of example 4 (stiffness method)

NTRA	NTRAJE	NTRA	NTRAJE	NTRA	NTRAJE	NTRAJE	NTRAJE
e=0.1E-04	e=0.1E-04	e=0.1E-01	e=0.1E-01	e=0.1E-01	e=0.1E-04	e=0.1E-01	e=0.1E-01
$E_v, ND=10$	$E_v, ND=10$	$E_v, ND=1$	$E_c, ND=1$	$E_c, ND=1$	$E_v, ND=1$	$E_c, ND=0.1$	$E_v, ND=0.1$
45.326	24.289	32.246	9.010	18.895	88.685	50.295	57.797

Table 10.9 Final execution time in seconds for example 4

Vertical load at node 5	CGST-SC	CGST-SC-R1	CGST-SC-R3	CGST-SC-R20
	$e = 0.1E-01$	$e = 0.1E-01$	$e = 0.1E-01$	$e = 0.1E-04$
	$E_v, NDIV = 10$	$E_v, NDIV = 10$	$E_v, NDIV = 10$	$E_v, NDIV = 10$
10	2.59444	2.58805	2.58881	2.59929
20	5.19120	5.19236	5.20513	5.20629
30	9.18493	9.19781	9.21069	9.18700
40	12.56039	12.54247	12.55356	12.56698
50	16.16411	16.15798	16.10670	16.13505
60	20.00019	20.03265	20.15185	20.03777
Ultimate load at nodes	60.0	60.0	60.0	60.0
Total time	18.352	8.341	8.100	23.289

Table 10.10 Studies of example 4 with the conjugate gradient method

Vertical load at node 5	CGST-R20	CGST-R1	CGST-SC-	CGST-SC	CGST-SC-R3	CGST-SC-R20
	$e = 0.1E-04$	$e = 0.1E-03$	$e = 0.1E-01$	$e = 0.1E-01$	$e = 0.1E-01$	$e = 0.1E-01$
	$E_c, NDIV = 100$	$E_c, NDIV = 100$	$E_c, NDIV = 100$	$E_v, NDIV = 100$	$E_v, NDIV = 100$	$E_v, NDIV = 100$
10	2.39074	2.39073	2.38709	2.43875	2.42996	2.42996
20	5.53920	5.53932	5.54673	5.67127	5.66641	5.66641
30	8.85385	8.85385	8.84670	9.07256	9.07034	9.07034
40	12.14833	12.14826	12.12706	12.43622	12.45783	12.45783
50	15.60010	15.60255	15.59573	16.06023	16.00423	16.00423
60	19.30125	19.30205	19.25522	20.12381	20.06815	20.06815
Ultimate load at node 5	70.0	70.0	70.0	63.0	63.0	63.0
Total time	68.880	67.365	28.924	49.885	37.381	36.993

Table 10.11 Studies of example 4 with the conjugate gradient method

Node number	ND = 10			ND = 1			ND = 0.1 (NTRAJE)		
	x(ft)	y(ft)	z(ft)	x(ft)	y(ft)	z(ft)	x(ft)	y(ft)	z(ft)
1	-0.12523	-0.70147	12.98974	0.14499	-0.82658	10.96289	0.17286	-0.83462	11.16048
2	0.00150	0.00263	9.94333	0.00486	0.00498	9.52403	0.04997	0.04459	9.70974
3	-1.15214	-0.35194	14.28172	-0.83871	-0.42002	12.32271	-0.83831	-0.41661	12.46288
4	0.16457	0.00185	7.41783	0.16782	0.00418	7.27157	0.16743	0.00223	7.35455
5	0.44985	-0.34744	24.75501	0.94314	-0.40682	21.43947	1.06463	-0.41086	21.53689
6	-0.16294	0.00214	7.41845	-0.16234	0.003286	7.23879	-0.16289	-0.01538	7.66064
7	-0.58849	0.22985	11.72856	-0.35019	0.05853	9.96671	-0.36766	0.03515	10.11346
8	0.11765	-0.11346	7.41738	0.11655	-0.11655	7.25975	0.11913	-0.11439	7.35455
13	0.07230	-0.19202	6.85170	0.17949	-0.25338	5.82834	0.21278	-0.26697	5.97339
14	-0.10438	-0.12580	6.84569	-0.07320	-0.14791	5.82013	-0.07244	-0.15228	5.96360
15	-0.06632	0.07439	8.67995	0.07181	-0.03247	7.64370	0.08598	-0.02649	7.80458
16	0.01383	-0.16349	8.67028	0.00256	-0.16245	7.24261	0.00250	-0.16270	7.35455

Table 10.12 Final displacements at selected nodal points of example 4 with CGST-SC

Node number	ND = 10			ND = 1			ND = 0.1		
	x(ft)	y(ft)	z(ft)	x(ft)	y(ft)	z(ft)	x(ft)	y(ft)	z(ft)
1	0.27359	-0.86781	10.0700	0.19985	-0.85125	11.01545	0.17286	-0.83462	11.16048
2	0.00821	0.00607	9.83813	0.00496	0.00427	9.62922	0.04997	0.04459	9.70974
3	-0.69630	-0.42909	11.44717	-0.81036	-0.42046	12.31465	-0.83831	-0.41661	12.46288
4	0.16799	0.00031	7.41189	0.16728	0.00214	7.31420	0.16743	0.00223	7.35455
5	1.23035	-0.42756	19.98091	1.09900	-0.41994	21.37359	1.06463	-0.41086	21.53689
6	0.15948	0.00304	7.41889	-0.16220	0.00214	7.31420	-0.16289	-0.01538	7.66064
7	-0.26702	-0.02783	9.20658	-0.34611	0.02315	9.98363	-0.36766	0.03515	10.11346
8	0.12009	-0.11293	7.41889	0.11903	-0.11440	7.31420	0.11913	-0.11439	7.35455
13	0.26052	-0.26222	5.62411	0.22462	-0.27030	5.90625	0.21278	-0.26697	5.97339
14	-0.05712	-0.16526	5.61385	-0.06991	-0.15367	5.89609	-0.07244	-0.15228	5.96360
15	0.13411	-0.07449	7.13549	0.09941	-0.03733	7.69462	0.08598	-0.02649	7.80458
16	0.00927	-0.16781	7.13002	0.00249	-0.16270	7.31420	0.00250	-0.16270	7.35455

Table 10.13 Final displacements at selected nodal points of example 4 with NTRAJE

Member	Load at node 5					
	ND = 0.1		ND = 1		ND = 10	
	Slackening	Reloading	Slackening	Reloading	Slackening	Reloading
5 - 6	13.7	62.5	14.0	63.0	30.0	70.0
9 - 10	15.5	-	16.0	-	30.0	-
17 - 18	18.2	-	19.0	-	30.0	-
11 - 12	22.6	-	23.0	-	30.0	-
3 - 4	29.9	-	30.0	-	40.0	-
7 - 8	42.4	-	43.0	-	50.0	-
1 - 2	57.9	-	59.0	-	60.0	-
15 - 16	61.1	-	62.0	-	70.0	-

Table 10.14 Example 4 : Loading history of members going "slack" (NTRAJE)

Member	Load at node 5			
	ND = 1		ND = 10	
	Slackening	Reloading	Slackening	Reloading
5 - 6	14.0	62.0	30.0	70.0
9 - 10	16.0	-	30.0	-
17 - 18	18.0	-	30.0	-
11 - 12	23.0	-	30.0	-
3 - 4	30.0	-	30.0	-
7 - 8	43.0	-	50.0	-
1 - 2	57.0	-	60.0	-
15 - 16	61.0	-	70.0	-

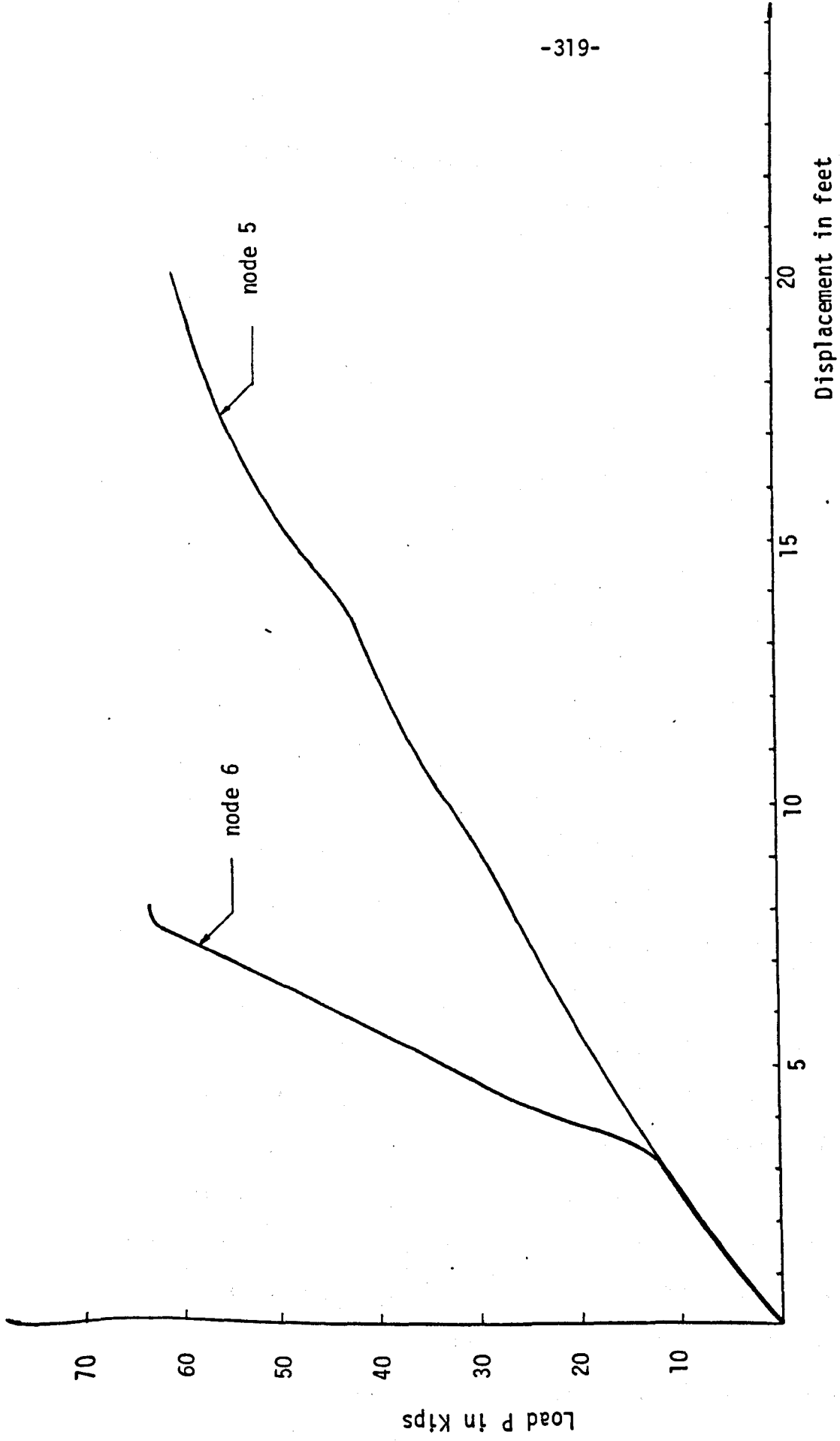
Table 10.15 Example 4 : Loading history of members going "slack" (CGST-SC)

Plots of the load P versus the vertical displacements at joints 5 and 6 are shown in Figure 10.5. The two nodal displacements have produced almost coincident graphs up to the point when member 5-6 becomes slack. From then on node 6 follows a totally different curve until, when P reaches 62.5 kips, it again reloads. It is of interest to see that both curves have the characteristics of a "softening" structure.

10.5 Conclusions

The conjugate gradient method and the Newton Raphson method can be used very efficiently to study the ultimate carrying capacity of cable structures. In both methods the loads need to be applied in increments. Different load increments, however, produce different characteristics of the structure as it deflects from its initial configuration to its ultimate load capacity, and could very easily lead to erroneous results. The problem is extremely path dependent and this was demonstrated by the fact that the conjugate gradient method with and without reinitialization gave different results. The same happened with the scaled and unscaled versions of the method.

The total computer time required for each method to predict the ultimate load is not readily comparable, since different load increments and termination parameters have a profound effect on the total execution time. The NTRAJE method, however, gave generally the fastest results. For larger load increments a more accurate behaviour was expected from the conjugate gradient



method than from the Newton Raphson method, because the stress-strain curve is followed at more frequent intervals by the conjugate gradient method. This expected increase in accuracy did not, however, occur.

By updating the slope of the stress-strain curve at each iteration, the methods gave better results than by keeping it constant inside each load increment. The use of small values for the termination parameter ϵ , for each load increment, can have a great effect on the final execution time yet give only slight improvement on the predicted displacements and the final ultimate load.

The members were checked for slackening, reloading and rupturing, throughout this study, at the end of each load increment, which rather limited an improved behaviour of the methods for greater load increments. An alternative technique could be to check the members in each iteration, or after a specified number of iterations and not necessarily after convergence at a load increment. It is thought that this second approach should suit better the iterative nature of dynamic relaxation. This is an area in which dynamic relaxation could prove to be very effective if full use were made of the controllable smooth curves for the displacements as they build up from their initial configuration to their final values. Larger load increments could perhaps be implemented with intermediate checks to predict the load increment in which the first member of the structure will rupture. Smaller load increments could then be used to predict the exact ultimate carrying capacity of the structure.

CHAPTER 11

GENERAL CONCLUSIONS AND SUGGESTIONS FOR FURTHER WORK

11.1. Conclusions

In an effort to select the best method of solution suitable for the static nonlinear analysis of cable supported structures, a number of different algorithms have been developed and compared. The methods were classified into three main categories ; (a) the conjugate gradient algorithms, (b) the relaxation methods and (c) the stiffness methods. It was shown that the conjugate gradient method, the Francel's method, the dynamic relaxation method, the Tchebycheff method and the Jacobi semi-iterative method all, in fact, belong to the same family of iterative methods named "three term recursion formulae". They use the same number of vectors, they perform the same iterative process and they differ only in the way the scalar or relaxation parameters are evaluated. In other words they approach the minimum from different paths.

It is very difficult to select in a general way the best method for the nonlinear solution of cable structures. Each method performs differently for different types of structures. When the criterion for comparison is the computer cost, then the stiffness method with Newton Raphson iterations in conjunction with Jennings's compact store elimination algorithm (NTRAJE) gave the more economical results for medium to large size problems. For very small problems the same method with the

semi-bandwidth storage scheme produced the best results. Taking into account further improvements of the method that have been reported recently, by introducing relaxation coefficients to scale down the overestimated displacements, the NTRAJE method is a very powerful technique for the solution of cable supported structures.

When, on the other hand, the criterion for comparison is the computer storage requirements, then it is obvious that all the vector methods are superior to stiffness methods. Also, some of the vector methods can combine the inherent property of requiring less storage with fast convergence to the solution giving thus a very competitive computer cost and requiring only relatively small computers.

The gradient methods have been applied in two categories ; those without linear search, the linearized methods, and those with one or two dimensional linear search. The first category has the advantage of being more straightforward while the second category of methods, with the exception of the memory gradient method (CGMEM), produced faster results. For problems with moderate nonlinearity the CGFRIN method produced competitive results, while for highly nonlinear problems the simple conjugate gradient algorithm with Newton Raphson iterations never failed to converge and reached the required accuracy in reasonable execution time. The memory gradient method, with the scalar parameter β being calculated from the minimization of the total potential energy with respect to β and not as in all other

methods from the K-orthogonality condition, produced extremely slow results in all but the small problem of the single cable. This confirms the usefulness of the method to optimization problems with a few numbers of unknowns.

The methods using one dimensional linear search, gave similar results. When the required convergence was not very strict, then Fletcher and Reeves method with Davidon's linear search (CGFR) and Buchholdt's method with a fourth order polynomial representation of the total potential energy (CGBUC) produced the quickest results. As the termination parameter becomes smaller, in other words as we begin to test the "well behaviour" of the methods, the above mentioned methods failed to reach the required accuracy whereas the methods using Stanton's bracketing technique converged to the required accuracy. In particular, the CGST method with the regula-falsi bisection algorithm to approximate the minimum in the bracketed interval, gave the more consistent and accurate results.

The relaxation methods, also, have been applied in two categories ; those using the principle of dynamic relaxation and the successive overrelaxation methods. The successive overrelaxation method , although for linear problems with tri-diagonal matrices having a convergence rate twice as fast as dynamic relaxation, produced much slower convergence than the dynamic relaxation when applied to nonlinear problems. The automatic adjustment of the relaxation parameter ω based on Carre's algorithm (SORESC) produced faster and more consistent

results than Hageman's algorithm (SORESH) and in all cases both methods gave better results than the SORES method with the optimum parameter being constant through the iteration process.

The dynamic relaxation method has been applied in three different forms. The method using an "a priori" evaluation of the iteration parameters gave very competitive results for problems with moderate nonlinearity. As the problem became more and more nonlinear the need to adjust the iteration parameters became obvious when the method failed to reach the equilibrium position and diverged. The time required for the evaluation of the maximum and minimum eigenvalues of the stiffness matrix was reduced to an average of 10% of the total execution time.

The principle of kinetic damping gave very satisfactory results for most of the problems investigated in this work. The method has the advantage of requiring only the determination of the maximum eigenvalue of the current stiffness matrix and an approximation to this value can be very easily obtained from the Gershgorin bound theorem. The combination of the conjugate gradient algorithm and the dynamic relaxation method (CGTCH) gave unsatisfactory results. It is believed, however, that in problems with ill-conditioned matrices, such as cable supported structures with flexible boundaries, the method could produce better convergence when the transformation from the ill-conditioned system to a system less ill-conditioned will be justified.

The automatic adjustment technique (DRAUT) for the relaxation parameters produced the best results of all the relaxation methods. For the particular case of the hyperbolic paraboloid of example 3 the method reached the required accuracy in almost the same execution time as the NTRAJE method. In all other cases, the DRAUT method gave similar results to the DRKV and CGST methods. From the two divergence criteria used in DRAUT and DRK methods, the one with the velocity-difference criterion produced the more consistent and reliable results.

The diagonal matrix scaling technique gave in all cases better results than the unscaled methods. Only for the single cable of example 1 did the initial scaling technique give inferior results to the unscaled version. This is because the changes involved in the stiffness matrix as the structure deforms towards its final equilibrium state are too big, making the scaling effects negligible. An updated process for the diagonal coefficient of the stiffness matrix every so often will, however, improve the convergence. The scaling effect was more powerful when applied to the conjugate gradient methods than to the relaxation methods. This fact indicates that the conjugate gradient methods are more sensitive to ill-conditioned problem than the dynamic relaxation methods. Reinitializations applied to the conjugate gradient methods always improved the convergence, and in particular this technique had greater influence on the unscaled versions of the methods.

The problem of evaluating the extreme eigenvalues of the stiffness matrix was investigated by comparing the efficiencies

of a number of iterative methods. The power method is the simplest to use and gave very satisfactory results for the maximum eigenvalue. The evaluation of the minimum eigenvalue needs a more careful approach and could lead to erroneous results. The coordinate relaxation method was, in all cases, inferior to the conjugate gradient type of methods. The modifications proposed by Fried for evaluating the scalar parameter β in the same way as in the memory gradient method did not produce fast enough results. The same happened when the Bradbury and Fletcher orthogonalization process was applied to eliminate the dependence of the convergence of the method on the initial estimate of the final eigenvector. The best results, however, were obtained using the simple conjugate gradient algorithm with the scalar α being evaluated from the minimization of the Rayleigh quotient with respect to α , and the scalar β from the A-orthogonality condition. The method also remained unaffected by the choice of the initial estimate for the final eigenvector.

Path dependent problems created by the slackening of the members, and by nonlinear stress-strain relationships were studied. For the particular problems of example 4 considered in this work, when only slackening of members is allowed to occur, the stiffness methods with Newton Raphson iterations gave the correct results with only one increment of the applied load. However, there is always the danger when applying the NTRAJE method of jumping into another configuration and producing erroneous results. The same could happen with the conjugate gradient method since there is no way to control the

interim displacement states until the final equilibrium position is achieved. Only the dynamic relaxation method with automatic adjustment of the relaxation parameters can safeguard convergence by a proper control of the iteration parameters to ensure always that the method is overdamped and thus never exceeding the final equilibrium position in the course of the iterations. By using incremental load analysis this inefficiency of the two above mentioned methods can be overcome, but at the cost of increased execution time.

In problems with nonlinear stress-strain relationships the NTRAJE method gave the fastest results. The improvement in convergence by the use of the conjugate gradient method was negligible and the method required the same load increments as the stiffness method with Newton Raphson iterations. It is believed, however, that dynamic relaxation with controllable iteration parameters could reach the required solution using higher load increments in less computer time. All the checks for loading, reloading and slackening of the members can be performed after a number of iterations and not necessarily at the end of a load increment, allowing a greater flexibility in the selection of the optimum load increment. It is in this area of path dependent problems that the method could be extremely effective.

11.2. Suggestions for future work

The most obvious extension to this work would be to

apply the dynamic relaxation method with automatic adjustment of the relaxation parameters to the ultimate load analysis of cable supported structures. This is an area of path dependent problems where the inherent properties of dynamic relaxation can be utilized, allowing for greater load increments to be handled with a consequent reduction in the required computer time. A more generalised ultimate load analysis, with the inclusion of buckling of struts would also be an interesting subject for investigation.

A comparison of the efficiencies of various methods of analysis for cable structures supported by flexible boundaries would be another useful subject for investigation. It is believed that the conjugate gradient methods would be affected more seriously by the high condition number. The zig-zag behaviour involved in the p directions could make the conjugate gradient methods inferior to the dynamic relaxation method. Also of interest would be the response of the conjugate gradient-Tchebycheff method to this type of structure. The application of another type of combined method, the symmetric overrelaxation-Tchebycheff method, could also produce good convergence characteristics in this area with ill-conditioned matrices.

The use of block operations in the gradient and relaxation methods can further improve the convergence of the methods. The extension of the comparison to a greater number of stiffness methods could also be of interest.

The inclusion of more elaborate matrix storage techniques and linear solution procedures is an aspect to be investigated. The effect of backing storage techniques and more sophisticated nonlinear solution methods on the total execution time and computer cost is another area worthy of study.

Perhaps of greatest relevance would be a study of the methods examined in this work when applied to the problems of form-finding of prestressed configurations and the optimization of cable systems. Time dependent loading and the possible effects of flutter are also problems of particular importance in the design of light-weight long span cable systems.

REFERENCES

1. Abadie, J., "Integer and nonlinear programming", North-Holland Publishing Company, 1970.
2. Aizawa, M.; Tanaka, S. and Tsubota, H., "Theoretical analysis of pretensioned cable structures", 2nd Int. Conf. on Space Structures, Guildford, England, September 1975.
3. Allen, D. N., "Relaxations methods in engineering and science", McGraw Hill Book Company Inc., 1954.
4. Almroth, B. O. and Brogan, F. A., "Automated choice of procedures in computerised structural analysis", Computers and Structures, Vol. 7, 1977, pp 335-342.
5. Argyris, J. H., "Recent advances in matrix methods of structural analysis", The Mac.Millan Company New York, 1965.
6. Argyris, J. H., "Recent advances in matrix methods of structural analysis", "Progress in aeronautical sciences", Pergamon Press New York, 1964, edited by D. Kucheman and L. H. G. Sterne.
7. Argyris, J. H. and Scharpf, D. W., "Large deflection analysis of prestressed networks", J. of Struct. Div., ASCE, ST3, March 1972, pp 633-654.
8. Asplund, S. O., "Force-method analysis of orthogonal cable nets", Int. Symp. on Wide Span Surface Structures, Stuttgart, 1976.
9. Avent, R., "Nonlinear field analysis of structural nets", J. of Struct. Div., ASCE, paper No. 6556, Vol. 95, ST5, May 1969, pp 889-907.
10. Bandel, H. K., "Das orthogonale seilnetz hyperbolisch-parabolischer form unter verticalen lastzustanden und temperaturanderung", Der Baningenieur, Berlin, West Germany, Vol. 34, 1959.
11. Bandel, H. K., "Das hangende seil unter raumlicher belastung und temperaturanderung", Der Baningernieur, Berlin, West Germany, Vol. 37, 1962, pp 145-146.

12. Barnes, M. R., "Pretensioned cable networks", Conrad, Vol. 3, No. 3, April 1971.
13. Barnes, M. R., "Dynamic relaxation analysis of tension networks", Int. Conf. on Tension Structures, London, April 1974.
14. Barnes, M. R., "Applications of dynamic relaxation to the design and analysis of cable, membrane and pneumatic structures", 2nd Int. Conf. on Space Structures, Guildford, England, September 1975.
15. Barnes, M. R., "Explicit dynamic analysis and model correlation of tension structures", Int. Symp. on Wide Span Surface Structures, Stuttgart, April 1976.
16. Barnes, M. R., "Interactive graphical design on tension surface structures", Int. Symp. on Wide Span Surface Structures, Stuttgart, April 1976.
17. Barnes, M. R.; Topping, B. H. V.; Wakefield, D. S., "Aspects of form-finding using dynamic relaxation", Int. Conf. on Slender Structures, London, September 1977.
18. Barnes, M. R., "Form-finding and analysis of tension space structures by dynamic relaxation", Ph.D. Thesis, The City University, London, October 1977.
19. Baron, F. and Venkatesan, M. S., "Nonlinear analysis of cable and truss structures", J. of Struct. Div., ASCE, paper No. 7937, February 1971, pp 679-709.
20. Basu, A. K. and Dawson, J. M., "Orthotropic sandwich plates", Proc. Inst. Civ. Engrs., 1970, pp 87-115.
21. Discussion on the above paper, Proc. Inst. Civ. Engrs., 1971, pp 49-55.
22. Bauer, F. L., "Optimally scaled matrices", Numerische Mathematik, Vol. 5, 1963, pp 73-78.
23. Bechman, F. S., "The solution of linear equations by the conjugate gradients", "Mathematical methods for digital computers", edited by A. Ralston and H. S. Wilf, John Wiley and Sons, New York 1960.

24. Bhupinder, P. S. and Bhusham L. D., "Membrane analogy for anisotropic cable networks", J. of Struct. Div., ASCE, ST5, paper No. 10544, May 1974, pp 1053-1066.
25. Bender, C. F. and Shavitt, I., "An iterative procedure for the calculation of the lowest real eigenvalue and eigenvector of a nonsymmetric matrix", J. Computational Physics, Vol. 6, 1970, pp 146-149.
26. Bergan, P. G. and Clough, R. W., "Convergence criteria for iterative processes", AIAA, Vol. 10, No. 8, August 1972, pp 1107-1108.
27. Bergan, P. G. and Soreide, T., "A comparative study of different numerical solution techniques as applied to nonlinear structural problem", Comp. Meth. in Appl. Mech. and Engng. Vol. 2, 1973.
28. Bogner, F. K.; Mallet, R. H.; Minich, M. D. and Smith, L. A., "Development and evaluation of energy search methods of non-linear structural analysis", AFFDL-TR-65-113, Air Force Flight Dynamics Lab., Wright-Patterson Air Force Base, Ohio, October 1965.
29. Bogner, F. K., "Analysis of tension structures", Proc. of the Second Conf. on Matrix Methods in Struct. Mech., AFFDL-TR-68-150, pp 1253-1270.
30. Booth, A. D., "An application of the method of steepest descent to the solution of nonlinear simultaneous equations", Quarterly Journal of Mechanics and Applied Mathematics, Vol. 2, 1949, pp 460-468.
31. Box, G. E. P. and Wilson, K. B., "On the experimental attainment of optimum condition", J. of Royal Statistical Soc., Vol. 13, 1951, pp 1-45.
32. Box, G. E. P.; Davies, D. and Swann, W. H., "Non-linear optimization techniques", Monograph, No. 5, Imperial Chemical Industries Ltd., 1969.
33. Bracken, J. and McCormick, G. P., "Selected applications of nonlinear programming", John Wiley & Sons, Inc., 1968.
34. Bradbury, W. W. and Fletcher, R., "New iterative methods for solution of the eigenproblem", Numerische Mathematik, Vol. 9, 1966, pp 259-267.

35. Braga, F. and Care, A., "Study on cable networks subject to loads however distributed", Int. Conf. on Tension Structures, London, April 1974.
36. Breddia, C. and Connor, J., "Geometrically nonlinear finite element analysis", J. of Struct. Div., ASCE, paper No. 6516, April 1969, pp 463-483.
37. Brew, J. S., "The application of dynamic relaxation to the solution of nonlinear structural plane frames", MSc. thesis, Univ. of Manchester 1968.
38. Brew, J. S. and Brotton, D. M. "Nonlinear structural analysis by dynamic relaxation", Int. J. for Num. Methods in Engng., Vol. 3, 1971, pp 463-483.
39. Brooks, S. H., "A discussion of random methods for seeking maxima ", Operation Research, Vol. 6, 1958, pp 244-251.
40. Brooks, D. F. and Brotton, D. M., "Formulation of a general space frame program for a large computer", The Structural Engineer, Vol. 44, November 1966, pp 381-396.
41. Brooks, D. F. and Brotton, D. M., "Computer systems for analysis of large frameworks", J. of Struct. Div., ASCE, December 1967, pp 1-23.
42. Bubner, E., "Net structures - a survey", Int. Conf. on Tension Structures, London, April 1974.
43. Budianski, B., "Remarks on theories of solid and structural mechanics", Harvard Univ., Cambridge, Mass., 1967.
44. Buchanan, G. R. and Akin, J. E., "The deflection analysis of structural nets using the reflection method", Int. Conf. on Space Structures, Guildford, England, 1966.
45. Buchanan, G. R., "Two-dimensional cable analysis", J. of Struct. Div., ASCE, paper No. 7436, ST7, July 1970, pp 1581-1587.
46. Buchholdt, H. A., "The behaviour of small prestressed cable roofs subjected to uniformly distributed loading", Int. Conf. on Space Structures, Guildford, England, 1966.

47. Buchholdt, H. A., "Deformation of prestressed cable nets", Acta Polytechnica Scandinavica Tronheim, Norway, No. ci 38, 1966, pp 3-17.
48. Buchholdt, H. A.; Davies, M. and Hussey, M. J. L., "The analysis of cable nets", J. Inst. Maths. Appls. Vol. 4, 1968, pp 339-358.
49. Buchholdt, H. A., "The configuration of prestressed cable nets", Acta Polytechnica Scandinavica, ci 54, Norges Tekiske Videnskaps Academi Trondheim 1968.
50. Buchholdt, H. A., "A non-linear deformation theory applied to two dimensional pretensioned cable assemblies", Proc. Inst. Civil Engrs., Vol. 42, 1969, pp 124-141.
51. Discussion on the above paper, Proc. Inst. Civil Engrs., Vol. 43, 1969, pp 665-673.
52. Buchholdt, H. A. and Reeves, D. J. E., "Cable structures", Conf. on Steel in Architecture, London, November 1969.
53. Buchholdt, H. A., "Pretensioned cable girders", Proc. Inst. Civil Engrs., paper No. 7198, Vol. 45, March 1970, pp 453-469.
54. Buchholdt, H. A., "Tension structures", J. Inst. Struct. Eng., February 1970.
55. Buchholdt, H. A., "The Newton-Raphson approach to skeleton assemblies having significant displacements", Acta Polytechnica Scandinavica, ci 72, 1971.
56. Buchholdt, H. A. and McMillan, B. R., "Iterative methods for the solution of pretensioned cable structures and pin-jointed assemblies having significant geometrical displacements", IASS Symp. on Tension Structures and Space frames, Tokyo and Kyoto 1971.
57. Buchholdt, H. A. and McMillan, B. R. "A nonlinear vector-method for the analysis of vertically and laterally loaded cables and cable assemblies", Proc. Inst. Civil Engrs., Vol. 55, paper No. 7586, March 1973, pp 211-228.
58. Buchholdt, H. A.; Das, N. K. and Al-Hilli, A. J., "A gradient method for the analysis of cable structures with flexible boundaries", Int. Conf. on Tension Structures, London, April 1974.

59. Buchholdt, H. A. and Dixon, R., "The design and analysis of the cable roof for Odsal Sports Centre", 2nd Int. Conf. on Space Structures, Guildford, England, 1975.
60. Buchholdt, H. A., "The behaviour of circular saddle shaped nets with flexible boundaries", Int. Symp. on Wide Span Surface Structures, Stuttgart, 1976.
61. Buchholdt, H. A., "Cable roofs - dreams and realities, the Riyadh Stadium", Cable Structures Research Centre, Polytechnic of Central London, May 1977.
62. Bunce, J. W., "A note on the estimation of critical damping in DR", Int. J. for Num. Methods in Engng., Vol. 4, 1972, pp 301-304.
63. Bunce, H. W. and Brown, E. H., "The finite deflection of plane frames", Int. J. Mech. Sci., Vol. 15, 1973, pp 189-198.
64. Burley, E. and Harvey, R. C. "Behaviour of tension structures subjected to uniformly distributed cable loading", Int. Conf. on Tension Structures, London, April 1974.
65. Butler, A. A. W., "Long span cable roof structures", Proc. Inst. Civil Engrs., part 1, Vol. 52, November 1972, pp 331-353.
66. Discussion on the above paper, Proc. Inst. Civil Engrs., Vol. 54, November 1973, pp 507-524.
67. Cantrell, J., "On the relation between the memory gradient method and the Fletcher and Reeves method", J. of Opt. Theory and Applications, Vol. 4, No. 1, 1969.
68. Carre, B. A., "The determination of the optimum acceleration factor", Comp. J., Vol. 4, 1961, pp 73-78.
69. Cassell, A. C.; Kinsey, P. J. and Sefton, D. J., "Cylindrical shell analysis by dynamic relaxation", Proc. Inst. Civil Engrs., Vol. 39, January 1968.
70. Discussion on the above paper, Proc. Inst. Civil Engrs., June 1968, pp 241-250.

71. Cassell, A. C. and Hobbs, R. E., "Dynamic relaxation", Proc. IUTAM Symp. High Speed Computing in Elastic Structures, Univ. of Liege, 1970.
72. Cassell, A. C., "Shells of revolution under arbitrary loading and the use of frictitious densities in dynamic relaxation", Proc. Inst. Civil Engrs., Vol. 45, 1970, pp 65-78.
73. Cassell, A. C. and Hobbs, R. E., "Technical note - numerical stability of dynamic relaxation of nonlinear structures", Int. J. for Num. Methods in Engng., 1976, pp 1407 - 1410.
74. Cauchy, A., "Methode Generale pour la resolution des systemes d'equations simultanees", Compt. Rend., Vol. 25, 1847, pp 536-538.
75. Chaundhury, N. K.; Brotton, D. M. and Merchant, W., "A numerical method for dynamic analysis of structural frame frameworks", Int. J. Mech. Sci., Vol. 8, 1966, pp 149-162.
76. Cohen, A., "Rate of convergence of several conjugate gradient algorithms", SIAM Num. Anal., Vol. 9, No. 2, June 1972, pp 248-259.
77. Collatz, L., "Eigwertanfgaben mit technisheu Anwendungen", 2nd edition, Leipzig, 1963.
78. Conrad, V. and Wallach, Y., "A faster SSOR Algorithm", Num. Math., Vol. 27, 1977, pp 371-372.
79. Cundall, P. A., "The measurement and analysis of accelerations in rock slopes", PhD. thesis, University of London, 1971.
80. Cundall, P. A., "Explicit finite difference methods in geomechanics", Proc. E. F. Conf. Num. Methods in Geomechanics, Blacksburg, Va., June 1976.
81. Curtis, A. R. and Reid, J. K., "The solution of large sparse unsymmetric systems of linear equations", Information Processing 71 - North Holland Publishing Company 1972, pp 1240-1245.
82. Daniel, J. W., "The CG method for linear and nonlinear operator equations", Soc. for Ind. and Appl. Math. J. of Num. Anal., Vol. 4, 1967, pp 10-26.

83. Daniel, J. W., "The conjugate gradient method for linear and nonlinear operator equations", SIAM J. Num. Anal., Vol. 4, 1967, pp 10-26.
84. Daniel, J. W., "Convergence of the conjugate gradient method with computational convenient modifications", Numerical Mathematics, Vol. 10, 1967, pp 125-131.
85. Daniel, J. W., "The approximate minimization of functionals", Prentice-Hall Inc. 1971.
86. Davidon, W. C., "Variable metric method for minimization", Research and Development Report ANL-5990 (Rev.), U.S. Atomic Energy Commission, Argonne National Laboratories, 1959.
87. Davidson, I., "The analysis of cracked structures", Transactions of the 3rd Int. Conf. on Struct. Mech. and in Reactor Technology, Vol. 3, part H, 1975.
88. Day, A. S., "An introduction to dynamic relaxation", The Engineer 1965, pp 218-221.
89. Day, A. S., "Analysis of plates by dynamic relaxation with special reference to boundary conditions", Symp. on Use of Electronic Digital Computers in Struct. Eng., Univ. of Newcastle, July 1966.
90. Day, A. S. and Bunce, J. W., "The analysis of hanging roofs", The Arup Journal, September 1969.
91. Day, A. S. and Bunce, J. W., "Analysis of cable networks", Civil Enging.and Public Works Review, April 1970, pp 363-386.
92. Dean, D. L. and Ugarte, C. P., "Analysis of structural nets", Pubs. Int. Assoc. Bridge Struct. Enging., Vol. 23, 1963, pp 71-89.
93. De Donato, O. and Franchi, A., "A modified gradient method for finite element elastoplastic analysis by quadratic programming", Computer Methods in Appl. Mech. and Enging., Vol. 2, 1973, pp 107-131.

94. Engeli, M.; Ginsburg, T.; Rutishauser, H. and Stiefel, E., "Refined iterative methods for computation of the solution and the eigenvalues of self-adjoint boundary value problems", Birkhauser Verlag, Basel/Stuttgart, 1959.
95. Epstein, M. and Tene, Y., "Nonlinear analysis of pin-jointed space trusses", J. of Struct. Div., ASCE, paper No. 8357, ST9, September 1971, pp 289-302.
96. Eras, G. and Elze, H., "Zur berechnung und statish vorteilhaften formgebung von seilnetzwerken", Hanging Roofs, North Holland Publishing Company, Amsterdam, 1963.
97. Esquillan, N. and Saillard, Y., "Hanging roofs", Proc. of the IASS Collog. on Hanging Roofs, Continuous Mettalic Shell Roofs and Superficial Lattice Roofs, Paris, 9 - 11 July , 1962.
98. Evans, D. J., "The use of preconditioning in iterative methods for solving linear equations with symmetric positive definite matrices", J. Inst. Maths. Applics., Vol. 4, 1967, pp 295-314.
99. Evans, D. J., "The analysis and application of sparse matrix algorithms in the finite element method", "The mathematics of finite elements and applications", edited by J. R. Whiteman, 1973, pp 427-447.
100. Evans, D. J., "Software for numerical mathematics", Academic Press 1974.
101. Faddeev, D. K. and Faddeeva, V. N., "Computational methods of linear algebra", W. H. Freeman and Co., 1963.
102. Feder, D. P., "Automatic lens design methods", J. of the American Optical Society, Vol. 47, No. 10, 1957.
103. Fiacco, V. A. and McCormick, G. P., "Nonlinear programming: Sequential unconstrained minimization techniques", John Wiley and Sons Inc., New York, k968.
104. Finkel, R. W., "The method of resultant descents for the minimization of an arbitrary function", paper No. 71, presented at the 14th National Meeting of the Association of Computing Machinery, 1959.

105. Fix, G. J. and Larsen, K., "On the convergence of SOR iterations for finite element approximations to elliptic boundary value problems", SIAM J. Num. Anal., Vol. 8, No. 3, September 1971, pp 536-547.
106. Flanders, D. A. and Shortley, G., "Numerical determination of fundamental modes", J. Appl. Physics, Vol. 21, 1950, pp 1326-1332.
107. Fletcher, R. and Powell, M. J. D., "A rapidly convergent descent method for minimization", The Computer Journal, Vol. 6, 1963, pp 163-168.
108. Fletcher, R. and Reeves, C. M., "Function minimization by conjugate gradients", Computer Journal, Vol. 7, 1964, pp 149-154.
109. Foster, E. P. and Beaufait, F. W., "Theoretical and experimental analysis of cable net roof system with precast panels", Int. Conf. on Tension Roof Structures, London, April 1974.
110. Foster, E. P., "Experimental and finite element analysis of cable roof structures including precast panels", PhD. thesis, Vanderbilt University, August 1974, Nashville, Tennessee.
111. Fox, L., "Introduction to numerical analysis", Oxford Univ. Press, 1965.
112. Fox, L. and Stanton, E. L., "Developments in structural analysis by direct energy minimization", AIAA Journal, Vol. 6, No. 6, June 1968, pp 1036-1042.
113. Fox, R. L. and Kapoor, M. P., "A minimization method for the solution of the eigenproblem arising in structural dynamics", Proc. 2nd Conf. on Matrix Methods on Struct. Mechanics, Wright Patterson Air Force Base, Ohio, 1968, AFFDL-TR-68-150, pp 271-301.
114. Frankel, S. P., "Convergence rates of iterative treatments of partial differential equations", Mathematical Tables and Other Aids to Computation, Vol. 4, 1950, pp 72-73.
115. Fried, I., "Move on gradient iterative methods in finite element analysis", AIAA Journal, Vol. 4, 1969, pp 739-741.

116. Fried, I., "Gradient methods for finite element eigenproblems", AIAA Journal, Vol. 4, 1969, pp 739-741.
117. Fried, I., "A gradient computational procedure for the solution of large problems arising from the finite element discretization method", Int. J. of Num. Methods in Enging., Vol. 2, 1970, pp 477-494.
118. Fried, I., "N-step conjugate gradient minimization scheme for nonquadratic functions", AIAA Journal, Vol. 9, No. 11, November 1971, pp 2286-2287.
119. Fried, I., "Condition of finite element matrices generated from nonuniform meshes", AIAA Journal, Vol. 10, No. 2, February 1972, pp 219-221.
120. Fried, I., "Optimal gradient minimization scheme for finite element eigenproblems", Journal of Sound and Vibration, Vol. 20, 1972, pp 333-342.
121. Fried, I., "Bounds on the external eigenvalues of the finite element stiffness and mass matrices and their spectral condition number", Journal of Sound and Vibration, Vol. 22, 1972, pp 407-418.
122. Gallagher, R. H. and Zienkiewicz, O. C., "Optimum structural design, theory and applications", John Wiley and Son, 1973.
123. Geradin, M., "The computational efficiency of a new minimization algorithm for eigenvalue analysis", Journal of Sound and Vibration, Vol. 19, 1971, pp 319-331.
124. Gero, J. S., "The analysis of cable networks using an iteration technique", Architectural Science Review, Vol. 10, March 1967, pp 2-5.
125. Gero, J. S.; Ding, C. D. and Cowan, H. J., "Research in space structures in the Department of Architectural Science", Univ. of Sidney, Space Structures, Blackwell Scientific Publications, Oxford 1967.
126. Gero, J. S., "The behaviour of cable network structures", 2nd Int. Conf. on Space Structures, Guildford, England, September 1975.

127. Golub, G. H. and Varga, R. A., "Chebyshev semi-iterative methods, successive overrelaxation iterative methods", Num. Mathematics, Vol. 3, 1964, pp 147-148.
128. Gragg, E. E. and Lavy, A. V., "Study on a super memory gradient method for the minimization of functions", J. of Optimization Theory and Applications, Vol. 4, No. 3, 1969.
129. Greenberg, D. P., "Inelastic analysis of suspension roof structures", J. of Struct. Div., ASCE, paper No. 7284, ST5, May 1970, pp 905-930.
130. Greenberg, D. P., "An equivalent stiffness method for suspension roof analysis", Proc. of the 9th Congress of the International Assoc. for Bridge and Structural Enging., Amsterdam 1972.
131. Hageman, L. A., "The estimation of acceleration parameters for the Chebyshev polynomial and the SOR methods", WAPD-TM-1038, June 1972.
132. Hangeman, L. A. and Porching, T. A., "Aspects on nonlinear block successive overrelaxation", SIAM J. Numerical Analysis, Vol. 12, No. 3, June 1975, pp 316-335.
133. Hangai, Y. and Kawamata, S., "Nonlinear analysis of space frames and snap-through buckling of reticulated shell structures", IASS Symp. on Tension Structures and Space Frames, Tokyo and Kyoto, 1971.
134. Haug, E. and Powell, G. H., "Analytical shape finding of cable nets", IASS Symp. on Tension Structures and Space Frames, Tokyo and Kyoto, 1971.
135. Haug, E. and Powell, G. H., Discussion of "Inelastic analysis of suspension roof structures" by D. P. Greenberg, J. of Struct. Div., ASCE, Vol. 97, No. ST4, April 1971, pp 1360-1363.
136. Hestenes, M. R. and Karush, W., "A method of gradients for the calculation of the characteristic roots and vectors of a real symmetric matrix", J. of Research of the Nat. Bureau of Standards, Vol. 47, No. 1, July 1951, pp 45-61.

137. Hestenes, M. R. and Stiefel, E., "Method of conjugate gradients for solving linear systems", J. of Research of the Nat. Bureau of Standards, B, Vol. 49, 1952, pp 409-436.
138. Hestenes, M. R., "The conjugate gradient method for solving linear systems", Proc. Symposia on Applied Mathematics, Vol. VI, Numerical Analysis, McGraw Hill, New York 1956, pp 83-102.
139. Hodgins, W. R., "On the relation between DR and semi-iterative matrix methods", Numerische Mathematik, Vol. 9, 1967, pp 446-451.
140. Holland, J. A., "DR applied to local effects", Conf. on Prestressed Concrete Vessels, I.C.E., London 1967, Group H, paper No. 51, pp 587 - 595.
141. Holm S., "Coordinate overrelaxation methods for the eigenproblem", Report UMINF-33-73, Unea University, 1973.
142. Hood, C. G., "A general stiffness method for the solution of nonlinear cable networks with arbitrary loading", Computers and Structures, Vol. 6, 1976, pp 391-396.
143. Hook, P. M., "The application of DR to non-linear structural problems", PhD. thesis, University of Birmingham, 1974.
144. Howson, W. P. and Wootton, L. R., "Some aspects of the aerodynamics and dynamics of tension-roof structures", Int. Conf. on Tension Structures, London, April 1974.
145. Irons, B. M., "A frontal solution program for the finite element analysis", Int. J. for Num. Methods in Enging., Vol. 2, 1970, pp 5-32.
146. Irons, B. M. and Hamza, M. M. A., "Comment on a note by Winifred L. Wood", Int. J. for Num. Methods in Enging., 1973, pp 430 - 431.
147. Irvine, H. M. and Sinclair, G. B., "Suspended elastic cable under the action of concentrated vertical loads", Int. J. Solids and Struct., Vol. 12, No. 4, 1976, pp 309-317.

148. Iwegbue, I. E. and Brotton, D. M., "A numerical integration method for computing the flutter speeds of suspension bridges in erection conditions", Proc. Inst. Civil Engrs., Part 2, Vol. 63, 1977, pp 785-802.
149. Jacobson, D. H. and Oksman, W., "An algorithm that minimizes homogeneous functions of N variables in N+2 iterations and rapidly minimizes general functions", Technical Report No. 618, Division of Enging. and Appl. Physics, Harvard Univ., Cambridge, Mass., October 1970.
150. Jawerth, D., "Forspand hangkonstruktion med mot varandra apande linor Byggmastaren, No. 10, 1959.
151. Jawerth, D., "Vorgespannte hangkonstruktion aus gegensinning gekrumnten seilen mit diagonalver spannung", Der Stahlbau, Berlin, West Germany, Vol. 28, No. 5, May 1959, pp 126-171.
152. Jennings, A., "The free cable", The Engineer, 214 (5579), 1962, pp 1111-1112.
153. Jennings, A., "A compact storage scheme for the solution of symmetric linear simultaneous equations", Computer Journal, Vol. 9, 1966, pp 281-285.
154. Jennings, A., "Frame analysis including change of geometry", J. of Struct. Div., ASCE, ST3, paper No. 5839, March 1968, pp 627-644.
155. Jennings, A., "A sparse matrix scheme for the computer analysis of structures", Int. J. of Comp. Math., Vol 2, 1968, pp 1 - 21.
156. Jennings, A., "Matrix computation for engineers and scientists", John Wiley and Sons, 1977.
157. Jennings, A. and Malik, G. M., "The solution of sparse linear equations by the CG method", Int. J. for Num. Methods in Enging., Vol. 12, 1978, pp 141-158.
158. Jensen, J. J., "Beregning og utforming av tan og membrankonstruksjoner", Report, Div. of Struct. Mech., The Norwegian Institute of Technology, Trondheim, January 1970, pp 1 - 23.

159. Jensen, J. J., "An investigation of the static and dynamic behaviour of suspension structures", IASS Sump. on Tension Structures and Space Frames, Tokyo and Kyoto, 1971.
160. Johnatowski, J. J. and Birnstiel, C., "Inelastic stiffened suspension space structures", J. of Struct. Div., ASCE, Vol. 96, paper No. 7364, ST6, June 1970, pp 1143-1166.
161. Johnatowski, J. J., "Tensile roof structures: An inelastic analysis", Int. Conf. on Tension Roof Structures, London, April 1970.
162. Johnson, D. and Brotton, D. M., "A finite deflection analysis for space structures", Int. Conf. on Space Structures, Univ. of Surrey, England, 1966.
163. Kahan, W., "Relaxation methods for an eigenproblem", Technical Report, CS-44, Computer Science Department Stanford University, 1966.
164. Kammerer, W. J. and Nashed, M. Z., "Convergence of the CG method", SIAM J. of Numerical Analysis, Vol. 9, No. 2, 1972.
165. Kao, R., "A comparison of Newton-Raphson methods and incremental procedures for geometrically nonlinear analysis", Computers and Structures, Vol. 4, 1974, pp 1091-1097.
166. Kar, A. K. and Okazaki, C. Y., "Convergence in highly nonlinear cable net problems", J. of Struct. Div., ASCE, paper No. 7107, ST2, February 1970, pp 321-334.
167. Kar, A. K., "An initial-value approach to the analysis of rectangular cable roof nets", Phd. thesis, The Pennsylvania State University, University Park, Pa, 1971.
168. Klynyev, V. V. and Kokonkin-Scherback, N. I., "On the minimization of the number of arithmetic operations for the solution of linear algebraic systems of equations", Technical Report CS24. Stanford Univ., Stanford Calif. 1965.
169. Krishna, P. and Sparks, S. R., "An influence coefficient method for pretensioned cable systems", Proc. Inst. Civil Engrs., Vol. 41, November 1968, pp 543 - 548.

170. Krishna, P. and Sparks, S. R., "Analysis of pretensioned cable systems", Proc. Inst. Civil Engrs., Vol. 39, January 1968, pp 103-109.
1971. Discussion on the above paper, Proc. Inst. Civil Engrs., Vol. 40, August 1968, pp 531-537.
172. Krishna, P. and Natarajan, P. R., "Analysis of doubly curved suspended cable network", Int. Association for Shell Structures, Bulletin, No. 34, June 1968.
173. Krishna, P., "Theoretical analysis of pretensioned cable networks", IASS Symp. on Tension Structures and Space Frames, Tokyo and Kyoto, 1971.
174. Krishna, P. and Argrawal, T. P., "Approximate analysis of tension structures", Int. Conf. on Tension Structures, London, 1974.
175. Kawaguchi, M. and Chin, Y., "On nonlinearity of prestressed suspension roofs", Reports of the Technical College, Hosei University, No. 17, March 1968.
176. Kawamata, S. and Magara, E., "Analysis of cable nets in mixed formulation", Recent Advances in Matrix Methods of Structural Analysis and Design, 1971.
177. Kawamata, S.; Magara, E. and Kunita, J., "Analysis of cable nets in mixed formulations", Proc. of the 1974 Int. Conf. on Finite Element Methods in Engineering, The Univ. of New South Wales, Australia, 1974.
178. Kiefer, J., "Sequential minimax search for a maximum", Proc. Amer. Math. Soc., Vol. 4, 1953.
179. Kiefer, J., "Optimum experimental designs", J. of the Royal Statistical Soc., Vol. 21, 1959, pp 272-319.
180. Lanzos, C., "Applied analysis", Prentice Hall, London, 1956, page 169.
181. Lavi, A. and Vogl, T. P., "Recent advances in optimization techniques", John Wiley and Sons, Inc., 1966.

182. Lehman, F. G., "Simultaneous equations solved by over-relaxation", Proc. 2nd, ASCE, Conf., Elect. Comp., September 1960.
183. Lowe, P. A., "Prediction of loadings causing universability of reinforced concrete and composite highway bridges", PhD. thesis, University of London, July 1969.
184. Lowe, P. A. and Flint, A. R., "Prediction of collapse loadings for composite highway bridges", Proc. Inst. Civil. Engrs., paper No. 7351, 1971, pp 645-659.
185. Lynch, R. D.; Kelsey, S. and Saxe, H. C., "The application of DR to the finite element method of structural analysis", Technical Report No. THEMIS-UND-68-1, University of Notre Dame, September 1968.
186. Malik, G. M., "Relaxation and gradient methods for solving large systems of structural equations", PhD. thesis, The Queens University Belfast, 1976.
187. Mallet, R. H., "A mathematical programming approach to nonlinear structural analysis", E.D.C. Report No. 2-65-10, Case Institute of Technology, Cleveland, Ohio, November 1965.
188. Mallett, R. H. and Berke, L., "Automated methods for large deflection and instability analysis of three dimensional truss and frame assemblies", AFFDL TR-66-102, Air Force Flight Dynamics Laboratory, Wright Patterson Air Force Base, Ohio, December 1966.
189. Mallet, R. H. and Schmit Jr, L. A., "Nonlinear structural analysis by energy search", J. of Struct. Div., ASCE, paper No. 5285, June 1967, pp 221-234.
190. Mallet, R. H. and Marcal, P. V., "Finite element analysis of nonlinear structures", J. of Struct. Div., ASCE, paper No. 6115, ST9, September 1968, pp 2081-2105.
191. Martin, H. C., "On the derivation of stiffness matrices for the analysis of large deflection and stability problems", Proc. 1st Conf. on Matrix Methods in Structural Mechanics, AFFDL-TR-66-80, 1966.
192. Melosh, J. R. and Bamford, R. M., "Efficient solution of load-deflection equations", J. of Struct. Div., ASCE, April 1969, pp 661-676.

193. Meyer, R. R., "On convergence of algorithms with restart", SIAM J. Num. Analysis, Vol. 13, No. 5, 1976, pp 696-704.
194. Meyer, R. R., "Solution of linear equations - state of the art", J. of Struct. Div., ASCE, July 1973, pp 1507-1525.
195. Meyer, R. R., "Special problems related to linear equation solvers", J. of Struct. Div., ASCE, April 1975, pp 869-870.
196. Michalos, J. and Birnstiel, C., "Movements of a cable due to changes in loading", J. of Struct. Div., ASCE, Vol. 127, Part II, 1962.
197. Miele, A. and Cantrell, J. W., "Study on a memory gradient . . method for the minimization of functions", J. of Optimization Theory and Applications, Vol. 3, No. 6, 1969, pp 459-470.
198. Mirsky, L., "An introduction to linear algebra", Oxford University Press, Oxford, 1963.
199. Mollman, H., "A study in the theory of suspension structures", Akademisk Forlag, 1965.
200. Mollman, H. and Mortensen, P. L., "The analysis of prestressed suspended roofs (cable nets)", Int. Conf. on Space Structures, Guildford, England, 1966.
201. Mollman, H., "The analysis of shallow cables", Bygningsstatistiske Meddr, Vol. 41, No. 3, 1970.
202. Mollman, H., "Analysis of plane prestressed cable structures", J. of Struct. Div., ASCE, ST10, October 1970, pp 2059-2082.
203. Mollman, H., "Analytical solutions for a cable net over a rectangular plan", IASS Symp. on Tension Structures and Space Frames, Tokyo and Kyoto, 1971.
204. Mollman, H., "Analysis of hanging roofs using the displacement method", Acts Polytechnica Scandinavica Ci 68, Copenhagen, 1971, pp 1-52.

205. Mollman, H., "Analysis of hanging roofs by means of the displacement method", Polytekisk Forlag, May 1972.
206. Mollman, H., "Analysis of prestressed cable systems supported by elastic boundary structures", Int. Conf. on Tension Structures, London, April 1974.
207. Mondkar, D. P. and Powell, G. H., "Towards optimal in core equation solving", Computers and Structures, Vol. 4, 1974, pp 531-548.
208. Morales, R. C., "Shear-volume method of solving tension in cables", J. of Struct. Div., ASCE, paper No. 5318, Vol. 94, January 1968, pp 111-118.
209. Murray, T. M., "Application of divert energy minimization to the static analysis of cable supported structures", PhD. thesis, University of Kansas, 1970.
210. Murray, T. M. and Willems, N., "Analysis of inelastic suspension structures", J. of Struct. Div., ASCE, paper No. 2792, December 1971, pp 2791-2805.
211. Nayak, G. C. and Zienkiewicz, O. C., "Note on the alpha constant stiffness method for the analysis of nonlinear problems", Int. J. of Num. Methods in Enging., Vol. 4, 1972, pp 579-582.
212. Newmark, N. M., "A method of computation for structural dynamics", J. of Mech. Div., ASCE, No. EM3, Vol. 85, 1959.
213. Ng, F. W. and Kettleborough, C. F., "Three dimensional transient thermoelastic stresses in constrained spherical fuel elements", 1st Int. Conf. on Struct. Mech. in Reactor Technology, paper D3/5, Berlin West Germany, September 1971.
214. Nisbet, R. M., "Acceleration of the convergence in Nesbet's algorithm for eigenvalues and eigenvectors of large matrices", J. Comp. Physics, Vol. 10, 1972, pp 614-619.
215. Noesgen, J., "A contribution to the loading bearing behaviour of prestressed cable net structures", Int. Conf. on Tension Structures, London, April 1974.

216. O'Brien, W. T. and Francis, A. J., "Cable movements under two dimensional loads", J. of Struct. Div., ASCE, Vol. 90, paper No. 3229, June 1964.
217. O'Brien, W. T., "General solution of suspended cable problems", J. of Struct. Div., ASCE., Vol. 43, paper No. 5085, February 1967.
218. Oden, J. T., "Finite element applications in nonlinear structural analysis", Proc. of the Conf. on Finite Element Methods, Vanderbilt University, Nashville, Tennessee, November 1969.
219. Ortega, J. M. and Rheinboldt, W. C., "Iterative solution of nonlinear equations in several variables", Academic Press, 1970.
220. Ostrowski, A. M., "Solution of equations and systems of equations", 2nd edition, Academic Press, New York, 1966.
221. Otter, J. R. H. and Day, A. S., "Tidal computations", The Engineer, January 1960.
222. Otter, J. R. H., "Computations for prestressed concrete reactor pressure vessels using dynamic relaxation", Nuclear Structural Engineer, Vol. 1, 1965, pp 61-75.
223. Otter, J. R. H.; Cassell, A. C. and Hobbs, R. E., "Dynamic relaxation", Proc. Inst. Civil Engrs., paper No. 6986, Vol. 35, December 1966, pp 633-656.
224. Discussion on the above paper, Proc. Inst. Civil Engrs., Vol. 37, August 1967, pp 723-750.
225. Otter, J. R. H., "DR compared with other iterative finite difference methods", Nuclear Eng. Design, Vol. 3, January 1966, pp 183-185.
226. Otto, F., "Tensile structures", The MIT press, 1969.
227. Otto, F., "Wide span structures in natural science, arts and technics", Int. Symp. on Wide Span Surface Structures, Stuttgart, April 1976.

228. Pearson, J. D., "On variable metric methods of minimization", Technical paper, RAC-TP-302, Research Analysis Corporation, McLean, Virginia, February 1968.
229. Peters, S., "Zur Berechnung allgemeiner flachentragwerke mit hilfe der dynamischen relaxation", Ingenieur Archiv, Vol. 49, 1972, pp 42-57.
230. Polak, E., "On primal and dual methods for solving discrete optimal control problems", 2nd Int. Conf. on Comp. Methods in Optimization Problems, San Remo, Italy, September 1968.
231. Polak, E. and Ribiere, G., "Note sur la convergence de methodes de directions conjugees", Ibid, Vol. 3, 1969, pp 35-43.
232. Poljak, B. T., "The method of CG in external problems", Z. Vychisl. Mat. i Mat. Fiz. Vol. 9, 1969, pp 35-43 (in Russian).
233. Porter Jr., D. S. and Fowler, D. W., "The analysis of nonlinear cable net systems and their supporting structures", Computers and Structures, Vol. 3, 1973, pp 1109-1123.
234. Poskitt, T., "Numerical solution of nonlinear structures", J. of Struct. Div., ASCE, paper No. 5362, August 1967, pp 69-94.
235. Discussion on the above paper, J. of Struct. Div., ASCE, June 1968, pp 1613-1627.
236. Powell, M. J. D., "An efficient method for finding the minimum of a function of several variables without calculating derivations", The Computer J., Vol. 7, 1964.
237. Pugsley, A., "The theory of suspension bridges", Edward Arnold Ltd., London 1957.
238. Pugsley, A., "A flexibility coefficient approach to suspension bridge theory", J. of the Inst. of Civil Engrs., No. 5, 1948-49, March 1949.
239. Rabinowitz, P., "Numerical methods for nonlinear algebraic equations", Gordon and Breach Science Publishers Ltd., 1970.

240. Rajasekarom, S. and Murray, D. W., "Incremental F.E. matrices", J. of Struct. Div., ASCE, paper No. 10226, December 1973, pp 2423-2438.
241. Ramberg, W. and Osgood, W. R., "Description of stress strain curves by three parameters", National Advisory Committee for Aeronautics, TN 902, July 1943.
242. Reid, J. K., "Large sparse sets of linear equations", Academic Press, 1971.
243. Reid, J. K., "A discussion on a modified CG method", Int. J. for Num. Methods in Enging., Vol. 7, 1973, pp 431-432.
244. Rodriques, J. S., "Node numbering optimization in structural analysis", J. of Struct. Div., ASCE, Vol. 101, ST2, 1975, pp 361-376.
245. Row, D. G.; Powell, G. H. and Moudkar, D. P., "Solution of progressively changing equilibrium equations for nonlinear structures", Computers and Structures, Vol. 7, 1977, pp 659- 655.
246. Ruhe, A., "SOR-methods for the eigenvalue problem", Report UNINF-37-73, Unea University, 1973.
247. Rushton, K. R., "DR solutions of elastic-plate problems", J. Strain Analysis, Vol. 3, No. 1, 1968.
248. Rushton, K. R., "The DR used for stress analysis", Recent Advances in Stress Analysis, 1968, pp 3-42.
249. Rushton, K. R., "Large deflection of variable thickness plates", Int. J. Mech. Sci., Vol. 10, 1968, pp 723-735.
250. Rushton, K. R. and Laing, L. M., "A digital computer solution of the Laplace equation using the dynamic relaxation method", The Aeronautical Quarterly, Vol. 19, 1968.
251. Rushton, K. R., "Post buckling of tapered plates", Int. J. Mech. Sci., Vol. 11, 1969, pp 461-480.

252. Rushton, K. R. and Hook, P. M., "Large deflection of plates and beams obeying non-linear stress-strain laws", J. of Strain Analysis, Vol. 9, No. 3, 1974, pp 178-184.
253. Saafan, A. S., "Theoretical analysis of suspension roofs", J. of Struct. Div., ASCE, paper No. 7107, February 1970, pp 393-405.
254. Saitoh, M. and Kurok, F., "The analysis, design and construction of a cable net suspension structure", 2nd Int. Conf. on Space Structures, Guildford, England, September 1975.
255. Sandi, H. and Hagiescu, S., "Influence of the boundary structure on behaviour of cable girders", Int. Conf. on Tension Structures, London, April 1974.
256. Sayar, K. F., "On the statics of a tension roof structure", Int. Conf. on Tension Structures, London, April 1974.
257. Schwarz, H. R., "The method of coordinate overrelaxation for $(A-\lambda B)x = 0$ ", Num. Math. Vol. 23, 1974, pp 135-151.
258. Schwarz, H. R., "The eigenvalue problem $(A-\lambda B)x = 0$ for symmetric matrices of high order", Computer Methods in Applied Mechanics and Engineering, Vol. 3, 1974, pp 11-28.
259. Schechter, S., "On the choice of relaxation parameters for nonlinear problems", "Numerical solution of systems of nonlinear algebraic equations", Edited by G. D. Byrne and C. A. Hall, Academic Press 1973.
260. Schlaich, J., "Lecture on cable structures", Int. Symp. on Wide Span Surface Structures, Stuttgart, April 1976.
261. Schmit, L. A.; Bogner, F. K. and Fox, R. L., "Finite deflection structural analysis using plate and shell discrete elements", AIAA J., Vol. 6, No. 5, May 1968, pp 781-791.
262. Schmit, L. A.; Stanton, E. L.; Gibson, W. and Goble, G. G., "Developments in discrete element finite deflection structural analysis by function minimization", Report AFFDL-TR-68-126, September 1968, Air Force Flight Dynamics Laboratory, Air Force Wright Patterson Base, Ohio.

263. Shavitt, I.; Bender, C. F.; Pipano, A. and Hosteny, R. P., "The iterative calculation of several of the lowest or highest eigenvalues and corresponding eigenvectors of very large symmetric matrices", J. Computational Physics, Vol. 11, 1973, pp 90-108.
264. Sheldon, J. W., "On the numerical solution of elliptic difference equations", Math. Tables Aids, Comput., Vol. 9, 1955, pp 101-112.
265. Shore, S. and Bathish, G. N., "Membrane analysis of cable roofs", Space Structures, Blackwell Publications, Oxford, 1967.
266. Shortley, G., "Use of Tschebysheff polynomial operators in the numerical solution of boundary-value problems", J. Appl. Physics, Vol. 24, No. 4, 1953, pp 392-396.
267. Schleyer, F. K., "Die berechnung von seilnetzen", IASS Colloquium on Hanging Roofs, Paris, 1962.
268. Schleyer, F. K., "Analysis of cable nets and cable structures", "Tensile structures", edited by F. Otto, Vol. 2, pp 98-168, MIT press 1969.
269. Sewell, M. J., "The static perturbation technique in buckling problems", J. Mech. Phys. Solids, Vol. 13, 1965, pp 247-265.
270. Sewell, M. J., "A general theory of equilibrium paths through critical points", Proc. Royal Soc., A306, 1968, pp 201-238.
271. Siev, A., "A general analysis of prestressed nets", Publications International Association for Bridge and Structural Engineering, Vol. 23, 1963, pp 283-292.
272. Siev, A. and Eidelman, J., "Stress analysis of prestressed suspended roofs", J. Struct. Div., ASCE, Vol. 90, paper No. 4008, 1964, pp 103-121.
273. Sofronie, R., "The response to wind of tension roof structures", Int. Conf. on Tension Roof Structures, London, April 1970.
274. Sorenson, H. W., "Comparison of some conjugate direction procedures for function minimization", J. of Franklin Inst., Vol. 288, No. 6, December 1969, pp 421-442.

275. Stamenkovic, A., "Local strength of flat slabs at column heads", PhD. thesis, University of London, December 1969.
276. Stein, E., "The design of pretensioned cable networks in the shape of hyperbolic paraboloids with edge cables", Hanging Roofs, North Holland Publishing Company, Amsterdam, 1963.
277. Striclin, J. A.; Haisler, W. E. and Von Rieseemann, W. A., "Geometrically non-linear structural analysis by direct stiffness method", J. of Struct. Div., ASCE, ST9, September 1971, pp 2299-2313.
278. Subcommittee on Cable Suspended Structures of the Task Committee on Special Structures, of the Committee on Metals of the Structural Division, "Cable-suspended roof construction state-of-the-art".
279. Takahashi, I., "A note on the conjugate gradient methods", International Processing in Japan, Vol. 5, 1965, pp 45-49.
280. Tanaka, S.; Tsubota, H. and Aizawa, M., "Theoretical analysis of pretensioned cable structures", Annual Report of Kajima Institute of Construction Technology, Vol. 21, 1972, pp 747-766.
281. Thomson, J. M. T. and Walker, A. C., "The nonlinear perturbation analysis of discrete structural systems", Int. J. Solids and Structures, Vol. 4, 1968, pp 757-768.
282. Thornton, C. H. and Birnstiel, C., "Three dimensional suspension structures", J. of Struct. Div., ASCE, Vol. 93, ST2, paper No. 5196, 1967, pp 247-270.
283. Tene, Y. and Epstein, M., "Nonlinear space trusses with tension only members", IASS Symp. on Tension Structures and Space Frames, Tokyo and Kyoto, 1971.
284. Tillerson, J. R.; Striclin, J. A. and Haisler, W. E., "Numerical methods for the solution of nonlinear problems in structural analysis", ASME, AMD, Vol. 6, November 1973, pp 67-101.
285. Topping, B. H. V., "The application of dynamic relaxation to the design of tension structures", PhD. thesis, The City University, London 1978.

286. Tottenham, H. and Williams, P. G., "Cable net: continuous system analysis", J. of Mech. Div., ASCE, Vol. 96, EM3, June 1970, pp 277-293.
287. Tottenham, H. and Khan, M. A., "Elastic non-linear analysis of prestressed cable networks using equivalent continuum theory", IAAS Symp. on Tension Structures and Space Frames, Tokyo and Kyoto, 1971.
288. Tuma, F. Y. and Galletly, G. D., "Large deflection analysis of plates using DR", Canadian Congress of Applied Mechanics, 28th May to June 1st, Montreal, Canada, 1973.
289. Turner, M. J.; Dill, E. H.; Martin, H. C. and Melosh, R. J., "Large deflections of structures subjected to heating and external loads", J. of Aerospace Sciences, Vol. 27, February 1960.
290. United States Steel Corporation Booklet, Bethlehem, Pa, 1969, "Design fundamentals of cable roof structures".
291. Urelius, D. E. and Fowler, D. W., "Behaviour of prestressed cable truss structures", J. of Struct. Div., ASCE, paper No. 10747, ST8, August 1974, pp 1624-1641.
292. Discussion on the above paper, J. of Struct. Div., ASCE, August 1975, pp 1710-1712.
293. Van Dyke, M., "Perturbation methods in fluid mechanics", Chapter 2, Academic Press, New York, 1964.
294. Varga, I. S., "Fraklin park zoo - a tension structure", 2nd Int. Conf. on Space Structures, Guildford, England, 1975.
295. Wachspress, E. L., "Iterative solution of elliptic systems", Prentice Hall Inc., 1966.
296. Walker, A. C., "A method of solution for non-linear simultaneous algebraic equations", Int. J. for Num. Methods in Enging., Vol. 1, 1969, pp 177-180.
297. Walsh, J., "Numerical analysis - an introduction", Academic Press, 1966.

298. Ward, J. K., "The vibration of simple span bridges by dynamic relaxation", MSc. thesis, Imp. College of Science and Technology, London 1969.
299. Warlick, C. H. and Young, D. M., "A priori methods for the determination of the optimum relaxation factor for the successive overrelaxation method", TNN-105, Computation Center, University of Texas.
300. Whiteman, J. R., "The mathematics of finite element and applications", Academic Press 1973.
301. Wilde, D. J., "Optimum seeking methods", Prentice Hall, Inc. 1964.
302. Williams, P. G., "Analysis of a cable net treated as a continuous system", PhD. thesis, University of Southampton, 1969.
303. Williams, F. W., "Rapid reduction of banded stiffness matrices", J. of Struct. Div., ASCE, May 1973, pp 967-971.
304. Wilkinson, J. H., "Error analysis of direct methods of matrix inversion", J. Ass. Comput. Mech., Vol. 8, 1961, pp 281-330.
305. Wilkinson, J. H., "The algebraic eigenvalue problem", Oxford Univ. Press, 1965.
306. Wilson, E. L.; Bathe, K. J. and Doherty, W. P., "Direct solution of large systems of linear equations", Computers and Structures, Vol. 4, 1974, pp 363-372.
307. Wood, W. L., "Comparison of DR with three other iterative methods", The Engineer, 1967, pp 683-687.
308. Wood, W. L., "Note on a modified CG method", Int. J. for Num. Methods in Enging., Vol. 7, 1973, pp 228-232.
309. Wozniakowski, H., "Numerical stability of the Chebyshev Method for the solution of large linear systems", Numerische Mathematik, Vol. 28, 1977, pp 191-209.

310. Young, D. M., "Iterative methods for solving partial difference equations of elliptic type", Trans. Amer. Math. Soc., Vol. 76, 1954, pp 92-111.
311. Young, D. M., "On the solution of large systems of linear algebraic equations with sparse positive definite matrices", "Numerical solution of systems of nonlinear algebraic equations", edited by G. D. Byrne and C. A. Hall, Academic Press 1973.
312. Zetlin, L., "Elimination of flutter in suspension roofs", Hanging Roofs, North Holland Publishing Company, Amsterdam, 1963.
313. Zetlin, L., "Steel cable creates novel structural space systems", Engineering Journal of AISC, Vol. 1, No. 1, January 1964.
314. Zienkiewicz, O. C., "The finite element method in engineering science", McGraw Hill, London, 1971.
315. Barnes, M.R., "An investigation of vibration decay in a model pneumatic dome", Int. Symp. on wide Surface Structures, Stuttgart, April 1976.
316. Forsythe, G.E. and Wasow, W.R., "Finite difference methods for partial differential equations", John Wiley and Sons, 1960.